Voltammetric Studies of Paracetamol with Some Functional Amines at Different pH Media

by

Md. Hafizur Rahman

A thesis submitted in partial fulfillment of the requirements for the degree of
Master of Science (M.Sc.) in Chemistry

Khulna University of Engineering & Technology
Khulna 9203, Bangladesh
February 2016

Dedicated

To My Parents

Rabeya Khatun and Md. Abdus Sattar

Who have desired underprivileged life to continue my smile.

Declaration

This is to certify that the thesis work entitled "Voltammetric Studies of Paracetamol with Some Functional Amines at Different pH Media" has been carried out by Md. Hafizur Rahman in the Department of Chemistry, Khulna University of Engineering & Technology, Khulna, Bangladesh. The above thesis work or any part of this work has not been submitted anywhere for the award of any degree or diploma.
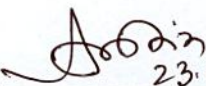
Signature of Supervisor   Signature of Candidate
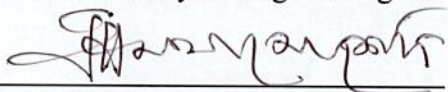
Approval

This is to certify that the thesis work submitted by Md. Hafizur Rahman entitled "Voltammetric Studies of Paracetamol with some Functional Amines at Different pH Media" has been approved by the board of examiners for the partial fulfillment of the requirements for the degree of Master of Science in the Department of Chemistry, Khulna University of Engineering & Technology, Khulna, Bangladesh in February 2016.

BOARD OF EXAMINERS

1. _____
   23.02.16
   Dr. Md. Abdul Motin
   Professor, Department of Chemistry
   Khulna University of Engineering & Technology

   Chairman
   (Supervisor)

2. _____
   23.02.16
   Head
   Department of Chemistry
   Khulna University of Engineering & Technology

   Member

3. _____
   Dr. Mohammad Abu Yousuf
   Professor, Department of Chemistry
   Khulna University of Engineering & Technology

   Member

4. _____
   Dr. Mohammad Hasan Morshed
   Professor, Department of Chemistry
   Khulna University of Engineering & Technology

   Member

5. _____
   23.02.16
   Dr. Md. Rezaul Haque
   Professor, Chemistry Discipline
   Khulna University

   Member
   (External)

Acknowledgements

Abstract

Electroactive paracetamol adducts such as paracetamol-diethylamine and paracetamol-diisopropylamine were synthesized electrochemically. The products has been studied by Cyclic voltammetry (CV), Controlled potential coulometry (CPC), Differential pulse voltammetry (DPV) and Chronoamperometry (CA) techniques using Glassy carbon (GC), Gold (Au) and Platinum (Pt) electrodes. The studies have been carried out in variation of paracetamol, diethylamine and diisopropylamine concentration, buffer solution of different pH, different electrodes and scan rate.

After the insertion of diethylamine and diisopropylamine in paracetamol solution at the second scan of CV potential, new anodic and cathodic peaks appeared at the negative potential. In the presence of nucleophiles with paracetamol as Michael acceptors the oxidation and reduction peak shifted with respect of pure paracetamol. Also the anodic and cathodic peak current changes significantly compared with the pure paracetamol that indicates the participation of reaction of p-quinoneimine with diethylamine and diisopropylamine. The products generated from the reaction of paracetamol with diethylamine and diisopropylamine are assumed to be N-(3-(diethylamino)-4-hydroxyphenyl)acetamide and N-(3-(diisopropylamino)-4-hydroxyphenyl)acetamide respectively that undergo electron transfer at more negative potentials than the paracetamol.

The influence of pH of paracetamol in presence of diethylamine and diisopropylamine was studied by varying pH from 3 to 9. For diethylamine and diisopropylamine, it is observed that at pH 3-5, no new anodic peak appeared after monotonous cycling. In the pH 7, the p-dienone endures nucleophilic attack by the amines that voltammetric new anodic peaks A_1 and A_2 appeared after monotonous cycling. Whereas in pH 9, the voltammogram display a new peak at the first scan of potential. In lieu of diethylamine and diisopropylamine, the maximum peak current is observed at pH 7. The slopes of the peak potential, E_p vs pH plot was determined graphically as the anodic peaks of paracetamol-diethylamine (37 mV/pH for first anodic peak A_3) and paracetamol-diisopropylamine (23 mV/pH for first anodic peak A_3) at 0.1V/s in the 2nd cycle. This ascribed that the oxidation reaction of

paracetamol-diethylamine and paracetamol-diisopropylamine adducts proceeded via the $2e^-/2H^+$ process. This also indicates that during the reaction not only electron but also proton are released from the paracetamol-amine adduct. The reaction was strongly influenced by the pH as well as concentration of diethylamine and diisopropylamine. The reaction was mostly favorable in 150mM of diethylamine and 150mM of diisopropylamine with fixed 2mM of paracetamol at pH 7. The electrochemical reaction of paracetamol-diethylamine and paracetamol-diisopropylamine adduct are facilitated in neutral media.

The effect of scan rate on cyclic voltammogram of paracetamol in presence of diethylamine and diisopropylamine were also investigated. The peak currents of both the anodic and the corresponding cathodic peaks increase with the increase of scan rate. The nearly proportionality of the anodic and corresponding cathodic peak ascribes that the peak current of the reactant at each redox reaction is controlled by diffusion process. The current function, $I_p/v^{1/2}$ of paracetamol-amine derivatives were found to be decreased exponentially with increasing scan rate. In all the studies of paracetamol-amine derivatives have been found to undergo electrochemical reaction with ECE (electron transfer-chemical reaction- electron transfer) type mechanism.

Controlled-potential coulometry was studied of catechol in presence of diethylamine and diisopropylamine. During the course of coulometry, the appeared peaks height increase proportionally to the advancement of coulometry, parallel to the decrease in the height of paracetamol peak. These observations also indicate the participation of reaction of paracetamol with the studied nucleophiles. The electro-synthesized products originated from the bulk electrolysis of paracetamol with diethylamine and diisopropylamine were isolated. The formations of new products were also ascertained by FTIR spectra.

Contents

LIST OF TABLES

LIST OF FIGURES

CHAPTER I

Introduction

1.1 General

Electrochemistry provides very interesting and versatile means for the study of electro-synthesis and characterization of electro-active compounds. Recently, the terms molecular electrochemistry or dynamic electrochemistry have been used to study the mechanistic events of functional drug compounds [1-4]. The majority of electroactive drugs are characterized by the generation of a reactive intermediate at the electrode by electron transfer and subsequent chemical reactions. The electrochemical generation and study of the intermediates may be advantageous because of the mild reaction conditions employed and the additional selectivity introduced in voltammetric experiments.

Voltammetry is an analytic method based on electrochemistry. The common characteristic of all voltammetric techniques is that they involve the application of a potential (E) to an electrode and the monitoring of the resulting current (i) flowing through the electrochemical cell. In many cases the applied potential is varied or the current is monitored over a period of time (t). Thus, all voltammetric techniques can be described as some function of E, i, and t. They are considered active techniques (as opposed to passive techniques such as potentiometry) because the applied potential forces a change in the concentration of an electroactive species at the electrode surface by electrochemically reducing or oxidizing it. The current-potential-curve gives information about the amount and identity of the substances in the measured solution. Oxidations as well as reductions can be observed and characterized. The current-potential curve shows the measured current against the applied potential difference between the working electrode and the counter electrode. A voltammetric cell consists of a working electrode, on which the oxidation and reduction processes are taking place. There has to be a counter and a reference electrode too. In the cyclic voltammetry the potential is continuously changed until a previously defined potential is reached. Then the potential is changed in the other

direction, until the starting potential is reached again. Instead of changing the potential and measuring the current continuously, in differential pulse voltammetry a rectangular pulse potential is applied and the current is measured only shortly before the pulse and at the end of the pulse.

Electrochemical methods have proved to be very sensitive for the determination/ electrochemical study of organic molecules, including drugs and related molecules in pharmaceutical dosages forms and biological fluids and their oxidisible property. Although regarded to be safe at therapeutic doses, acetaminophen is known to cause acute hepatic centrilobular necrosis in humans when consumed in large doses [5, 6]. The mechanism of acetaminophen-induced toxicity has come under extensive study and circumstantial evidence for the involvement of the cytochrome P460 mixed function oxidize in the formation of an electrophilic reactive intermediate is strong [7-14]. When a larger dose is administered, the level of glutathione is depleted and the quinoneimine reacts with cell macromolecules leading to cell damage or death [15]. However, unlike phenacetin, acetanilide and their combinations, paracetamol is not considered carcinogenic at therapeutic doses [16]. The nucleophilic attacks toward paracetamol that lead to the formation of dienone derivatives with more or less positive oxidation potentials are followed by more E (electron transfer) steps and C (chemical reaction) steps depends on the structure of intermediates by EC reaction [17]. The following drug or drug making compounds for example nicotinamide, diethylamine, metronidazole, diisopropylamine, pyridoxine etc. may be used as nucleophiles. Among them diethylamine and diisopropylamine are also used as a precursor to two herbicides, dilate and triallate, as well as formation of certain organosulfur drugs [18]. Due to weak alkaline nature it may act a neutral nucleophile and presence of one lone pair electron on nitrogen enables it to take participation in 1,4-Michael addition reaction with dienone.

The electrocatalytic activity of paracetamol in presence of diethylamine and diisopropylamine were studied in the research for three different electrodes (GC, Au and Pt) and various concentrations of diethylamine (100-250mM) and diisopropylamine (100-250mM) at different scan rates. Because of significance of acetoaminophen as biologically important compounds [19] in this direction that demands detail electrochemical studies of paracetamol in the presence of diethylamine and diisopropylamine as representative of

secondary aliphatic and aromatic amines. Although people have used the above drug or drug making compounds enormously but the reaction mechanism of most of the compounds are still unknown.

The objective of the present study is thus a fundamental pursuit to have better insight of the possible redox interactions of acetaminophen with diisopropylamine and diethylamine compounds. These compounds undergo oxidation and/or reduction on the electrode surface within the potential range. The electro activity of such compounds depends upon the pH of the medium, nature of the electrode and active electrophore present in their structures. Their redox behavior can be influenced by the change in pH, substituents, concentration and scan rate.

1.2.1 Paracetamol

Paracetamol, known as *N*-(4-hydroxyphenyl)acetamide or acetaminophen is a medication used to treat pain and fever reducer. It's molecular formula is $C_8H_9NO_2$ (Figure 1.1). Paracetamol consists of a benzene ring core, substituted by one hydroxyl group and the nitrogen atom of an amide group in the para (1,4) position [20]. The amide group is acetamide (ethanamide). It is an extensively conjugated system, as the lone pair on the hydroxyl oxygen, the benzene π-cloud, the nitrogen lone pair, the π-orbital on the carbonyl carbon, and the lone pair on the carbonyl oxygen are all conjugated. The presence of two activating groups also makes the benzene ring highly reactive toward electrophilic aromatic substitution. As the substituents are ortho, para-directing and para with respect to each other, all positions on the ring are more or less equally activated. The conjugation also greatly reduces the basicity of the oxygens and the nitrogen, while making the hydroxyl acidic through delocalization of charge developed on the phenoxide anion.
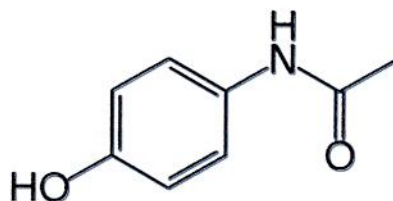
Figure 1.1: Structure of paracetamol

1.2.2 Use of Paracetamol

Paracetamol is a widely used over-the-counter pain medication and antipyretic (fever reducer) [21]. It is classified as a mild analgesic. It is commonly used for the relief of headaches and other minor aches and pains and is a major ingredient in numerous cold and flu remedies. In combination with opioid analgesics, paracetamol can also be used in the management of more severe pain such as post-surgical and cancer pain. Though paracetamol is used to treat inflammatory pain, it is not generally classified as an NSAID because it exhibits only weak anti-inflammatory activity.

1.2.3 Diethylamine

Diethylamine is an organic compound with the molecular formula $(C_2H_5)_2NH$ shown in Figure 1.2. This secondary amine is a colorless, flammable gas with an ammonia-like odor. It is used as a corrosion inhibitor and in the production of rubber, resins, dyes and pharmaceuticals. Diethylamine is commonly encountered commercially as a solution in water at concentrations up to around 40%. It is also found as a natural product.
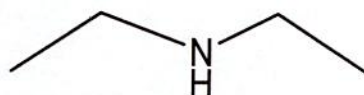
Figure 1.2: Structure of diethylamine

1.2.4 Natural occurrence of Diethylamine

Diethylamine is found quite widely distributed in animals and plants, and is present in many foods at the level of a few mg/kg [22].

1.2.5 Use of Diethylamine

Diethylamine is a precursor to several industrially significant compounds. It reacts with carbon disulfide to give dimethyl dithiocarbamate, a precursor to a family of chemicals widely used in the vulcanization of rubber. The solvents diethylformamide and diethylacetamide are derived from diethylamine. It is raw material for the production of

many agrichemicals and pharmaceuticals, such as dimefox and diphenhydramine, respectively. The chemical weapon tabun is derived from diethylamine. The surfactant lauryl diethylamine oxide is found in soaps and cleaning compounds. Unsymmetrical diethylhydrazine, a rocket fuel, is prepared from diethylamine.

1.2.6 Diisopropylamine

The IUPAC name of Diisopropylamine is N-(1-Methylethyl)-2-propanamine, it is also named as 2-Propaneamine as shown in Figure 1.3. The product's categories are pharmaceutical intermediates; heterocyclic Compounds. Besides, it is a clear colorless liquid with an ammonia-like odor, which should be sealed in a cool, ventilated warehouse. And it can react violently with oxidizing agents and strong acids. It may be incompatible with isocyanates, halogenated organics, peroxides, phenols (acidic), epoxides, anhydrides, and acid halides. In addition, its molecular formula is $C_6H_{15}N$ and molecular weight is 101.19.
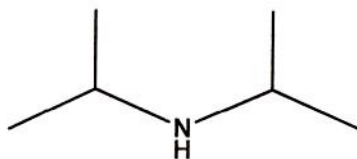
Figure 1.3: Structure of Diisopropylamine

1.2.7 Use of Diisopropylamine

Diisopropylamine is primarily used as a precursor to two herbicides, dilate and triallate, as well as certain sulfenamides used in the vulcanization of rubber [23]. It is also used to prepare N,N-Diisopropylethylamine (Hünig's base) by alkylation with diethyl sulfate. It is also used as catalyst for polymerization. Anti-eroding lubricant agent and emulsifying agent, Intermediate for pharmaceuticals, coating materials, pesticide, rubber chemicals, fiber, alkylalkanolamines and other organic products, additive in petroleum industry and solvent for hydrocarbon extraction.

1.3 Literature review

An enormous survey of literature, it is seen that very limited works on the electro-oxidation of paracetamol in presence of nucleophiles have been performed [24-26, 19]. The electro-oxidation of paracetamol in presence of some other nucleophiles such as malononitrile, fluoxetine, sertraline, nortriptyline and diemethylamine [24-26, 19] were studied. A. Asghari et al [24] studied of electrochemical oxidation of paracetamol in the presence of malononitrile as a nucleophile in a phosphate buffer solution (0.15 mol/L, pH 7), using cyclic voltammetric techniques. The results indicated that the *N*-acetyl-*p*-benzoquinone-imine derived from paracetamol participates in a 1,4-Michael-type addition reaction with the malononitrile to form the corresponding paracetamol derivatives. Nematollahi et al [26] reported on the electrochemical Synthesis and Kinetic Evaluation of Electrooxidation of Acetaminophen in the Presence of Antidepressant Drugs (fluoxetine, sertraline and nortriptyline). They showed the drug-drug interaction (DDI) between acetaminophen and some of antidepressant drugs (fluoxetine, sertraline and nortriptyline) by means of cyclic voltammetry and Controlled-potential coulometry. The reaction between N-acetyl-p-benzoquinone-imine (NAPQI) produced from electrooxidation of acetaminophen and antidepressant drugs cause to reduce the concentration of NAPQI and decreases the effective concentration of antidepressants. Hadi Shafiei et al [19] reported on experimental and computational study on the rate constant of electrochemically generated *N*-acetyl-*p* -quinoneimine with dimethylamine. Their results showed the participation of electrochemically generated *N*-acetyl-*p*-quinoneimine in Michael reaction with dimethylamine.

For the quantitative determination of paracetamol in different systems, various analytical methods have been executed such as spectrofluorimetric analysis [27], solid-phase molecular fluorescence [28], spectrophotometric analysis [29-31], HPLC [32-35]. However, these methods are time consuming or solvent-usage intensive. Moreover, these methods face the drawbacks of being expensive, laborious and requiring pretreatment of the samples. Compared to other options, electroanalytical methods have the advantages of simplicity and high sensitivity. But, despite of these advantages, there are a few electrochemical methods for simultaneous determination and/ or electrochemical analysis of paracetamol. Goyal et al. [36, 37] have been studied

voltammetric analysis of paracetamol. Lau et al. [38] reported the electrochemical analysis of ascorbic acid, paracetamol and caffeine by differential pulse voltammetry (DPV). Zen and Ting [39] studied the use of Nafion/ruthenium oxide pyrochlore chemically modified electrode for the voltammetric study of paracetamol and caffeine in drug formulations by square-wave voltammetry. Lourenc et al. [40] reported the voltammetric study of paracetamol and caffeine in pharmaceutical formulations. Sanghavi and Srivastava [41] have studied the use of an in situ surfactant-modified multi-walled carbon nanotube paste electrode for voltammetric analysis of paracetamol, aspirin and caffeine. Wangfuengkanagul et al [42] reported the electrochemical analysis of acetaminophen. Habibi et al [43, 44] reported the Electro-chemical oxidation of acetaminophen and dopamine.

Since electrochemical oxidation very often parallels with the cytochrome P450 catalyzed oxidation in liver microsomes, studying the anodic oxidation of acetaminophen in the presence of nucleophiles is of interest. Therefore, with the aim of investigating of the reactivity of intermediate *N*-acetyl-*p* quinoneimine toward amines, as well as estimation of observed rate constant of this reaction, we will investigate the electrochemical oxidation of acetaminophen in aqueous solutions in the presence of diethylamine and diisopropylamine as a model for amine important compounds such as drugs, amino acids, peptides and proteins. In this research work cyclic voltammetry (CV), differential pulse voltammetry (DPV), controlled potential coulometry (CPC) and chronoamperometry (CA) techniques will be used to study the interaction and the mechanism of the redox process of paracetamol with diethylamine and diisopropylamine for three different electrodes (Au, GC and Pt), different pH (3-9) and various concentration (100-250 mM of nucleophiles). To the best of our knowledge, the electrochemical study of paracetamol in presence of diethylamine and diisopropylamine at different conditions (concentration, pH, scan rate etc) has not been reported before this work.

1.4 Objectives of the thesis

Attempt will be made in the present research work to show a systematic study of electro-synthesis and mechanism of redox process of biologically important paracetamol containing amine derivatives which may help to understand the role of paracetamol drugs

and their derivatives in the biological processes. Electrochemical study of nucleophilic substitution reactions of paracetamol in presence of diethylamine and diisopropylamine were carried out in different conditions.

The specific aims of this study are:

- ➢ to synthesize biologically important paracetamol-amine derivatives electrochemically.
- ➢ to diagnose the mechanism of the redox processes of these compounds at different pH and at different scan rate.
- ➢ to study the effect of pH, scan rate, concentration on the voltammogram.
- ➢ to identify the most favorable condition (concentration, pH) for the reaction.
- ➢ to know the redox interaction of the species by Cyclic voltammetry (CV), Controlled potential coulometry (CPC), Differential pulse voltammetry (DPV) and Chronoamperometry (CA) techniques.
- ➢ to characterize the new features of the species by electrochemical and spectral analysis.

CHAPTER II

Theoretical Background

Electroanalytical chemistry includes a group of quantitative analytical methods that are based upon the electrical and chemical properties of an analyte solution. There are two general types of electrochemical methods. Electroanalytical methods are a class of techniques in analytical chemistry which study an analyte by measuring the potential (volts) and/or current (amperes) in an electrochemical cell containing the analyte. These methods can be broken down into several categories depending on which aspects of the cell are controlled and which are measured. The three main categories are potentiometry (the difference in electrode potentials is measured), coulometry (the cell's current is measured over time), and voltammetry (the cell's current is measured while actively altering the cell's potential). Voltammetry applies a constant and/or varying potential at an electrode's surface and measures the resulting current with a three electrode system. This method can reveal the reduction potential of an analyte and its electrochemical reactivity. This method in practical terms is nondestructive since only a very small amount of the analyte is consumed at the two-dimensional surface of the working and auxiliary electrodes. In practice the analyte solutions is usually disposed of since it is difficult to separate the analyte from the bulk electrolyte and the experiment requires a small amount of analyte. Electrodes are employed for electrochemical determination of organic molecules as well as metal ions. The electrode can act as a source (for reduction) or a sink (for oxidation) of electrons transferred to or from the species in solution:

$$O + ne \rightarrow R$$
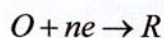
Where, O and R are the oxidized and reduced species. In order for the electron transfer to occur, there must be a correspondence between the energies of the electron orbitals where transfer takes place in the donor and acceptor. In the electrode this level is the highest filled orbital, which in a metal is Fermi energy level. In the soluble species it is the orbital of the valence electron to be given or received. For reduction, there is a minimum energy that the transferable electrons from the electrode must have before the transfer can occur, which corresponds to a sufficiently negative potential. For an oxidation, there is a

maximum energy that the lowest unoccupied level in the electrode can have in order to receive electrons from the species in solution, corresponding to a sufficiently positive potential.

In order to study electrode reactions, reproducible experimental conditions must be created which enable minimization of all unwanted factors that can contribute to the measurements and diminish their accuracy. That means to suppress migration effects, confine the interfacial region as close as possible to the electrode, and minimize solution resistance. These objectives are achieved by the addition of large amount (around 1 mol dm^{-3}) of inert electrolyte, the electroactive species being at a concentration of 5 mM or less [45].

Since an electrode predominantly attracts positively and negatively charged species, which may or may not undergo reaction at the surface, it should be remembered that the species may adsorb at the electrode surface. This makes it clear that in the description of any electrode process we have to consider the transport of species to the electrode surface as well as the electrode reaction itself. This transport can occur by diffusion, convection or migration.

2.1 Mass transfer process in voltammetry

Mass transfer is the movement of material from one location to another in solution. In electrochemical systems, three modes of mass transport are generally considered which a substance may be carried to the electrode surface from bulk solution including diffusion, convection and migration. Any of these or more than one might be operating in a given experiment which is depended on the experimental conditions.

In general, there are three types of mass transfer processes:

- Migration
- Diffusion
- Convection

2.1.1 Migration

Migration is the movement of ions through a solution as a result of electrostatic attraction between the ions and the electrodes. It is the primary cause of mass transfer in the bulk of the solution in a cell. This motion of charged particle through solution, induced by the charges on the electrodes is called migration [46]. This charge movement constitutes a

current. This current is called migration current. The larger the number of different kinds of ions in a given solution, the smaller is the fraction of the total charge that is carried by a particular species. Electrolysis is carried out with a large excess of inert electrolyte in the solution so the current of electrons through the external circuit can be balanced by the passage of ions through the solution between the electrodes, and a minimal amount of the electroactive species will be transported by migration. Migration is the movement of charged species due to a potential gradient. In voltammetric experiments, migration is undesirable but can be eliminated by the addition of a large excess of supporting electrolytes in the electrolysis solution. The effect of migration is applied zero by a factor of fifty to hundred ions excess of an inert supporting electrolyte.

2.1.2 Diffusion

Diffusion refers to the process by which molecules intermingle as a result of their kinetic energy of random motion. Whereas a concentration difference between two regions of a solution, ions or molecules move from the more concentrated region to the dilute and leads to a disappearance of the concentration difference.

The one kind of mode of mass transfer is diffusion to an electrode surface in an electrochemical cell. The rate of diffusion is directly proportional to the concentration difference. When the potential is applied, the cations are reduced at the electrode surface and the concentration is decreased at the surface film. Hence a concentration gradient is produced. Finally, the result is that the rates of diffusion current become larger.

2.1.3 Convection

By mechanical way reactants can also be transferred to or from an electrode. Thus forced convection is the movement of a substance through solution by stirring or agitation. This will tend to decrease the thickness of the diffuse layer at an electrode surface and thus decrease concentration polarization. Natural convection resulting from temperature or density differences also contributes to the transport of species to and from the electrode [47]. At the same time a type of current is produced. This current is called convection current. Removing the stirring and heating can eliminate this current. Convection is a far more efficient means of mass transport than diffusion.

2.2 Cyclic voltammetry (CV)

Cyclic voltammetry is a very versatile electrochemical technique which allows to probe the mechanics of redox and transport properties of a system in solution. This is accomplished with a three electrode arrangement whereby the potential relative to some reference electrode is scanned at a working electrode while the resulting current flowing through a counter (or auxiliary) electrode is monitored in a quiescent solution. The technique is ideally suited for a quick search of redox couples present in a system; once located, a couple may be characterized by more careful analysis of the cyclic voltammogram. More precisely, the controlling electronic is designed such that the potential between the reference and the working electrodes can be adjusted but the big impedance between these two components effectively forces any resulting current to flow through the auxiliary electrode. Usually the potential is scanned back and forth linearly with time between two extreme values – the switching potentials using triangular potential waveform (see Figure 2.1). When the potential of the working electrode is more positive than that of a redox couple present in the solution, the corresponding species may be oxidized (i.e. electrons going from the solution to the electrode) and produce an anodic current. Similarly, on the return scan, as the working electrode potential becomes more negative than the reduction potential of a redox couple, reduction (i.e. electrons flowing away from the electrode) may occur to cause a cathodic current. By IUPAC convention, anodic currents are positive and cathodic currents negative.
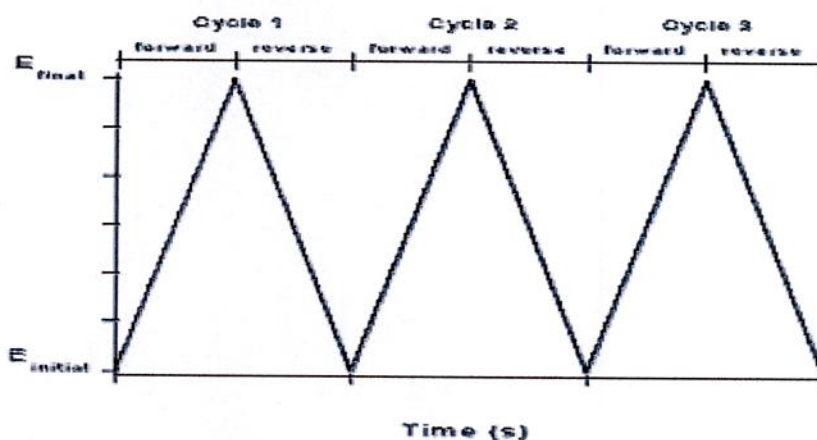
Figure 2.1: A cyclic voltammetry potential waveform with switching potentials

The magnitude of the observed faradaic current can provide information on the overall rate of the many processes occurring at the working electrode surface. As is the case for any

12

multi–step process, the overall rate is determined by the slowest step. For an redox reaction induced at a working electrode, the rate determining step may be any one of the following individual step depending on the system: rate of mass transport of the electro-active species, rate of adsorption or de-sorption at the electrode surface, rate of the electron transfer between the electro-active species and the electrode, or rates of the individual chemical reactions which are part of the overall reaction scheme.

For the oxidation reaction involving n electrons

$$Red \; \rightleftarrows \; Ox + ne^-$$
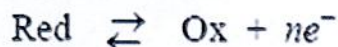
the *Nernst Equation* gives the relationship between the potential and the concentrations of the oxidized and reduced form of the redox couple at equilibrium (at 298 K):

$$E = E^{0'} + \frac{0.059}{n} \log_{10} \frac{[Ox]_c}{[Red]}$$

where E is the applied potential and E^{v} the formal potential; [OX] and [Red] represent surface concentrations at the electrode/solution interface, *not* bulk solution concentrations. Note that the Nernst equation may or may not be obeyed depending on the system or on the experimental conditions.
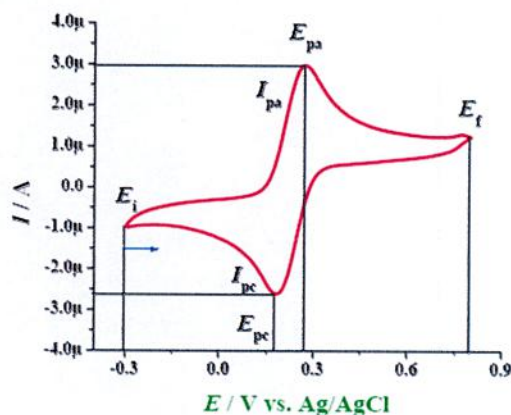
Figure 2.2: The expected response of a reversible redox couple during a single potential cycle

A typical voltammogram is shown in Figure 2.2. The scan shown starts at a slightly negative potential, *(A)* up to some positive switching value, *(D)* at which the scan is reversed back to the starting potential. The current is first observed to peak at E_{pa} (with value i_{pa}) indicating that an oxidation is taking place and then drops due to depletion of the reducing species from the diffusion layer. During the return scan the processes are reversed

13

(reduction is now occurring) and a peak current is observed at E_{pc} (corresponding value, i_{pc}).

Providing that the charge–transfer reaction is reversible, that there is no surface interaction between the electrode and the reagents, and that the redox products are stable (at least in the time frame of the experiment), the ratio of the reverse and the forward current $i_{pr}/i_{pf} = 1.0$ (in Figure 2.2 $i_{pa} = i_{pf}$ and $i_{pc} = i_{pr}$). In addition, for such a system it can be shown that:

- ❖ the corresponding peak potentials E_{pa} and E_{pc} are independent of scan rate and concentration

- ❖ the formal potential for a reversible couple $E^{0'}$ is centered between E_{pa} and E_{pc}: $E^{0'} = (E_{pa} + E_{pc})/2$

- ❖ the separation between peaks is given by $\Delta E_p = E_{pa} - E_{pc} = 59/n$ mV (for a n electron transfer reaction) at all scan rates (however, the measured value for a reversible process is generally higher due to uncompensated solution resistance and non-linear diffusion. Larger values of ΔE_p, which increase with increasing scan rate, are characteristic of slow electron transfer kinetics).

It is possible to relate the half-peak potential ($E_{p/2}$, where the current is half of the peak current) to the polarographic half-wave potential, $E_{1/2}$: $E_{p/2} = E_{1/2} \pm 29mV/n$ (The sign is positive for a reduction process.)

Simply stated, in the forward scan, the reaction is $O + e^- \rightarrow R$, R is electrochemically generated as indicated by the cathodic current. In the reverse scan, $R \rightarrow O + e^-$, R is oxidized back to O as indicated by the anodic current. The CV is capable of rapidly generating a new species during the forward scan and then probing its fate on the reverse scan. This is a very important aspect of the technique [48].
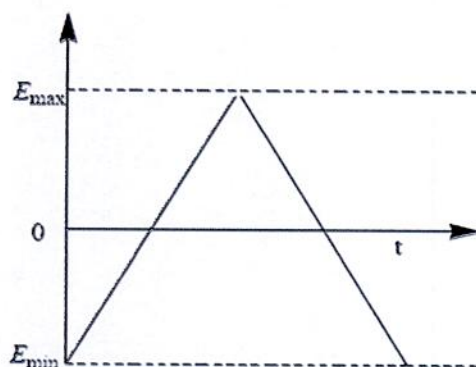
Figure 2.3: Variation of potential with time in cyclic voltammetry

A characteristic feature is the occurrence of peaks, identified by the peak potential E_p, which corresponds to electron transfer reactions. The repetitive triangular potential excitation signal for CV causes the potential of the working electrode to sweep backward and forward between two designate values (the switching potentials).

In cyclic voltammetry of reversible system, the product of the initial oxidation or reduction is then reduced or oxidized, respectively, on reversing the scan direction.

Adsorbed species lead to changes in the shape of the cyclic voltammogram, since they do not have to diffuse from the electrode surface. In particular, if only adsorbed species are oxidized or reduced, in the case of fast kinetics the cyclic voltammogram is symmetrical, with coincident oxidation and reduction peak potentials [49].

Cyclic voltammetry is one of the most versatile techniques for the study of electroactive species, as it has a provision for mathematical analysis of an electron transfer process at the electrode [50-53]. It is an electroanalytical tool for monitoring and recognition of many electrochemical processes taking place at the surface of electrode and can be used to study redox processes in biochemistry and macromolecular chemistry [54].

2.2.1 Single electron transfer process

Based upon the values of electrochemical parameters, i.e., peak potential E_p, half peak potential ($E_{p/2}$), half wave potential ($E_{1/2}$), peak current (I_p), anodic peak potential E_{pa}, cathodic peak potential E_{pc} etc, it can be ascertained whether a reaction is reversible, irreversible or quasi-reversible. The electrochemical parameters can be graphically obtained from the voltammogram as shown in the Figure 2.3.

Three types of single electron transfer process can be studied.

         a. Reversible process. b. Irreversible process and c. Quasi-reversible.

2.2.1(a) Reversible processes

The peak current for a reversible couple (at 25°C), is given by the Randles-Sevcik equation: $i_p = (2.69 \times 10^5) \, n^{3/2} A C D^{1/2} v^{1/2}$

where n is the number of electrons, A the electrode area (in cm^2), C the concentration (in mol/cm^3), D the diffusion coefficient (in cm^2/s), and v the scan rate (in V/s). Accordingly, the current is directly proportional to concentration and increases with the square root of the scan rate. The ratio of the reverse-to-forward peak currents, i_{pr}/i_{pf}, is unity for a simple reversible couple. This peak ratio can be strongly affected by chemical reactions coupled to the redox process. The current peaks are commonly measured by extrapolating the preceding baseline current. The position of the peaks on the potential axis (E_p) is related to the formal potential of the redox process. The formal potential for a reversible couple is centered between E_{pa} and E_{pc}:

$$E° = (E_{pa} + E_{pc})/2$$

The separation between the peak potentials (for a reversible couple) is given by:

$$\Delta E_p = E_{pa} - E_{pc} = 59 mV/n$$

Thus, the peak separation can be used to determine the number of electrons transferred, and as a criterion for a Nernstian behavior. Accordingly, a fast one-electron process exhibits a ΔE_p of about 59 mV. Both the cathodic and anodic peak potentials are independent of the scan rate. It is possible to relate the half-peak potential ($E_{p/2}$, where the current is half of the peak current) to the polarographic half-wave potential, $E_{1/2}$

$$E_{p/2} = E_{1/2} \pm 29 mV/n$$

(The sign is positive for a reduction process.) For multi electron-transfer (reversible) processes, the cyclic voltammogram consists of several distinct peaks, if the E° values for the individual steps are successively higher and are well separated. An example of such mechanism is the six-step reduction of the fullerenes C_{60} and C_{70} to yield the hexaanion products C_{60}^{6-} and C_{70}^{6-} where six successive reduction peaks can be observed.

The situation is very different when the redox reaction is slow or coupled with a chemical reaction. Indeed, it is these "nonideal" processes that are usually of greatest chemical interest and for which the diagnostic power of cyclic voltammetry is most useful. Such information is usually obtained by comparing the experimental voltammograms with those derived from theoretical (simulated) ones.
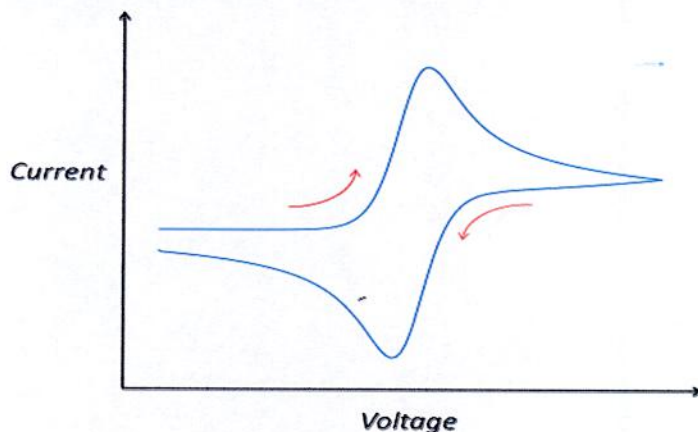
Figure 2.4: Reversible cyclic voltammogram of redox process

2.2.1(b) Irreversible processes

For irreversible processes (those with sluggish electron exchange), the individual peaks are reduced in size and widely separated. Totally irreversible systems are characterized by a shift of the peak potential with the scan rate:

$$E_p = E° - (RT/\alpha n_a F)[0.78 - \ln(k°/(D)^{1/2}) + \ln (\alpha n_a F v/RT)^{1/2}]$$

where α is the transfer coefficient and n_a is the number of electrons involved in the charge-transfer step. Thus, E_p occurs at potentials higher than $E°$, with the overpotential related to $k°$ and a. Independent of the value $k°$, such peak displacement can be compensated by an appropriate change of the scan rate. The peak potential and the half-peak potential (at 25°C) will differ by 48/αn mV. Hence, the voltammogram becomes more drawn-out as α**n** decreases.
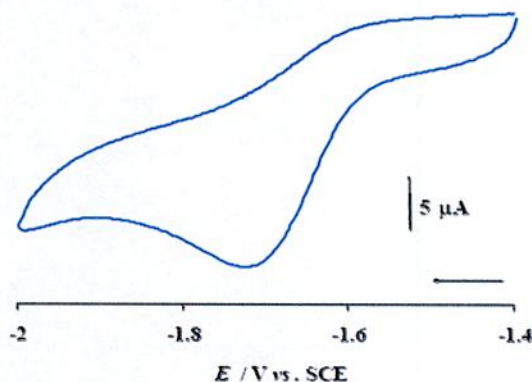
Figure 2.5: Cyclic voltammogram of irreversible redox process

2.2.1(c) Quasi-reversible process

Quasi-reversible process is termed as a process, which shows intermediate behavior between reversible and irreversible processes. In such a process the current is controlled by both the charge transfer and mass transfer.

Cyclic voltammogram for quasi-reversible process is shown in Figure 2.6 [55].
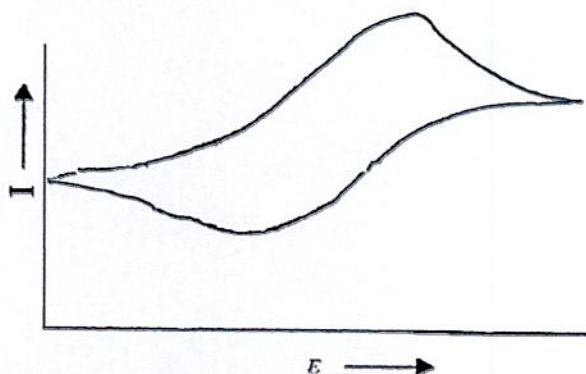
Figure 2.6: Cyclic voltammogram of quasi-reversible redox process

For quasi-reversible process the value of standard heterogeneous electron transfer rate constant, k_{sh}^o lies in the range of 10^{-1} to 10^{-5} cm sec^{-1} [56]. An expression relating the current to potential dependent charge transfer rate was first provided by Matsuda and Ayabe [57].

$$I(t) = C_{o(0,t)} k_{sh}^o Exp\left[-\frac{\alpha nF}{RT}\left\{E(t) - E^o\right\}\right] - C_{R(0,t)} k_{sh}^o Exp\left[-\frac{\beta nF}{RT}\left\{E(t) - E^o\right\}\right] \ldots.2.1$$

where k_{sh}^o is the heterogeneous electron transfer rate constant at standard potential E^0 of redox system. α is the transfer coefficient and $\beta = 1 - \alpha$. In this case, the shape of the peak and the various peak parameters are functions of α and the dimensionless parameter, Λ, defined as [58]

$$\Lambda = \frac{k_{s,h}}{D^{1/2}(nF/RT)^{1/2}\upsilon^{1/2}} \quad \dots\dots\dots\dots\dots\dots\dots\dots\dots2.2$$

when $D_o = D_R = D$

D_o and D_R are the diffusion coefficients of oxidized and reduced species respectively.

For quasi-reversible process current value is expressed as a function of $\psi(E)$ [58].

$$I = nFAC_o^* \frac{k_{sh}^o}{\Lambda}\psi(E) \quad \dots\dots\dots\dots\dots\dots\dots\dots\dots2.3$$

where $\psi(E)$ is expressed as

$$\psi(E) = \frac{I}{nFAC_o^* D_o^{1/2}(nF/RT)^{1/2}\upsilon^{1/2}} \quad \dots\dots\dots\dots\dots2.4$$

It is observed that when $\Lambda \geq 10$, the behavior approaches that of a reversible system [59]. For three types of electrode processes, Matsuda and Ayabe [57] suggested following zone boundaries.

- Reversible (Nernstian)

  $k_{sh}^o \geq 0.3\upsilon^{1/2}$ cm s^{-1}

- Quasi-reversible

  $0.3\upsilon^{1/2} \geq k_{sh}^o \geq 2\times10^{-5}\upsilon^{1/2}$ cm s^{-1}

- Totally irreversible

  $k_{sh}^o \leq 2\times10^{-5}\upsilon^{1/2}$ cm s^{-1}

2.2.2 Multi electron transfer processes

Multi-electron transfer process usually takes place in different steps. A two-step mechanism each characterized by its own electrochemical parameters is called an "EE mechanism".

A two step reversible "EE mechanism" is represented as;

$$O + n_1 e \leftrightarrow R_1 \qquad\qquad\qquad (E_1^o)\dots\dots\dots\dots\dots2.5$$

$$R + n_1 e \leftrightarrow R_2 \qquad\qquad (E_2^o)\dots\dots\dots\dots\dots 2.6$$

Each heterogeneous electron transfer step is associated with its own electrochemical parameters i.e., k_{sh}^o and α_i, where $i = 1, 2$ for the 1st and 2nd electron transfer respectively. The value of k_{sh}^o for first reversible electron transfer limiting case can be calculated as [60]:

$$k_{sh} = k_{sh}^o \exp\left[-\alpha 1 F \Delta E^o / 2RT\right]\dots\dots\dots\dots\dots\dots.2.7$$

where

$$\Delta E^o = E_2^o - E_1^o$$

For ΔE^0 greater than 180 mV, shape of wave does not dependent on the relative values of E^0, otherwise shapes of peak and peak currents depend upon ΔE^0 [61]. Based on the value of ΔE^0, we come across different types of cases as shown in the Figure 2.6.

Types of two electron transfer reactions

Case 1: $\Delta E^0 \geq 150$ mV peaks separation

When $\Delta E^0 \geq 150$ mV the EE mechanism is termed as "disproportionate mechanism [62]. Cyclic voltammogram consists of two typical one-electron reduction waves. The heterogeneous electron transfer reaction may simultaneously be accompanied by homogenous electron transfer reaction, which in multi-electron system leads to disproportionation which can be described as:

$$R_1 \rightarrow O + n_1 e \dots\dots\dots\dots\dots\dots\dots\dots\dots\dots2.8a$$

$$R_1 + n_2 e \rightarrow R_2 \dots\dots\dots\dots\dots\dots\dots\dots\dots2.8b$$

$$2R_1 \leftrightarrow O + R_2 \dots\dots\dots\dots\dots\dots\dots\dots\dots\dots2.8c$$

$$k_{disp} = \frac{[O][R_2]}{[R_1]^2} \dots\dots\dots\dots\dots\dots\dots\dots\dots2.9$$

$$\ln k_{disp} = \left[\frac{nF}{RT}\right](E_2^o - E_1^o) \dots\dots\dots\dots\dots\dots\dots2.10$$

Case 2: $\Delta E^0 < 100$ mV ----- Peaks overlapped

In this case, the individual waves merge into one broad distorted wave whose peak height and shape are no longer characteristics of a reversible wave. The wave is broadened

similar to an irreversible wave, but can be distinguished from the irreversible voltammogram, in that the distorted wave does not shift on the potential axis as a function of the scan rate.

Case 3: $\Delta E^0 = 0$ mV ----- Single peak

In this case, in cyclic voltammogram, only a single wave would appear with peak current intermediate between those of a single step one electron and two electron transfer reactions and $E_p - E_p/2 = 56$ mV.
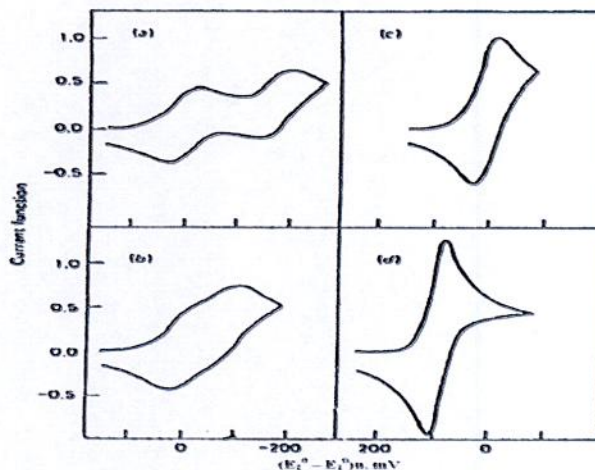
Figure 2.7 Cyclic voltammograms for a reversible two-step system (a) $\Delta E^0 = -180$ mV, (b) $\Delta E^0 = -90$ mV, (c) $\Delta E^0 = 0$ mV, (d) $\Delta E^0 = 180$ mV. (Taken from ref. [63])

Contrary to the convention the direction of the current in these voltammograms has been shown cathodic above the base line and anodic below the base line.

Case 4: $E^0_1 < E^0_2$ ----2nd Reduction is easy than 1st one

If the energy required for the second electron transfer is less than that for the first, one wave is observed, having peak height equal to $2^{3/2}$ times that of a single electron transfer process. In this case, $E_p - E_p/2 = 29$ mV. The effective E^0 for the composite two electron wave is given by $\dfrac{(E^o_1 + E^o_2)}{2}$ as reported in literature [63].

2.3 Pulse techniques

The basis of all pulse techniques is the difference in the rate of decay of the charging and the faradaic currents following a potential step (or pulse). The charging current decays considerably faster than the faradaic current. A step in the applied potential or current represents an instantaneous alteration of the electrochemical system. Analysis of the evolution of the system after perturbation permits deductions about electrode reactions and their rates to be made. The potential step is the base of pulse voltammetry. After applying a pulse of potential, the capacitive current dies away faster than the faradic one and the current is measured at the end of the pulse. This type of sampling has the advantage of increased sensitivity and better characteristics for analytical applications. At solid electrodes there is an additional advantage of discrimination against blocking of the electrode reaction by adsorption [49].

2.3.1 Differential pulse voltammetry (DPV)

The potential wave form for differential pulse voltammetry (DPV) is shown in Figure 2.8. The potential wave form consists of small pulses (of constant amplitude) superimposed upon a staircase wave form. Unlike normal pulse voltammetry (NPV), the current is sampled twice in each Pulse Period (once before the pulse, and at the end of the pulse), and the difference between these two current values is recorded and displayed.
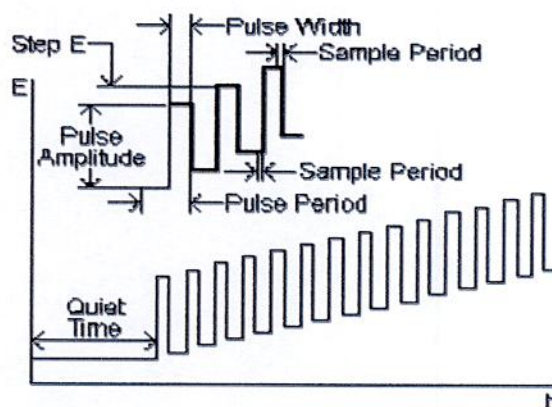
Figure 2.8: Scheme of application of potential

The important parameters for pulse techniques are as follows:

- Pulse amplitude is the height of the potential pulse. This may or may not be constant depending upon the technique.

- Pulse width is the duration of the potential pulse.

- Sample period is the time at the end of the pulse during which the current is measured.

- For some pulse techniques, the pulse period or drop time must also be specified. This parameter defines the time required for one potential cycle, and is particularly significant for polarography (i.e., pulse experiments using a mercury drop electrode), where this time corresponds to the lifetime of each drop (i.e., a new drop is dispensed at the start of the drop time, and is knocked off once the current has been measured at the end of the drop time - note that the end of the drop time coincides with the end of the pulse width).

Quantitative treatments for reversible systems demonstrated that, with only R (positive sign) or only O (negative sign) initially present, the following equation can be written as

$$E_{max} = E_{1/2} \pm \frac{\Delta E}{2} \dots\dots\dots\dots\dots\dots\dots\dots\dots\dots\dots\dots\dots\dots2.11$$

where ΔE is the pulse amplitude.

2.4 Chronoamperometry (CA)

As with all pulsed techniques, chronoamperometry (**CA**) is one of the simplest potential wave forms. The potential is changed instantaneously from the initial potential to the first step potential, and it is held at this value for the first step time. This is a single potential step experiment. In **CA**, the current is monitored as a function of time. The Faradaic current which is due to electron transfer events and is most often the current component of interest decays as described in the Cottrell equation. Since the current is integrated over relatively longer time intervals, CA gives a better signal to noise ratio in comparison to other amperometric technique. A chronoamperometric curve at a disk microelectrode varies from the Cottrell behavior to the steady state current. When potential is stepped to a diffusion-controlled potential domain at the disk electrode with radius, a, in the solution

including electroactive species with the concentration, c^*, and the diffusion coefficient, D, the responding current, I, at the electrolysis time, t, has been expressed as [64, 65]

$$I = 4nFc^*Da\left(1 + 0.71835\tau^{-1/2} + 0.05626\tau^{-3/2} - 0.00646\tau^{-5/2}\right)\ldots.\ 2.12$$

$$I = 4nFc^*Da\left[(\pi/4\tau)^{1/2} + \pi/4 + 0.094\tau^{1/2}\right]\ldots\ldots\ldots\ldots.2.13$$

where $\tau = 4Dt/a^2$. Equations 2.12 and 2.13 are valid for $\tau > 1.44$ and $\tau < 0.82$, respectively. Some expressions for the chronoamperometric curves obtained by finite difference or the related methods [66-71] are closed to Equation (2.12) and (2.13). When τ is small enough to neglect the third term in Equation (2.13), the potential-depending current for the reversible case is expressed by

$$I = \left(\pi^{1/2}nFD^{1/2}a^2t^{-1/2} + \pi nFDa\right)c^*(1+e^{-\varsigma})^{-1}\ldots\ldots.2.14$$

where $\varsigma = (F/RT)(E - E^{0'})$

The Cottrell plot (I vs. $t^{-1/2}$) gives the slope and the intercept, respectively

$$s = \pi^{1/2}nFD^{1/2}a^2c^*(1+e^{-\varsigma})^{-1}$$

$$p = \pi nFDa\, c^*(1+e^{-\varsigma})^{-1}$$

The ratio of the square of the slope to the intercept is

$$s^2/p = nFa^3\, c^*(1+e^{-\varsigma})^{-1}\ \text{ or }\ n\left(1+e^{-\varsigma}\right)^{-1} = s^2/pFa^3\, c^*\ \ldots 2.15$$

This equation does not include D, and hence is the basic equation of evaluating n without knowing D from the chronoamperometric curves.

CHAPTER III

Experimental

During the course of the present work a number of techniques were involved which were in general standard ones. Constant efforts for attaining the ideal conditions for the experiments were always attempted. The thoroughly cleaned glass pieces were dried in electric oven. The smaller pieces of apparatus were dried in electric oven and stored in a desiccator, while larger pieces of apparatus were used directly from the oven.

The electrochemical behavior of paracetamol with different amines such as diethylamine, diisopropylamine in aqueous buffer solution at different pH has been measured using Cyclic Voltammetry (CV) and Differential Pulse Voltammetry (DPV) at glassy carbon (GC), Gold (Au) electrode, platinum electrode (Pt). Details of the instrumentation are given in the following sections. The source of different chemicals, the instruments and brief description of the methods are given below.

3.1 Chemicals

All chemicals, solvents and ligands used in the electrochemical synthesis and analytical work were analytical grade. The used chemicals were-

Sl. No.	Chemicals	Molecular formula	Molar mass	Reported purity	Producer
1.	Diethylamine	$C_4H_{11}N$	73.14	99%	E-Merck, Germany
2.	Diisopropylamine	$C_6H_{15}N$	101.19	99%	Merck, India
3.	Paracetamol	$C_8H_{10}O_2N_2$	151.16	99%	Collected from Gonosastho Pharmaceuticals, Bangladesh
4.	Sodium Acetate	CH_3COONa	136.08	99%	E-Merck, Germany
5.	Potasium Chloride	KCl	74.6	99.5%	E-Merck, Germany
6.	Sodium Di-hydrogen Ortho Phosphate	$NaH_2PO_4.2H_2O$	156.01	98-100%	Loba Chemie Pvt. Ltd., India

Sl. No.	Chemicals	Molecular formula	Molar mass	Reported purity	Producer
7.	Di-sodium Hydrogen Ortho Phosphate	$Na_2HPO_4.2H_2O$	177.99	97-100%	Fisher Scientific UK Ltd.
8.	Sodiun Hydroxide	NaOH	40.0	97%	E-Merck, Germany
9.	Hydrochloric acid	HCl	36.5	37%	Sigma-Aldrich, Germany

3.2 Equipments

During this research work the following instruments were used-

- The electrochemical studies (CV, DPV) were performed with a computer controlled potentiostats/ galvanostats (µstat 400, Drop Sens, Spain)
- A Pyrex glass micro cell with teflon cap
- Glassy carbon (GC)/ Gold (Au)/ Platinum (Pt) as working electrode (BASi, USA)
- Three carbon rods (Local market Dhaka, Bangladesh)
- Ag/ AgCl as reference electrode (BASi, USA)
- Liquid micro size (0.05um) polishing alumina (BAS Inc. Japan)
- Pt wire as counter electrode (Local market, Dhaka, Bangladesh)
- A HR 200 electronic balance with an accuracy of ± 0.0001g was used for weighting and
- A pH meter (pH Meter, Hanna Instruments, Italy) was employed for maintaining the pH of the solutions.

3.3 Cyclic voltammetry (CV)

In several well established electrochemical techniques for the study of electrochemical reactions, we have chosen the CV technique to study and analyze the redox reactions occurring at the polarizable electrode surface. This technique helps us to understand the mechanism of electron transfer reaction of the compounds as well as the nature of adsorption of reactants or products on the electrode surface. CV is often the first experiment performed in an electrochemical study. CV consists of imposing an excitation potential nature on an electrode immersed in an unstirred solution and measuring the current and its potential ranges varies from a few millivolts to hundreds of millivolts per

second in a cycle. This variation of anodic and cathodic current with imposed potential is termed as voltammogram [47].

The technique involves under the diffusion controlled mass transfer condition at a stationary electrode utilizing symmetrical triangular scan rate ranging from 1 mVs^{-1} to hundreds millivolts per second.

In CV the current function can be measured as a function of scan rate. The potential of the working electrode is controlled vs a reference electrode such as Ag/AgCl electrode. The electrode potential is ramped linearly to a more negative potential and then ramped is reversed back to the starting voltage. The forward scan produces a current peak for any analyte that can be reduced through the range of potential scan. The current will increase as the current reaches to the reduction potential of the analyte [72].

The current at the working electrode is monitored as a triangular excitation potential is applied to the electrode. The resulting voltammogram can be analyzed for fundamental information regarding the redox reaction. The potential at the working electrode is controlled vs a reference electrode, Ag/AgCl (standard NaCl) electrode. The excitation signal varies linearly with time. First scan positively and then the potential is scanned in reverse, causing a negative scan back to the original potential to complete the cycle. Signal on multiple cycles can be used on the scan surface. A cyclic voltammogram is plot of response current at working electrode to the applied excitation potential.

3.4 Important features of CV

An electrochemical system containing species 'O' capable of being reversibly reduced to 'R' at the electrode is given by,

$$O + ne^- = R \ldots\ldots\ldots\ldots\ldots\ldots\ldots\ldots\ldots\ldots 3.1$$

Nernst equation for the system is

$$E = E^0 + \frac{0.059}{n} \log \frac{C_0^s}{C_R^s} \ldots\ldots\ldots\ldots\ldots\ldots\ldots 3.2$$

Where,

E = Potential applied to the electrode

E^0 = Standard reduction potential of the couple versus reference electrode

n = Number of electrons in Equation (3.1)

C_0^s = Surface concentration of species 'O'

C_R^s = Surface concentration of species 'R'

A redox couple that changes electrons rapidly with the working electrode is termed as electrochemically reverse couple. The relation gives the peak current i_{pc}

$$i_{pc} = 0.4463\ nFA\ (D\alpha)^{1/2}C \ldots\ldots\ldots\ldots\ldots\ldots 3.3$$

$$\alpha = \left(\frac{nFv}{RT}\right) = \left(\frac{nv}{0.026}\right)$$

Where,

i_{pc} = peak current in amperes

F= Faraday's constant (approximately 96500)

A = Area of the working electrode in cm^2

v= Scan rate in volt/ sec

C= Concentration of the bulk species in mol/L

D= Diffusion coefficient in cm^2 /sec

In terms of adjustable parameters, the peak current is given by the Randless- Sevcik equation,

$$i_{pc} = 2.69 \times 10^5 \times n^{3/2} A D^{1/2} C v^{1/2} \ldots\ldots\ldots\ldots\ldots\ldots 3.4$$

The peak potential E_p for reversible process is related to the half wave potential $E_{1/2}$, by the expression,

$$E_{pc} = E_{1/2} - 1.11\left(\frac{RT}{nF}\right), \quad \text{at } 25^0C \ldots\ldots\ldots\ldots 3.5$$

$$E_{pc} = E_{1/2} - \left(\frac{0.0285RT}{n}\right) \ldots\ldots\ldots\ldots\ldots\ldots 3.6$$

The relation relates the half wave potential to the standard electrode potential

$$E_{1/2} = E^0 - \frac{RT}{nF}\ln\frac{f_{red}}{f_{ox}}\left(\frac{D_{ox}}{D_{ox}}\right)^{1/2}$$

$$E_{1/2} = E^0 - \frac{RT}{nF}\ln\left(\frac{D_{ox}}{D_{red}}\right)^{1/2} \ldots\ldots\ldots\ldots\ldots\ldots 3.7$$

Assuming that the activity coefficient f_{ox} and f_{red} are equal for the oxidized and reduced species involved in the electrochemical reaction.

From Equation (3.6), we have,

$$E_{pa} - E_{pc} = 2.22\left(\frac{RT}{nF}\right) \quad \text{at } 25^0C \dots\dots\dots\dots\dots 3.8$$

$$\text{or } E_{pa} - E_{pc} = \left(\frac{0.059}{n}\right) \quad \text{at } 25^0C \dots\dots\dots\dots \quad 3.9$$

This is a good criterion for the reversibility of electrode process. The value of i_{pa} should be close for a simple reversible couple,

$$i_{pa}/i_{pc} = 1 \dots\dots\dots\dots\dots\dots\dots 3.10$$

And such a system $E_{1/2}$ can be given by,

$$E_{1/2} = \frac{E_{pa} + E_{pc}}{2} \dots\dots\dots\dots\dots 3.11$$

For irreversible processes (those with sluggish electron exchange), the individual peaks are reduced in size and widely separated, Totally irreversible systems are characterized by a shift of the peak potential with the scan rate [73];

$$E_p = E^0 - (RT/\alpha n_a F)[0.78 - \ln(k^0/(D)^{1/2}) + \ln(\alpha n_a F\alpha/RT)^{1/2}]\dots\dots.3.12$$

Where α is the transfer coefficient and n_a is the number of electrons involved in the charge transfer step. Thus E_p occurs at potentials higher than E^0, with the over potential related to k^0 (standard rate constant) and α. Independent of the value k^0, such peak displacement can be compensated by an appropriate change of the scan rate. The peak potential and the half-peak potential (at 25^0 C) will differ by $48/\alpha n$ mV. Hence, the voltammogram becomes more drawn-out as αn decreases.

The peak current, given by

$$i_p = (2.99 \times 10^5)n(\alpha n_a)^{1/2}ACD^{1/2}v^{1/2}\dots\dots\dots.3.13$$

is still proportional to the bulk concentration , but will be lower in height (depending upon the value of α) . Assuming $\alpha = 0.5$, the ratio of the reversible –to– irreversible current peaks is 1.27 (i.e. the peak current for the irreversible process is about 80% of the peak for a reversible one). For quasi- reversible systems (with $10^{-1} > k^0 > 10^{-5}$ cm/s) the current is controlled by both the charge transfer and mass transport [57]. The shape of the cyclic voltammogram is a function of the ratio $k^0 (\pi vnFD/RT)^{1/2}$. As the ratio increases, the process approaches the reversible case. For small values of it, the system exhibits an irreversible behavior. Overall, the voltammograms of a quasi-reversible system are more drawn out and exhibit a larger separation in peak potential compared to a reversible system.

Unlike the reversible process in which the current is purely mass transport controlled, currents due to quasi-reversible process are controlled by a mixture of mass transport and charge transfer kinetics [74, 75]. The process occurs when the relative rate of electron transfer with respect to that of mass transport is insufficient to maintain Nernst equilibrium at the electrode surface.

3.5 Differential pulse voltammetry (DPV)

Differential pulse voltammetry (DPV) is a technique that is designed to minimize background charging currents. The waveform in DPV is a sequence of pulses, where a baseline potential is held for a specified period of time prior to the application of a potential pulse. Current is sampled just prior to the application of the potential pulse. The potential is then stepped by a small amount (typically < 100 mV) and current is sampled again at the end of the pulse. The potential of the working electrode is then stepped back by a lesser value than during the forward pulse such that baseline potential of each pulse is incremented throughout the sequence.

By contrast, in normal pulse voltammetry the current resulting from a series of ever larger potential pulse is compared with the current at a constant 'baseline' voltage. Another type of pulse voltammetry is square wave voltammetry, which can be considered a special type of differential pulse voltammetry in which equal time is spent at the potential of the ramped baseline and potential of the superimposed pulse. The potential wave form consists of small pulses (of constant amplitude) superimposed upon a staircase wave form [76]. Unlike NPV, the current is sampled twice in each pulse Period (once before the pulse, and at the end of the pulse), and the difference between these two current values is recorded and displayed.

3.6 Important features of DPV

Differential pulse voltammetry has these prominence:

i)   Current is sampled just prior to the application of the potential pulse.

ii)   Reversible reactions show symmetrical peaks and irreversible reaction show asymmetrical peaks.

iii)   The peak potential is equal to $E_{1/2}{}^{r}\text{-}\Delta E$ in reversible reactions, and the peak current is proportional to the concentration.

3.7 Chronoamperometry (CA)

Chronoamperometry is an electrochemical technique in which the potential of the working electrode is stepped and the resulting current from faradaic processes occurring at the electrode is monitored as a function of time. This technique has advantage of without knowing a value of a diffusion coefficient [77]. When potential is stepped from a non-reacting domain to E, a Cottrell plot (I vs. $t^{-1/2}$) shows the slope by the linear diffusion.

$$s = \pi^{1/2}nFD^{1/2}a^2c^*$$

together with the intercept for the edge effect

$$p = \pi nFDac^*$$

where a is the radius of the electrode, c^* is the concentration of the electroactive species, D is the diffusion coefficient. The ratio of the square of the slope, s, to the intercept, p, is

$$n = s^2 / pFa^3c^* \ \dots\dots\dots\dots\dots\dots\dots\dots\dots\dots\dots\dots\dots\dots.3.14$$

Since this equation does not include D, values of n can be determined from s and p without knowing D values.

3.8 Computer controlled potentiostats

The main instrument for voltammetry is the Potentiostats/ Galvanostats (µStat 400, DropSens, Spain), which will be applied to the desired potential to the electrochemical cell (i.e. between a working electrode and a reference electrode), and a current-to-voltage converter, which measures the resulting current, and the data acquisition system produces the resulting voltammogram.

3.9 Electrochemical cell

This research work was performed by a three electrode electrochemical cell. The voltammetric cell also contains a Teflon cap. The electrochemical reaction of interest takes place at the working electrode and the electrical current at this electrode due to electron

transfer is termed as faradic current. The counter electrode is driven by the potentiostatic circuit to balance the faradic process at the working electrode with an electron transfer of opposite direction.

3.10 Electrodes

Three types of electrodes are used in this research:

i)   Working electrodes are Glassy carbon (GC) electrode with 3.0 mm diameter disc, Gold (Au) & Platinum (Pt) electrode with 1.6 mm diameter disc and three carbon rods (diameter 6.0 mm)

ii)   Ag/ AgCl (standard NaCl) electrode used as reference electrode from BASi, USA

iii)   Counter electrode is a Pt wire

The working electrode is an electrode on which the reaction of interest is occurring. The reference electrode is a half-cell having a known electrode potential and it keeps the potential between itself and the working electrode. The counter electrode is employed to allow for accurate measurements to be made between the working and reference electrodes.

3.11 Preparation of electrodes

In this study, Glassy carbon (GC), Gold (Au) and Platinum (Pt) electrodes purchase from the BASi, USA are used as working electrode. Electrode preparation includes polishing and conditioning of the electrode. The electrode was polished with 0.05μm alumina powder on a wet polishing cloth. For doing so a part of the cloth was made wet with deionized water and alumina powder was sprinkled over it. Then the electrode was polished by softly pressing the electrode against the polishing surface at least 10 minutes. The electrode surface would look like a shiny mirror after thoroughly washed with deionized water.

3.12 Removing dissolved oxygen from solution

Dissolved oxygen can interfere with observed current response so it is needed to remove it. Experimental solution was indolented by purging for at least 5-10 minutes with 99.99% pure and dry nitrogen gas (BOC, Bangladesh). By this way, traces of dissolved oxygen were removed from the solution.

3.13 Electrode polishing

Materials may be adsorbed to the surface of a working electrode after each experiment. Then the current response will degrade and the electrode surface needs to clean. In this case, the cleaning required is light polishing with 0.05μm alumina powder. A few drops of polish are placed on a polishing pad and the electrode is held vertically and the polish rubbed on in a figure-eight pattern for a period of 30 seconds to a few minutes depending upon the condition of the electrode surface. After polishing the electrode surface is rinsed thoroughly with deionized water.

3.14 Experimental procedure

The electrochemical cell filled with solution 50mL of the experimental solution and the Teflon cap was placed on the cell. The working electrode together with reference electrode and counter electrode was inserted through the holes. The electrodes were sufficiently immersed. The solution system is deoxygenated by purging the nitrogen gas for about 10 minutes. The solution has been kept quiet for 10 seconds. After determining the potential window the voltammogram is taken at various scan rates, pH and concentrations from the Drop View Software.

3.15 Preparation of buffer solutions

Acetate Buffer Solution: To prepare acetate buffer (pH 3.0-5.0) solution definite amount of sodium acetate was dissolved in 0.1M acetic acid in a volumetric flask and the pH was measured. The pH of the buffer solution was adjusted by further addition of acetic acid and / or sodium acetate.

Phosphate Buffer Solution: Phosphate buffer solution (pH 6.0-8.0) was prepared by mixing a solution of 0.1M sodium dihydrogen ortho-phosphate ($NaH_2PO_4.2H_2O$) with a solution of 0.1M disodium hydrogen ortho-phosphate ($Na_2HPO_4.2H_2O$). The pH of the prepared solution was measured with pH meter.

Hydroxide Buffer Solution: To prepare hydroxide buffer (pH 9.0) solution definite amount of sodium hydroxide was dissolved in 0.1M sodium bicarbonate in a volumetric flask. The pH of the prepared solution was measured with pH meter.

Figure 3.1: Experimental setup (Software controlled Potentiostats (µstat 400))

CHAPTER IV

Results and Discussion

The electrochemical behavior of paracetamol in presence of diethylamine and diisopropylamine in buffer solution of different pH has been studied at different scan rates by Cyclic voltammetry (CV), Controlled potential coulometry (CPC), Differential pulse voltammetry (DPV) and Chronoamperometry (CA) techniques using Glassy carbon (GC), Gold (Au) and Platinum (Pt) electrodes. The techniques provide important information regarding nucleophilic substitution reaction of paracetamol with diethylamine, diisopropylamine and their mixtures.

4.1 Electrochemical behavior of Paracetamol

Figure 4.1 shows the cyclic voltammograms of (first cycle) 2 mM paracetamol of GC (3 mm) electrode in buffer solution of pH 7. The voltammogram at the $0.1Vs^{-1}$ scan rate has one anodic peak at 0.46 V and corresponding cathodic peak at 0.04 V versus Ag/AgCl. In the subsequent potential cycles no new anodic or cathodic peak appeared. This can be attributed that paracetamol showed one anodic peak related to its transformation to N-acetyl-*p*-quinoneimine and corresponding cathodic peak related to its transformation to paracetamol from N-acetyl-*p*-quinoneimine (Scheme 1) within a quasi-reversible two-electron transfer process [19]. The anodic and corresponding cathodic peak current ratios are slowly decreased with increasing the scan rates which is tabulated in Table 4.1. It can be also considered as criteria for the stability of *p*-quinoneimine produced at the surface of electrode [78] under the experimental conditions. In other words, any hydroxylation [79-82] or dimerization [83, 84] reactions are too slow that can be observed in the time-scale of cyclic voltammetry [78]. The corresponding peak potentials at different scan rates are tabulated in Table 4.1. The corresponding peak potential difference increases with the increase of scan rate that indicates there is a limitation according to ohomic potential drop or charge transfer kinetics [85].

4.2 Electrochemical behavior of Paracetamol + Diethylamine

Figure 4.2 shows the cyclic voltammograms of (first cycle) only 150 mM diethylamine at GC (3 mm) electrode in buffer solution of pH 7. Pure diethylamine is electrochemically inactive having no redox peaks in the potential range investigated.

Figure 4.3 shows the CV of paracetamol (2 mM) in the presence of diethylamine (150 mM) at Glassy carbon (GC) electrode in the first scan of potential at pH 7. In the first scan of potential, it shows one anodic peak and three cathodic peaks (red line). Two new reduction peaks (C_1 and C_2) appear at - 0.12 V and 0.10 V after the addition of 150 mM diethylamine to the solution at first scan of potential (Figure 4.3). The reduction peaks shifted by the addition of diethylamine. Figure 4.4 shows the CV of paracetamol (2 mM) in the presence of diethylamine (150 mM) in the second scan of potential (red line). In the second scan of potential, it shows three anodic peaks at 0.0 V, 0.33 V and 0.66 V and three cathodic peaks at - 0.13 V, 0.0 V and 0.41V respectively. Upon addition of diethylamine to paracetamol solution, the anodic peak A_3 shifted and new anodic peaks A_1 and A_2 appear. In the second scan of potential (Figure 4.4), new oxidation peak appears at 0.0 V and 0.33 V and new reduction peak appears at -0.13 V and 0.0 V. The newly appearance of A_1 and A_2 & C_1 and C_2 peaks and also shifting of the positions of peaks A_3 and C_3 in the presence of diethylamine indicates that it is due to follow up reaction of paracetamol with diethylamine (Scheme 1). This observation can be explained by considering nucleophilic attack of diethylamine to *p*-quinoneimine. The nucleophilic attack of diethylamine to *p*-quinoneimine reduces the *p*-quinoneimine concentration in reaction layer, consequently the A_3 and C_3 peaks shifted, whereas in the same time produces paracetamol-diethylamine adduct and consequently the peaks A_1 and A_2 & C_1 and C_2 appears. In the first scan of potential, the anodic peak of paracetamol in presence of diethylamine is very similar to only paracetamol (Figure 4.3). But in the second scan of potential the peak current of A_3 (red line) decreases significantly compared with that of only paracetamol (blue line). The peak current ratios in the first and second scan of potential of paracetamol-diethylamine at different scan rate are tabulated in the Table 4.2 and 4.3, respectively. The peak current ratio for the peaks A_2 and A_3 (I_{pa2}/I_{pa3}) increased firstly, which is indicative of a chemical reaction of diethylamine (2) with the *p*-quinoneimine (1a) produced at the surface of electrode. These observations may ascribe the formation of N-(3-(diethylamino)-4-

36

hydroxyphenyl)acetamide or N-(2-(diethylamino)-4-hydroxyphenyl)acetamide through nucleophilic substitution reaction (Scheme 1). If the constituent is such that the potential for the oxidation of product is lower, then further oxidation of the product is lower, the further oxidation and further addition may occur [86]. In the case of paracetamol in presence of diethylamine, the oxidation of diethylamine substituted *p*-quinoneimine is easier than the oxidation of parent paracetamol. This substitution product can also be attacked by diethylamine, however, it was not observed during the voltammetric experiments because of the low activity of *p*-quinoneimine 4 toward 2.

The corresponding peak potential differences (ΔE) in the first and second scan of potential are tabulated in Table 4.2 and 4.3. The peak separation potential increases with the increasing of scan rate that indicates there is a limitation according to ohomic potential drop or charge transfer kinetics [85]. The half wave potentials ($\Delta E_{1/2}$) of paracetamol-diethylamine in aqueous buffer solution at different scan rates are tabulated in Table 4.2. The $\Delta E_{1/2}$ value of paracetamol-diethylamine is $\approx 0.53V$ which is higher than only paracetamol in aqueous buffer solution ($\approx 0.19V$).

4.3 Subsequent cycles of CV of Paracetamol + Diethylamine

Figure 4.5 shows the cyclic voltammograms of the first 15 cycles of 2 mM paracetamol in presence of 150 mM diethylamine of GC (3 mm) electrode in buffer solution of pH 7 for the potential range between - 0.3 V to 1.0 V. The voltammogram at 0.1 Vs^{-1} has one anodic peak at 0.63V and three cathodic peaks at - 0.13 V, 0.02 V and 0.4V when considered the first scan of potential (red line). In the subsequent potential cycles two new anodic peaks appeared at -0.05V and 0.28 V and intensity of the first anodic peak current increases progressively on cycling but the third anodic peak current decreases and shifted positively on cycling. This can be attributed to produce of the paracetamol-diethylamine adduct through nucleophilic substitution reaction in the surface of electrode (Scheme 1). The successive decrease in the height of the paracetamol oxidation and reduction peaks with cycling can be ascribed to the fact that the concentrations of paracetamol-diethylamine adduct formation increased by cycling leading to the decrease of concentration of paracetamol or quinoneimine at the electrode surface. The positive shift of the third anodic peak in the presence of diethylamine is probably due to the formation of

a thin film of product at the surface of the electrode, inhibiting to a certain extent the performance of electrode process. Along with the increase in the number of potential cycles the first and second anodic peak current increased upto 10 cycles and then the peak current almost unchanged with subsequent cycle (Figure 4.5). This may be due to the block of electrode surface by the newly formed species after more cycling.

4.4 Effect of pH of Paracetamol + Diethylamine

The influence of pH on the cyclic voltammogram of paracetamol in presence of diethylamine at GC (3 mm) electrode in the first and second scan of potential was studied at pH from 3 to 9 (Figure 4.6 and 4.7). The voltammetric behavior of 2 mM paracetamol in the presence of 150 mM diethylamine at pH 3-5 shows that no new anodic peak appeared after repetitive cycling, indicating that the reaction between *p*-quinoneimine and diethylamine has not occurred. This can be attributed to the fact that at pH 3-5, the nucleophilic property of amine groups is diminished through protonation (Figure 4.7). In the pH 7, the *p*-quinoneimine undergoes diethylamine attack by the amine through an addition reaction reflected that voltammetric new anodic peaks A_1 and A_2 appeared after repetitive cycling (Figure 4.7). Whereas, in the higher pH range (e.g., pH 9), the cyclic voltammograms of paracetamol show irreversible behavior. It was thus suggested that the oxidation of paracetamol followed by an irreversible chemical reaction with hydroxyl ion, especially in alkaline solutions [87]. However amines in this condition can also act as nucleophiles. The peak position of the redox couple is found to be dependent upon pH.

Figures 4.8 and 4.9 show the plot of oxidation peaks (A_3 and A_2) current, I_p against pH of solution in the second scan of potential. It is seen that the maximum peak current is obtained at pH 7 for the second scan of potential suggested that nucleophilic addition reaction is most favorable in neutral media. Figure 4.10 and 4.11 shows the plot of peak potential, E_p values against pH in the first and second scan of potential. As shown, the peak potential for A_3 peak shifted to the negative potentials by increasing pH. This is expected because of participation of proton in the reaction of paracetamol with diethylamine. From the Figure 4.10, the slopes of the plot was determined graphically as the anodic peaks (41 mV/pH for peak A_3) at 0.1V/s, which is close to the theoretical value (30mV/pH) for two-electron, two-proton transfer process. From the Figure 4.11 the slopes

of the plot was determined graphically as the anodic peaks (37 mV/pH for the peak A_3) at 0.1V/s, which is close to the theoretical value for two-electron, two-proton transfer process. This indicates that both the oxidation of the paracetamol and paracetamol-diethylamine adduct proceeded via the $2e^-/2H^+$ processes. This also suggests that during the reaction not only electron but also proton are released from the paracetamol-diethylamine adduct.

The peak current ratio (I_{pc3}/I_{pa3}) increases with decreasing pH. This can be related to protonation of amine and inactivation of it towards Michael addition reaction with *p*-quinoneimine (**2a**). This suggests that the rate of coupling reaction is pH dependent and enhanced by increasing pH. The peak current of the redox couple also is found to be dependent upon pH (Table 4.4-4.5). At pH 7, the difference between the peak current ratio (I_{pc3}/I_{pa3}) in the presence and absence of paracetamol is maximum. Consequently, in this study buffer solution of pH 7 has been selected as suitable medium for electrochemical study of paracetamol in the presence of diethylamine. This ascribed that the electrochemical oxidation of paracetamol in presence of diethylamine is facilitated in neutral media and hence the rate of electron transfer is faster.

4.5 Effect of scan rate of Paracetamol + Diethylamine

Figures 4.12 and 4.13 show the CV of first and second cycle of 2mM paracetamol in presence of 150mM diethylamine of GC (3mm) electrode in buffer solution (pH 7) at different scan rates. The peak current of both the anodic and the corresponding cathodic peaks increases with the increase of scan rate. The cathodic peaks are shifted towards left and the anodic peaks are to the right direction with increase in scan rate. As can be seen in Figure 4.12 and 4.13, the cathodic peak for reduction of p-quinoneimine is disappeared in the scan rate of 0.05 V/s. By increasing the scan rate, the cathodic peak for reduction of *p*-quinoneimine begins to appear and increase. The anodic and cathodic peak current, peak current ratio and peak potential difference are tabulated in Tables 4.2-4.3.

Figures 4.14 and 4.15 show the plots of the anodic and cathodic net peak currents of 2mM paracetamol + 150mM diethylamine for second cycle against the square-root of the scan rates where the net current means the second peak subtracted from the first one by the scan-stopped method [86]. The nearly proportionality of the anodic and cathodic peaks

suggests that the peak current of the reactant at each redox reaction is controlled by diffusion process [83]. The corresponding peak current ratio (I_{pa3}/I_{pc3}) vs scan rate for a mixture of paracetamol + diethylamine decreases with increasing scan rate firstly and then after 0.2V/s, it is almost unchanged (Figure 4.16, left scale). The anodic peak current ratio (I_{pa2}/I_{pa3}) vs scan rate for a mixture of paracetamol and diethylamine firstly increases and then after 0.25V/s scan rate it decreases slowly (Figure 4.16, right scale). On the other hand, the value of current function ($I_p/v^{1/2}$) was found to be decreased with increasing scan rate (Figure 4.17). The exponential nature of the current function versus the scan rate plot is indicative of an electron transfer-chemical reaction-electron transfer (ECE) mechanism for electrode process [88]. This confirms the reactivity of *p*-quinoneimine (**1a**) towards diethylamine (**2**) firstly increases at slow scan rate and then at higher scan rate it decreases.

The reactivity of paracetamol towards diethylamine is pH and concentration dependent. So the voltammetric behavior of the above systems verified at different pH, concentration and scan rate. Figures 4.18-4.23 show the CV at different scan rate for first and second cycle of 2mM paracetamol in presence of 150mM diethylamine at different pH (3-9). From the figures it is seen that the voltammograms at lower pH (3-5) is irreversible. At lower scan rate the cathodic peak is almost absent, with the increasing of scan rate cathodic peak is appeared. The voltammograms at relatively higher pH (7-9) is quasi-reversible and the formation of adduct is occurred. Figures 4.24-4.29 show the plots of the anodic and cathodic net peak currents against the square-root of the scan rates at the same condition. The nearly proportionality of the anodic and the cathodic peaks for the studied all pH suggests that the peak current of the reactant at each redox reaction is controlled by diffusion process. The peak currents and peak potentials are tabulated in Table 4.6-4.11. Figures 4.30-4.35 show the CV of 2mM paracetamol in presence of 100mM-250mM of diethylamine at different scan rate at pH 7. Figures 4.36-4.41 show the plots of the anodic and cathodic net peak currents against the square-root of the scan rates in same condition. The peak currents and peak potentials are tabulated in Table 4.12-4.17. The nearly proportionality of the anodic and the cathodic peaks for the studied all pH and concentration suggests that the peak current of the reactant at each redox reaction is controlled by diffusion process. Although most of the lines have non zero intercept.

Scheme 1

Step-1:

Acetaminophen or
N-acetyl-p-aminophen or
N-(4-hydroxyphenyl)acetamide

N-acetyl-p-quinoneimine or
N-(4-oxocyclohexa-2,5-dien-1-ylidene)acetamide
1a

Step-2:

diethylamine
2

1a

N-(3-(diethylamino)-4-hydroxyphenyl)acetamide
3

N-(2-(diethylamino)-4-hydroxyphenyl)acetamide

Step-3:

N-(3-(diethylamino)-4-hydroxyphenyl)acetamide

N-(2-(diethylamino)-4-hydroxyphenyl)acetamide
3

(*E*)-*N*-(3-(diethylamino)-4-oxocyclohexa-2,5-dien-1-ylidene)acetamide

(*E*)-*N*-(2-(diethylamino)-4-oxocyclohexa-2,5-dien-1-ylidene)acetamide
4

4.6 Concentration effect of Diethylamine

Figures 4.42 and 4.43 show the variation of voltammogram pattern by the addition of different concentration of diethylamine (100, 150, 200 and 250mM) into fixed concentration of paracetamol (2mM) for the first and second cycle of GC (3mm) electrode at pH 7 and scan rate 0.1V/s. From Figure 4.42 (1st cycle), it is seen that no new anodic

peak appears but two new cathodic peaks (C_1 and C_2) appears. In the second scan of potential the anodic peaks shifted positively and two new anodic peaks appeared upon addition of diethylamine upto 200 mM which suggests the formation of paracetamol-diethylamine adduct (Figure 4.43). The net current intensity of the newly appeared anodic and cathodic peak increases with the increase of diethylamine composition upto ~150 mM of diethylamine (Figure 4.44) where the net current means the peak current is measured from the baseline consideration. After further addition of diethylamine (>150mM), the anodic and cathodic peak current is decreased (Figure 4.44). The nucleophilic substitution reaction of paracetamol in presence of diethylamine was maximum favorable up to 150mM of diethylamine at pH 7 (Figure 4.44). The corresponding peak current ratio (I_{pc3}/I_{pa3}) varies with the concentration of diethylamine. This is related to the increase of the homogenous reaction rate of following chemical reaction between p-quinoneimine **1a** and diethylamine **2** with increasing concentration of diethylamine up to 150mM. At higher concentration of diethylamine (>150mM), the excess electroinactive diethylamine may be deposited on the electrode surface and consequently the peak current decreased.

4.7 Concentration effect of Paracetamol

Figure 4.45 and 4.46 shows the variation of voltammogram by the addition of different concentration of paracetamol (2, 4, 6 and 8mM) into fixed concentration of diethylamine (150mM) for first and second cycle of GC (3mm) electrode at pH 7 and at scan rate 0.1V/s. In Figure 4.46, in contrast, with the addition of different concentration of paracetamol (2, 4, 6 and 8mM) into fixed concentration of diethylamine (150 mM), the anodic peak (A_3) current increases and shifted positively with the increase of paracetamol composition in the second scan of potential. The newly appearing anodic peak (A_2) is remaining at 2-4 mM of paracetamol and then further addition of paracetamol peak A_2 completely disappears (Figure 4.46). Appeared anodic peak disappears at higher concentration of paracetamol ascribed the non-availability of diethylamine for the formation of substitution reaction. Figure 4.47 shows the plots of peak currents against concentration of paracetamol species in the first scan of potential. The relation between paracetamol concentration (2, 4, 6 and 8 mM) and cyclic voltammetric anodic peak current (I_p) is increased for first anodic peak (A_3). With the increase in concentration there is a increase in A_3 peak current, which may be due to the presence of a large amount of electroactive species at higher concentration. Figure 4.48 shows the plots of peak current

for appeared peak A_2 against concentration of paracetamol species in the second scan of potential. In the second scan of potential the appeared anodic peak (A_2) is not occurred at higher concentration (>2mM).

4.8 Effect of electrode materials

Electrochemical properties of paracetamol in absence and presence of diethylamine was examined by different electrodes for example Glassy carbon (GC), Gold (Au) and Platinum (Pt) at different pH. The Cyclic voltammograms of 2 mM paracetamol + 150 mM diethylamine at GC, Au and Pt electrodes in the first and second scan of potential are shown in Figures 4.49-4.50.

The nature of voltammograms, the peak position and current intensity for the studied systems are different for different electrodes although the diameter of GC electrode (3mm) is higher than Au and Pt (1.6mm). The CV at Au electrode is little different from those of the GC and Pt electrodes. In case of GC electrode it shows three anodic and three cathodic peaks for the second scan of potential whereas at Pt electrode it shows two anodic and corresponding two cathodic peaks (Figure 4.50). For the GC electrode in the second cycle of potential two new oxidation and reduction peak appear at lower oxidation potential which can be attributed to the oxidation of adduct formed between the *p*-quinoneimine and diethylamine. Electrochemical properties of paracetamol with diethylamine for example change of pH, concentration, scan rate etc. were studied using Pt and Au electrodes. But among the electrodes, the voltammetric response of GC electrode was better than Pt and Au electrodes in the studied systems.

4.9 Controlled-potential coulometry of Paracetamol + Diethylamine

Controlled-potential coulometry was performed in 1 mM of paracetamol and 75 mM of diethylamine at potential 0.5V in buffer solution pH 7 by using the three carbon rods. The electrolysis progress was monitored by cyclic voltammetry (Figure 4.51). During the course of coulometry the peaks A_2 appeared and the height of the A_2 peak increase proportionally to the advancement of coulometry, parallel to the decrease in height of anodic peak A_3. All anodic and cathodic peaks disappeared after consumption of 4

electrons per paracetamol. These observations allow us to propose the pathway in Scheme 1 for the electro-oxidation of paracetamol (1) in the presence of diethylamine (2). According to our results, it seems that the addition reaction of 2 to *p*-quinoneimine (1a) reaction (2) is faster than other secondary reactions, leading to the intermediate 3. The oxidation of this compound (3) is easier than the oxidation of parent starting molecule (1) by virtue of the presence of electron-donating group. However, no over reaction was observed during the voltammetric experiments because of the low activity of the *p*-quinoneimine 4 toward addition reaction with diethylamine (2).

We have isolated the products (3) originated from paracetamol + diethylamine electro-synthesis process. In the electrosynthesis process small amount of reagent was used for the formation of reaction causing the yield of the product was limited. The product 3 was further confirmed by FTIR in the next section.

4.10 pH effect of DPV of Paracetamol + Diethylamine

Differential pulse voltammetry (DPV) technique was applied to make more clear for paracetamol-diethylamine addition reaction. DPV obtained for 2mM paracetamol in the presence of 150 mM diethylamine in first and second scan at different pH (3-9) was shown in Figures 4.52-4.53, using GC (3mm) electrode (E_{pulse} 0.02V, t_{pulse} 20s and scan rate 0.1V/s). In the buffer solution of pH 7, the voltammogram of paracetamol gave two well-developed wave in the presence of diethylamine at the second scan of potential (Figure 4.53). In pH 7, two new anodic peaks appeared at -0.14V and 0.26V. In pH 3-5 at the second scan of potential the appeared anodic peak A_2 is not found. As can be seen two completely separated anodic peaks with high current intensity are observed in pH 7, which can be attributed to the oxidations of *p*-quinoneimine-diethylamine new compound and *p*-quinoneimine, respectively. This result is consistent with the cyclic voltammetric result.

4.11 Effect of concentration of DPV of Paracetamol + Diethylamine

The effect of concentration of diethylamine on the differential pulse voltammograms of paracetamol was studied. Figures 4.54-4.55 show DPV for 2 mM of paracetamol solution containing buffer (pH 7) in the presence of various concentration of diethylamine from 100 to 250 mM at the surface of GC electrode at the first and second scan of potential. As

indicated in Figure 4.55, there are two separated anodic peaks appeared after addition of diethylamine into paracetamol. In this case, the increasing of the concentration of diethylamine from 100 to 150 mM leads to increasing of appeared anodic peak current. For further increase of concentration from 200 to 250 mM, the first and second anodic peak current decreases gradually. In lower concentration of diethylamine (<150 mM), the nucleophilic substitution reaction take place in comparable degree, whereas increasing the concentration of diethylamine (150 mM) make favorable nucleophilic attack of diethylamine toward *p*-quinoneimine generated at the surface of electrode. For further addition of diethylamine (>150mM) into paracetamol solution, the excess electroinactive diethylamine deposited on the electrode surface and hence the peak current decreases.

In this study comparatively high concentration of diethylamine (100-250mM) was used sequentially to determine the optimum condition for the nucleophilic substitution reaction of paracetamol + diethylamine. As the reaction was occurred at high concentration of nucleophiles, consequently the voltammetric peaks (DPV) for adduct appeared noticeably. In contrast, comparatively low concentration of diethylamine was used arbitrarily by Kiani et al [89], hence the appearing peak was not so prominent.

4.12 Effect of DPV of electrode materials

Figure 4.56 shows the differential pulse voltammograms of 2 mM of paracetamol + 150 mM of diethylamine at different electrodes in buffer solution pH 7 and scan rate 0.1V/s. At GC electrode the all anodic peaks are sharp than another electrodes. So, the reaction easily occurred at the surface of GC electrode.

4.13 Effect of deposition time change of DPV of Paracetamol + Diethylamine

Figure 4.57 shows the DPV of deposition time change (0, 10, 30, 60, 90, 120 and 150s) of 2mM paracetamol + 150mM diethylamine of pH 7. It is seen that the increasing of deposition time from 0 to 10s leads to develop two new peaks. When the deposition time increases 90s, more nucleophilic attack occurs and consequently more paracetamol-diethylamine adducts leads to decreasing in the concentration of *p*-quinoneimine and increasing in the concentration of paracetamol-diethylamine adduct at the surface of electrode. For further increase of deposition time from 90s to 150s, the appeared anodic

peak current decreases may be due to the electro-inactive diethylamine species deposit on the surface of electrode for the long time elapse.

4.14 Spectral analysis of paracetamol + diethylamine

The FTIR spectrum of the vibrational modes of the paracetamol-diethylamine adduct, paracetamol and diethylamine were taken (Figure 4.58). The paracetamol showed the O-H stretching band at 3390 cm^{-1} and N-H stretching band at 3120 cm^{-1}. The diethylamine showed the N-H stretching sharp band at 2965 cm^{-1}. The absorption peaks due to the N-H stretching vibration of diethylamine was disappeared but the paracetamol N-H stretching and O-H stretching at 3390 cm^{-1} was retained for the paracetamol-diethylamine adduct. The finger print region is different for the adduct from pure paracetamol and pure diethylamine.

4.15 Chronoamperometry of paracetamol + diethylamine

The short time chronoamperogram of 2mM paracetamol in presence of 150mM diethylamine in buffer solution in pH 7 at GC electrode is shown in Figures 4.59. The cottrell plots of the background-substracted current for paracetamol-diethylamine fell on straight line as is shown in Figures 4.60. From the Equation 4.1 the values of n (number of transfer electrons) was obtained from the slope and intercept of the cottrell plot. Determination of electron transfer number, n at different stepping potential is very essential for the estimation of redox interaction. When potential is stepped from a non-reacting domain to E, a cottrell plot (I vs $t^{-1/2}$) shows the slope by the linear diffusion

$s = \pi^{1/2} nFD^{1/2} a^2 c*$

together with the intercept for the edge effect

$p = \pi nFDac*$

where a is the radius of the electrode, c* is the concentration of the electroactive species, D is the diffusion coefficient. The ratio of the square of the slope, s, to the intercept, p, is

$n = s^2 / pFa^3 c*$ 4.1

Paracetamol-diethylamine adduct in buffer solution (pH 7), it is seen that total electron transfer numbers is found to be very high. This is may be due to the using of macro electrode.

4.16 Electrochemical behavior of Paracetamol + Diisopropylamine

The electrochemical behavior of paracetamol in the presence of diisopropylamine as nucleophile was studied in details. Figure 4.61 shows the cyclic voltammograms of the first cycle of 2mM paracetamol of GC (3mm) electrode in buffer solution of pH 7. The voltammogram at the $0.5Vs^{-1}$ scan rate has one anodic peak at 0.55V and cathodic peak at -0.15V. In the subsequent potential cycles no new anodic peak appeared. This can be attributed that paracetamol showed one anodic peak related to its transformation to *p*-quinoneimine and corresponding cathodic peak related to its transformation to paracetamol from *p*-quinoneimine (Scheme 2) within two-electron process. The anodic and corresponding cathodic peak current ratios at different scan rates are nearly unity which indicates that the redox reactions are reversible. It can be also considered as criteria for the stability of *p*-quinoneimine produced at the surface of electrode under the experimental conditions.

Figure 4.62 shows the cyclic voltammogram of the first cycle of only 150mM diisopropylamine at GC (3mm) electrode in buffer solution of pH 7. The voltammogram of diisopropylamine is electrochemically inactive having no redox peaks in the potential range investigated.

Figures 4.63-4.64 show the CV of pure paracetamol (blue line), pure diisopropylamine (black line) and paracetamol + diisopropylamine (red line) in the first and second cycle of GC electrode in pH 7 at scan rate 0.5V/s. From Figure 4.63, the CV of paracetamol (2mM) in the presence of diisopropylamine (150mM) in the first scan of potential (red line) shows one anodic and two cathodic peaks. A new reduction peak (C_2) appears at -0.05 V after the addition of 150mM diisopropylamine to the solution at first scan of potential (Figure 4.63). The reduction peak shifted by the addition of diisopropylamine. The peak current decreases significantly compared with the pure paracetamol, which may be due to the addition of paracetamol with diisopropylamine. In the second scan of potential (Figure 4.64) two new oxidation peaks also appear at -0.07V and 0.36V which can be attributed to the oxidation of adduct formed between the *p*-quinoneimine and diisopropylamine according to Scheme 2. In Figure 4.64, the second scan of potential paracetamol with diisopropylamine shows three anodic peaks at -0.07V, 0.36V and 0.68V and corresponding three cathodic peaks at -0.2V, -0.06V and 0.08V, respectively. Upon addition of

diisopropylamine to paracetamol solution, in the first scan of potential the cathodic peak C_3 decreases and new cathodic peak C_1 and C_2 appears. Also, in the second scan of potential a new anodic peak A_1 and A_2 appears and anodic peak A_3 decreases gradually. The newly appearance of A_1 and A_2 & C_1 and C_2 peaks and decreases of A_3 and C_3 peaks and also shifting of the positions of peaks A_3 and C_3 in the presence of diisopropylamine indicates that it is due to follow up reaction of paracetamol with diisopropylamine. This observation can be explained by considering nucleophilic attack of paracetamol to diisopropylamine. The nucleophilic attack of diisopropylamine to *p*-quinoneimine reduces the *p*-quinoneimine concentration in reaction layer, consequently the A_3 and C_3 peaks reduces, whereas in the same time produces paracetamol-diisopropylamine adduct and consequently the peaks A_1 and A_2 & C_1 and C_2 appears. In the first scan of potential, the anodic peak of paracetamol in presence of diisopropylamine is very similar to only paracetamol (Figure 4.63). But in the second scan of potential (Figure 4.64) the peak current of A_3 (red line) decreases significantly compared with that of pure paracetamol (blue line). The peak current ratio for the peaks A_3 and C_3 (I_{pa3}/I_{pc3}) decreased noticeably, which is indicative of a chemical reaction of paracetamol (**2**) with the *p*-quinone (**1a**) produced at the surface of electrode. These observations may ascribe the formation of N-(3-(diisopropylamino)-4-hydroxyphenyl)acetamide   or   N-(2-(diisopropylamino)-4-hydroxyphenyl)acetamide through nucleophilic substitution reaction (Scheme 2). If the constituent is such that the potential for the oxidation of product is lower, then further oxidation of the product is lower, the further oxidation and further addition may occur [86]. In the case of paracetamol in presence of diisopropylamine, the oxidation of paracetamol substituted *p*-quinoneimine is easier than the oxidation of parent paracetamol. This substitution product can also be attacked by diisopropylamine, however, it was not observed during the voltammetric experiments because of the low activity of *p*-quinoneimine **4** toward **2**.

The corresponding peak potential differences (ΔE) in the first and second scan are tabulated in Table 4.18 and 4.19. The peak potential differences are usually independent of scan rate. The peak separation potential increases with the increasing of scan rate that indicates there is a limitation according to ohomic potential drop or charge transfer kinetics [85].

Scheme 2

Step-1:

Acetaminophen or
N-acetyl-p-aminophen or
N-(4-hydroxyphenyl)acetamide

N-acetyl-p-quinoneimine or
N-(4-oxocyclohexa-2,5-dien-1-ylidene)acetamide
1a

Step-2:

diisopropylamine
2

1a

N-(3-(diisopropylamino)-4-
hydroxyphenyl)acetamide
3

N-(2-(diisopropylamino)-4-
hydroxyphenyl)acetamide

Step-3:

N-(3-(diisopropylamino)-4-
hydroxyphenyl)acetamide

N-(2-(diisopropylamino)-4-
hydroxyphenyl)acetamide
3

(*E*)-*N*-(3-(diisopropylam
ino)-4-oxocyclohexa-2,5
-dien-1-ylidene)acetamide
4

(*E*)-*N*-(2-(diisopropylam
ino)-4-oxocyclohexa-2,5
-dien-1-ylidene)acetamide

4.17 Subsequent cycles of CV of Paracetamol + Diisopropylamine

Figure 4.65 shows the cyclic voltammogram of the first 15 cycles of 2mM paracetamol + 150 mM diisopropylamine of GC (3mm) electrode in buffer solution of pH 7 for the potential range between -0.3V to 1.3V. The voltammogram at the $0.5Vs^{-1}$ scan rate has one anodic peak at 0.65V and two cathodic peaks at -0.01V and 0.27V when considered the first scan (blue line). In the subsequent potential cycles two new anodic peaks appeared

and intensity of the first two anodic peaks current increased progressively on cycling but the third anodic peak current decreases and shifted positively on cycling. This can be attributed to produce the paracetamol-diisopropylamine adduct through nucleophilic substitution reaction in the surface of electrode (Scheme 2). The successive decrease in the height of the paracetamol oxidation and reduction peaks with cycling can be ascribed to the fact that the concentrations of paracetamol-diisopropylamine adduct formation increased by cycling leading to the decrease of concentration of paracetamol or quinoneimine at the electrode surface. The positive shift of the third anodic peak in the presence of diisopropylamine is probably due to the formation of a thin film of product at the surface of the electrode, inhibiting to a certain extent the performance of electrode process.

4.18 Effect of pH of paracetamol + diisopropylamine

Cyclic voltammogram of paracetamol in the presence of 150mM diisopropylamine in the first and second cycle was studied by varying pH from 3 to 9 (Figure 4.66 and 4.67). The voltammetric behavior of paracetamol at pH 3-5 in the presence of 150mM diisopropylamine shows that no new anodic peak appeared after repetitive cycling indicating that the reaction between *p*-quinoneimine and diisopropylamine has not occurred. This can be attributed to the fact that at pH 3-5, the nucleophilic property of amine groups is diminished through protonation (Figure 4.67). At the pH 7 the quinoneimine undergoes diisopropylamine attack by the amine through an addition reaction reflected that voltammetric new anodic peak appeared after repetitive cycling. Whereas, in the higher pH range (e.g., pH 9), the cyclic voltammograms of paracetamol show irreversible behavior. In the first cycle of paracetamol + diethylamine shows a new anodic peak at pH 9. This is suggested that the hydroxyl group of basic solution formed adduct with paracetamol so prominently. It was also suggested that the oxidation of paracetamol followed by an irreversible chemical reaction with hydroxyl ion, especially in alkaline solutions [87]. However amines groups in this condition can also act as nucleophiles. The peak position of the redox couple is found to be dependent upon pH.

Figures 4.68 and 4.69 show the plot of oxidation peaks (A$_3$ and A$_2$) current, I_p against pH of solution in the second cycle. It is seen that the maximum peak current of the appeared peak is obtained at pH 7 suggested that nucleophilic addition reaction is most favorable in

neutral media (Figure 4.69). Figure 4.70 shows the plot of peak potential, E_p against pH in the second scan of potential. The peak potential for A_3 peak shifted to the negative potential by increasing of pH. The slope of the plot was determined graphically as the anodic peak (23 mV/pH for peak A_3) at 0.1V/s, which is close to the theoretical value (30mV/pH) for two electron- two proton transfer process. This suggest that during the reaction not only electron but also proton are released from the adduct. The peak current ratio (I_{pc3}/I_{pa3}) increases with decreasing pH. This can be related to protonation of amine and inactivation of it towards addition reaction with *p*-quinoneimine (**2a**). This suggests that the rate of coupling reaction is pH dependent and enhanced by increasing pH. The peak current of the redox couple also is found to be dependent upon pH which is tabulated in Table 4.20-4.21. At pH 7, the difference between the peak current ratio (I_{pc3}/ I_{pa3}) in the presence and absence of paracetamol is maximum. Consequently, in this study buffer solution of pH 7 has been selected as suitable medium for electrochemical study of paracetamol in the presence of diisopropylamine. This ascribed that the electrochemical oxidation of paracetamol in presence of diisopropylamine is facilitated in neutral media and hence the rate of electron transfer is faster.

4.19 Effect of scan rate of paracetamol + diisopropylamine

Figures 4.71 and 4.72 show the CV of first and second cycle of 2mM paracetamol in presence of 150mM diisopropylamine of GC (3mm) electrode in buffer solution (pH 7) at different scan rates. The peak current of both the anodic and the corresponding cathodic peaks increases with the increase of scan rate. The cathodic peaks are shifted towards left and the anodic peaks are to the right direction with increase in scan rate. Figures 4.73 and 4.74 show plots of the anodic and cathodic net peak currents of 2mM paracetamol + 150mM paracetamol for first and second cycle against the square-root of the scan rates where the net current means the second peak subtracted from the first one by the scan-stopped method [86]. The nearly proportionality of the anodic and the cathodic peaks suggests that the peak current of the reactant at each redox reaction is controlled by diffusion process [90]. As can be seen in Figure 4.72, the cathodic peak for reduction of *p*-quinoneimine is disappeared in the scan rate of 0.05 V/s. By increasing the scan rate, the cathodic peak for reduction of *p*-quinoneimine begins to appear and increase.

The corresponding peak current ratio (I_{pa3}/I_{pc3}) vs scan rate for a mixture of paracetamol + diisopropylamine decreases with increasing scan rate firstly and then after 0.45V/s, it is unchanged (Figure 4.75, left scale). The anodic peak current ratio (I_{pa2}/I_{pa3}) vs scan rate for a mixture of paracetamol and diisopropylamine firstly increases and then after 0.4V/s scan rate it is decreased (Figure 4.75, right scale). On the other hand, the value of current function ($I_p/v^{1/2}$) was found to be decreased with increasing scan rate (Figure 4.76). The exponential nature of the current function versus the scan rate plot is indicative of an electron transfer- chemical reaction- electron transfer (ECE) mechanism for electrode process [88]. This confirms the reactivity of *p*-quinoneimine (1a) towards diisopropylamine (2) firstly increases at intermediate scan rate and then at higher scan rates it is unfavorable.

The reactivity of paracetamol towards diisopropylamine is pH and concentration dependent. So the voltammetric behavior of the above systems verified at different pH, concentration and scan rate. Figures 4.77-4.82 show the CV at different scan rate for first and second cycle of 2mM paracetamol in presence of 150mM diisopropylamine at different pH (3-9). Figures 4.83-4.88 show the plots of the anodic and cathodic net peak currents against the square-root of the scan rates at the same condition. The peak currents and peak potentials are tabulated in Table 4.22-4.27. Figures 4.89-4.94 show the CV of 2mM paracetamol in presence of 100mM-250mM of diisopropylamine at different scan rate in pH 7. Figures 4.95-4.100 show the plots of the anodic and cathodic net peak currents against the square-root of the scan rates in same condition. The peak currents and peak potentials are tabulated in Table 4.28-4.33. The nearly proportionality of the anodic and the cathodic peaks for the studied all pH and concentration suggests that the peak current of the reactant at each redox reaction is controlled by diffusion process. Although most of the lines have non zero intercept.

4.20 Concentration effect of diisopropylamine

Figures 4.101 and 4.102 show the variation of voltammogram pattern by the addition of different concentration of diisopropylamine (100, 150, 200 and 250mM) into fixed concentration of paracetamol (2mM) for the first and second scan of potential of GC (3mm) electrode at pH 7 and scan rate 0.5V/s. From Figure 4.101, it is seen that no new anodic peak appears in the first scan of potential. In the second scan of potential the anodic

peaks shifted and a new anodic peak A_2 appeared at ~ 0.38V upon addition of paracetamol which suggests the formation of paracetamol-diisopropylamine adduct (Figure 4.102). The net current intensity of the newly appeared anodic peak increases with the increase of diisopropylamine composition upto ~150 mM of diisopropylamine. After further addition of diisopropylamine (>150 mM), the anodic and cathodic peak current is slightly decreased (Figure 4.102). The nucleophilic substitution reaction of paracetamol in presence of diisopropylamine was maximum favorable up to 150mM of diisopropylamine at pH 7 (Figure 4.104). The corresponding peak current ratio (I_{pc3}/I_{pa3}) varies with the concentration of diisopropylamine. This is related to the increase of the homogenous reaction rate of following chemical reaction between *p*-quinoneimine **1a** and diisopropylamine **2** with increasing concentration of paracetamol upto 150 mM. At higher concentration of diisopropylamine (>150mM), the excess electroinactive diisopropylamine may be deposited on the electrode surface and consequently the peak current decreased.

4.21 Concentration effect of paracetamol

Figures 4.105 and 4.106 show the variation of voltammogram by the addition of different concentration of paracetamol (2, 4, 6 and 8mM) into fixed concentration of diisopropylamine (150mM) for first and second cycle of GC (3mm) electrode at pH 7 and at scan rate 0.5V/s. In Figure 4.106, in contrast, with the addition of different concentration of paracetamol into fixed concentration of diisopropylamine of GC electrode, the anodic peak (A_3) current increases and shifted positively with the increase of paracetamol composition in the second scan of potential. The newly appearing anodic peak (A_2) is remaining at 2mM of paracetamol and then further addition of paracetamol (> 2mM) peak A_0 decreases (Figure 4.106). Appeared anodic peak decreases at higher concentration of paracetamol (> 2mM) ascribed the non-availability of diisopropylamine for the formation of substitution reaction. Figures 4.107-4.109 show the plots of peak currents against concentration of paracetamol species. The relation between paracetamol concentration (2, 4, 6 and 8 mM) and cyclic voltammetric anodic and cathodic peak current (I_p) is linear for anodic peak (A_3) (Figure 4.107 and 4.109). With the increase in concentration there is a gradual linear increase in A_3 peak current, which may be due to the presence of a large amount of electroactive species at higher concentration. The linear dependence of peak

current of paracetamol concentration is depicted from the calibration curve shown in Figure 4.109.

4.22 Effect of electrode materials

Electrochemical characteristics of paracetamol in absence and presence of diisopropylamine was examined by different electrodes like Glassy carbon (GC), Gold (Au) and Platinum (Pt) at different pH. The Cyclic voltammograms of 2 mM paracetamol + 150 mM diisopropylamine at GC, Au and Pt electrodes in the first and second scan of potential are shown in Figure 4.110-4.111.

The nature of voltammograms, the peak position and current intensity for the studied systems are different for different electrodes although the diameter of GC electrode (3mm) is higher than Au and Pt (1.6mm). The CV at Au electrode is different from those of the GC and Pt electrodes. At the Au electrode it shows only single anodic and cathodic peak for the second scan in the potential range was investigated (Figure 4.111). In case of GC electrode it shows two anodic and two cathodic peaks for the second scan of potential whereas at Pt electrode it shows one anodic and corresponding one cathodic peak (Figure 4.111). At GC electrode for the second cycle of potential a new oxidation appears at lower oxidation potential which can be attributed to the oxidation of adduct formed between the *p*-quinoneimine and diisopropylamine. Among the electrodes, the voltammetric response of GC electrode was better than Pt and Au electrodes in the studied systems.

4.23 Controlled-potential coulometry of paracetamol + diisopropylamine

Controlled-potential coulometry was performed in 1 mM of paracetamol and 75 mM of diisopropylamine at 0.5V in buffer solution pH 7 by using the three carbon rods. The electrolysis progress was monitored by cyclic voltammetry (Figure 4.112). During the course of coulometry the peaks A_2 appeared and the height of the A_2 peak increase proportionally to the advancement of coulometry, parallel to the decrease in height of anodic peak A_3. All anodic and cathodic peaks disappeared after consumption of 4 electrons per paracetamol. These observations allow us to propose the pathway in Scheme 2 for the electro-oxidation of paracetamol (1) in the presence of diisopropylamine (2). According to our results, it seems that the addition reaction of 2 to *p*-quinoneimine (1a)

(reaction (2) is faster than other secondary reactions, leading to the intermediate 3. The oxidation of this compound (3) is easier than the oxidation of parent starting molecule (1) by virtue of the presence of electron-donating group. However, no over reaction was observed during the voltammetric experiments because of the low activity of the *p*-quinoneimine 4 toward addition reaction with diisopropylamine (2).

We have isolated the products (3) originated from paracetamol + diisopropylamine electro-synthesis process. In the electro-synthesis process small amount of reagent was used for the formation of reaction causing the yield of the product was limited. The product 3 was further confirmed by FTIR in the next section.

4.24 pH effect of DPV of paracetamol + diisopropylamine

Differential pulse voltammetry (DPV) technique was applied to make more clear for paracetamol-diisopropylamine addition reaction. DPV obtained for 2mM paracetamol in the presence of 150 mM diisopropylamine in first and second scan at different pH (3-9) was shown in Figures 4.113-4.114, using GC (3mm) electrode (E_{pulse} 0.02V, t_{pulse} 20ms and scan rate 0.5V/s). It is observed that the peak position of the DPV of paracetamol + diisopropylamine was shifted. In the buffer solution of pH 7-9, the voltammogram of paracetamol gave two well-developed wave in the presence of diisopropylamine (Figure 4.114) except at pH 9 a new peak appeared in the first cycle (Figure 4.113). In pH 7, a new anodic peak appeared at 0.34V. In pH 3 and 5 at the second scan of potential the appeared anodic peak A_2 is not found. As can be seen two completely separated anodic peaks with high current intensity are observed in pH 7, which can be attributed to the oxidations of *p*-quinoneimine-diisopropylamine new compound and *p*-quinoneimine, respectively.

4.25 Effect of concentration of DPV of paracetamol + diisopropylamine

The effect of concentration of diisopropylamine on the differential pulse voltammograms of paracetamol was studied. Figures 4.115-4.116 show DPV for 2 mM of paracetamol solution containing buffer (pH 7) in the presence of various concentration of diisopropylamine from 100 to 250 mM at the surface of GC electrode at first and second scan of potential. As indicated in Figure 4.116, there are two separated anodic peaks appeared after addition of diisopropylamine into paracetamol. In this case, the increasing

of the concentration of diisopropylamine from 100 to 150 mM leads to increasing of appeared anodic peak current. For further increase of concentration from 200 to 250mM, the first and second anodic peak current decreases gradually. In lower concentration of diisopropylamine (<150 mM), the nucleophilic substitution reaction take place in comparable degree, whereas the concentration of 150 mM diisopropylamine make favorable nucleophilic attack of diisopropylamine toward *p*-quinoneimine generated at the surface of electrode. For further addition of diisopropylamine (>150mM) into paracetamol solution, the excess electroinactive diisopropylamine deposited on the electrode surface and hence the peak current decreases.

In this study comparatively high concentration of diisopropylamine (100-250mM) was used sequentially to determine the optimum condition for the nucleophilic substitution reaction of paracetamol with diisopropylamine. As the reaction was occurred 150 mM diisopropylamine of nucleophiles, consequently the voltammetric peaks (DPV) for adduct appeared noticeably.

4.26 Effect of DPV of electrode materials

Figures 4.117-4.118 show the differential pulse voltammograms of 2 mM of paracetanol + 150 mM of diisopropylamine at different electrodes in buffer solution of pH 7 and scan rate 0.5V/s. At GC electrode all anodic peaks are sharp than another electrodes. So, the reaction easily occurred at the surface of GC electrode.

4.27 Effect of deposition time change of DPV of paracetamol + diisopropylamine

Figure 4.119 shows the DPV of deposition time change (0, 30, 60, 90,120, 150 and 180s) of 2mM paracetamol + 150mM diisopropylamine of pH 7 at GC electrode. It is seen that the increasing of deposition time from 0 to 10s leads to develop two new peaks at -0.08V and 0.33V. When the deposition time increases 30s, more nucleophilic attack occurs and consequently more paracetamol-diisopropylamine adducts leads to decreasing in the concentration of *p*-quinoneimine and increasing in the concentration of paracetamol-diisopropylamine adduct at the surface of electrode. For further increase of deposition time from 30s to 180s, the first anodic peak current increases and second anodic peak current

decreases may be due to the electro-inactive diisopropylamine species deposit on the surface of electrode for the long time elapse.

4.28 Spectral analysis of Paracetamol + diisopropylamine

The FTIR spectrum of the vibrational modes of the paracetamol-diisopropylamine adduct, paracetamol and diisopropylamine were taken (Figure 4.120). The paracetamol showed the O-H stretching band at 3390 cm^{-1} and N-H stretching band at 3120 cm^{-1}. The diisopropylamine showed the N-H stretching sharp band at 2990 cm^{-1}. The absorption peaks due to the N-H stretching vibration of paracetamol was disappeared but the O-H stretching at 3390 cm^{-1} was retained for the paracetamol- diisopropylamine adduct and the finger print region is different for the adduct from pure paracetamol and pure diisopropylamine.

4.29 Chronoamperometry of paracetamol + diisopropylamine

The fast chronoamperogram of 2mM paracetamol in presence of 150mM diisopropylamine in buffer solution in pH 7 at GC electrode is shown in Figures 4.121. The cottrell plots of the background-substracted current for paracetamol- diisopropylamine fell on straight line as is shown in Figures 4.122. Determination of electron transfer number, n at different stepping potential is very essential for the estimation of redox interaction. It is seen that the total electron transfer numbers of paracetamol-diisopropylamine adduct is found to be very high. This is may be due to the effect of big electrode.

4.30 CV of Diisopropylamine + Diethylamine mixture with Paracetamol

Figures 4.123-4.124 show the comparison of CV and DPV at second scan of potential of paracetamol in presence of diisopropylamine, diethylamine and the mixture of diisopropylamine + diethylamine of pH 7 at GC electrode. The cyclic voltammogram of 2 mM paracetamol + 150 mM diisopropylamine shows the appeared anodic peaks at - 0.05 V and 0.33 V and appeared cathodic peaks at - 0.15 V and -0.03 V. The CV of paracetamol (2 mM) in the presence of diethylamine (150 mM) (blue line) in the second

scan of potential at the same condition shows two appeared anodic peaks at -0.05 V and 0.30 V and two appeared cathodic peaks at -0.18 V and -0.05 V (Figure 4.123). Red line shows the CV of paracetamol in presence of diisopropylamine + diethylamine mixture at the same condition. In the mixture two appeared anodic peaks obtained at -0.05 V and 0.44 V. The appeared anodic and cathodic peak current of mixture is lower than that of paracetamol-diethylamine and paracetamol-diisopropylamine.

Table 4.1 : Peak potential (E_p), corresponding peak potential difference (ΔE), half wave potential ($\Delta E_{1/2}$), peak current I_p (μA), corresponding peak current ratio (I_{pa}/I_{pc}) of 2mM paracetamol in aqueous buffer solution (pH 7) at different scan rate

v/Vs⁻¹	E_{pa3} /V	E_{pc3} /V	$\Delta E = E_{pc3} \sim E_{pa3}$	$\Delta E_{1/2}$/V	I_{pa3} /μA	I_{pc3} /μA	I_{pa3}/I_{pc3}
0.05	0.48	-0.10	0.58	0.19	35.77	-7.67	4.66
0.10	0.45	-0.10	0.38	0.26	53.04	-12.07	4.39
0.15	0.47	-0.11	0.46	0.24	64.60	-17.30	3.73
0.20	0.52	-0.13	0.65	0.19	72.85	-25.02	2.91
0.25	0.53	-0.13	0.66	0.20	73.33	-29.12	2.51
0.30	0.55	-0.19	0.74	0.18	74.74	-32.80	2.27
0.35	0.54	-0.18	0.72	0.18	84.64	-38.24	2.21
0.40	0.53	-0.14	0.67	0.19	104.04	-45.91	2.26
0.45	0.58	-0.21	0.79	0.18	91.85	-46.00	1.99

Table 4.2 : Peak potential (E_p), corresponding peak potential difference (ΔE), half wave potential ($\Delta E_{1/2}$), peak current (I_p), corresponding peak current ratio (I_{pa}/I_{pc}) of 150mM diethylamine + 2mM paracetamol in buffer solution (pH 7) of GC electrode at different scan rate (1st cycle)

v/Vs⁻¹	E_{pa3} /V	E_{pc3} /V	E_{pc2} /V	$\Delta E = E_{pa3} \sim E_{pc3}$	$\Delta E_{1/2}$/V	I_{pa3} /μA	I_{pc3} /μA	I_{pc2} /μA	I_{pa3}/I_{pc3}
0.05	0.63	0.44	-0.11	0.19	0.53	27.13	-13.07	-3.39	2.07
0.10	0.62	0.42	-0.11	0.20	0.52	45.27	-15.42	-3.55	2.93
0.15	0.64	0.41	-0.04	0.23	0.52	50.78	-24.11	-3.22	2.10
0.20	0.65	0.39	-0.05	0.26	0.52	59.50	-24.64	-3.35	2.41
0.25	0.67	0.44	-0.05	0.23	0.55	67.17	-20.85	-6.06	3.22
0.30	0.64	0.45	-0.01	0.19	0.54	81.81	-20.31	-6.93	4.02
0.35	0.69	0.50	-0.10	0.19	0.59	76.65	-18.86	-6.42	4.06
0.40	0.67	0.50	-0.06	0.17	0.58	88.07	-24.72	-8.32	3.56
0.45	0.67	0.48	-0.03	0.19	0.57	92.72	-23.00	-8.14	4.03
0.50	0.69	0.48	-0.10	0.21	0.58	95.52	-24.55	-9.69	3.89

Table 4.3 : Peak potential (E_p), corresponding peak potential difference (ΔE), half wave potential ($\Delta E_{1/2}$), peak current (I_p), peak current ratio (I_{pa}/I_{pc}) of 150mM diethylamine + 2mM paracetamol in buffer solution (pH 7) of GC electrode at different scan rate (2nd cycle)

v/Vs⁻¹	E_{pa2}/V	E_{pa3}/V	E_{pc3}/V	E_{pc2}/V	$\Delta E = E_{pa2}\sim E_{pc2}$	$\Delta E = E_{pa3}\sim E_{pc3}$	I_{pa2}/μA	I_{pa3}/μA	I_{pc3}/μA	I_{pc2}/μA	I_{pa2}/I_{pa3}	I_{pa3}/I_{pc3}
0.05	-	0.64	0.49	-	0	0.15	-	25.34	-8.71	-	-	3.90
0.10	0.33	0.66	0.41	-	0.33	0.25	4.16	31.17	-9.85	-3.13	0.13	3.16
0.15	0.32	0.63	0.41	-0.14	0.46	0.22	4.39	35.60	-19.67	-4.74	0.12	1.80
0.20	0.34	0.64	0.47	-0.17	0.51	0.17	7.22	41.61	-21.65	-4.42	0.17	1.92
0.25	0.36	0.67	0.47	-0.18	0.54	0.20	8.60	44.07	-21.57	-3.06	0.19	2.04
0.30	0.34	0.65	0.45	-0.12	0.46	0.20	11.27	48.38	-23.88	-3.67	0.23	2.02
0.35	0.40	0.69	0.52	-0.11	0.51	0.17	8.16	52.88	-23.81	-3.93	0.15	2.22
0.40	0.38	0.69	0.51	-0.19	0.57	0.18	9.16	58.26	-24.09	-4.34	0.15	2.41
0.45	0.37	0.66	0.45	-0.14	0.51	0.21	12.94	58.78	-21.72	-6.52	0.22	2.70
0.50	0.41	0.69	0.48	-0.15	0.56	0.21	12.99	66.45	-22.44	-9.08	0.19	2.96

Table 4.4 : Peak current I_p (μA), peak potential E_p (V) of 150mM diethylamine + 2mM paracetamol of GC electrode at scan rate 0.1V/s in different pH media (1st cycle)

pH	Peak Current I_p (μA)		Peak potential E_p(V)	
	A_3	C_3	A_3	C_3
3	54.71	-	0.65	-
5	43.84	-	0.64	-
7	45.27	-12.42	0.62	0.42
9	36.18	-12.66	0.40	-0.19

Table 4.5: Peak Current I_p (μA), peak potential E_p (V) of 150mM diethylamine + 2mM paracetamol of GC electrode at scan rate 0.1V/s in different pH media (2nd cycle)

pH	Peak Current I_p (μA)			Peak potential E_p (V)		
	A_2	A_3	C_3	A_2	A_3	C_3
3		39.68	-	0.66	-	-
5		34.02	-	0.71	-	-
7	4.16	39.17	-9.85	0.32	0.63	0.48
9		30.89	-	0.44	-	-0.19

Table 4.6 : Peak potential (E_p), corresponding peak potential difference (ΔE), peak current (I_p), corresponding peak current ratio (I_{pa}/I_{pc}) of 150mM diethylamine + 2mM paracetamol in buffer solution (pH 3) of GC electrode at different scan rate (1st cycle)

v/Vs^{-1}	E_{pa3}/V	E_{pc3}/V	$\Delta E=E_{pa3}\sim E_{pc3}$	I_{pa3}/μA	I_{pc3}/μA	I_{pa3}/I_{pc3}
0.05	0.65	-	0.65	38.35	-	-
0.10	0.65	0.28	0.35	54.71	-	-
0.15	0.66	0.28	0.36	62.35	-	-
0.20	0.67	0.30	0.37	75.82	-	-
0.25	0.68	0.20	0.47	83.83	-3.45	22.06
0.30	0.69	0.21	0.51	83.60	-7.12	11.03
0.35	0.68	0.13	0.58	85.09	-4.25	18.01
0.40	0.71	0.15	0.58	104.32	-4.08	21.82
0.45	0.69	0.09	0.46	107.13	-3.32	27.28
0.50	0.71	0.12	0.60	109.00	-7.03	14.17

Table 4.7 : Peak potential (E_p), corresponding peak potential difference (ΔE), peak current (I_p), corresponding peak current ratio (I_{pa}/I_{pc}) of 150mM diethylamine + 2mM paracetamol in buffer solution (pH 3) of GC electrode at different scan rate (2nd cycle)

v/Vs^{-1}	E_{pa3}/V	E_{pc3}/V	$\Delta E = E_{pa3} \sim E_{pc3}$	I_{pa3}/μA	I_{pc3}/μA	I_{pa3}/I_{pc3}
0.05	0.66	0.05	0.61	28.51	-11.38	2.50
0.10	0.66	0.20	0.46	43.84	-12.66	3.46
0.15	0.67	0.20	0.47	58.07	-17.79	3.26
0.20	0.68	0.22	0.46	62.73	-23.72	2.64
0.25	0.69	0.24	0.45	72.76	-28.08	2.59
0.30	0.71	0.18	0.53	75.23	-33.85	2.22
0.35	0.72	0.12	0.60	83.67	-35.68	2.34
0.40	0.71	0.11	0.60	85.72	-39.71	2.15
0.45	0.70	0.14	0.56	89.04	-41.00	2.17
0.50	0.71	0.12	0.59	90.20	-44.54	2.02

Table 4.8: Peak potential (E_p), corresponding peak potential difference (ΔE), half wave potential ($\Delta E_{1/2}$), peak current (I_p), corresponding peak current ratio (I_{pa}/I_{pc}) of 150mM diethylamine + 2mM paracetamol in buffer solution (pH 5) of GC electrode at different scan rate (1st cycle)

v/Vs^{-1}	E_{pa3}/V	E_{pc3}/V	$\Delta E = E_{pc3} \sim E_{pa3}$	$\Delta E_{1/2}$/V	I_{pa3}/μA	I_{pc3}/μA	I_{pa3}/I_{pc3}
0.05	0.64		0.64	0.32	28.51	-7.38	3.86
0.10	0.70		0.70	0.35	43.84	-12.66	3.46
0.15	0.64		0.64	0.32	58.07	-17.79	3.26
0.20	0.71		0.71	0.35	62.73	-23.72	2.64
0.25	0.67		0.67	0.33	72.76	-39.08	1.86
0.30	0.68		0.68	0.34	75.23	-31.85	2.36
0.35	0.66		0.66	0.33	83.67	-35.68	2.34
0.40	0.72	-0.02	0.74	0.35	85.72	-42.66	2.00
0.45	0.74	-0.01	0.75	0.36	89.04	-44.30	2.00
0.50	0.73	0.00	0.73	0.36	90.20	-47.48	1.89

Table 4.9: Peak potential (E_p), corresponding peak potential difference (ΔE), half wave potential ($\Delta E_{1/2}$), peak current (I_p), corresponding peak current ratio (I_{pa}/I_{pc}) of 250mM diethylamine + 2mM paracetamol in buffer solution (pH 5) of GC electrode at different scan rate (2nd cycle)

v/Vs^{-1}	E_{pa3}/V	E_{pc3}/V	$\Delta E = E_{pc3} \sim E_{pa3}$	$\Delta E_{1/2}$/V	I_{pa3}/μA	I_{pc3}/μA	I_{pa3}/I_{pc3}
0.05	0.68	-	0.68	0.28	25.52	-	-
0.10	0.71	-	0.71	0.29	34.02	-	-
0.15	0.65	-	0.65	0.28	47.62	-	-
0.20	0.72	-	0.72	0.28	49.72	-	-
0.25	0.67	-	0.67	0.29	65.10	-	-
0.30	0.68	-	0.68	0.29	67.16	-	-
0.35	0.67	-	0.67	0.30	74.59	-	-
0.40	0.73	-0.01	0.74	0.29	65.60	-13.39	4.89
0.45	0.74	-0.02	0.76	0.29	77.28	-13.02	5.93
0.50	0.73	0.00	0.73	0.29	79.03	-10.05	7.86

Table 4.10: Peak potential (E_p), corresponding peak potential difference (ΔE), half wave potential ($\Delta E_{1/2}$), peak current (I_p), corresponding peak current ratio (I_{pa}/I_{pc}) of 150mM diethylamine + 2mM paracetamol in buffer solution (pH 9) of GC electrode at different scan rate (1st cycle)

v/Vs^{-1}	E_{pa3}/V	E_{pc3}/V	$\Delta E = E_{pc3} \sim E_{pa3}$	$\Delta E_{1/2}$/V	I_{pa3}/μA	I_{pc3}/μA	I_{pa3}/I_{pc3}
0.05	0.38	-0.08	0.46	0.15	25.72	-7.75	3.31
0.10	0.40	-0.11	0.51	0.14	36.18	-14.95	2.42
0.15	0.43	-0.13	0.56	0.15	46.14	-21.38	2.15
0.20	0.41	-0.11	0.52	0.15	56.01	-25.02	2.23
0.25	0.41	-0.09	0.50	0.16	60.35	-29.72	2.03
0.30	0.40	-0.06	0.46	0.17	67.31	-36.47	1.84
0.35	0.44	-0.14	0.58	0.15	71.72	-37.02	1.93
0.40	0.41	-0.09	0.50	0.16	79.59	-42.59	1.86
0.45	0.43	-0.10	0.53	0.16	73.17	-41.39	1.76
0.50	0.45	-0.11	0.56	0.17	80.03	-47.72	1.67

Table 4.11: Peak potential (E_p), corresponding peak potential difference (ΔE), half wave potential ($\Delta E_{1/2}$), peak current (I_p), corresponding peak current ratio (I_{pa}/I_{pc}) of 150mM diethylamine + 2mM paracetamol in buffer solution (pH 9) of GC electrode at different scan rate (2nd cycle)

v/Vs^{-1}	E_{pa3}/V	E_{pc3}/V	$\Delta E = E_{pc3} \sim E_{pa3}$	$\Delta E_{1/2}/V$	$I_{pa3}/\mu A$	$I_{pc3}/\mu A$	I_{pa3}/I_{pc3}
0.05	0.43	-0.09	0.52	0.17	22.55	-7.38	3.05
0.10	0.44	-0.19	0.63	0.12	30.89	-12.66	2.43
0.15	0.47	-0.14	0.61	0.16	37.64	-17.79	2.11
0.20	0.45	-0.12	0.57	0.16	43.86	-23.72	1.84
0.25	0.43	-0.11	0.54	0.16	51.26	-39.08	1.31
0.30	0.41	-0.08	0.49	0.16	58.29	-31.85	1.83
0.35	0.49	-0.16	0.65	0.16	59.04	-35.68	1.65
0.40	0.42	-0.09	0.51	0.16	67.37	-42.66	1.57
0.45	0.44	-0.12	0.56	0.16	62.60	-44.30	1.41
0.50	0.46	-0.13	0.59	0.16	64.36	-47.48	1.35

Table 4.12: Peak potential (E_p), corresponding peak potential difference (ΔE), half wave potential ($\Delta E_{1/2}$), peak current Ip (μA), corresponding peak current ratio (I_{pa}/I_{pc}) of 100mM diethylamine and 2mM paracetamol in buffer solution (pH 7) at GC electrode and at different scan rate (1st cycle)

v/Vs^{-1}	E_{pa3}/V	E_{pc3}/V	$\Delta E = E_{pa3} \sim E_{pc3}$	$\Delta E_{1/3}/V$	$I_{pa3}/\mu A$	$I_{pc3}/\mu A$	I_{pa3}/I_{pc3}
0.05	0.59	-0.18	0.77	0.20	27.08	-6.89	3.93
0.10	0.63	-0.19	0.82	0.22	38.49	-7.46	5.15
0.15	0.64	-0.19	0.83	0.22	47.06	-10.50	4.48
0.20	0.66	-0.19	0.85	0.23	48.01	-6.68	7.18
0.25	0.62	-0.03	0.65	0.29	70.43	-12.70	5.54
0.30	0.65	-0.06	0.71	0.29	63.86	-12.30	5.19
0.35	0.66	-0.08	0.74	0.29	74.34	-16.61	4.47
0.40	0.66	-0.11	0.77	0.27	76.56	-18.40	4.16
0.45	0.68	-0.12	0.80	0.28	75.50	-17.55	4.30
0.50	0.63	-0.04	0.67	0.29	81.82	-22.15	3.69

Table 4.13: Peak potential (E_p), corresponding peak potential difference (ΔE), peak current (I_p), peak current ratio (I_{pa}/I_{pc}) of 100mM diethylamine + 2mM paracetamol in buffer solution (pH 7) of GC electrode at different scan rate (2nd cycle)

v/Vs^{-1}	E_{pa3}/V	E_{pa2}/V	E_{pc3}/V	E_{pc2}/V	$\Delta E = E_{pa3}\sim E_{pc1}$	$\Delta E = E_{pa2}\sim E_{pc2}$	$I_{pa2}/\mu A$	$I_{pa3}/\mu A$	$I_{pc3}/\mu A$	$I_{pc2}/\mu A$	I_{pa3}/I_{pc3}	I_{pa2}/I_{pa3}
0.05	0.61			-0.16	0.61	0.16		24.39	-10.58		2.305	0
0.10	0.64			-0.19	0.64	0.19		33.05	-11.48		2.87	0
0.15	0.66			-0.20	0.66	0.20		38.06	-9.07		4.19	0
0.20	0.67	0.38			0.67	0.38	5.74	41.24				0.13
0.25	0.63	0.37			0.63	0.37	9.14	43.06				0.21
0.30	0.66	0.38	0.48	-0.18	0.18	0.56	10.08	44.48	-18.79	-10.07	2.36	0.22
0.35	0.67	0.39	0.48	-0.19	0.19	0.58	12.37	51.79	-18.10	-9.11	2.86	0.23
0.40	0.67	0.39	0.44	-0.10	0.23	0.49	15.19	63.70	-24.11	-12.56	2.64	0.23
0.45	0.68	0.40	0.52		0.16	0.40	13.57	63.55				0.21

Table 4.14 : Peak potential (E_p), corresponding peak potential difference (ΔE), half wave potential ($\Delta E_{1/2}$), peak current (I_p), corresponding peak current ratio (I_{pa}/I_{pc}) of 200mM diethylamine + 2mM paracetamol in buffer solution (pH 7) of GC electrode at different scan rate (1st cycle)

v/Vs^{-1}	E_{pa3}/V	E_{pc3}/V	E_{pc2}/V	$\Delta E = E_{pa3}\sim E_{pc3}$	$\Delta E_{1/2}/V$	$I_{pa3}/\mu A$	$I_{pc3}/\mu A$	$I_{pc2}/\mu A$	I_{pa3}/I_{pc3}
0.05	0.63	-0.18	0.49	0.81	0.22	21.63	-26.37	-6.39	0.82
0.10	0.63	-0.16	0.49	0.79	0.23	32.87	-26.74	-7.62	1.22
0.15	0.66	-0.09	0.46	0.75	0.28	42.10	-21.67	-12.52	1.94
0.20	0.65	-0.07	0.49	0.72	0.29	50.06	-19.28	-11.96	2.59
0.25	0.65	-0.04	0.49	0.69	0.30	60.29	-22.43	-13.15	2.68
0.30	0.66	-0.08	0.47	0.74	0.29	62.17	-29.12	-17.88	2.13
0.35	0.68	-0.11	0.48	0.79	0.28	66.76	-24.51	-16.13	2.72
0.40	0.68	-0.13	0.49	0.81	0.27	64.55	-33.41	-18.43	1.93
0.45	0.68	-0.13	0.47	0.81	0.27	65.03	-32.88	-18.95	1.97
0.50	0.68	-0.15	0.47	0.83	0.26	77.33	-38.86	-15.75	1.98

Table 4.15: Peak potential (E_p), corresponding peak potential difference (ΔE), half wave potential ($\Delta E_{1/2}$), peak current (I_p), corresponding peak current ratio (I_{pa}/I_{pc}) of 200mM diethylamine + 2mM paracetamol in buffer solution (pH 7) of GC electrode at different scan rate (2nd cycle)

v/Vs^{-1}	E_{pa2}/V	E_{pa3}/V	E_{pc3}/V	$\Delta E=E_{pa3}\sim E_{pc3}$	$I_{pa2}/\mu A$	$I_{pa3}/\mu A$	$I_{pc3}/\mu A$	I_{pa3}/I_{pc3}
0.05		0.65	-0.18	0.83		15.36	-5.04	3.04
0.10	0.36	0.63	-0.19	0.82	2.06	25.65	-8.66	2.96
0.15	0.38	0.66	-0.11	0.77	3.78	28.68	-10.99	2.60
0.20	0.37	0.65	-0.10	0.75	8.02	33.90	-15.86	2.13
0.25	0.37	0.65	-0.07	0.72	11.33	36.30	-22.17	1.63
0.30	0.38	0.66	-0.08	0.74	12.46	39.24	-26.98	1.45
0.35	0.43	0.68	-0.13	0.81	11.26	35.91	-22.97	1.56
0.40	0.41	0.68	-0.12	0.80	16.85	38.50	-28.35	1.35
0.45	0.42	0.69	-0.13	0.82	14.59	45.65	-32.09	1.42
0.50	0.44	0.69	-0.16	0.85	16.42	46.73	-30.05	1.55

Table 4.16 : Peak potential (E_p), corresponding peak potential difference (ΔE), half wave potential ($\Delta E_{1/2}$), peak current (I_p), corresponding peak current ratio (I_{pa}/I_{pc}) of 250mM diethylamine + 2mM paracetamol in buffer solution (pH 7) of GC electrode at different scan rate (1st cycle)

v/Vs^{-1}	E_{pa3}/V	E_{pc3}/V	$\Delta E=E_{pa3}\sim E_{pc3}$	$I_{pa3}/\mu A$	$I_{pc3}/\mu A$	I_{pa3}/I_{pc3}
0.05	0.61	-0.15	0.76	25.93	-8.46	3.06
0.10	0.66	-0.19	0.85	35.03	-2.45	14.29
0.15	0.61	-0.08	0.69	43.78	-14.83	2.95
0.20	0.63	-0.05	0.68	49.26	-16.00	3.07
0.25	0.66	0.01	0.65	52.5	-16.56	3.17
0.30	0.64	-0.09	0.73	50.34	-21.89	2.29
0.35	0.63	0.02	0.61	65.1	-23.82	2.73
0.40	0.63	0.03	0.60	73.94	-22.23	3.32
0.45	0.70	-0.15	0.85	77.91	-22.23	3.50
0.50	0.66	-0.08	0.74	83.29	-22.32	3.73

Table 4.17 : Peak potential (E_p), corresponding peak potential difference (ΔE), peak current I_p (μA), corresponding peak current ratio (I_{pa}/I_{pc}) of 250mM diethylamine + 2mM paracetamol in buffer solution (pH 7) of GC electrode at different scan rate (2nd cycle)

v/Vs^{-1}	E_{pa2}/V	E_{pa3}/V	E_{pc3}/V	E_{pc2}/V	$\Delta E = E_{pc2} \sim E_{pa2}$	$\Delta E = E_{pc3} \sim E_{pa3}$	$I_{pa2}/\mu A$	$I_{pa3}/\mu A$	$I_{pc3}/\mu A$	$I_{pc2}/\mu A$	I_{pa2}/I_{pa3}	I_{pa3}/I_{pc3}
0.05		0.63		-0.17	0.17	0.63		21.66	-8.37			-2.58
0.10		0.65		-0.17	0.17	0.65		25.44				
0.15	0.33	0.61	0.07	-0.16	0.49	0.54	6.96	41.58	-8.59	-4.22	0.16	-4.84
0.20	0.34	0.63	0.06	-0.16	0.50	0.57	7.85	43.83	-11.65	-4.22	0.17	-3.76
0.25	0.36	0.65	0.04	-0.17	0.53	0.61	10.95	45.23	-12.68	-3.23	0.24	-3.56
0.30	0.39	0.65	-0.07		0.39	0.72	14.67	47.97	-14.02		0.30	-3.42
0.35	0.37	0.64	0.00		0.37	0.64	15.08	48.68	-17.50		0.30	-2.78
0.40	0.36	0.63	0.03		0.36	0.60	15.96	49.92	-23.36		0.31	-2.13
0.45	0.45	0.70	-0.17		0.45	0.87	17.58	50.71	-17.22		0.34	-2.94
0.50	0.40	0.67	-0.09		0.40	0.76	19.43	52.00	-19.69		0.37	-2.64

Table 4.18 : Peak potential (E_p), corresponding peak potential difference (ΔE), peak current (I_p), corresponding peak current ratio (I_{pa}/I_{pc}) of 150mM diisopropylamine + 2mM paracetamol in buffer solution (pH 7) of GC electrode at different scan rate (1st cycle)

v/Vs^{-1}	E_{pa3}/V	E_{pc3}/V	$\Delta E = E_{pc3} \sim E_{pa3}$	$I_{pa3}/\mu A$	$I_{pc3}/\mu A$	I_{pa3}/I_{pc3}
0.05	0.65	-	-	18.99	-	-
0.10	0.68	-	-	45.69	-	-
0.15	0.67	0.10	0.57	49.07	-8.59	5.71
0.20	0.67	0.14	0.53	66.60	-11.65	5.71
0.25	0.67	0.14	0.53	69.39	-12.68	5.47
0.30	0.70	0.06	0.64	65.53	-14.02	4.67
0.35	0.65	0.12	0.53	75.89	-17.50	4.33
0.40	0.69	0.11	0.58	85.84	-23.36	3.67
0.45	0.68	0.10	0.58	62.09	-17.22	3.60
0.50	0.73	0.06	0.67	85.40	-19.69	4.33

67

Table 4.19: Peak potential (E_p), corresponding peak potential difference (ΔE), peak current (I_p), corresponding peak current ratio (I_{pa}/I_{pc}) of 150mM diisopropylamine + 2mM paracetamol in buffer solution (pH 7) of GC electrode at different scan rate (2nd cycle)

v/Vs^{-1}	E_{pa2} /V	E_{pa3} /V	E_{pc3} /V	$\Delta E = E_{pc3} \sim E_{pa3}$	I_{pa2} /μA	I_{pa3} /μA	I_{pc3} /μA	I_{pa3}/ I_{pc3}
0.05	-	0.65	-	0.65	-	32.08	-1.10	29.16
0.10	-	0.68	-	0.68	-	38.14	-2.19	17.41
0.15	-	0.68	0.04	0.64	-	40.58	-2.72	14.91
0.20	-	0.66	0.09	0.57	-	50.01	-2.47	20.24
0.25	0.36	0.67	0.04	0.63	4.25	53.31	-3.45	15.45
0.30	0.45	0.71	0.04	0.67	5.27	45.54	-7.12	7.80
0.35	0.37	0.68	0.09	0.59	6.48	56.95	-4.25	13.40
0.40	0.38	0.69	0.08	0.61	5.27	61.24	-4.08	15.00
0.45	0.38	0.68	0.10	0.58	7.02	55.06	-3.32	19.59
0.50	0.44	0.72	0.10	0.62	13.53	70.71	-7.03	10.05

Table 4.20 : Peak Current I_p (μA), peak potential E_p (V) of 150mM diisopropylamine + 2mM paracetamol of GC electrode at scan rate 0.1V/s in different pH media (1st cycle)

pH	Peak Current I_p (μA)		Peak potential E_p (V)	
	A_2	C_3	A_2	C_3
3		99.69		0.70
5		106.78		0.67
7		85.40		0.73
9	22.45	60.95	0.38	0.68

Table 4.21 : Peak Current I_p (μA), peak potential E_p (V) of 150mM diisopropylamine + 2mM paracetamol of GC electrode at scan rate 0.1V/s in different pH media (2nd cycle)

pH	Peak Current I_p (μA)		Peak potential E_p (μA)	
	A_2	C_3	A_2	C_3
3		91.65		0.70
5		97.65		0.68
7	13.53	70.71	0.44	0.72
9	11.08	56.04	0.38	0.68

Table 4.22 : Peak potential (E_p), corresponding peak potential difference (ΔE), peak current (I_p), corresponding peak current ratio (I_{pa}/I_{pc}) of 150mM diisopropylamine + 2mM paracetamol in buffer solution (pH 3) of GC electrode at different scan rate (1st cycle)

v/Vs^{-1}	E_{pa3} /V	E_{pc3} /V	$\Delta E=E_{pc3}\sim E_{pa3}$	I_{pa3}/μA	I_{pc3}/μA	I_{pa3}/ I_{pc3}
0.05	0.66	-	0.66	33.31	-	-
0.10	0.66	0.28	0.38	61.94	-	-
0.15	0.67	0.28	0.39	55.06	-	-
0.20	0.67	0.30	0.37	69.98	-	-
0.25	0.68	0.20	0.48	76.11	-3.45	22.06
0.30	0.68	0.21	0.47	78.55	-7.12	11.03
0.35	0.70	0.13	0.57	76.58	-4.25	18.01
0.40	0.70	0.15	0.55	97.06	-4.08	21.82
0.45	0.71	0.09	0.62	90.60	-3.32	27.28
0.50	0.70	0.12	0.58	99.66	-7.03	14.17

Table 4.23 : Peak potential (E_p), corresponding peak potential difference (ΔE), peak current I_p (μA), corresponding peak current ratio (I_{pa}/I_{pc}) of 150mM diisopropylamine + 2mM paracetamol in buffer solution (pH 3) of GC electrode at different scan rate (2nd cycle)

v/Vs^{-1}	E_{pa3}/V	E_{pc3}/V	$\Delta E = E_{pc3} \sim E_{pa3}$	I_{pa3}/μA	I_{pc3}/μA	I_{pa3}/I_{pc3}
0.05	0.66	0.05	0.61	28.59	-	-
0.10	0.66	0.20	0.46	39.68	-9.67	5.14
0.15	0.67	0.20	0.47	47.54	-11.63	3.83
0.20	0.68	0.22	0.45	56.96	-15.37	3.70
0.25	0.69	0.24	0.44	65.76	-19.34	3.34
0.30	0.71	0.18	0.50	68.77	-23.45	2.83
0.35	0.72	0.12	0.57	64.90	-27.00	2.58
0.40	0.71	0.11	0.58	82.40	-29.23	3.00
0.45	0.70	0.14	0.58	92.57	-33.11	2.42
0.50	0.71	0.12	0.58	82.93	-35.12	2.60

Table 4.24 : Peak potential (E_p), corresponding peak potential difference (ΔE), peak current I_p (μA), corresponding peak current ratio (I_{pa}/I_{pc}) of 150mM diisopropylamine + 2mM paracetamol in buffer solution (pH 5) of GC electrode at different scan rate (1st cycle)

v/Vs^{-1}	E_{pa3}/V	E_{pc3}/V	$\Delta E = E_{pc3} \sim E_{pa3}$	I_{pa3}/μA	I_{pc3}/μA	I_{pa3}/I_{pc3}
0.05	0.68	-	-	30.29	-	-
0.10	0.68	0.09	0.59	44.03	-2.52	17.47
0.15	0.66	0.20	0.46	57.12	-5.35	10.67
0.20	0.66	0.23	0.43	69.01	-8.03	8.59
0.25	0.66	0.16	0.50	75.36	-7.82	9.63
0.30	0.67	0.14	0.53	83.62	-10.81	7.73
0.35	0.66	0.16	0.50	91.84	-11.97	7.67
0.40	0.67	0.18	0.49	98.08	-13.79	7.11
0.45	0.66	0.19	0.47	102.67	-16.20	6.33
0.50	0.67	0.14	0.53	106.78	-15.90	6.58

Table 4.25: Peak potential (E_p), corresponding peak potential difference (ΔE), peak current I_p (μA), corresponding peak current ratio (I_{pa}/I_{pc}) of 150mM diisopropylamine + 2mM paracetamol in buffer solution (pH 5) of GC electrode at different scan rate (2nd cycle)

v/Vs^{-1}	E_{pa3}/V	E_{pc3}/V	$\Delta E = E_{pc3} \sim E_{pa3}$	I_{pa3}/μA	I_{pc3}/μA	I_{pa3}/I_{pc3}
0.05	0.70		0.70	24.04	-	-
0.10	0.69	0.10	0.59	34.44	-3.95	8.71
0.15	0.67	0.18	0.49	47.93	-4.27	11.22
0.20	0.66	0.19	0.47	58.71	-6.39	9.18
0.25	0.67	0.17	0.50	66.12	-7.41	8.92
0.30	0.67	0.15	0.52	73.74	-10.09	7.30
0.35	0.67	0.17	0.50	83.49	-12.52	6.66
0.40	0.67	0.18	0.49	88.33	-14.24	6.20
0.45	0.67	0.17	0.50	93.92	-14.75	6.36
0.50	0.68	0.15	0.53	97.65	-15.67	6.23

Table 4.26: Peak potential (E_p), corresponding peak potential difference (ΔE), half wave potential ($\Delta E_{1/2}$), peak current I_p (μA), corresponding peak current ratio (I_{pa}/I_{pc}) of 150mM diisopropylamine + 2mM paracetamol in buffer solution (pH 9) of GC electrode at different scan rate (1st cycle)

v/Vs^{-1}	E_{pa2}/V	E_{pa3}/V	E_{pc3}/V	$\Delta E = E_{pc3} \sim E_{pa3}$	$\Delta E_{1/2}$/V	I_{pa2}/μA	I_{pa3}/μA	I_{pc3}/μA	I_{pa3}/I_{pc3}
0.05	0.33	0.62	-0.15	0.77	0.235	6.33	21.05	-6.77	3.109
0.10	0.34	0.64	-0.05	0.69	0.295	10.01	30.52	-9.21	3.31
0.15	0.36	0.66	-0.18	0.84	0.24	11.00	37.06	-10.62	3.48
0.20	0.37	0.63	-0.05	0.68	0.29	10.06	38.08	-12.70	2.99
0.25	0.37	0.67	-0.10	0.77	0.285	14.21	41.40	-17.29	2.39
0.30	0.36	0.65	-0.05	0.70	0.30	16.81	54.23	-18.12	2.99
0.35	0.36	0.64	-0.03	0.67	0.305	18.44	57.79	-26.65	2.16
0.40	0.36	0.66	-0.08	0.74	0.29	19.40	58.84	-29.32	2.00
0.45	0.38	0.66	-0.08	0.74	0.29	21.45	59.35	-30.38	1.95
0.50	0.38	0.67	-0.10	0.77	0.285	22.45	60.93	-33.69	1.80

Table 4.27: Peak potential (E_p), corresponding peak potential difference (ΔE), half wave potential ($\Delta E_{1/2}$), peak current I_p (μA), corresponding peak current ratio (I_{pa}/I_{pc}) of 150mM diisopropylamine + 2mM paracetamol in buffer solution (pH 9) of GC electrode at different scan rate (2nd cycle)

v/Vs^{-1}	E_{pa2}/V	E_{pa3}/V	E_{pc3}/V	$\Delta E = E_{pc3} \sim E_{pa3}$	$\Delta E_{1/2}$/V	I_{pa2}/μA	I_{pa3}/μA	I_{pc3}/μA	I_{pa3}/I_{pc3}
0.05	0.34	0.65	-0.02	0.67	0.315	2.33	21.76	-4.23	5.14
0.10	0.35	0.65	-0.04	0.69	0.305	5.93	27.48	-6.39	4.30
0.15	0.36	0.67	-0.07	0.74	0.30	9.17	35.50	-8.76	4.05
0.20	0.35	0.64	-0.05	0.69	0.295	11.31	36.23	-11.98	3.02
0.25	0.38	0.67	-0.09	0.76	0.29	12.94	38.41	-14.34	2.67
0.30	0.36	0.64	-0.04	0.68	0.30	16.37	46.70	-17.66	2.64
0.35	0.36	0.65	-0.04	0.69	0.305	19.93	53.01	-23.13	2.29
0.40	0.37	0.66	-0.07	0.73	0.295	22.72	53.73	-26.14	2.05
0.45	0.38	0.66	-0.08	0.74	0.29	21.77	54.39	-23.59	2.30
0.50	0.38	0.68	-0.09	0.77	0.295	21.08	56.04	-26.92	2.081

Table 4.28 : Peak potential (E_p), corresponding peak potential difference (ΔE), peak current I_p (μA), corresponding peak current ratio (I_{pa}/I_{pc}) of GC electrode at different scan rate (1st cycle) of 100mM diisopropylamine + 2mM paracetamol in buffer solution (pH 7)

v/Vs^{-1}	E_{pa3}/V	E_{pc3}/V	$\Delta E = E_{pc3} \sim E_{pa3}$	I_{pa3}/μA	I_{pc3}/μA	I_{pa3}/I_{pc3}
0.05	0.65	0.07	0.58	31.44	-0.66	47.63
0.10	0.69	0.03	0.66	40.07	-2.92	13.72
0.15	0.65	0.11	0.54	52.90	-4.37	12.10
0.20	0.66	0.09	0.57	57.03	-5.29	10.78
0.25	0.67	0.08	0.59	59.89	-7.39	8.10
0.30	0.70	0.02	0.68	60.36	-7.63	7.91
0.35	0.69	0.04	0.65	65.06	-7.94	8.19
0.40	0.66	0.13	0.53	72.14	-9.50	7.59
0.45	0.70	0.07	0.63	78.64	-10.82	7.26
0.50	0.70	0.05	0.65	84.00	-11.95	7.02

Table 4.29: Peak potential (E_p), corresponding peak potential difference (ΔE), peak current I_p (μA), corresponding peak current ratio (I_{pa}/I_{pc}) of 100mM diisopropylamine + 2mM paracetamol in buffer solution (pH 7) of GC electrode at different scan rate (2nd cycle)

v/Vs⁻¹	E_{pa3}/V	E_{pc3}/V	$\Delta E = E_{pc3} \sim E_{pa3}$	I_{pa3}/μA	I_{pc3}/μA	I_{pa3}/I_{pc3}
0.05	0.67	0.02	0.65	25.06	-0.60	41.76
0.10	0.71	0.09	0.62	33.83	-3.51	9.63
0.15	0.66	0.07	0.59	45.00	-3.77	11.93
0.20	0.68	0.07	0.61	51.74	-6.15	8.41
0.25	0.67	0.05	0.62	55.66	-7.15	7.78
0.30	0.71	0.01	0.70	54.33	-6.74	8.06
0.35	0.70	0.03	0.67	62.08	-8.80	7.05
0.40	0.66	0.09	0.57	68.40	-9.95	6.87
0.45	0.69	0.05	0.64	72.54	-12.07	6.00
0.50	0.71	0.03	0.68	74.63	-13.70	5.44

Table 4.30: Peak potential (E_p), corresponding peak potential difference (ΔE), peak current (I_p), corresponding peak current ratio (I_{pa}/I_{pc}) of 200mM diisopropylamine + 2mM paracetamol in buffer solution (pH 7) of GC electrode at different scan rate (1st cycle)

v/Vs⁻¹	E_{pa3}/V	E_{pc3}/V	$\Delta E = E_{pc3} \sim E_{pa1}$	I_{pa3}/μA	I_{pc3}/μA	I_{pa3}/I_{pc3}
0.05	0.65		0.65	33.74		
0.10	0.66	0.08	0.58	45.84	-2.24	20.46
0.15	0.68	0.06	0.62	55.24	-4.32	12.78
0.20	0.67	0.09	0.58	68.56	-6.19	11.07
0.25	0.66	0.15	0.51	74.48	-6.93	10.74
0.30	0.65	0.13	0.52	49.80	-4.88	10.20
0.35	0.67	0.12	0.55	84.86	-9.21	9.21
0.40	0.66	0.12	0.54	95.65	-10.08	9.48
0.45	0.68	0.11	0.57	98.00	-10.90	8.99
0.50	0.67	0.13	0.54	92.11	-11.22	8.20

73

Table 4.31: Peak potential (E_p), corresponding peak potential difference (ΔE), peak current (I_p), corresponding peak current ratio (I_{pa}/I_{pc}) of 200mM diisopropylamine + 2mM paracetamol in buffer solution (pH 7) of GC electrode at different scan rate (2nd cycle)

v/Vs^{-1}	E_{pa3} /V	E_{pc3} /V	$\Delta E = E_{pc3} \sim E_{pa3}$	I_{pa3} /μA	I_{pc3} /μA	I_{pa3} / I_{pc3}
0.05	0.68	-	0.68	26.12	-	-
0.10	0.67	0.05	0.62	38.02	-4.79	7.93
0.15	0.69	0.05	0.64	44.79	-4.88	9.17
0.20	0.67	0.08	0.59	54.31	-4.52	12.01
0.25	0.67	0.12	0.55	64.34	-5.73	11.22
0.30	0.66	0.11	0.55	51.62	-6.22	8.29
0.35	0.68	0.09	0.59	72.94	-8.46	8.62
0.40	0.67	0.12	0.55	83.51	-9.97	8.37
0.45	0.68	0.10	0.58	84.94	-12.48	6.80
0.50	0.67	0.12	0.55	90.47	-13.51	6.69

Table 4.32: Peak potential (E_p), corresponding peak potential difference (ΔE), peak current (I_p), corresponding peak current ratio (I_{pa}/I_{pc}) of 250mM diisopropylamine + 2mM paracetamol in buffer solution (pH 7) of GC electrode at different scan rate (1st cycle)

v/Vs^{-1}	E_{pa3} /V	E_{pc3} /V	$\Delta E = E_{pa3} \sim E_{pc3}$	I_{pa3} /μA	I_{pc3} /μA	I_{pa3}/I_{pc3}
0.05	0.68	-0.02	0.70	28.42	-3.29	8.63
0.10	0.68	-0.04	0.72	38.62	-6.55	5.89
0.15	0.67	-0.04	0.71	42.04	-7.39	5.68
0.20	0.68	-0.08	0.76	53.61	-9.70	5.52
0.25	0.69	-0.09	0.78	59.66	-10.59	5.63
0.30	0.66	-0.03	0.69	68.95	-11.13	6.19
0.35	0.70	-0.10	0.80	73.38	-15.14	4.84
0.40	0.66	-0.03	0.69	56.74	-12.45	4.55
0.45	0.68	-0.04	0.72	73.00	-18.34	3.98
0.50	0.68	-0.04	0.72	71.41	-16.03	4.45

Table 4.33: Peak potential (E_p), corresponding peak potential difference (ΔE), half wave potential ($\Delta E_{1/2}$), corresponding peak current (I_p), corresponding peak current ratio (I_{pa}/I_{pc}) of 250mM diisopropylamine + 2mM paracetamol in buffer solution (pH 7) of GC electrode at different scan rate (2nd cycle)

v/Vs^{-1}	E_{pa3}/V	E_{pc3}/V	$\Delta E = E_{pc3} \sim E_{pa3}$	$\Delta E_{1/2}/V$	$I_{pa3}/\mu A$	$I_{pc3}/\mu A$	I_{pa3}/I_{pc3}
0.05	0.69	-0.04	0.73	0.32	24.47	-3.52	6.95
0.10	0.68	-0.06	0.74	0.31	35.02	-6.14	5.70
0.15	0.68	-0.05	0.73	0.31	39.70	-7.44	5.33
0.20	0.69	-0.08	0.77	0.30	46.53	-9.79	4.75
0.25	0.69	-0.08	0.77	0.30	52.61	-9.79	5.37
0.30	0.66	-0.02	0.68	0.32	61.14	-11.48	5.32
0.35	0.71	-0.08	0.79	0.31	61.93	-14.13	4.38
0.40	0.66	-0.04	0.70	0.31	55.67	-15.50	3.59
0.45	0.67	-0.04	0.71	0.31	63.82	-13.83	4.61
0.50	0.68	-0.05	0.73	0.31	59.68	-13.68	4.36

75
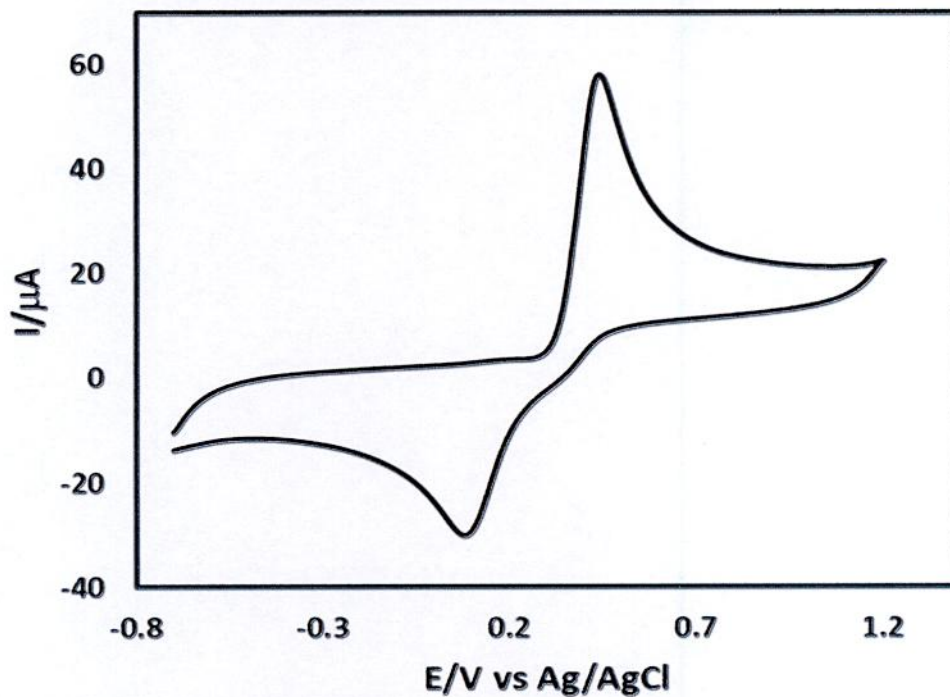
Fig. 4.1: Cyclic voltammogram of only 2mM paracetamol of GC electrode at scan rate 0.1V/s in buffer solution (pH 7) (1st cycle)
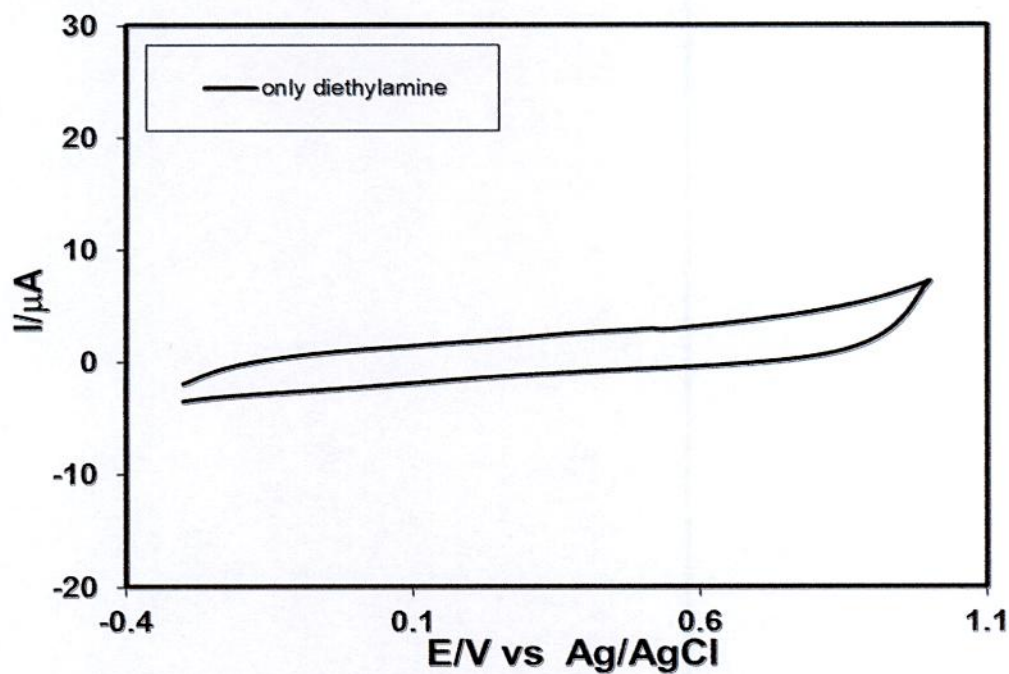
Fig. 4.2: Cyclic voltammogram of only 150mM diethylamine of GC electrode at scan rate 0.1V/s in buffer solution (pH 7) (1st cycle)

76
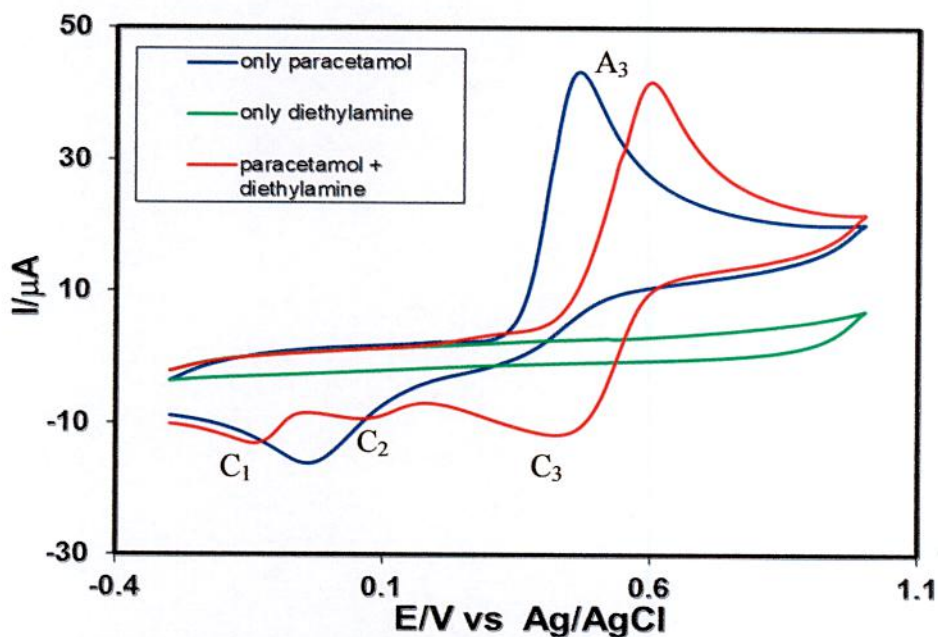
Fig. 4.3: Comparison of cyclic voltammogram of only 2mM paracetamol, only 150mM diethylamine, 2mM paracetamol + 150mM diethylamine of GC electrode at scan rate 0.1V/s in buffer solution (pH 7) (1st cycle), A_3= oxidation peak, C_1 and C_2= Appeared reduction peaks, C_3= reduction peak
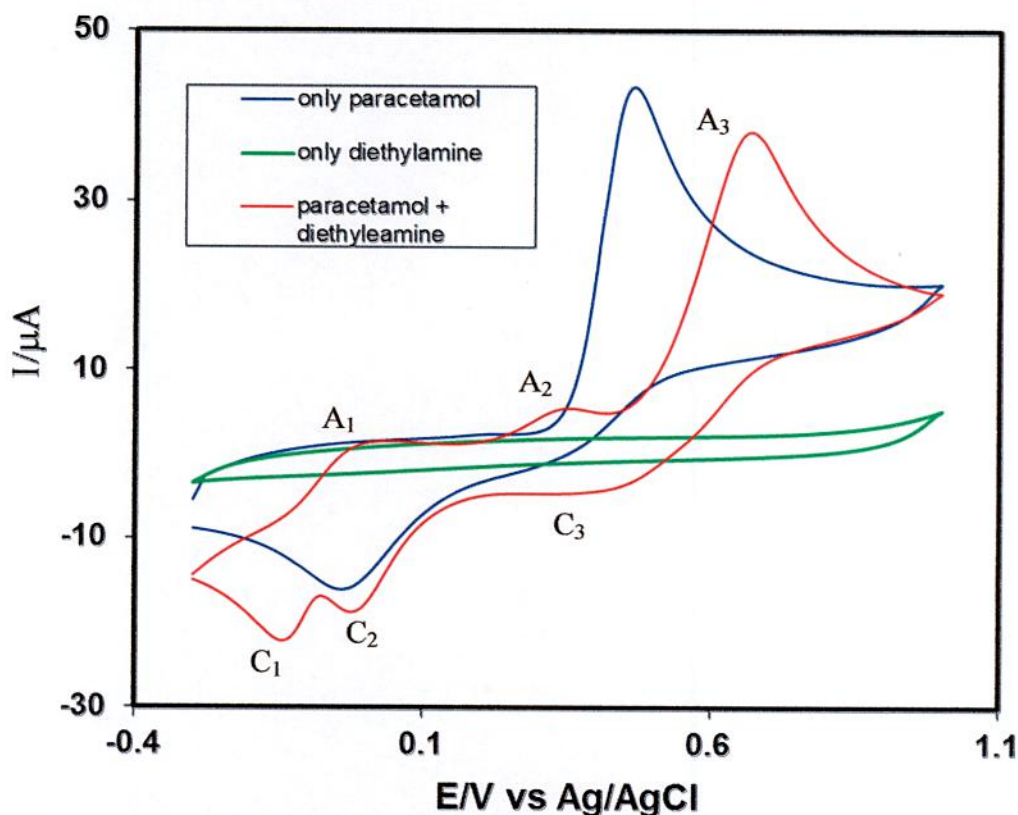
Fig. 4.4: Comparison of cyclic voltammogram of only 2mM paracetamol, only 150mM diethylamine and 2mM paracetamol + 150mM diethylamine of GC electrode at scan rate 0.1V/s in buffer solution (pH 7) (2nd cycle), A_1 and A_2= appeared oxidation peaks
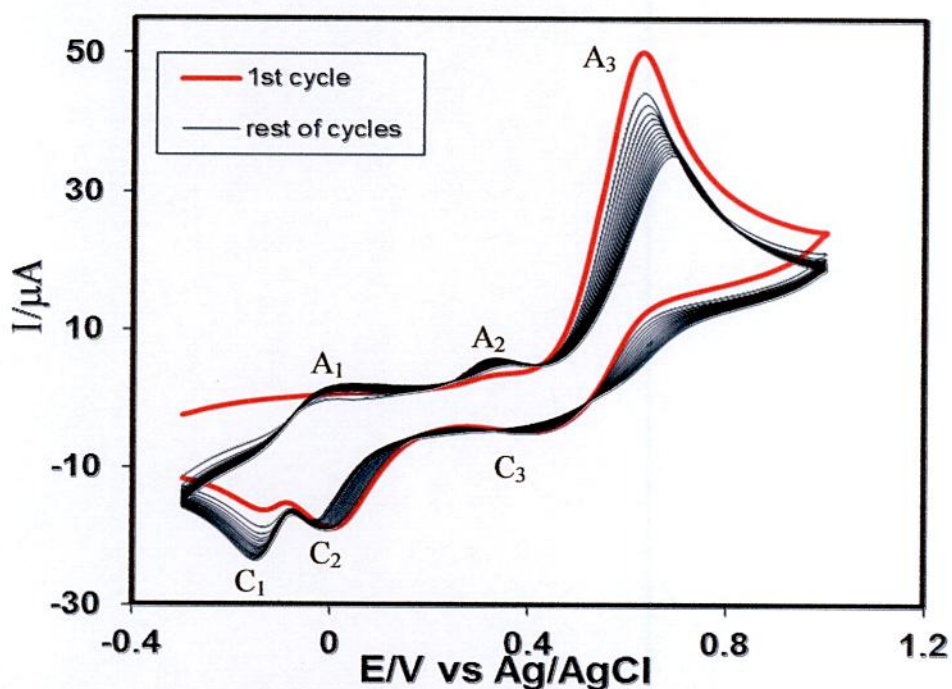
Fig. 4.5: Cyclic voltammogram of first 15 cycles of 2mM paracetamol + 150mM diethylamine of GC electrode at scan rate 0.1V/s in buffer solution (pH 7)
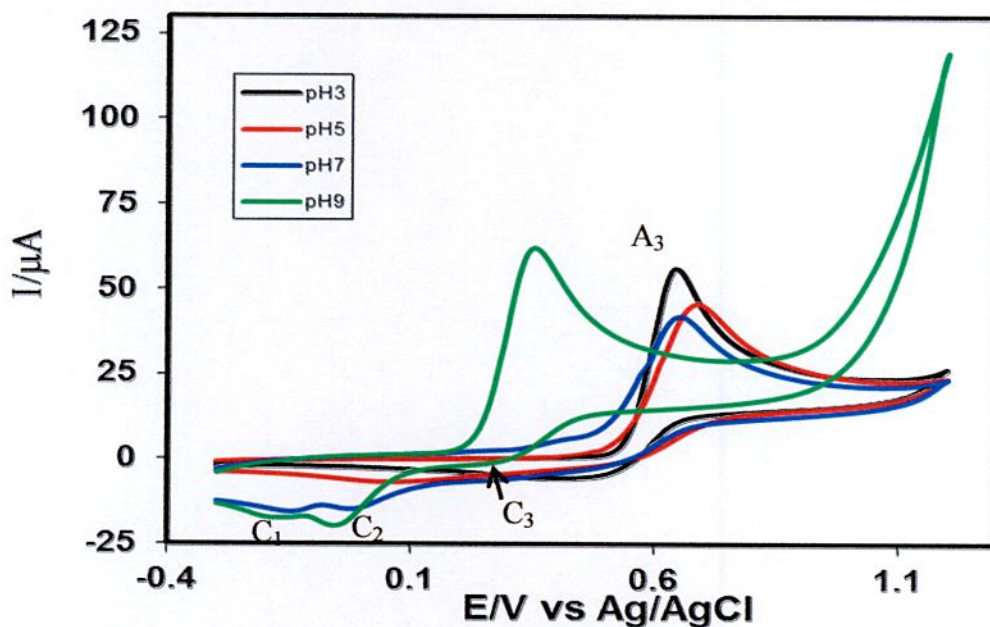
Fig. 4.6: Comparison of cyclic voltammogram of different pH (3, 5, 7 and 9) of 2mM paracetamol + 150mM diethylamine of GC electrode at scan rate 0.1V/s (1st cycle)
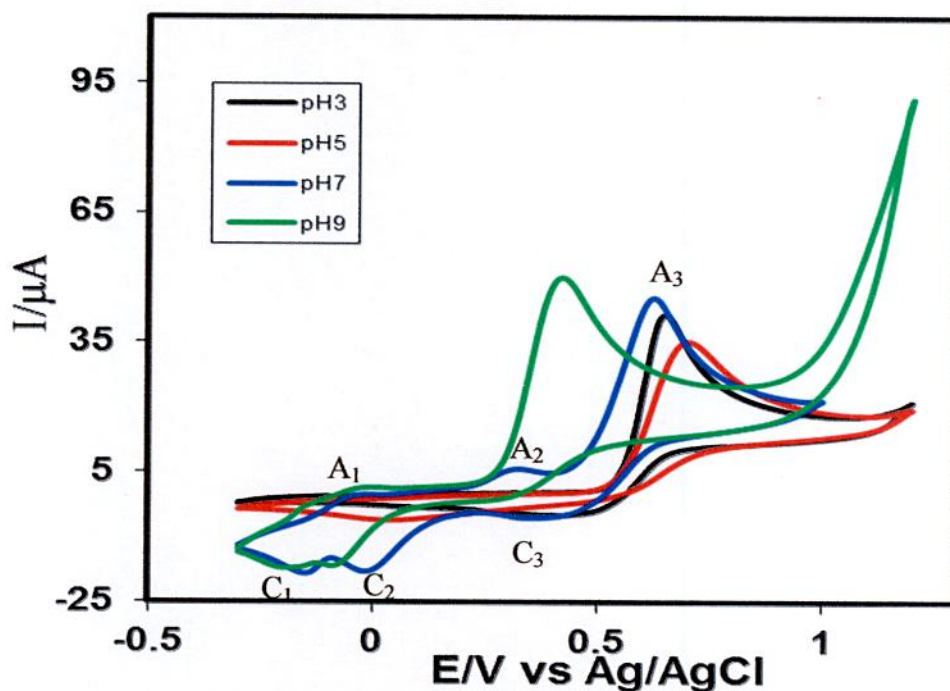
Fig. 4.7: Comparison of cyclic voltammogram of different pH   (3, 5, 7 and 9) of 2mM paracetamol + 150mM diethylamine of GC electrode at scan rate 0.1V/s (2nd cycle)
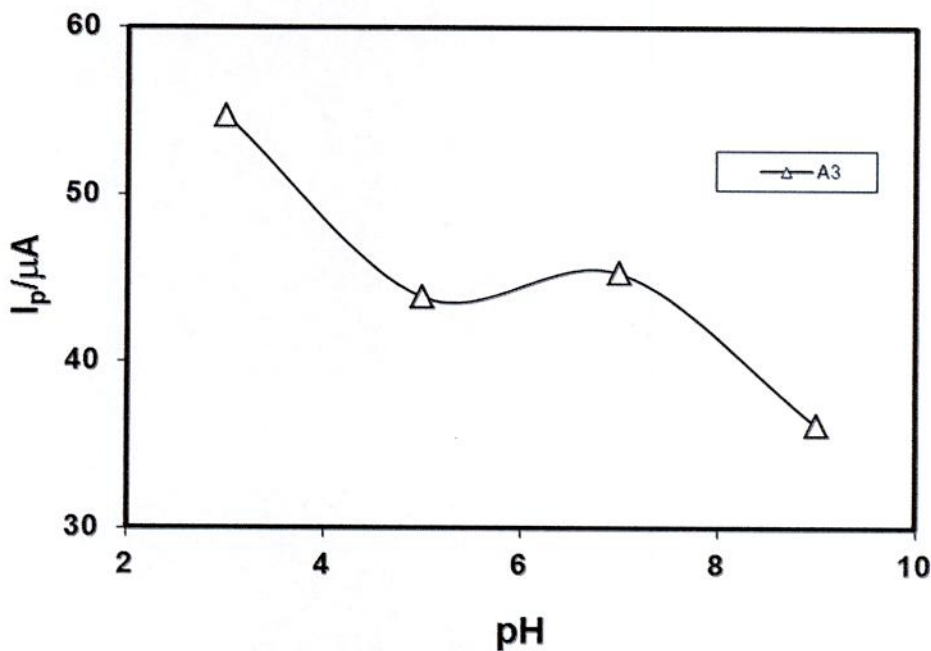
Fig. 4.8: Plots of peak current (I_p) versus pH (3, 5, 7 and 9) of 2mM paracetamol + 150mM diethylamine of GC electrode at scan rate 0.1V/s (2nd cycle)
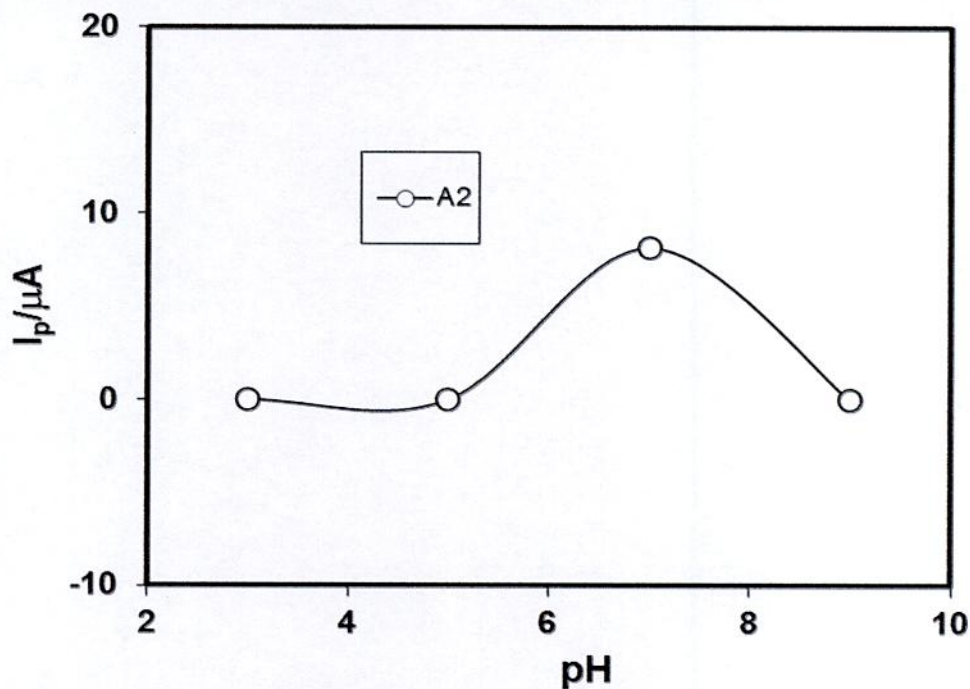
Fig. 4.9: Plots of peak current (I_p) versus pH (3, 5, 7 and 9) of 2mM paracetamol + 150mM diethylamine of GC electrode at scan rate 0.1V/s (2nd cycle)
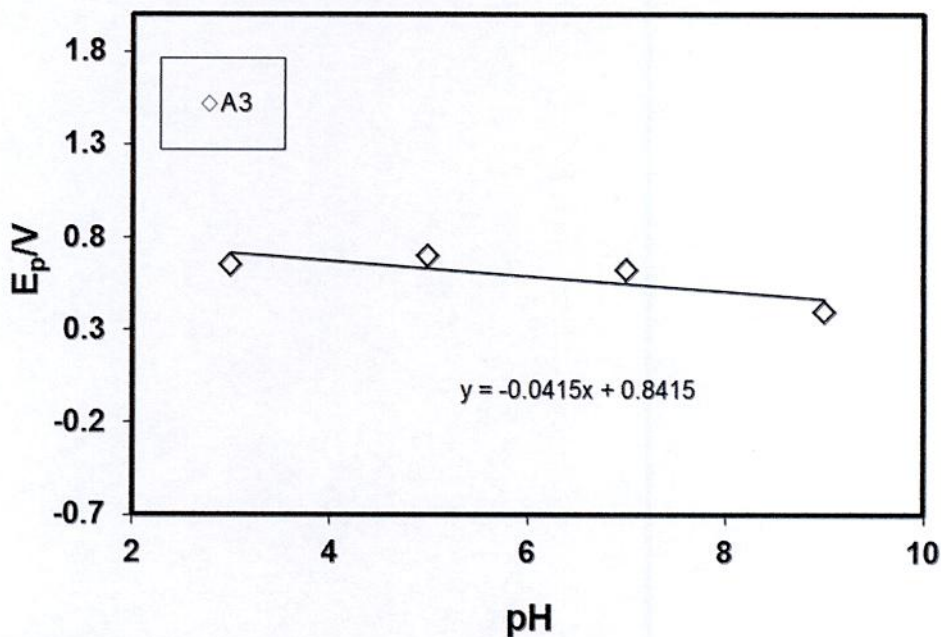
Fig. 4.10: Plots of peak potential (E_p) versus pH (3, 5, 7 and 9) of 2mM paracetamol + 150mM diethylamine of GC electrode at scan rate 0.1V/s (1st cycle)
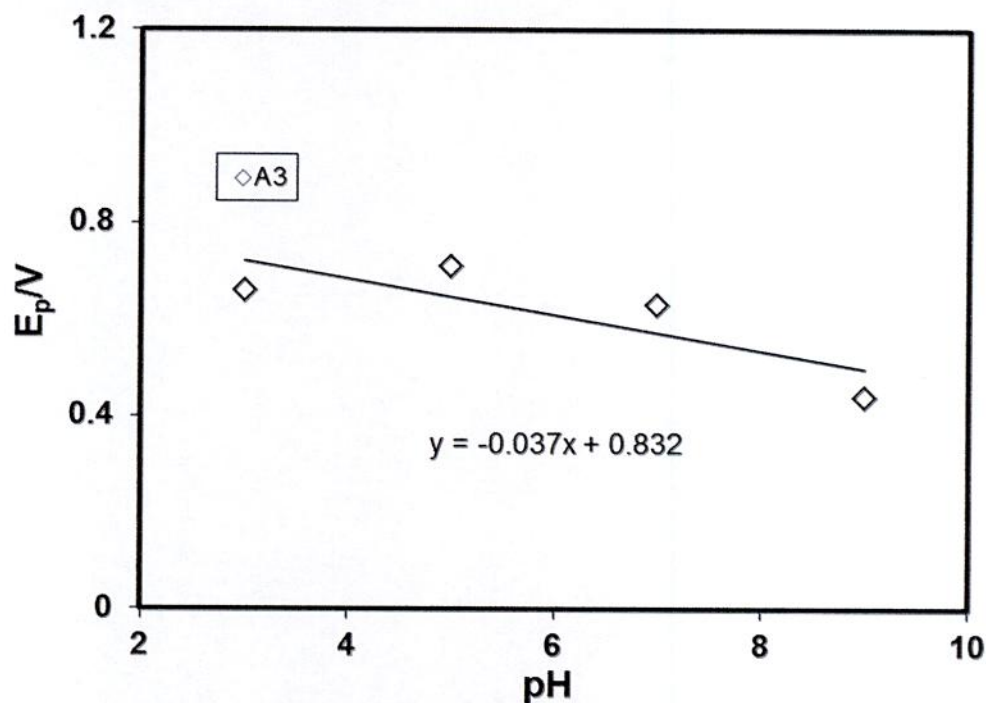
Fig. 4.11: Plots of peak potential (E_p) versus pH (3, 5, 7 and 9) of 2mM paracetamol + 150mM diethylamine of GC electrode at scan rate 0.1V/s (2nd cycle)
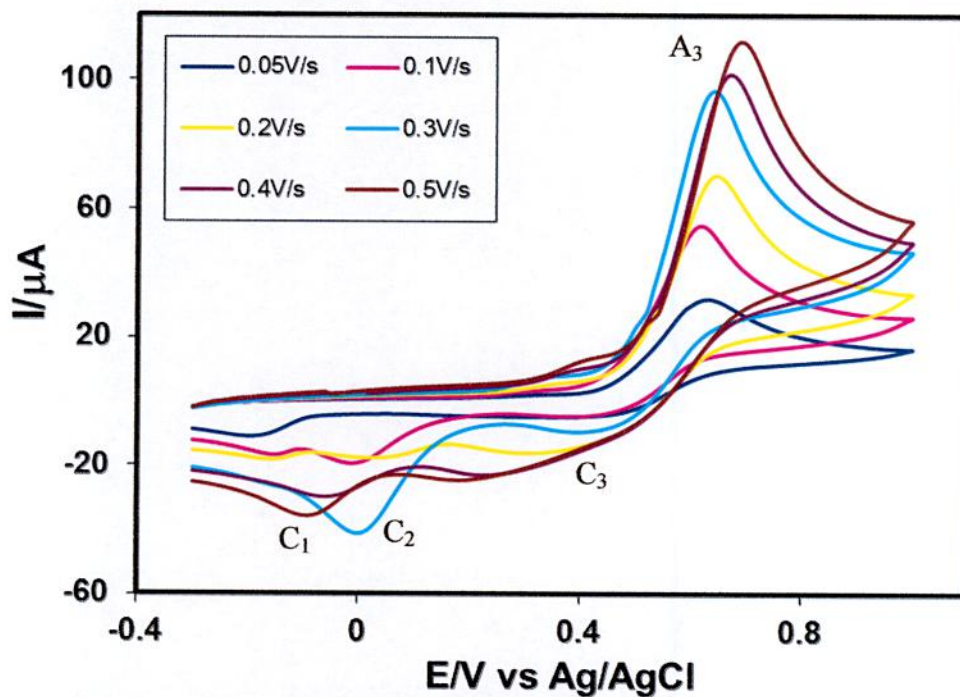
Fig. 4.12: Cyclic voltammogram of 2mM paracetamol + 150mM diethylamine of GC electrode at different scan rate in buffer solution (pH 7) (1st cycle)
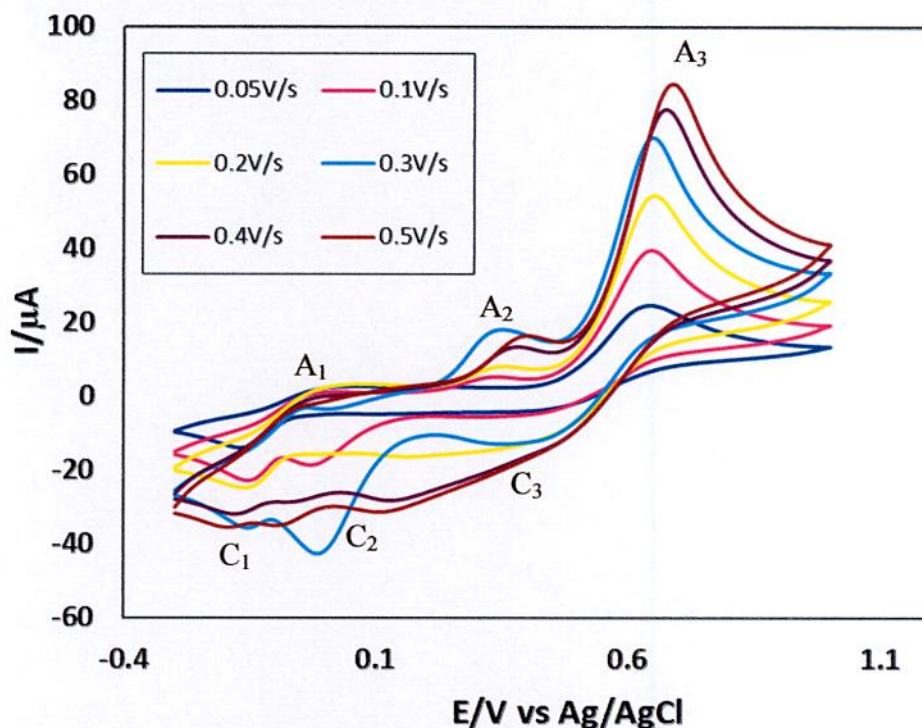
Fig. 4.13: Cyclic voltammogram of 2mM paracetamol + 150mM diethylamine of GC electrode at different scan rate (2nd cycle) in buffer solution (pH 7)
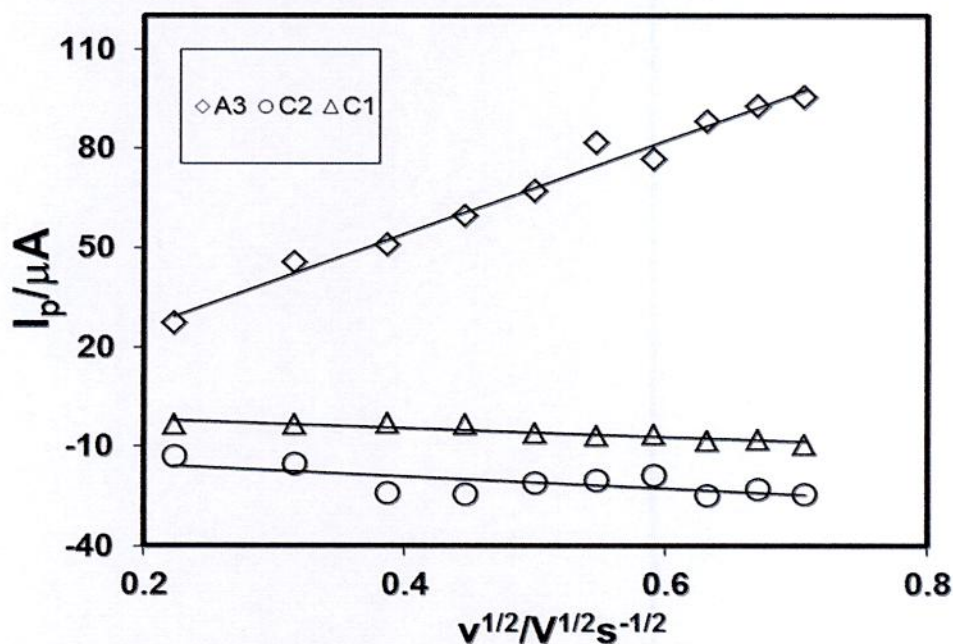
Fig. 4.14: Plots of peak current (I$_p$) versus square root of scan rate (v$^{1/2}$) of 2mM paracetamol + 150mM diethylamine of GC electrode in buffer solution (pH 7) at 1st cycle, A$_3$= oxidation peak, C$_1$= Appeared reduction peak and C$_2$= reduction peak
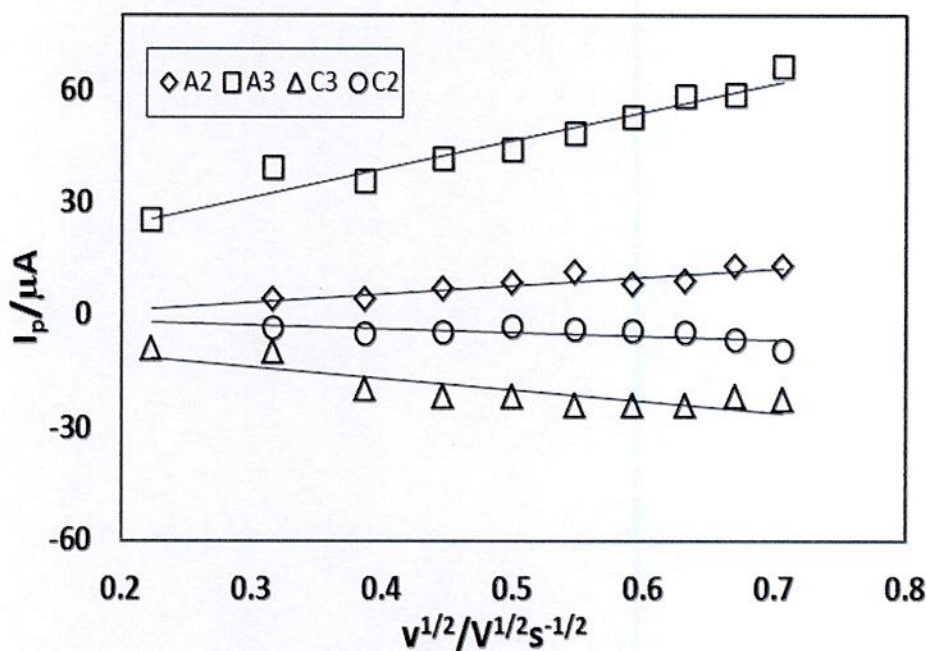
Fig. 4.15: Plots of peak current (I_p) versus square root of scan rate ($v^{1/2}$) of 2mM paracetamol + 150mM diethylamine of GC electrode in buffer solution (pH 7) at 2nd cycle (A_2= Appeared oxidation peak, A_3= 3rd oxidation peak, C_2= Appeared reduction peak and C_3= 3rd reduction peak)
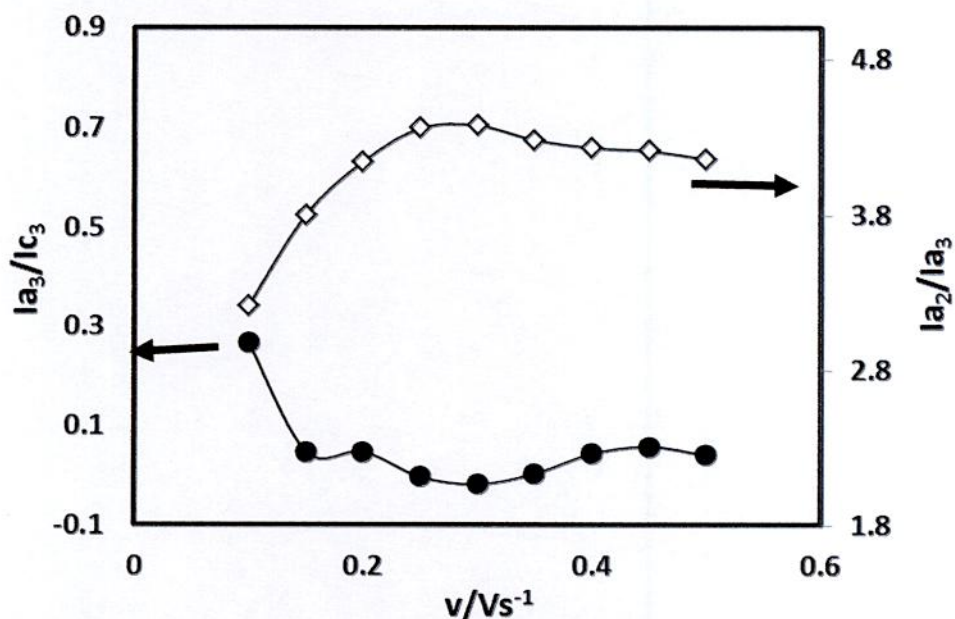
Fig. 4.16:Variation of peak current ratio of corresponding peak (I_{a3}/I_{c3}) and anodic peak (I_{a2}/I_{a3}) versus scan rate (v) of 150mM diethylamine + 2mM paracetamol in buffer solution (pH 7) of GC electrode (2nd cycle)
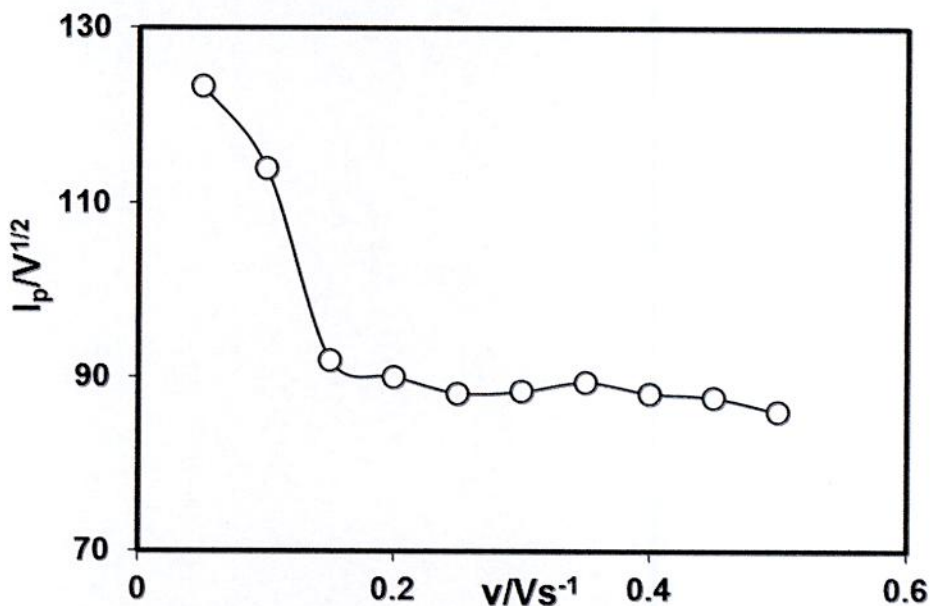
Fig. 4.17: Plots of current function ($I_p/v^{1/2}$) versus scan rate (v) of 150mM diethylamine + 2mM paracetamol of GC electrode in buffer solution (pH 7) at oxidation peak A_3
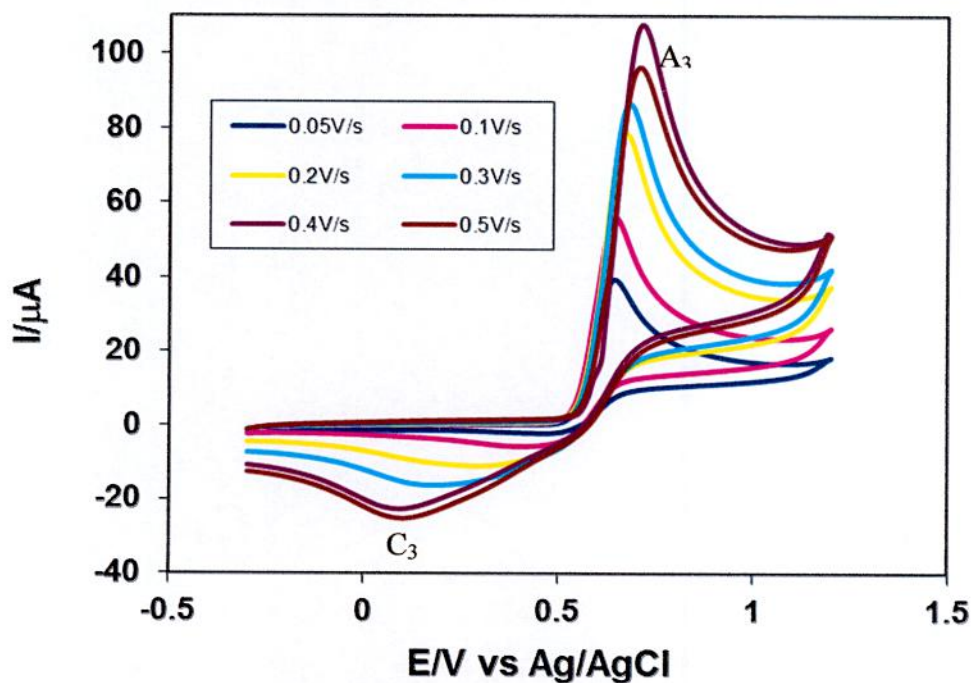
Fig. 4.18: Cyclic voltammogram of 2mM paracetamol + 150mM diethylamine at GC electrode in buffer solution (pH 3) at different scan rate (1st cycle)
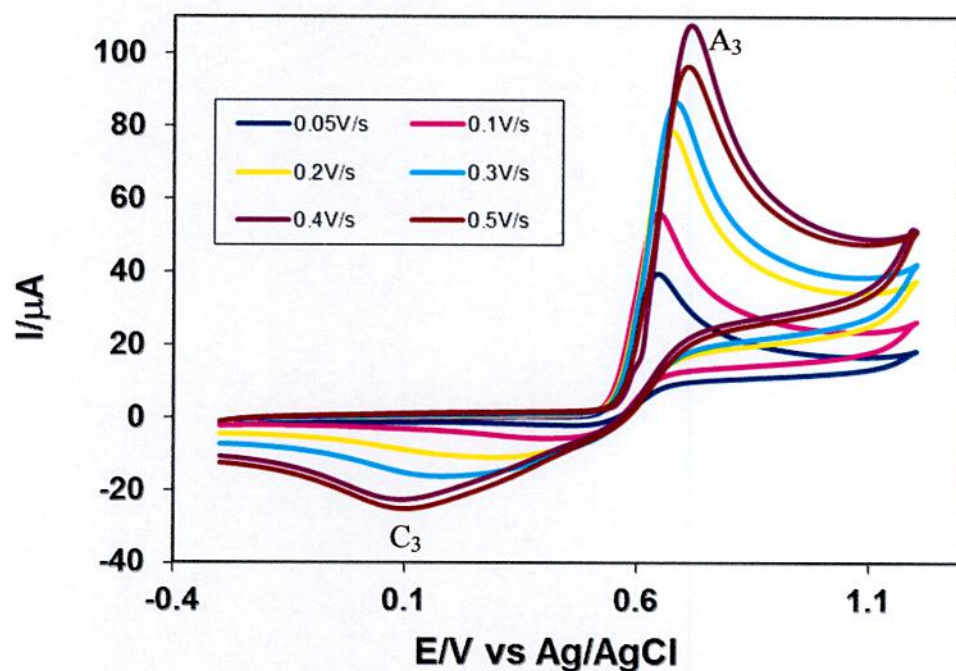
Fig. 4.19: Cyclic voltammogram of 2mM paracetamol + 150mM diethylamine of GC electrode in buffer solution (pH 3) at different scan rate (2nd cycle)
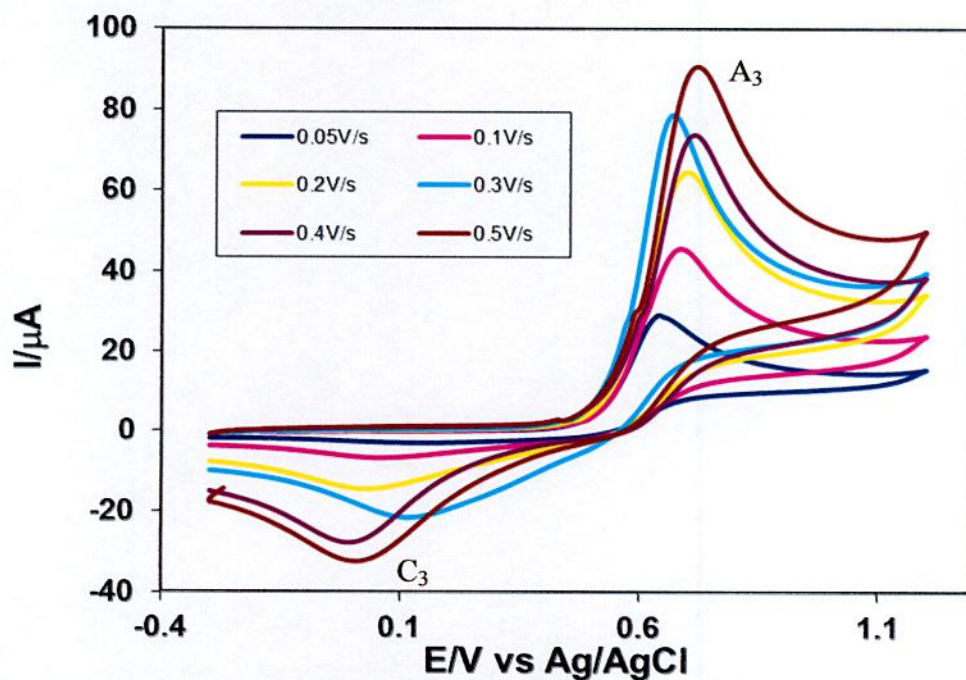
Fig. 4.20: Cyclic voltammogram of 2mM paracetamol + 150mM diethylamine of GC electrode in buffer solution (pH 5) at different scan rate (1st cycle)
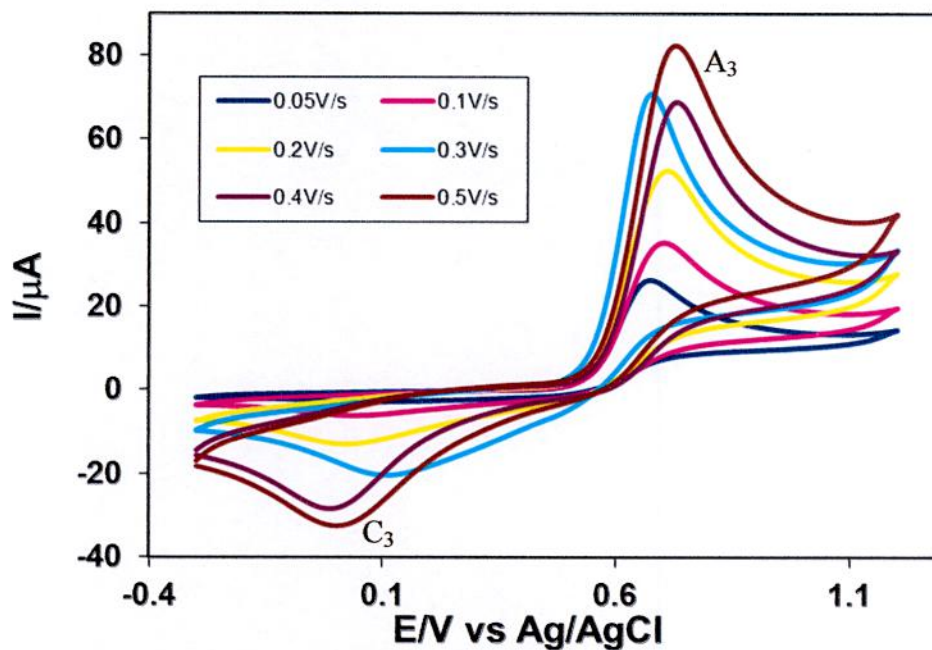
Fig. 4.21: Cyclic voltammogram of 2mM paracetamol + 150mM diethylamine of GC electrode in buffer solution (pH 5) at different scan rate (2nd cycle)
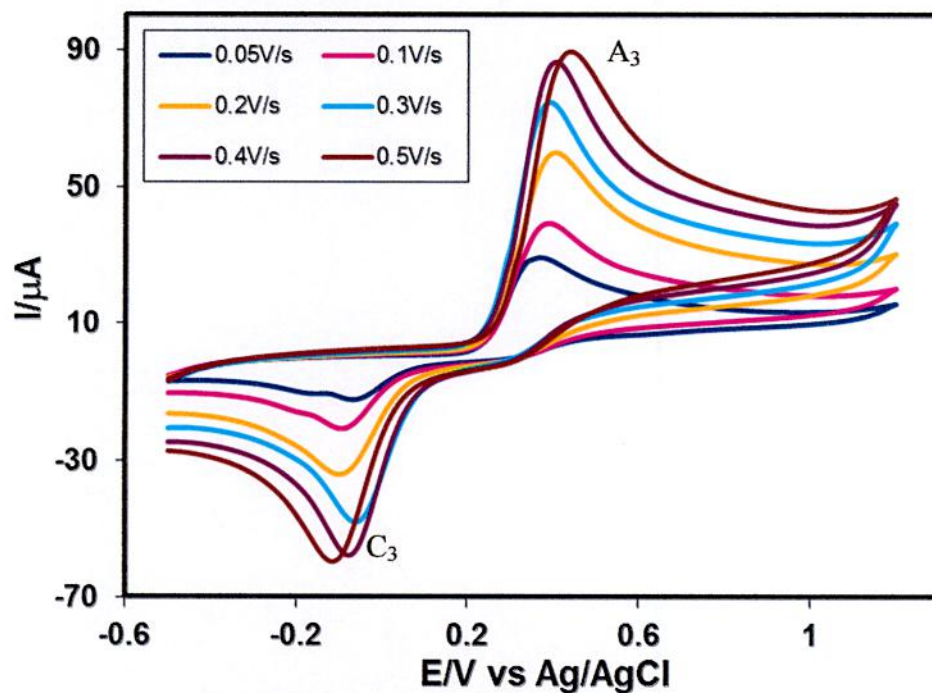
Fig. 4.22: Cyclic voltammogram of 2mM paracetamol + 150mM diethylamine of GC electrode in buffer solution (pH 9) at different scan rate (1st cycle)
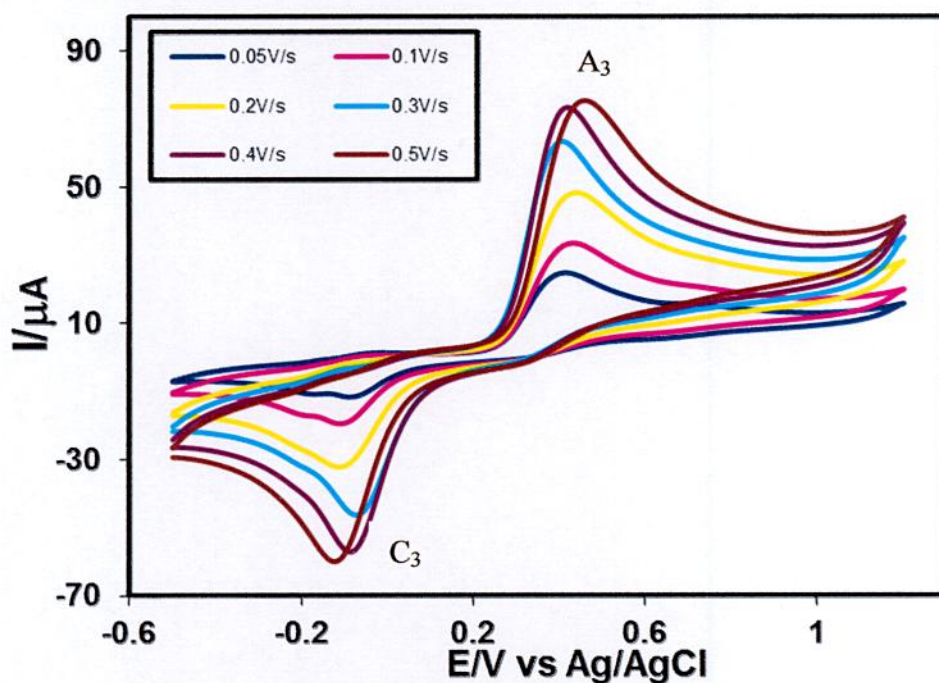
Fig. 4.23: Cyclic voltammogram of 2mM paracetamol + 150mM diethylamine of GC electrode in buffer solution (pH 9) at different scan rate (2nd cycle)
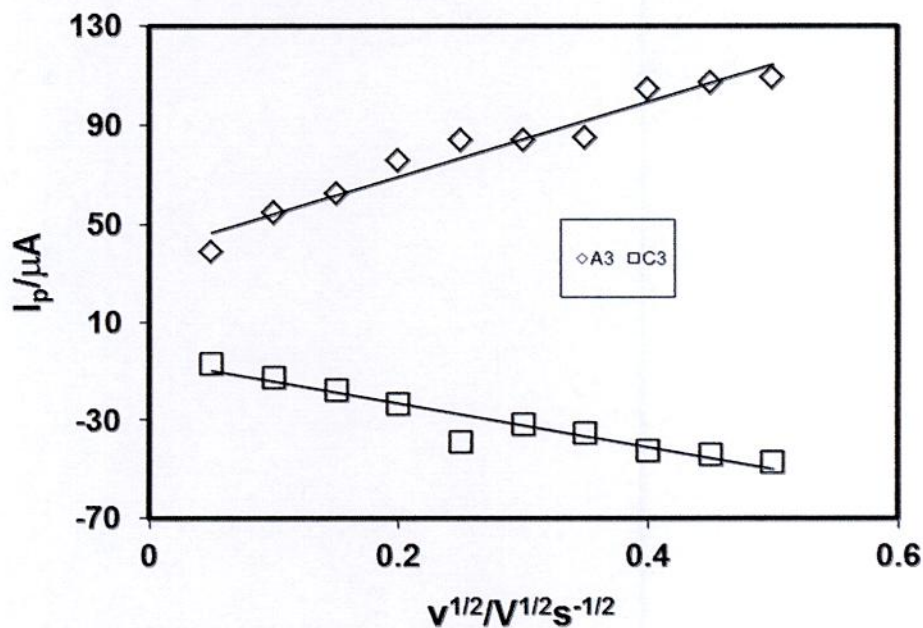
Fig. 4.24: Plots of peak current (I_p) versus square root of scan rate ($v^{1/2}$) of 2mM paracetamol + 150mM diethylamine of GC electrode in buffer solution (pH 3) (1st cycle)
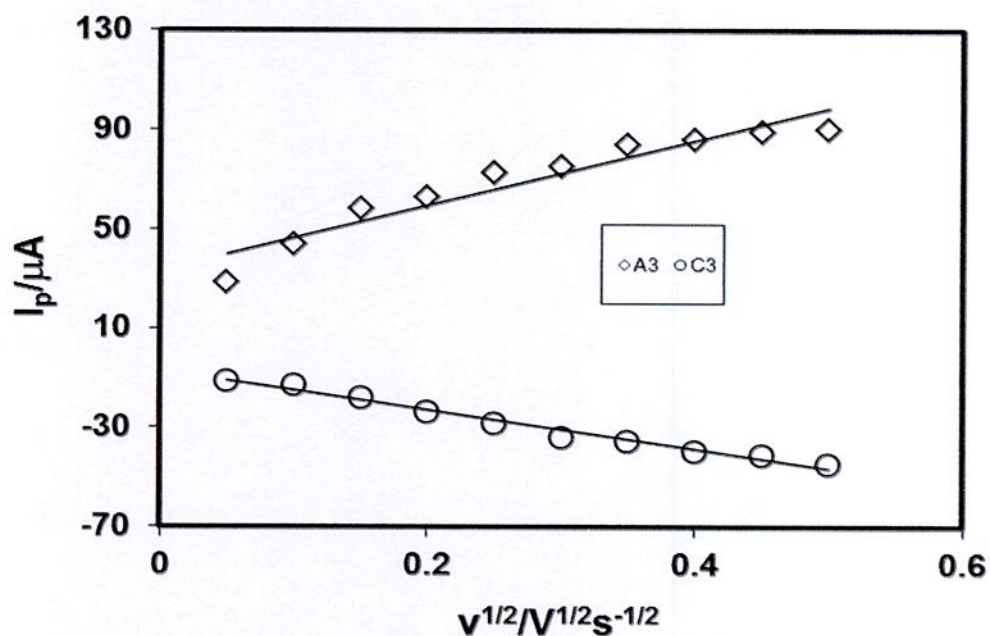
Fig. 4.25: Plots of peak current (I_p) versus square root of scan rate ($v^{1/2}$) of 2mM paracetamol + 150mM diethylamine of GC electrode in buffer solution (pH 3) (2nd cycle)
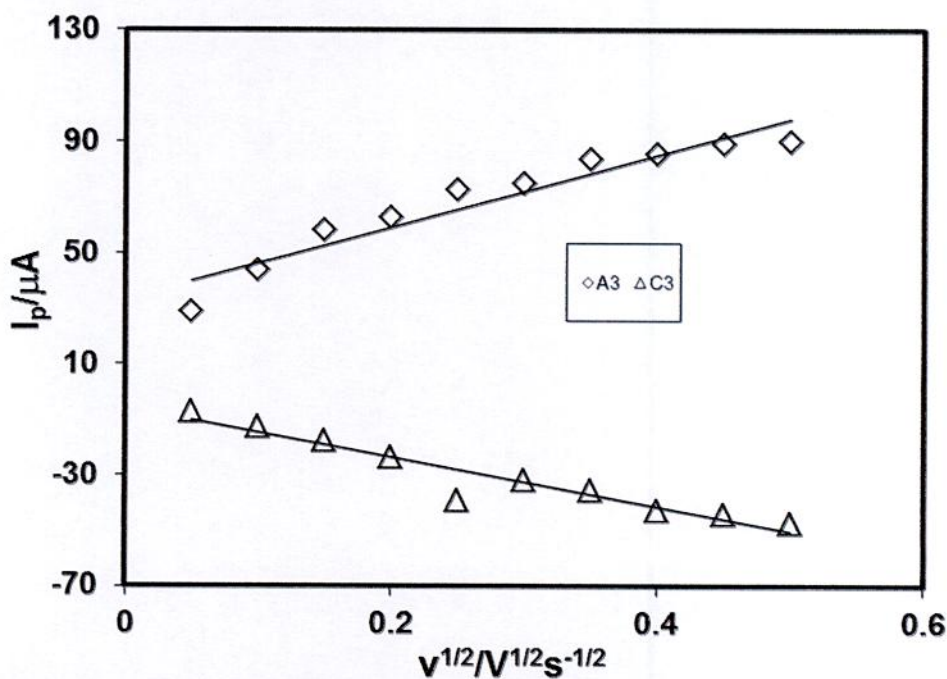
Fig. 4.26: Plots of peak current (I_p) versus square root of scan rate ($v^{1/2}$) of 2mM paracetamol + 150mM diethylamine of GC electrode in buffer solution (pH 5) at different scan rate (1st cycle)
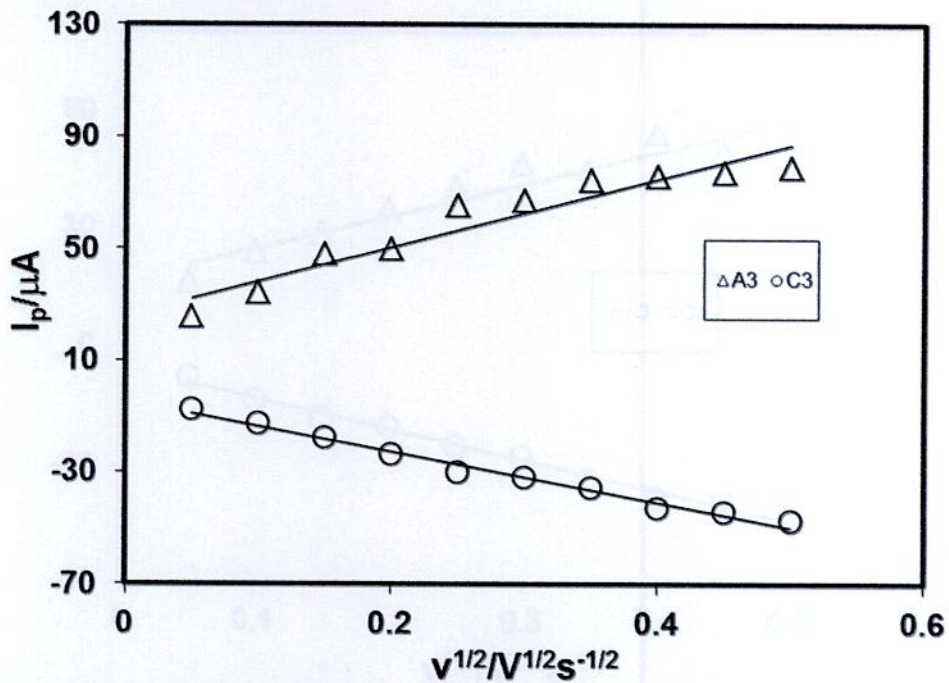
Fig. 4.27: Plots of peak current (I_p) versus square root of scan rate ($v^{1/2}$) of 2mM paracetamol + 150mM diethylamine of GC electrode in buffer solution (pH 5) at different scan rate (2nd cycle)
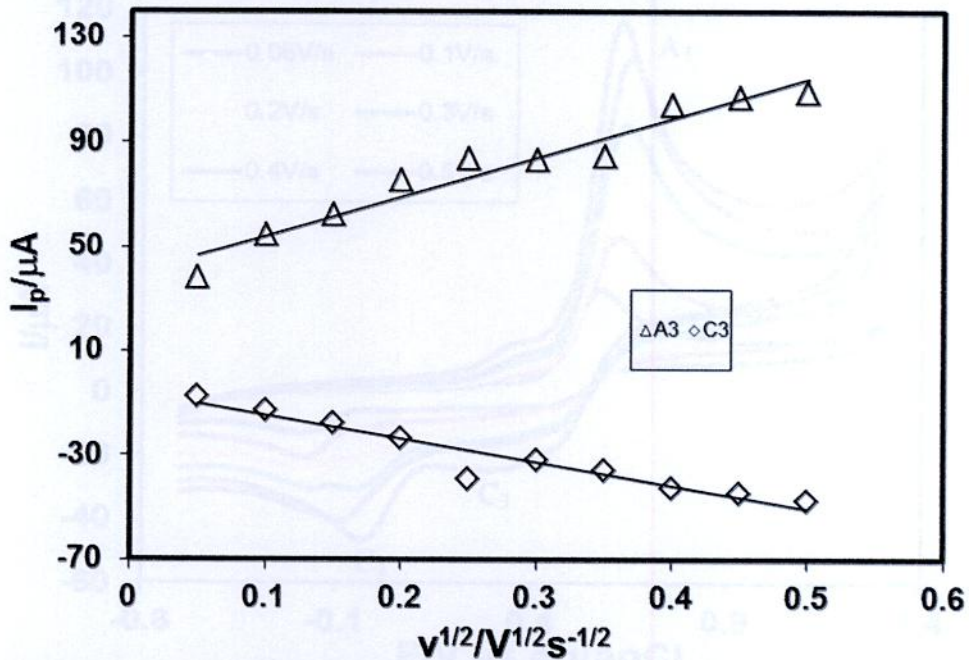
Fig. 4.28: Plots of peak current (I_p) versus square root of scan rate ($v^{1/2}$) of 2mM paracetamol + 150mM diethylamine at GC electrode in buffer solution (pH 9) at different scan rate (1st cycle)
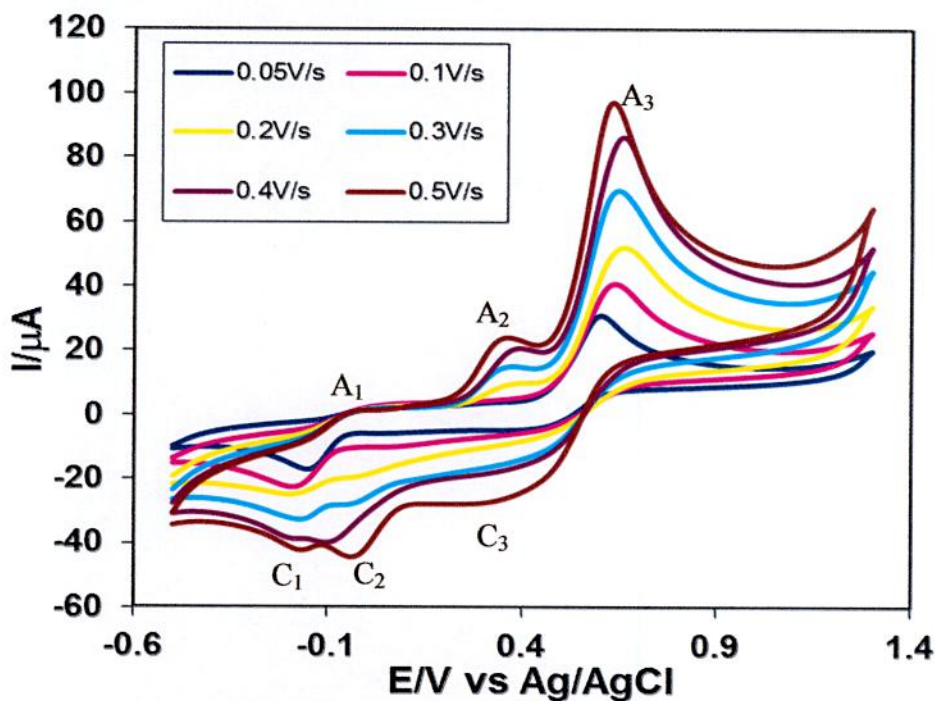
Fig. 4.31: Cyclic voltammogram of 2mM paracetamol + 100mM diethylamine of GC electrode in buffer solution (pH 7) at different scan rate (2nd cycle)
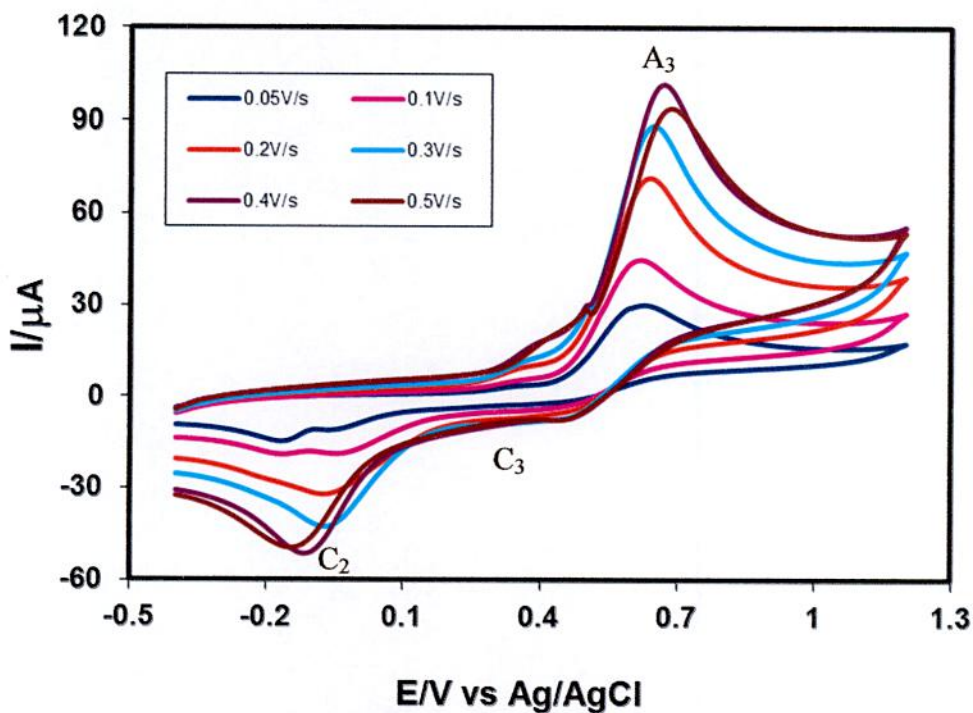
Fig. 4.32: Cyclic voltammogram of 2mM paracetamol + 200mM diethylamine of GC electrode in buffer solution (pH 7) at different scan rate (1st cycle)
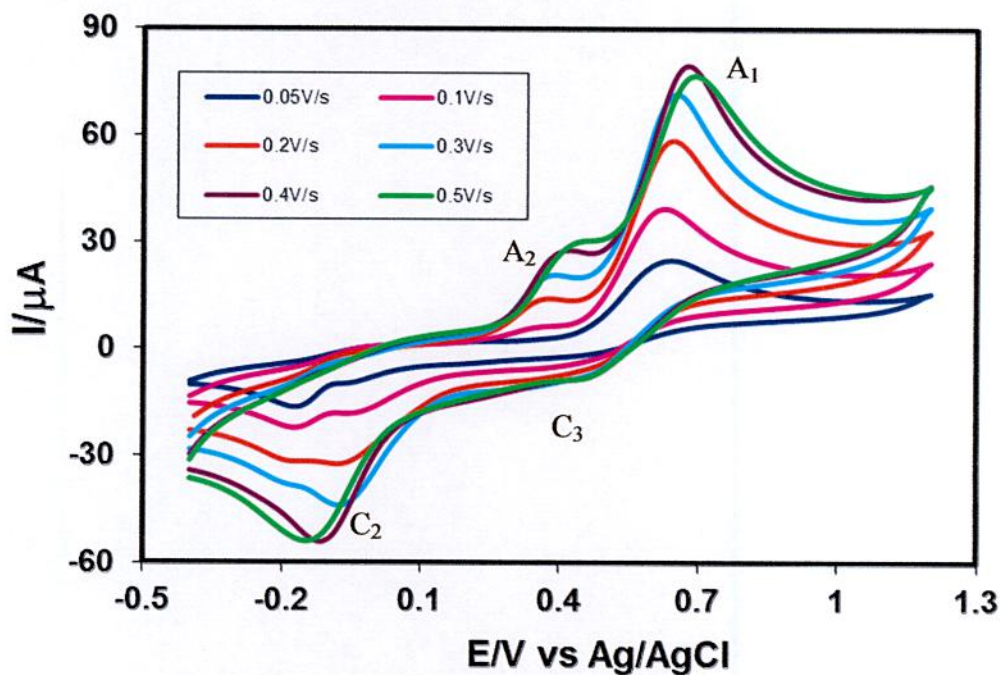
Fig. 4.33: Cyclic voltammogram of 2mM paracetamol + 200mM diethylamine of GC electrode in buffer solution (pH 7) at different scan rate (2nd cycle)
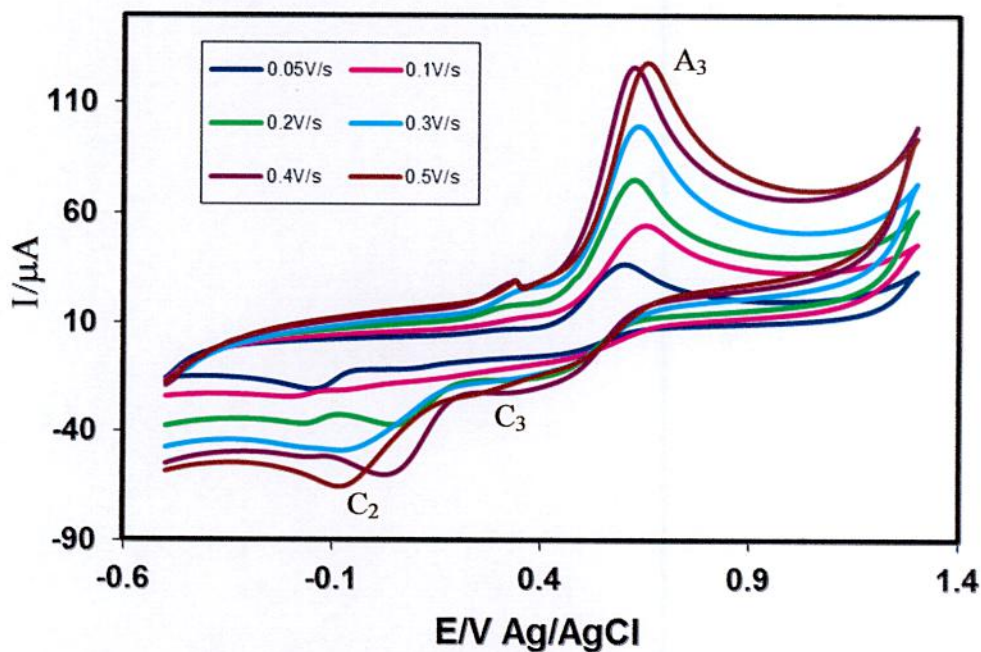
Fig. 4.34: Cyclic voltammogram of 2mM paracetamol + 250mM diethylamine of GC electrode in buffer solution (pH 7) at different scan rate (1st cycle)
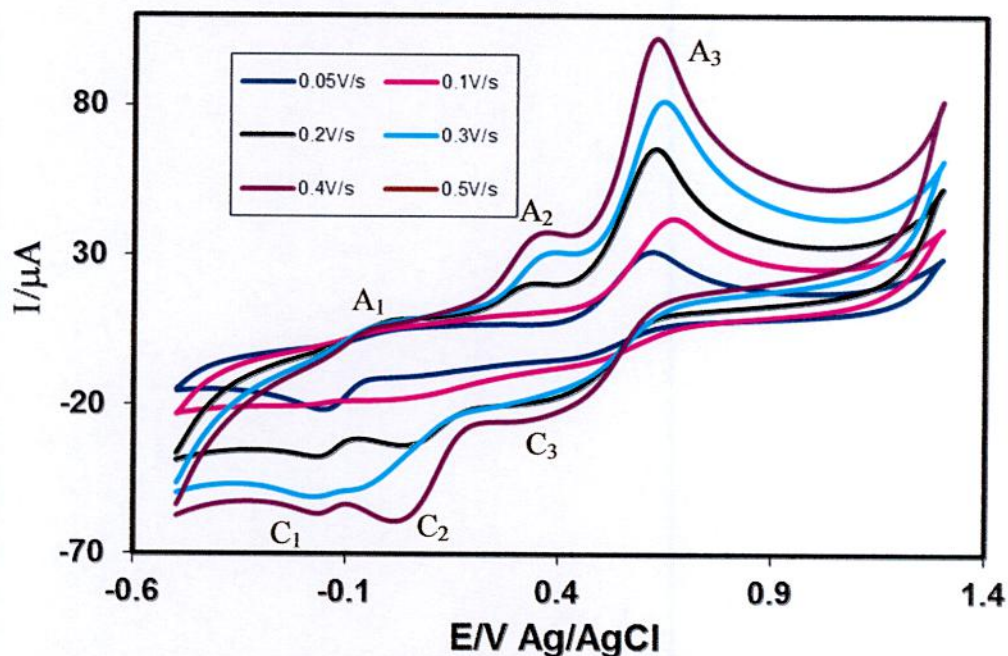
Fig. 4.35: Cyclic voltammogram of 2mM paracetamol + 250mM Diethylamine of GC electrode in buffer solution (pH 7) at different scan rate (2nd cycle)
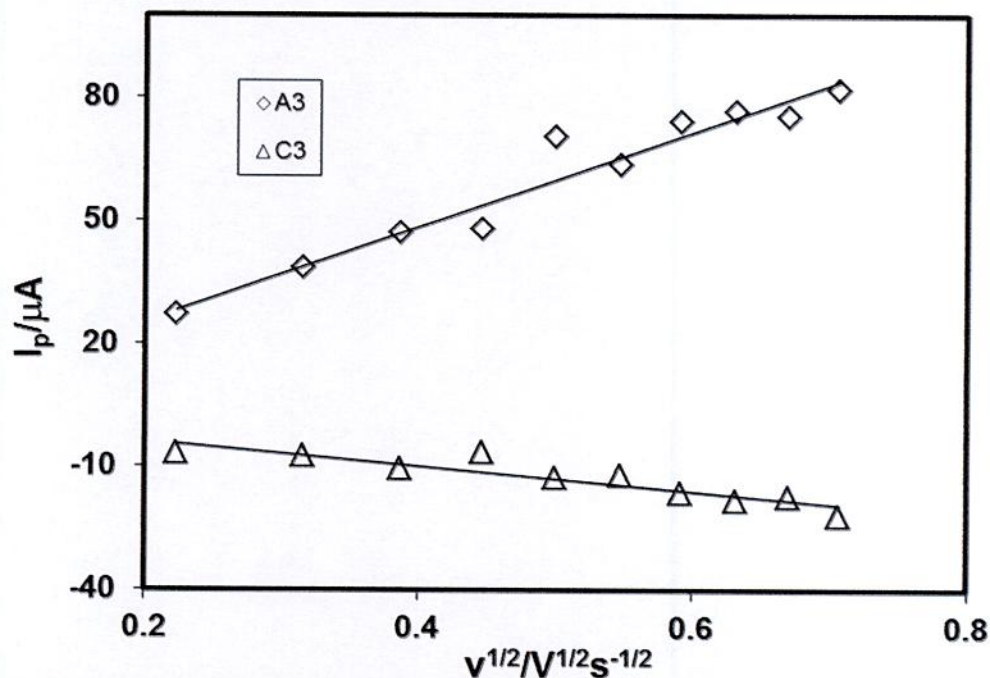
Fig. 4.36: Plots of peak current (I_p) versus square root of scan rate ($v^{1/2}$) of 2mM paracetamol + 100mM diethylamine of GC electrode in buffer solution (pH 7) (1st cycle)
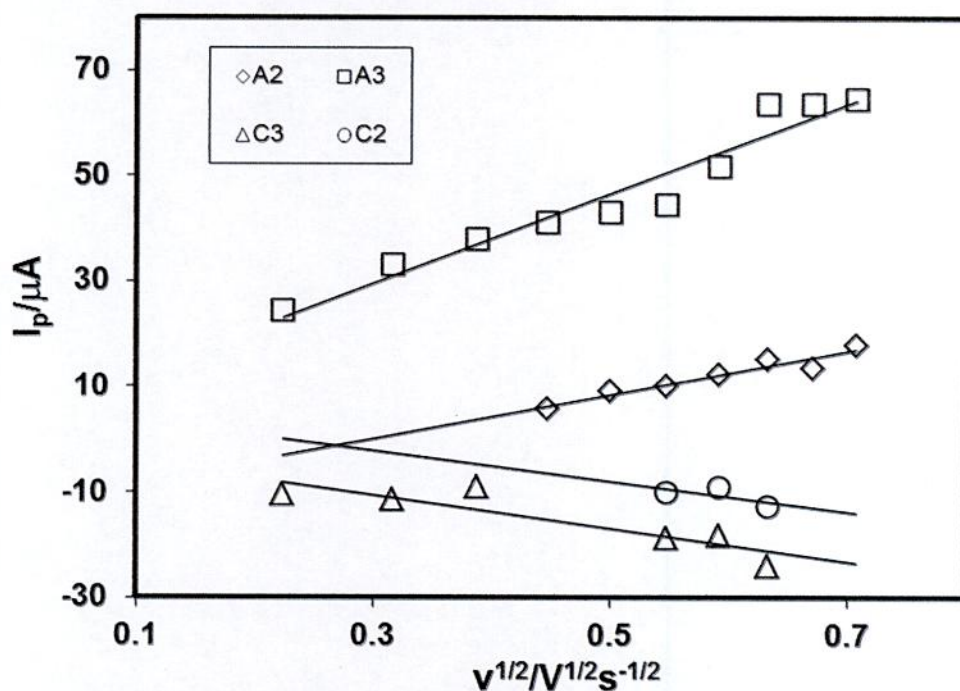
Fig. 4.37: Plots of peak current (I_p) versus square root of scan rate ($v^{1/2}$) of 2mM paracetamol + 100mM diethylamine of GC electrode in buffer solution (pH 7) (2nd cycle)
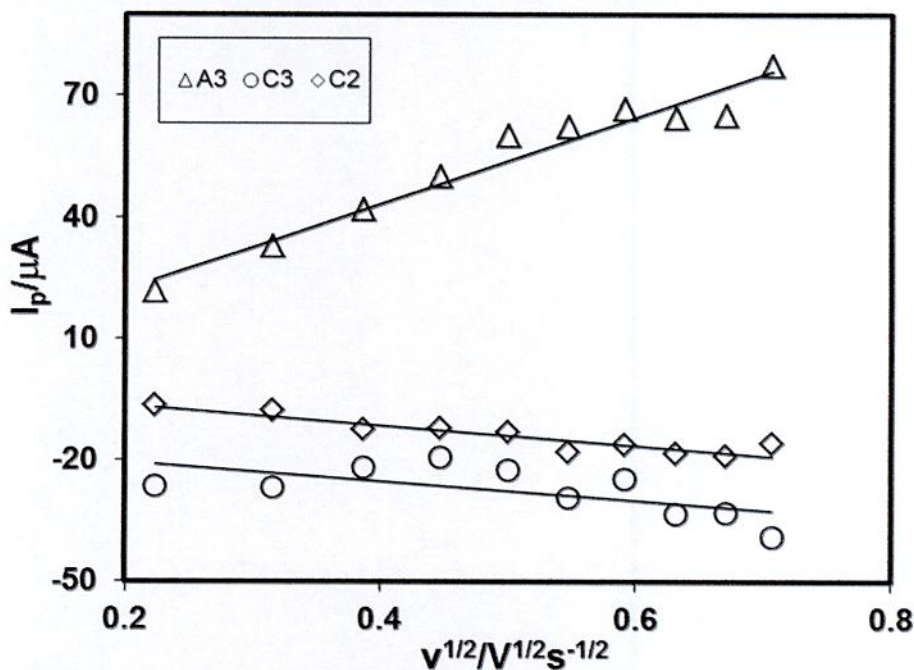
Fig. 4.38: Plots of peak current (I_p) versus square root of scan rate ($v^{1/2}$) of 2mM paracetamol + 200mM diethylamine of GC electrode in buffer solution (pH 7) (1st cycle)
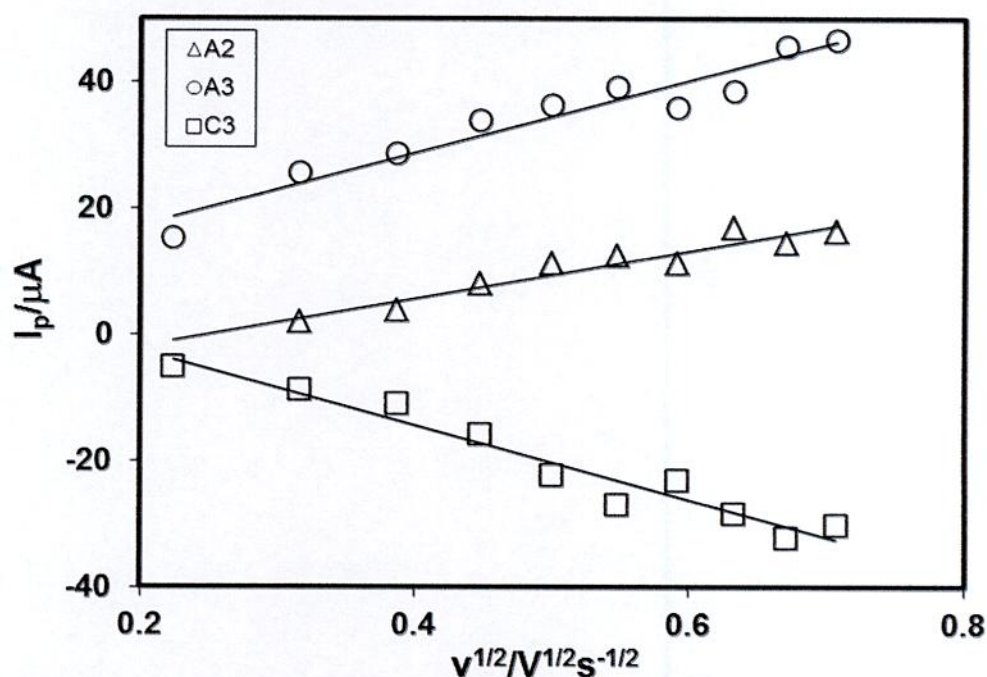
Fig. 4.39: Plots of peak current (I_p) versus square root of scan rate ($v^{1/2}$) of 2mM paracetamol + 200mM diethylamine of GC electrode in buffer solution (pH 7) (2nd cycle)
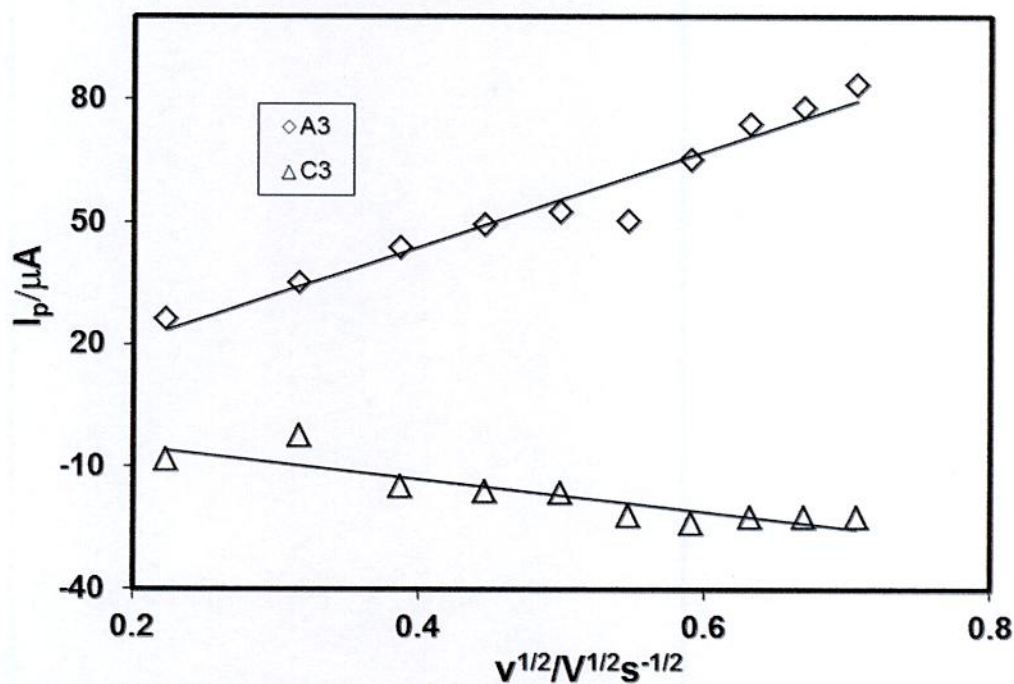
Fig. 4.40: Plots of peak current (I_p) versus square root of scan rate ($v^{1/2}$) of 2mM paracetamol + 250mM diethylamine of GC electrode in buffer solution (pH 7) at different scan rate (1st cycle)
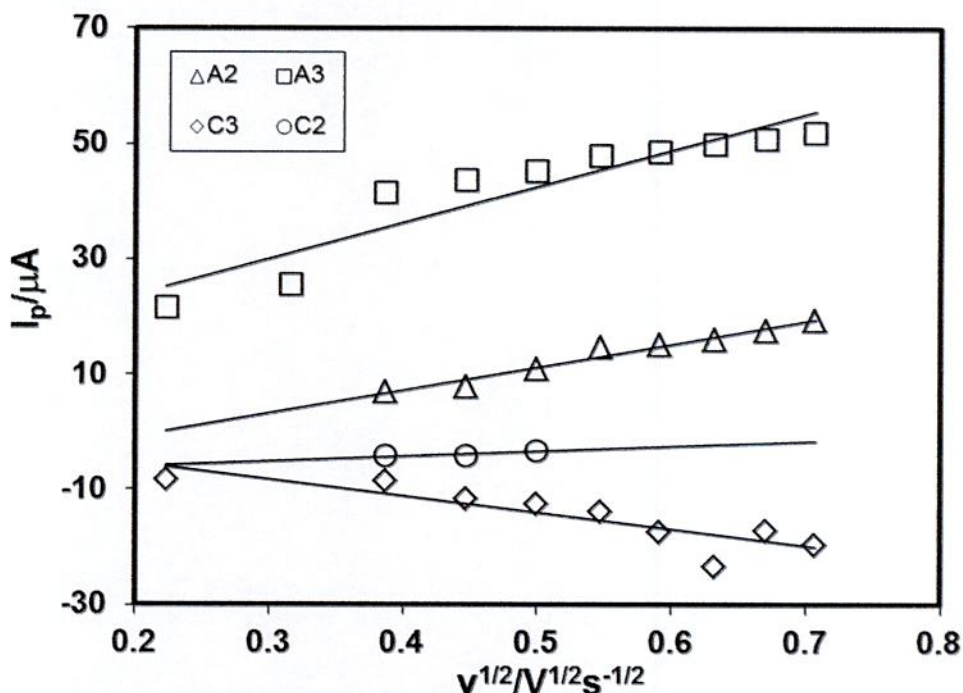
Fig. 4.41: Plots of peak current (I_p) versus square root of scan rate ($v^{1/2}$) of 2mM paracetamol + 250mM diethylamine at GC electrode in buffer solution (pH 7) at different scan rate (2nd cycle)
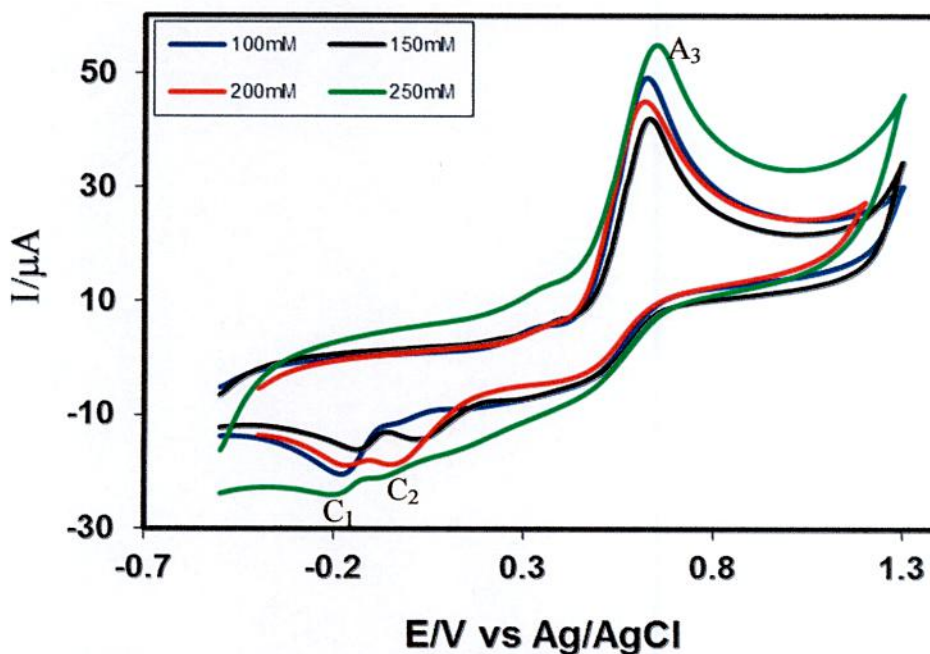
Fig. 4.42: Comparison of cyclic voltammogram of fixed 2mM paracetamol + different concentration (100, 150, 200 and 250mM) of diethylamine of GC electrode in buffer solution (pH 7) at scan rate 0.1V/s (1st cycle)
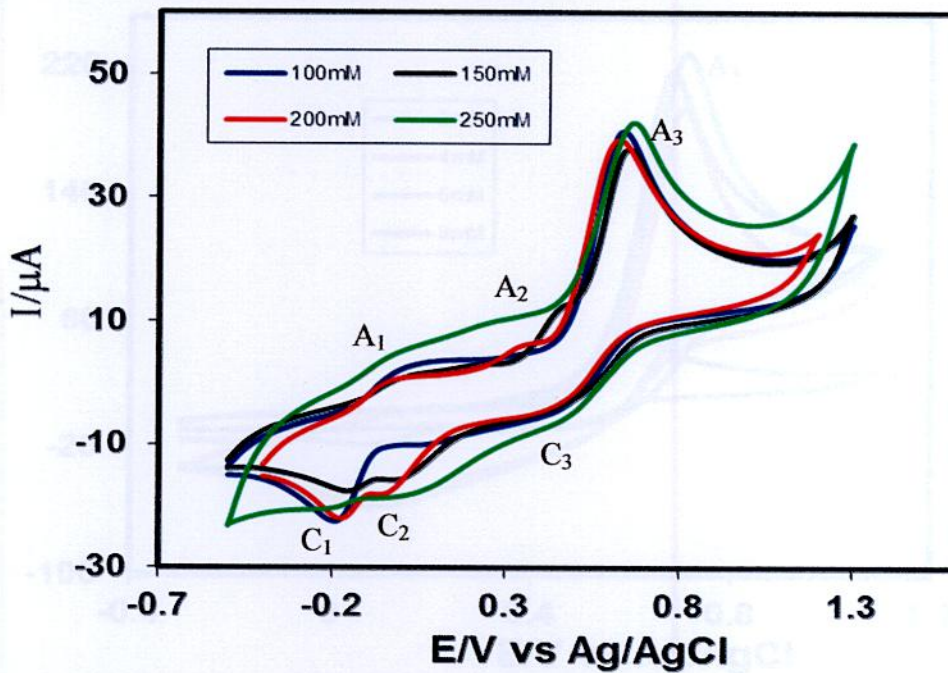
Fig. 4.43: Comparison of cyclic voltammogram of fixed 2mM paracetamol + different concentration (100, 150, 200, 250mM) of diethylamine of GC electrode at scan rate 0.1V/s in buffer solution (pH 7) (2nd cycle)
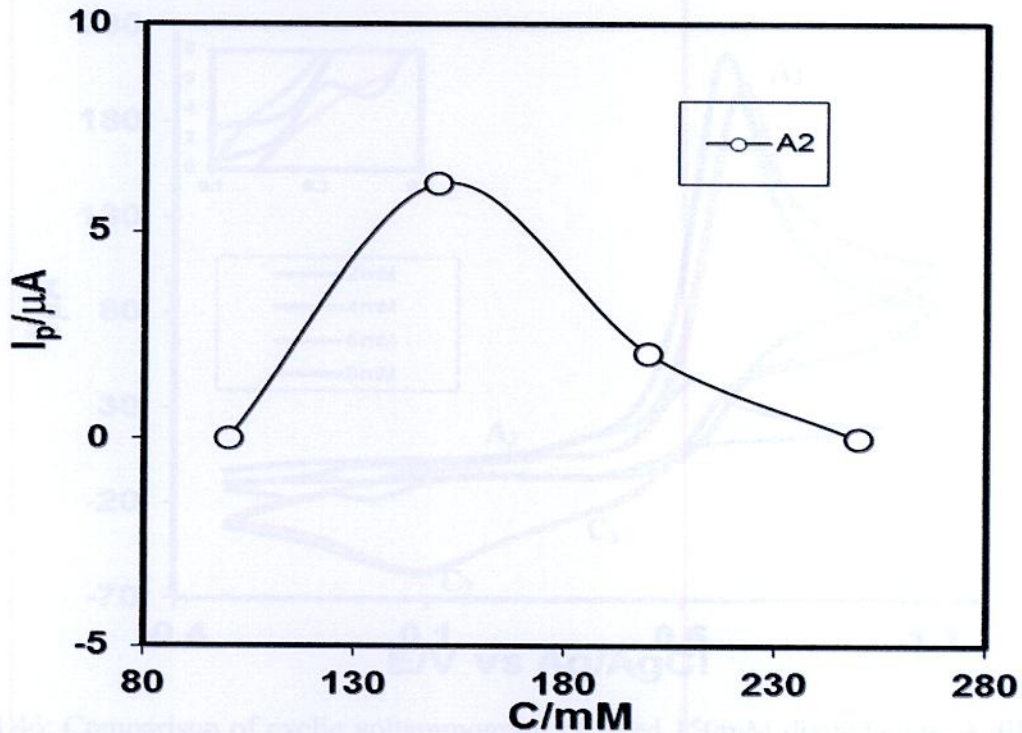
Fig. 4.44: Plots of peak current (I_p) versus different concentrations (C) (100, 150, 200 and 250mM) of diethylamine + 2mM paracetamol (fixed) of GC electrode at scan rate 0.1V/s in buffer solution (pH 7) (2nd cycle)
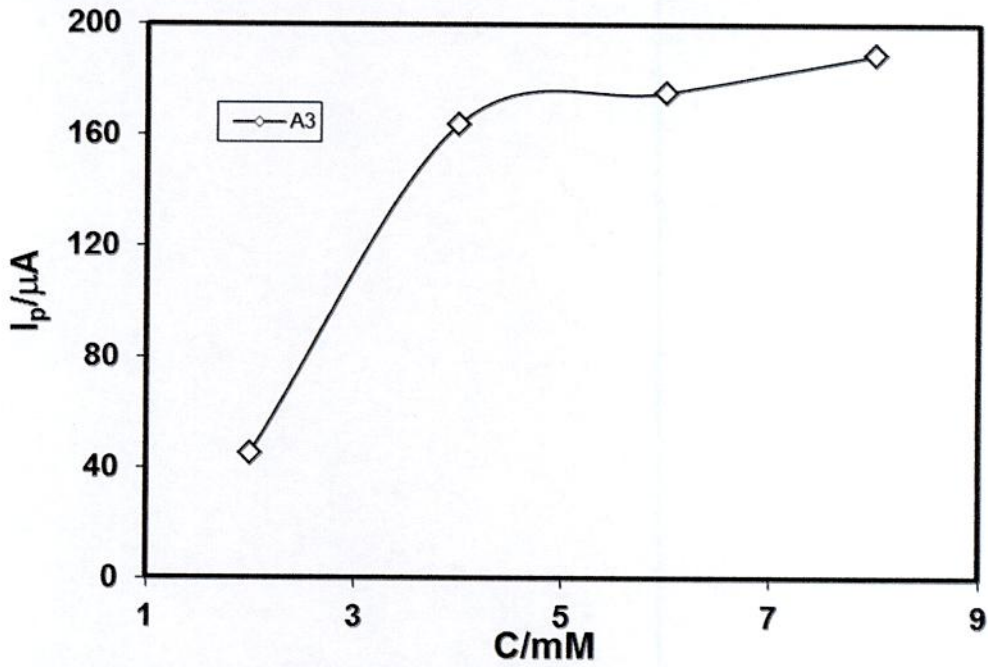
Fig. 4.47: Plots of peak current (I_p) versus different concentration (C) (2, 4, 6, 8mM) of paracetamol + 150mM diethylamine (fixed) of GC electrode (2nd cycle) at scan rate 0.1V/s in buffer solution (pH 7)
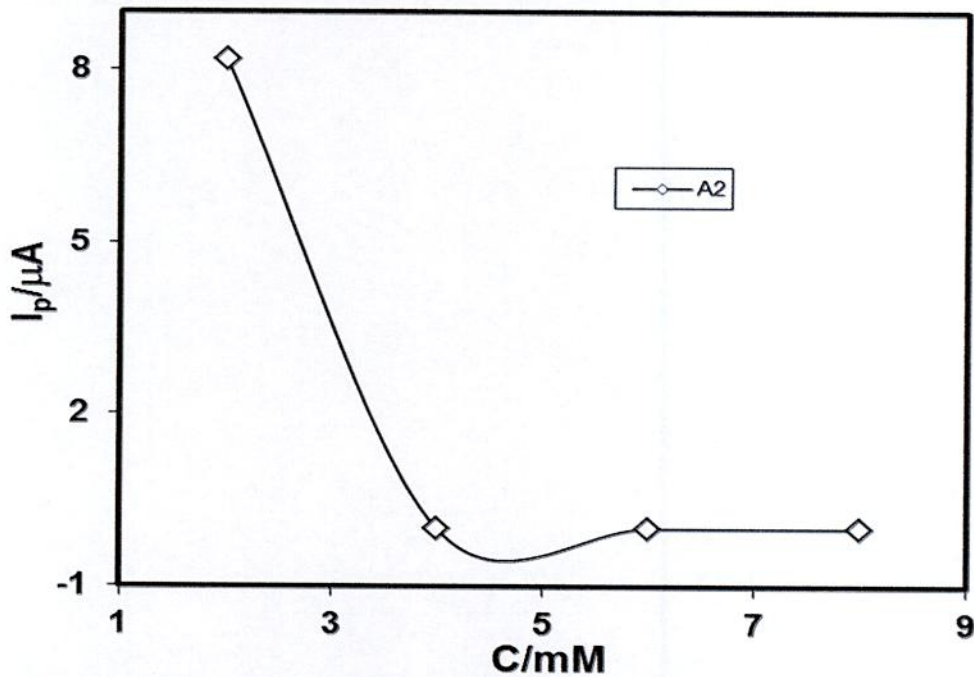
Fig. 4.48: Plots of peak current (I_p) versus different concentration (C) (2, 4, 6, 8mM) of paracetamol + 150mM diethylamine (fixed) of GC electrode at scan rate 0.1V/s (2nd cycle) in buffer solution (pH 7) for appeared peak (A_2)
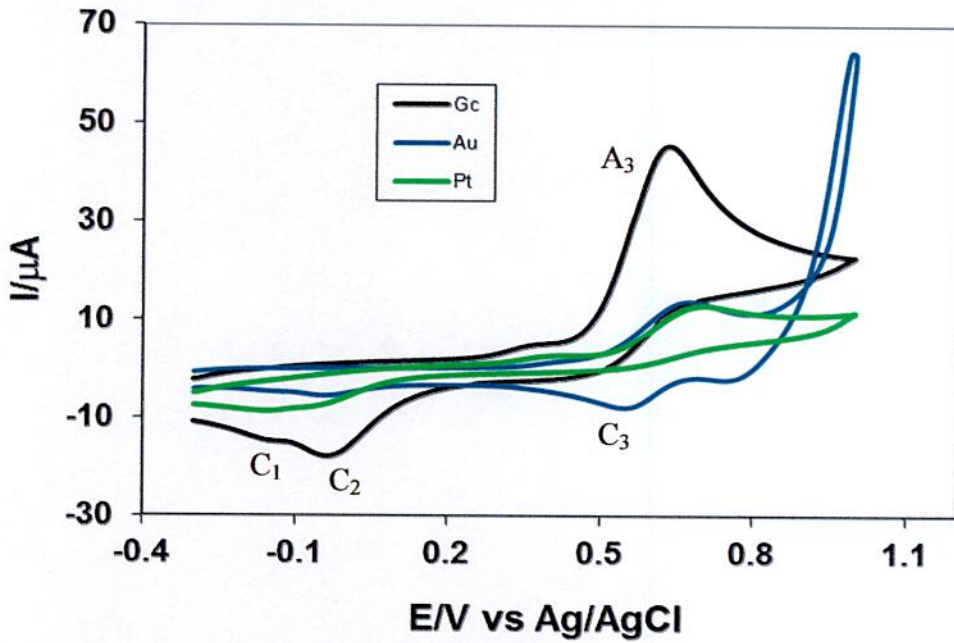
Fig. 4.49: Comparison of cyclic voltammogram of 2mM paracetamol + 150mM diethylamine of different electrode (GC, Au, Pt) at scan rate 0.1V/s (1st cycle) in buffer solution (pH 7), A_3= oxidation peak, C_3= reduction peak
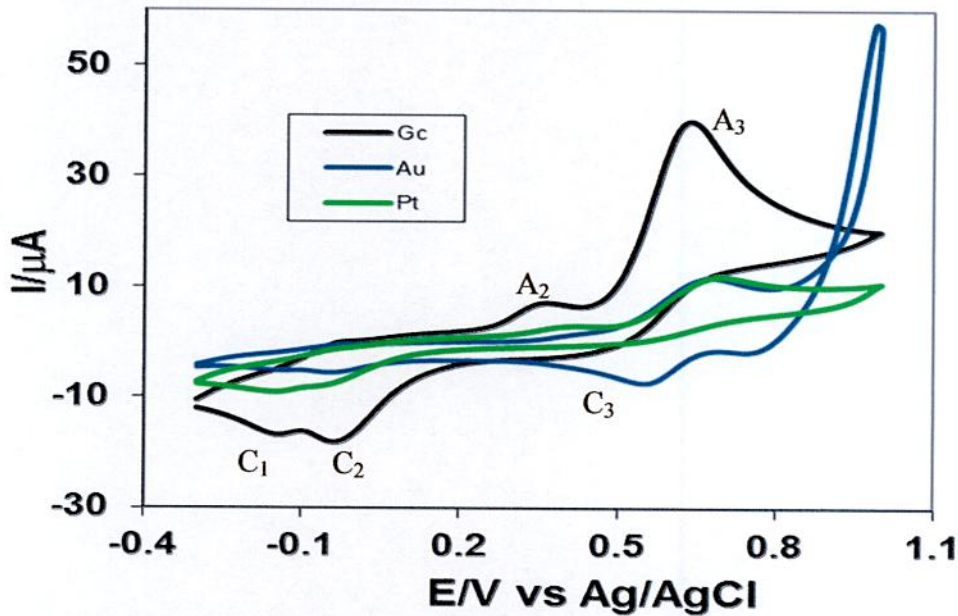
Fig. 4.50: Comparison of cyclic voltammogram of 2mM paracetamol + 150mM diethylamine of different electrode (GC, Au, Pt) at scan rate 0.1V/s (2nd cycle) in buffer solution (pH 7), A_2= appeared oxidation peak, C_2= appeared reduction peak
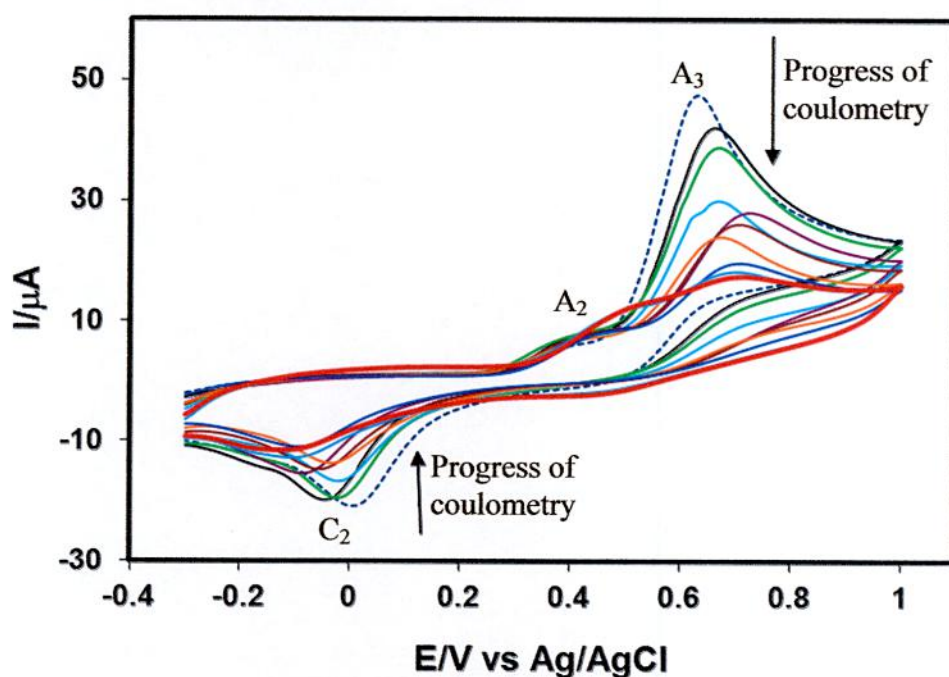
Fig. 4.51: Cyclic voltammogram of 1mM paracetamol + 75mM diethylamine during control potential coulometry of GC electrode in buffer solution (pH 7) at stepping potential 0.5V (time 0 to 18000s)
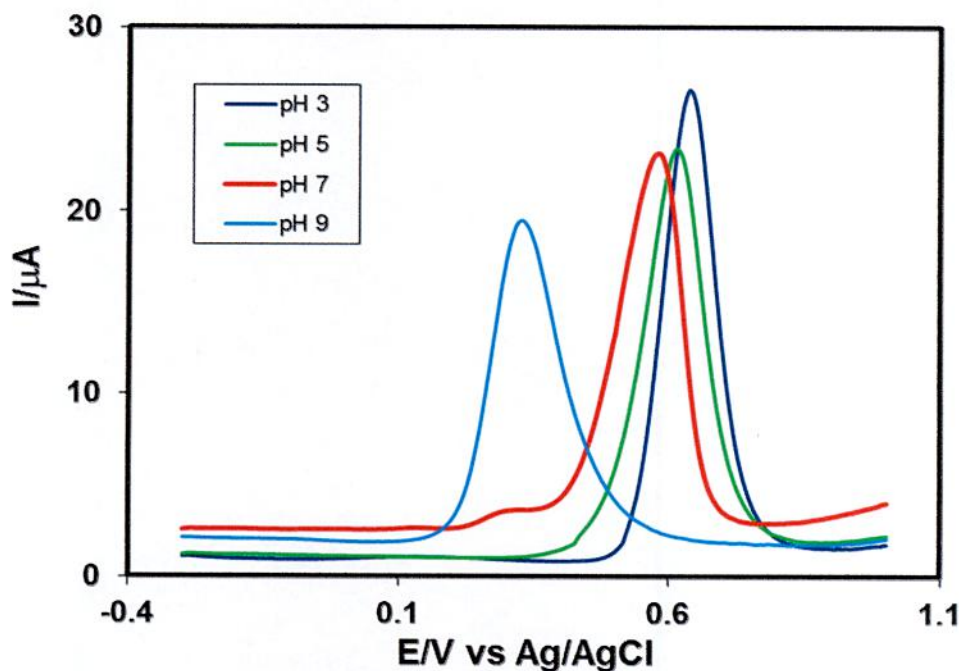
Fig. 4.52: Comparison of differential pulse voltammogram of 2mM paracetamol + 150mM diethylamine in different buffer solution of pH (3, 5, 7 and 9) at scan rate 0.1V/s (1st cycle), where E_{pulse} 0.02V and t_{pulse} 20.0s
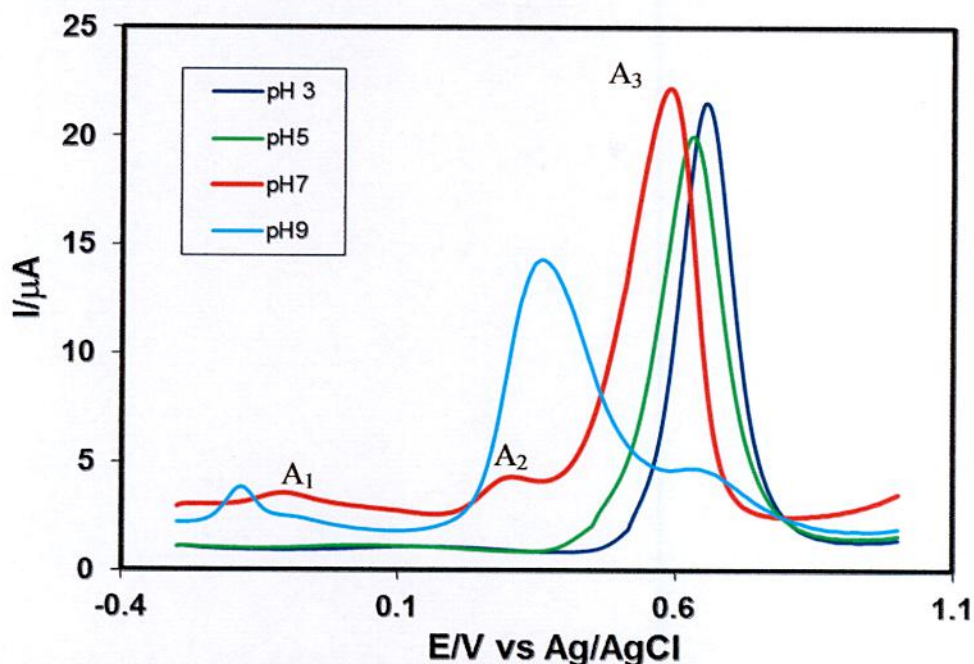
Fig. 4.53: Comparison of differential pulse voltammogram of 2mM paracetamol + 150mM diethylamine in different buffer solution of pH (3, 5, 7 and 9) at scan rate 0.1V/s (2nd cycle), E_{pulse} 0.02V and t_{pulse} 20.0s
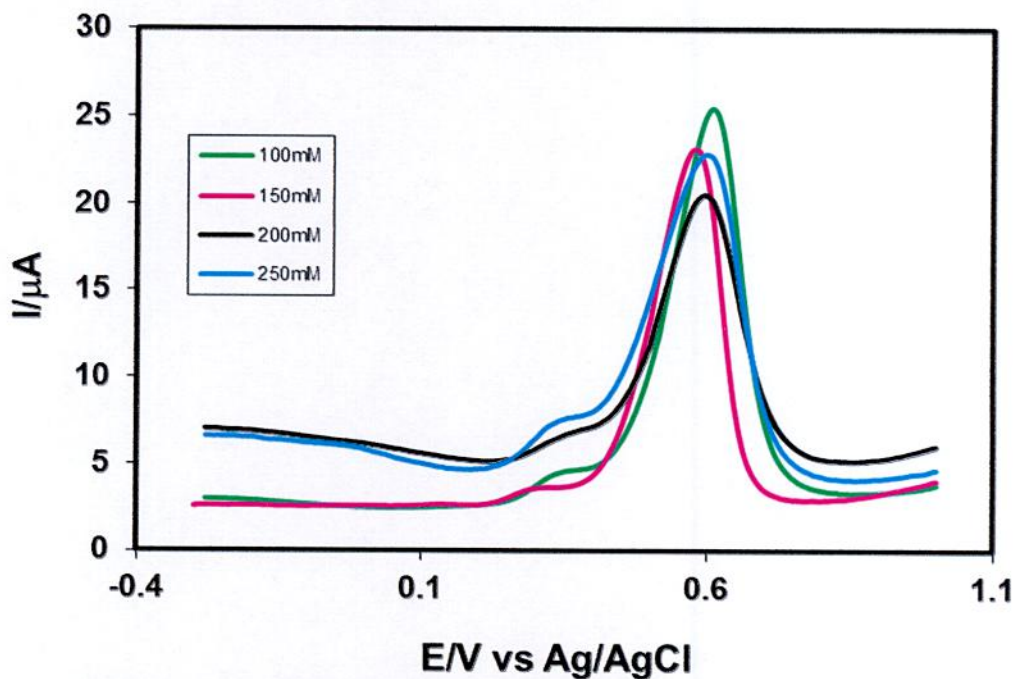
Fig. 4.54: Comparison of differential pulse voltammogram of fixed 2mM paracetamol + different concentration (100, 150, 200 and 250mM) of diethylamine of GC electrode in buffer solution (pH 7) at scan rate 0.1V/s (1st cycle), E_{pulse} 0.02V and t_{pulse} 20.0ms
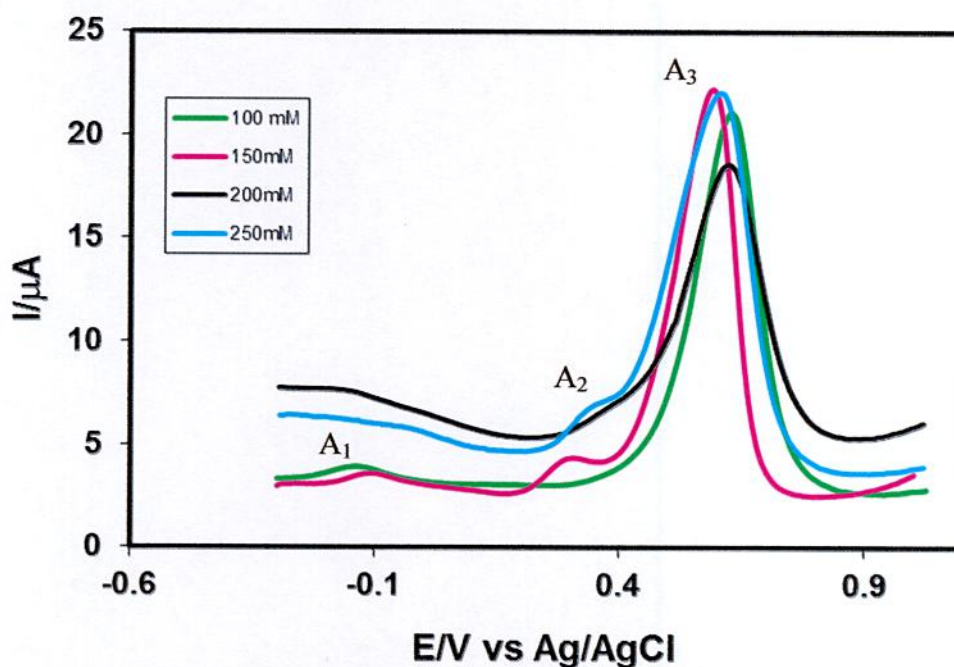
Fig. 4.55: Comparison of differential pulse voltammogram of fixed 2mM paracetamol + different concentration (100, 150, 200, 250mM) of diethylamine of GC electrode in buffer solution (pH 7) at scan rate 0.1V/s (2nd cycle), E_{pulse} 0.02V and t_{pulse} 20.0ms
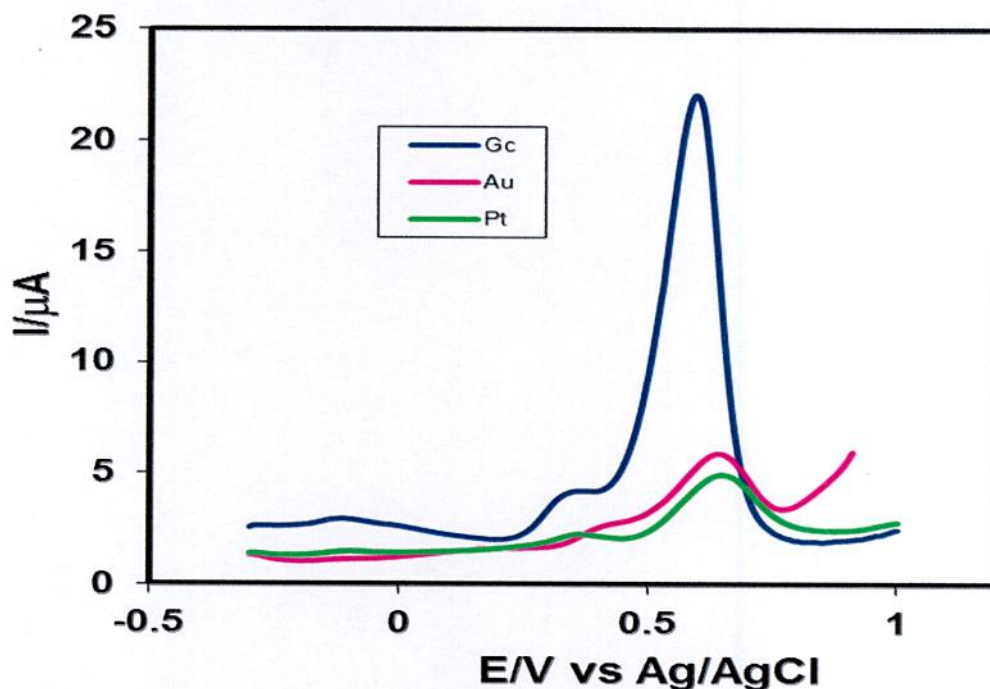
Fig. 4.56: Comparison of differential pulse voltammogram of 2mM paracetamol + 150mM diethylamine of different electrode (GC, Au, Pt) in buffer solution (pH 7) at scan rate 0.1V/s (2nd cycle), E_{pulse} 0.02V, t_{pulse} 20.0s
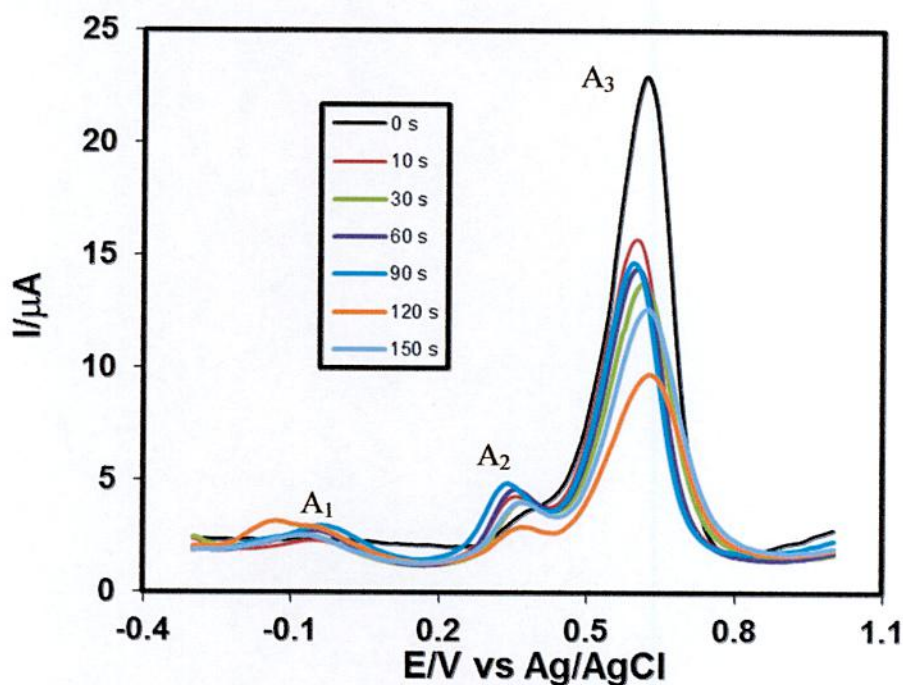
Fig. 4.57: Differential pulse voltammogram of deposition time change of 2mM paracetamol + 150mM diethylamine of GC electrode in buffer solution (pH 7) at scan rate 0.1V/s, E_{pulse} 0.02V, t_{pulse} 20.0ms and applied potential 0.5V
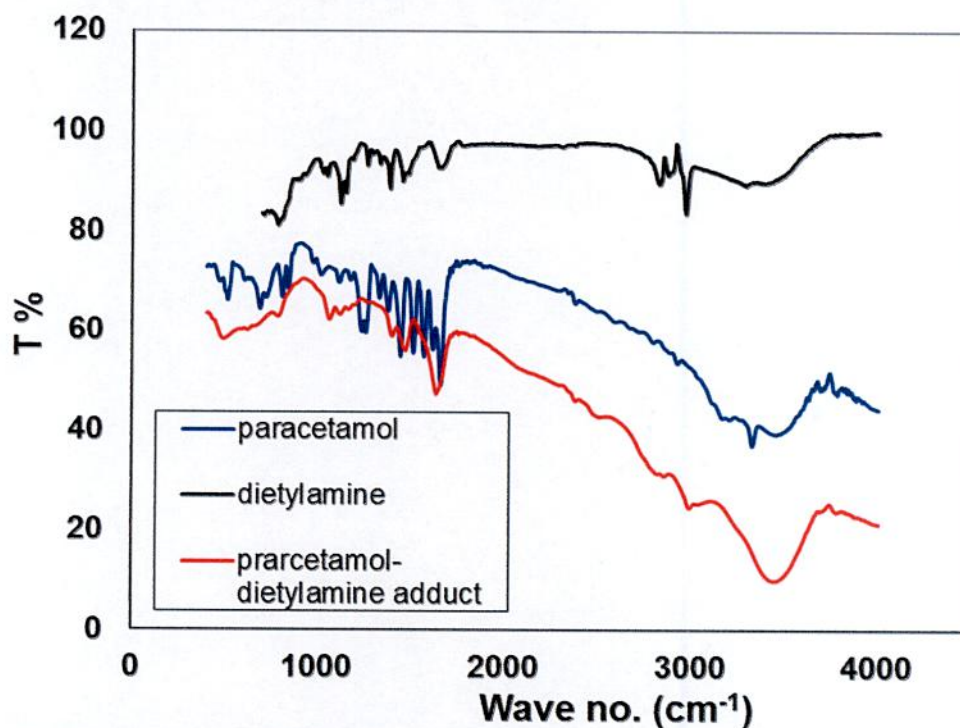
Fig. 4.58: Comparison of FTIR of only paracetamol, only diethylamine and paracetamol-diethylamine adduct
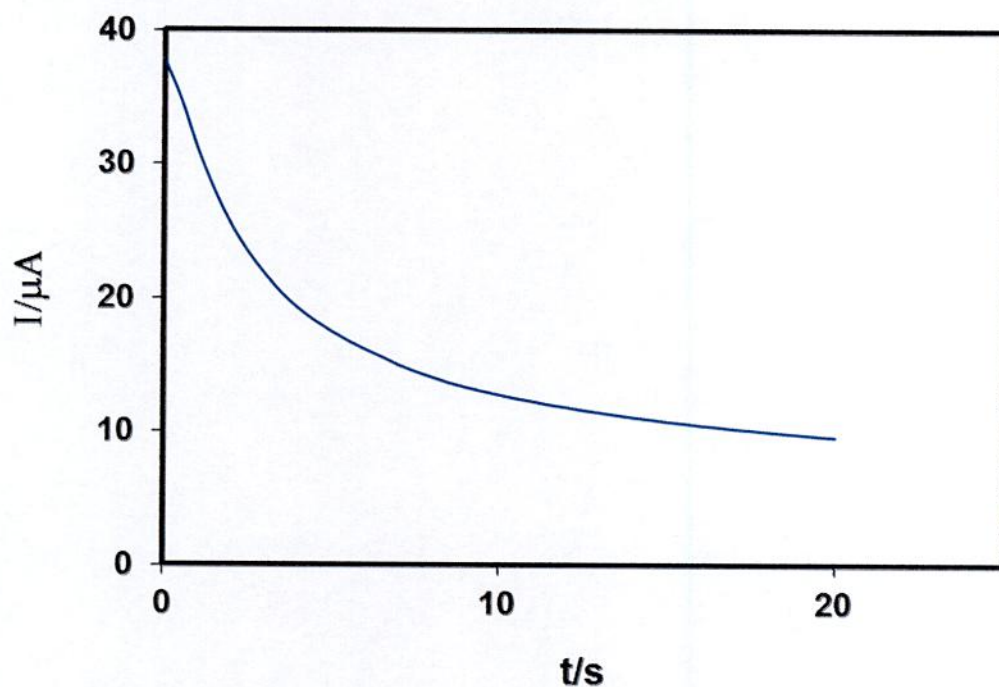
Fig. 4.59: Chronoamperogram of 2mM paracetamol + 150mM diethylamine of GC electrode in buffer solution (pH 7) at potential 0.31V and time 20s
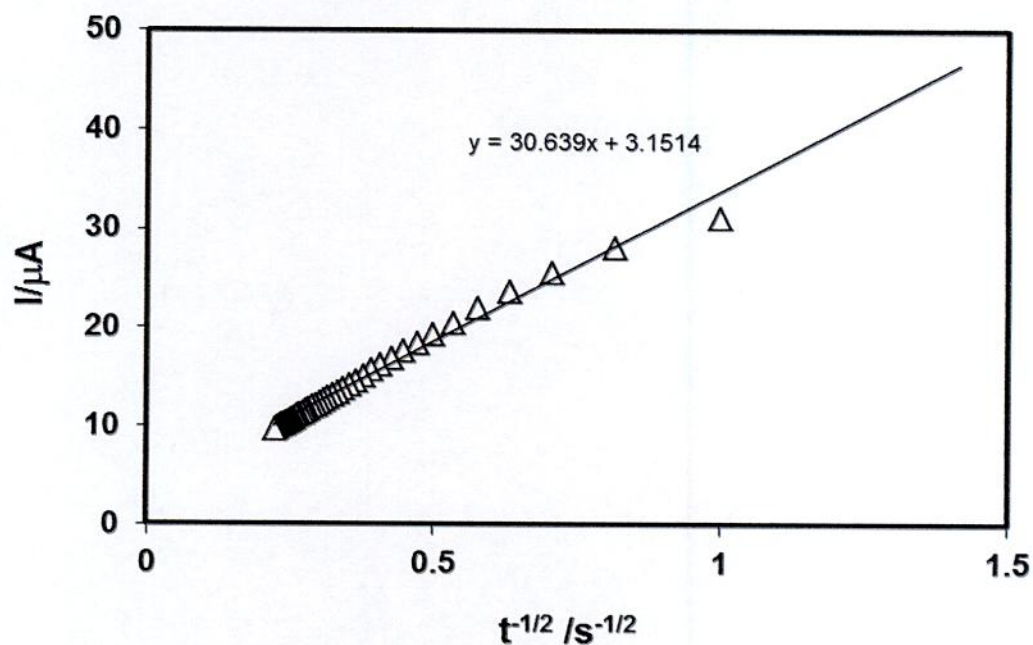
Fig. 4.60: Cottrell plots of the back-ground subtracted currents for 2mM paracetamol + 150mM diethylamine in buffer solution (pH 7) when the potential was stepped from 0.31V
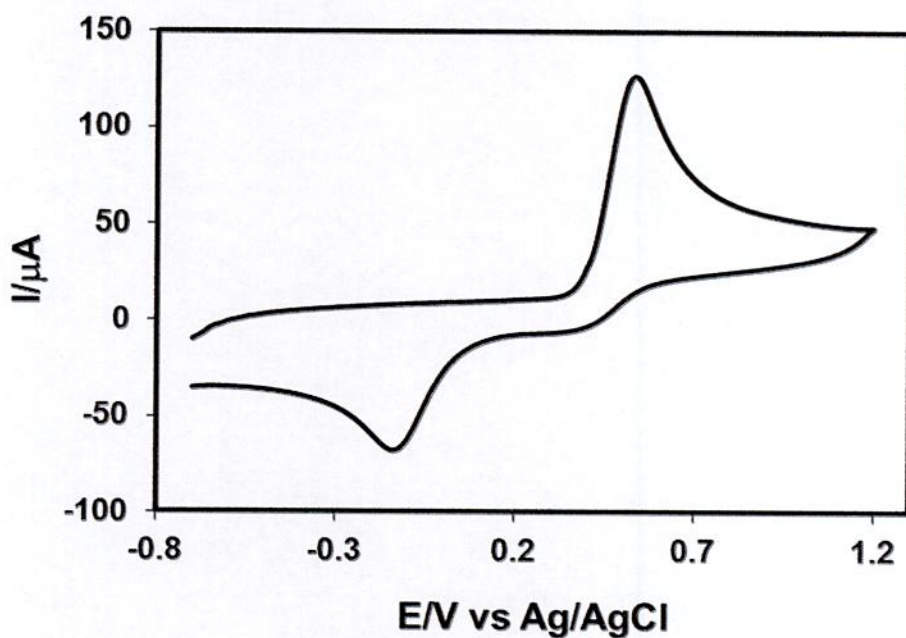
Fig. 4.61: Cyclic voltammogram of only 2mM paracetamol in buffer solution (pH 7) of GC electrode at scan rate 0.5V/s (1ˢᵗ cycle)
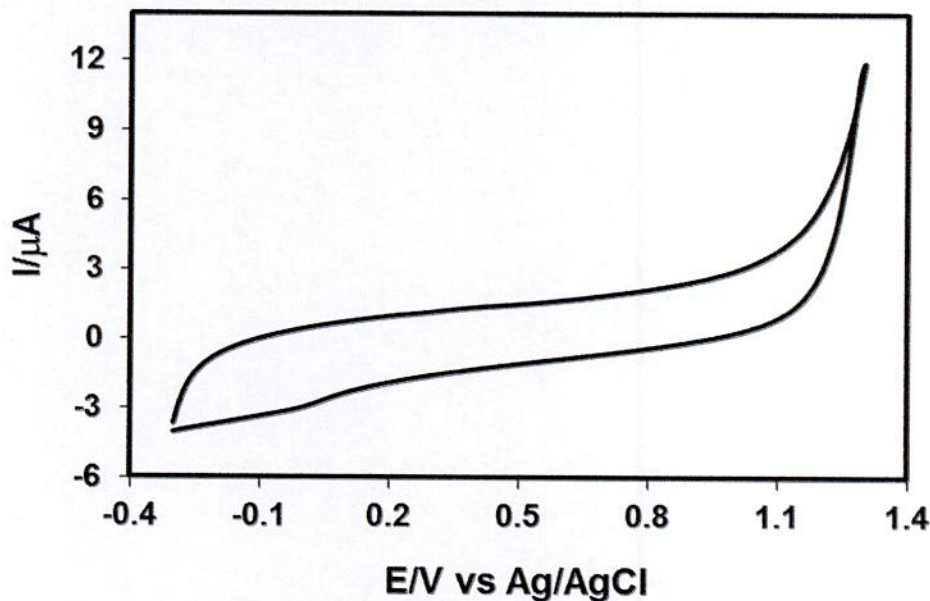
Fig. 4.62: Cyclic voltammogram of only 150mM diisopropylamine of GC electrode in buffer solution (pH 7) at scan rate 0.5V/s (1ˢᵗ cycle)
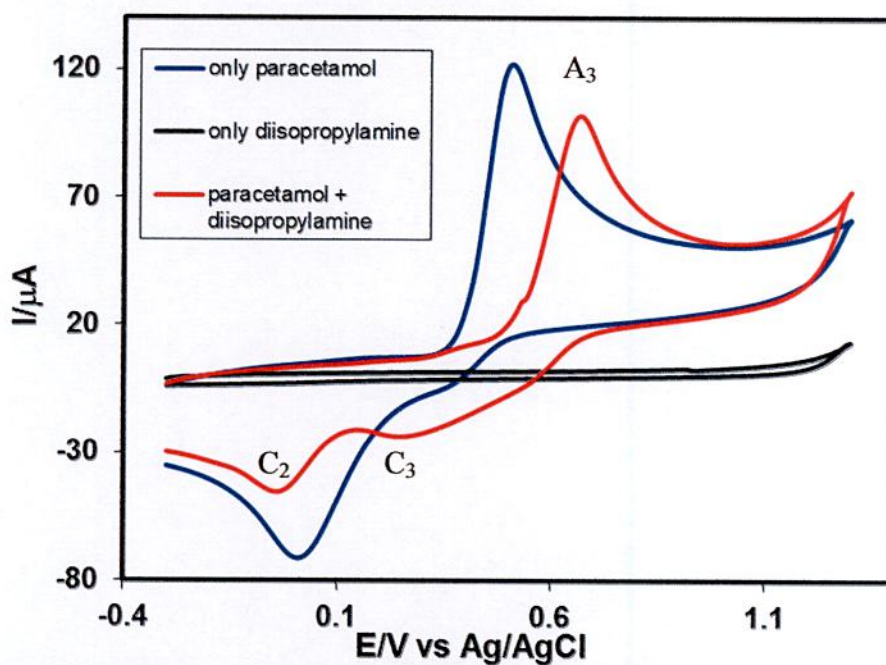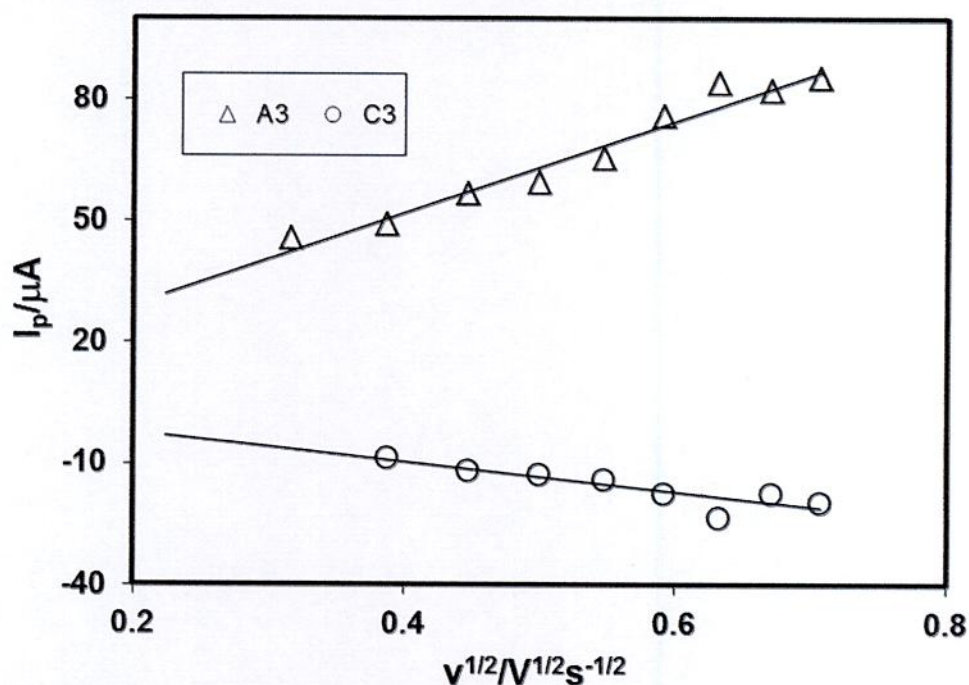
Fig. 4.63: Comparison of Cyclic voltammogram of 2mM paracetamol, 150mM diisopropylamine and 2mM paracetamol + 150mM diisopropylamine of GC electrode in buffer solution (pH 7) at scan rate 0.5V/s (1st cycle), where A_3= Oxidation peak, C_3= Reduction peak
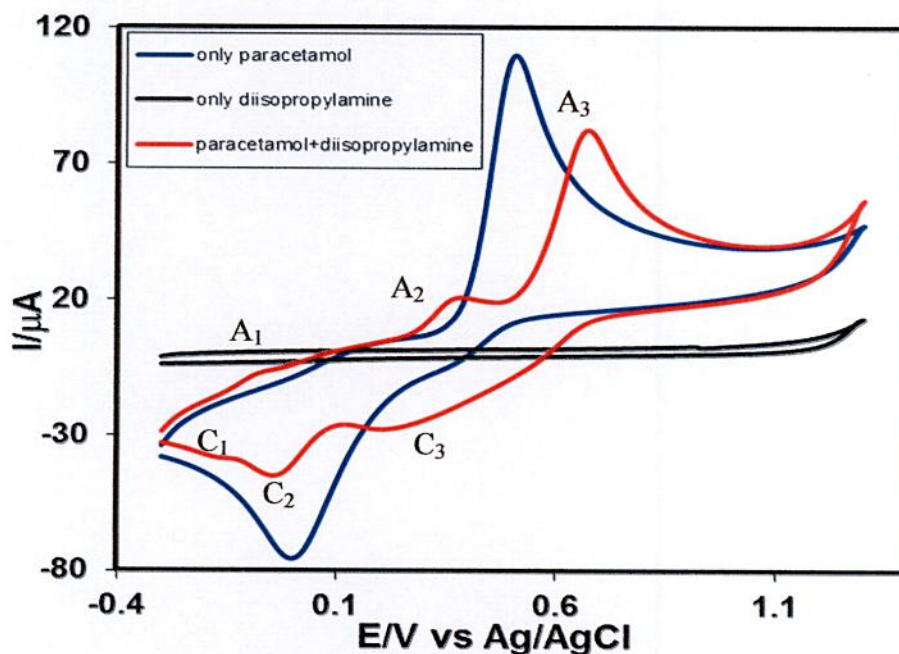
Fig. 4.64: Cyclic voltammogram of only 2mM paracetamol, only 150mM diisopropylamine and 2mM paracetamol + 150mM diisopropylamine of GC electrode in buffer solution (pH 7) at scan rate 0.5 V/s (2nd cycle), where A_1 and A_2= Appeared anodic peaks, A_3= Oxidation peak, C_1 and C_2 = Appeared reduction peaks, C_3 = Reduction peak
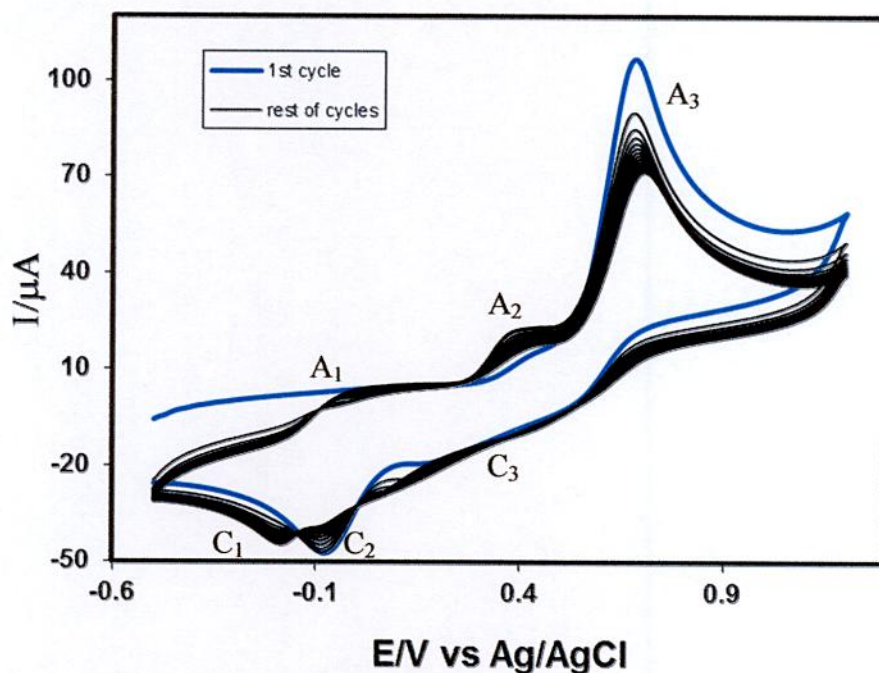
Fig. 4.65: Cyclic voltammogram of first 15 cycles of 2mM paracetamol + 150mM diisopropylamine of GC electrode in buffer solution (pH 7) at scan rate 0.5V/s
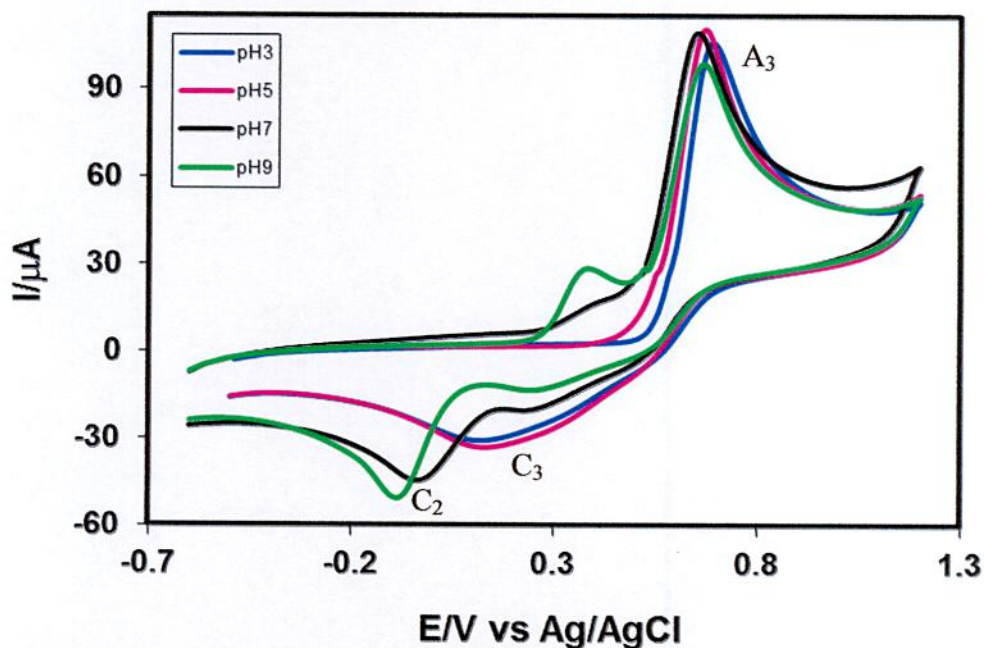
Fig. 4.66: Comparison of cyclic voltammogram of 2mM paracetamol + 150mM diisopropylamine at different pH (3, 5, 7 and 9) of GC electrode at scan rate 0.5V/s (1st cycle)
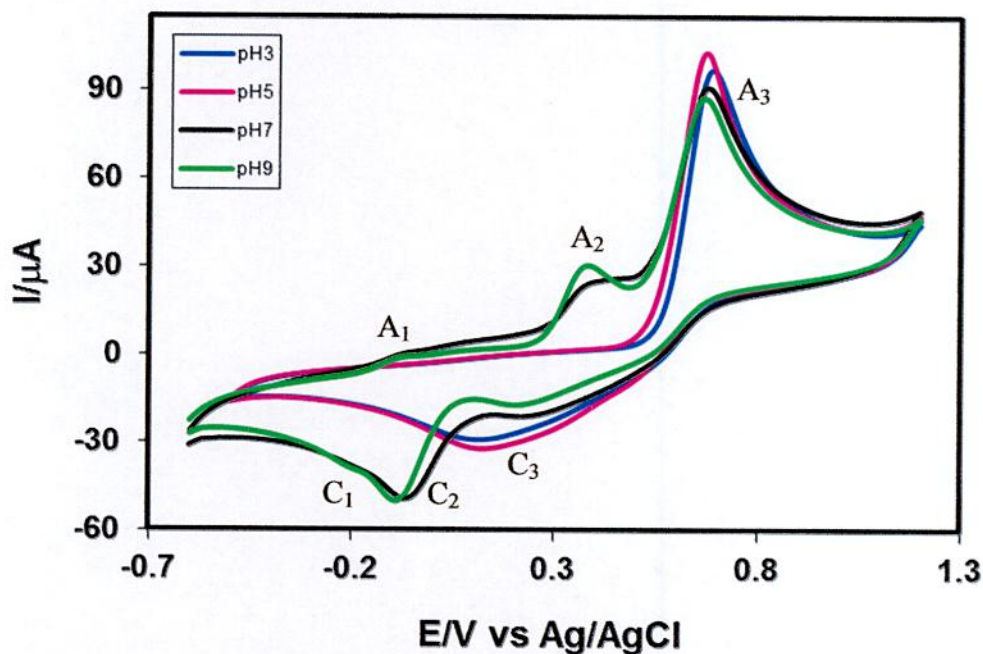
Fig. 4.67: Comparison of cyclic voltammogram of 2mM paracetamol + 150mM diisopropylamine at different pH different (3, 5, 7 and 9) of GC electrode at scan rate 0.5V/s (2nd cycle)
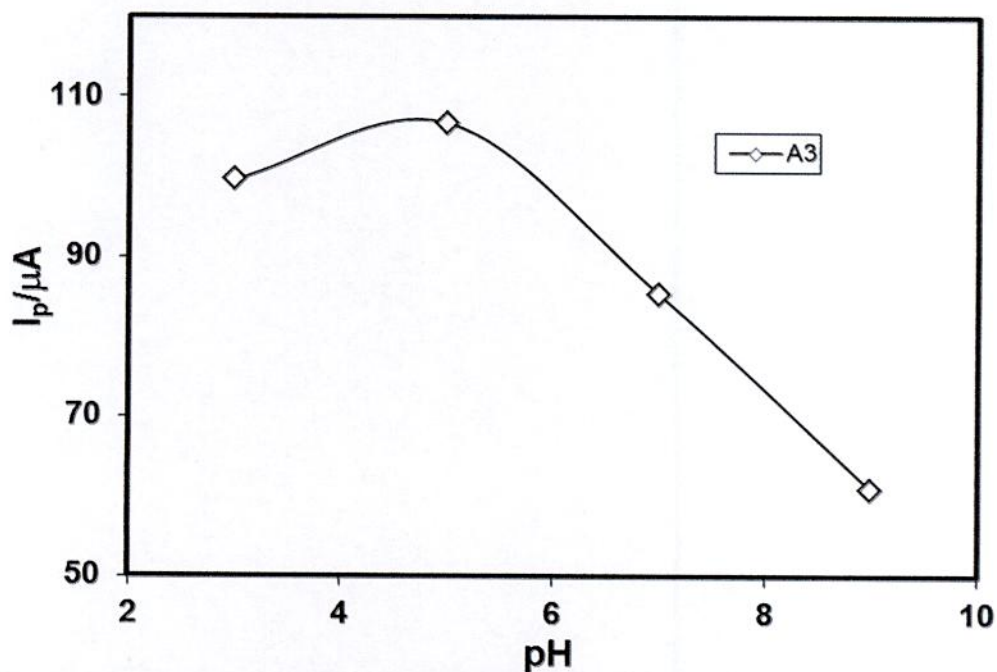
Fig. 4.68: Plots of peak current (I$_p$) versus different pH (3, 5, 7 and 9) of 2mM paracetamol + 150mM diisopropylamine of GC electrode at scan rate 0.5V/s (2nd cycle)
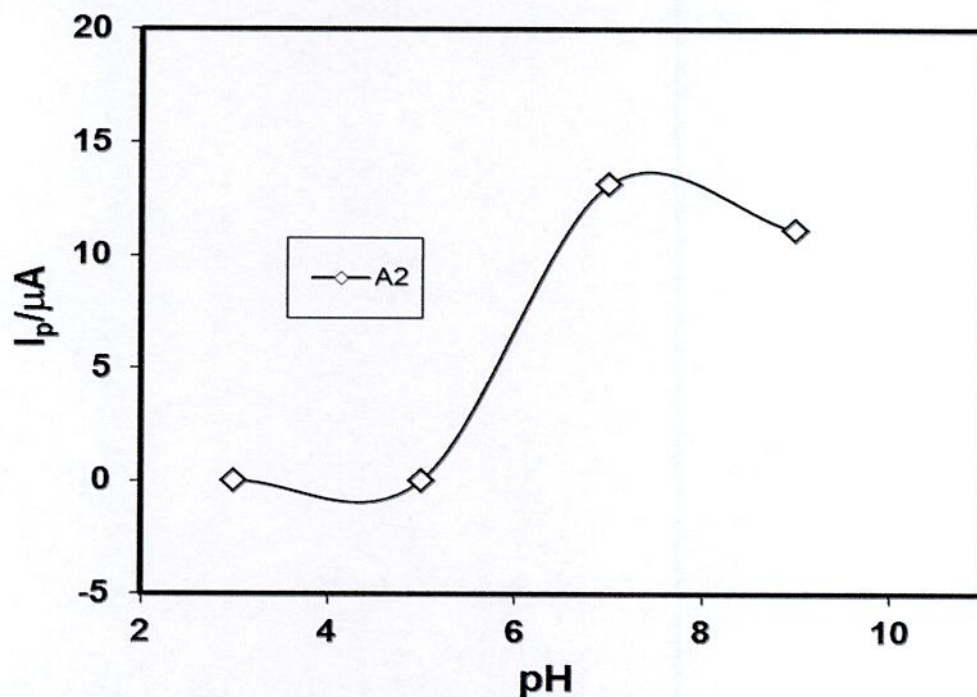
Fig. 4.69: Plots of peak current (I_p) versus different pH (3, 5, 7 and 9) of 2mM paracetamol + 150mM diisopropylamine of GC electrode at scan rate 0.5V/s (2nd cycle)
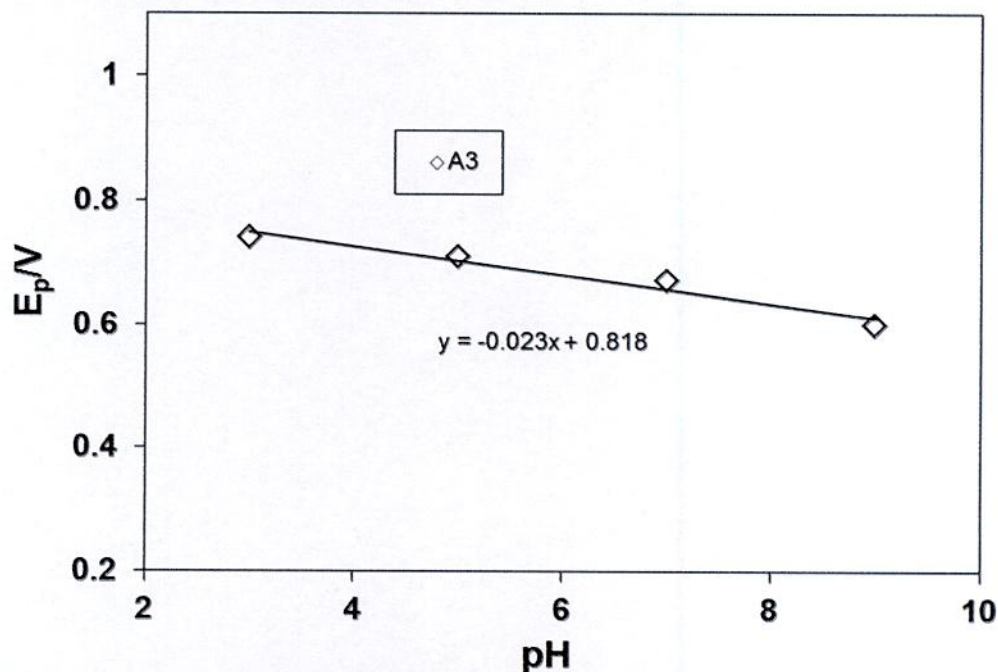
Fig. 4.70: Plots of peak potential (E_p) versus different pH (3, 5, 7 and 9) of 2mM paracetamol + 150mM diisopropylamine of GC electrode at scan rate 0.5V/s (2nd cycle)
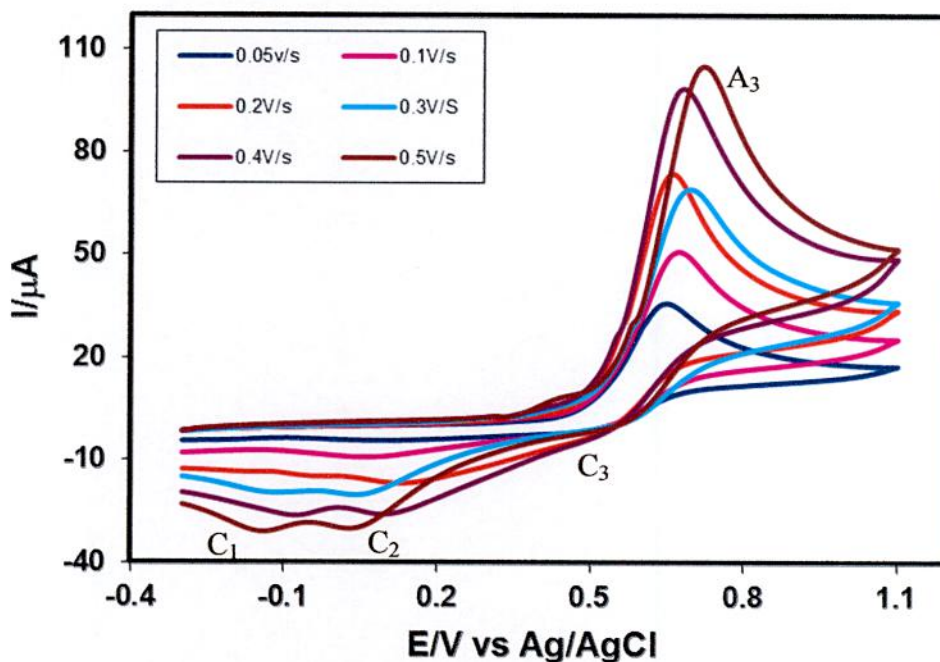
Fig. 4.71: Cyclic voltammogram of 2mM paracetamol + 150mM diisopropylamine of GC electrode in buffer solution (pH 7) at different scan rate (1st cycle)
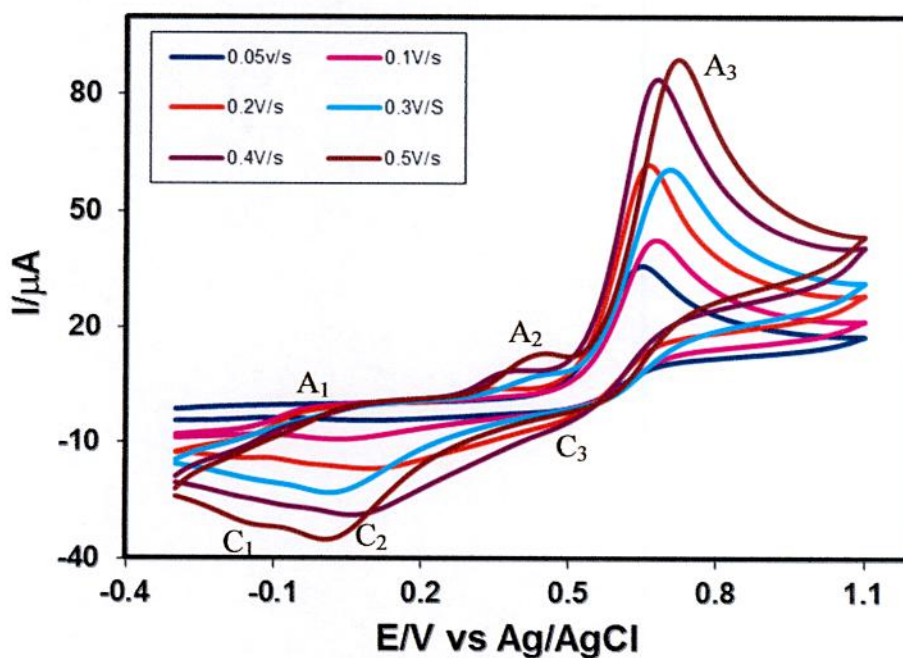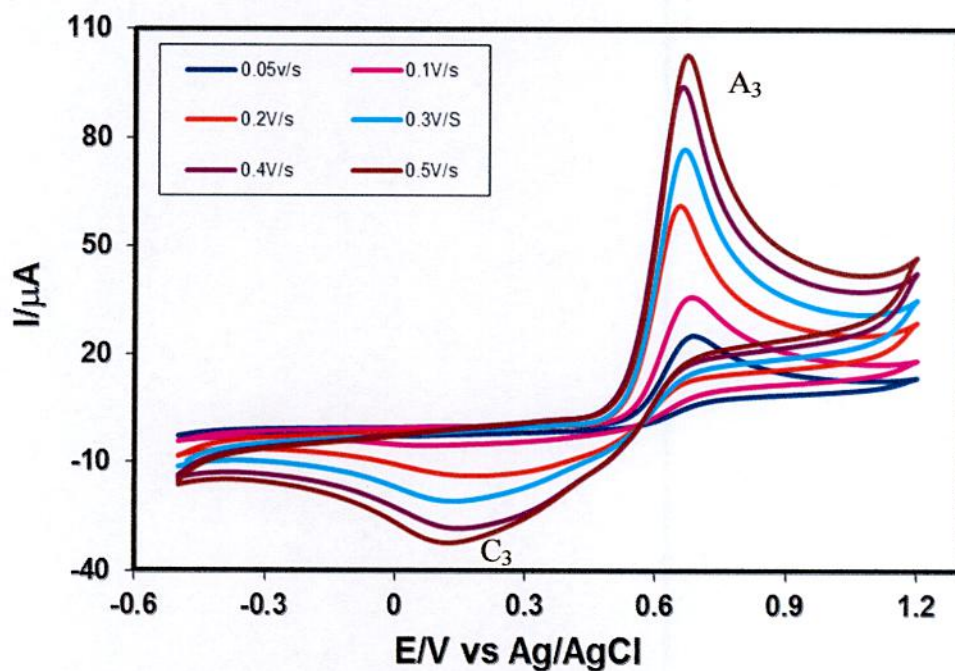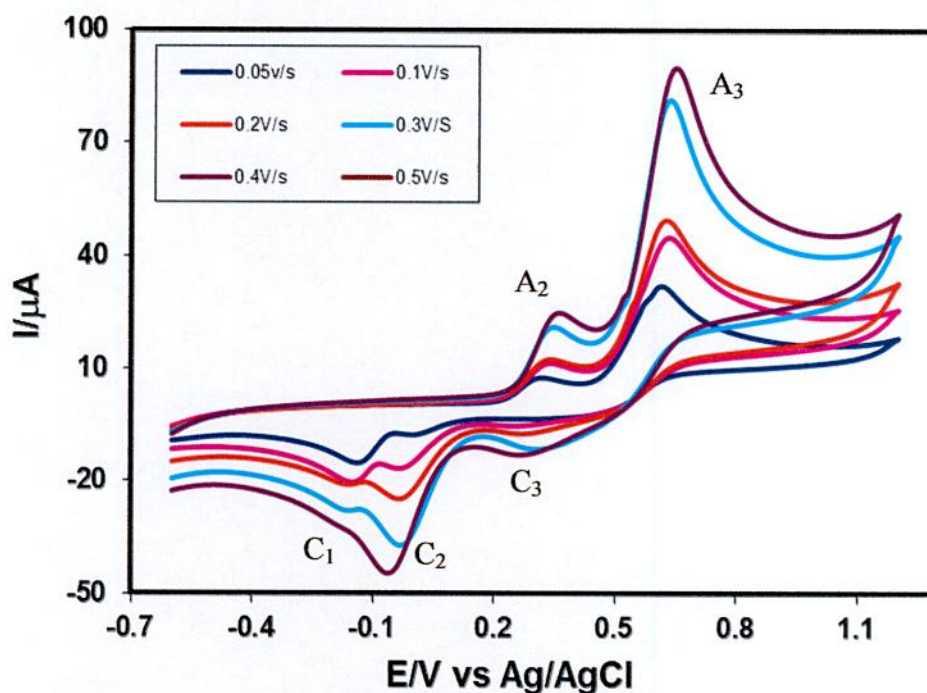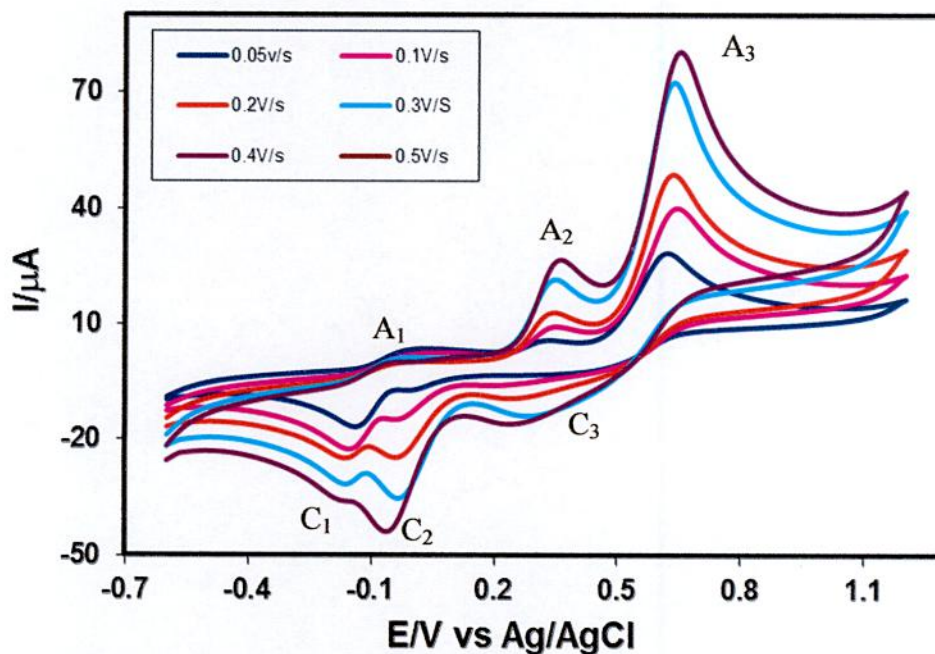

Fig. 4.72: Cyclic voltammogram of 2mM paracetamol + 150mM diisopropylamine of GC electrode in buffer solution (pH 7) at different scan rate (2nd cycle)
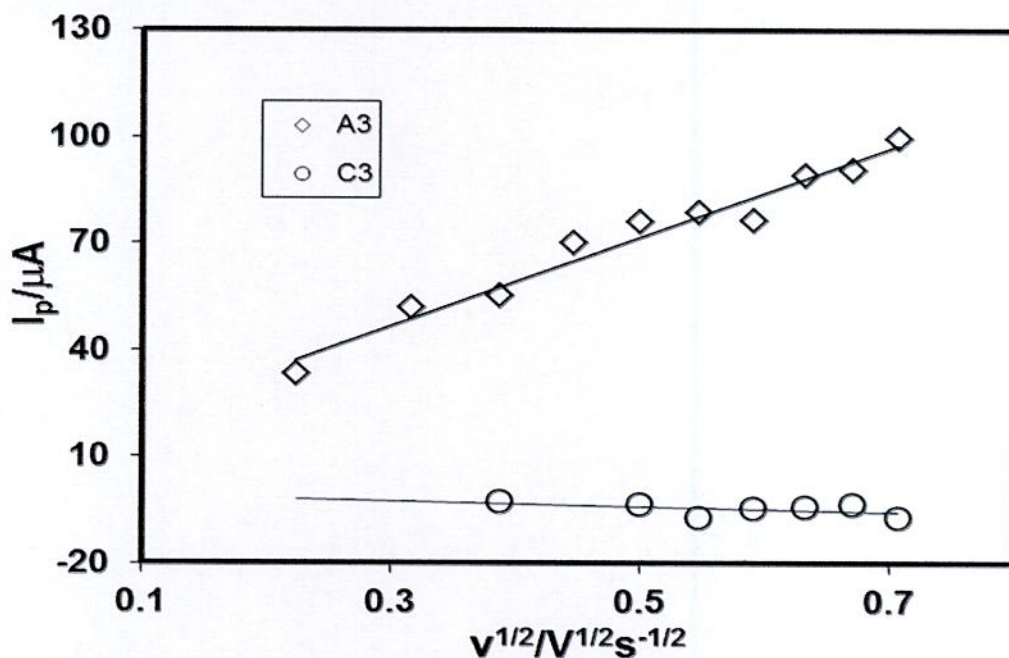
111

Fig. 4.73: Plots of peak current (I_p) versus square root of scan rate ($v^{1/2}$) of 2mM paracetamol + 150mM diisopropylamine of GC electrode in buffer solution (pH 7) (1st cycle)
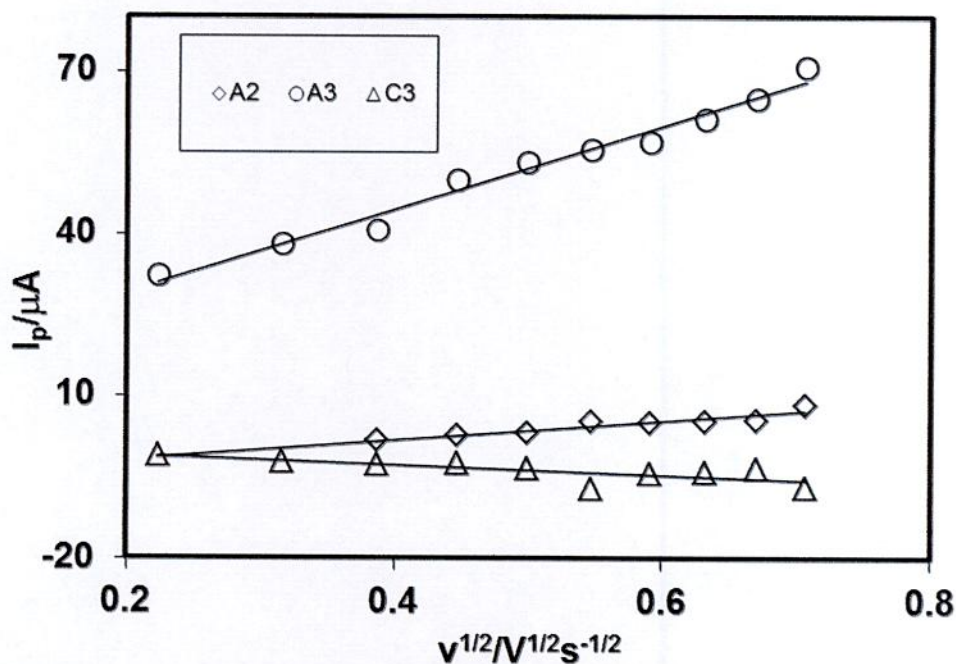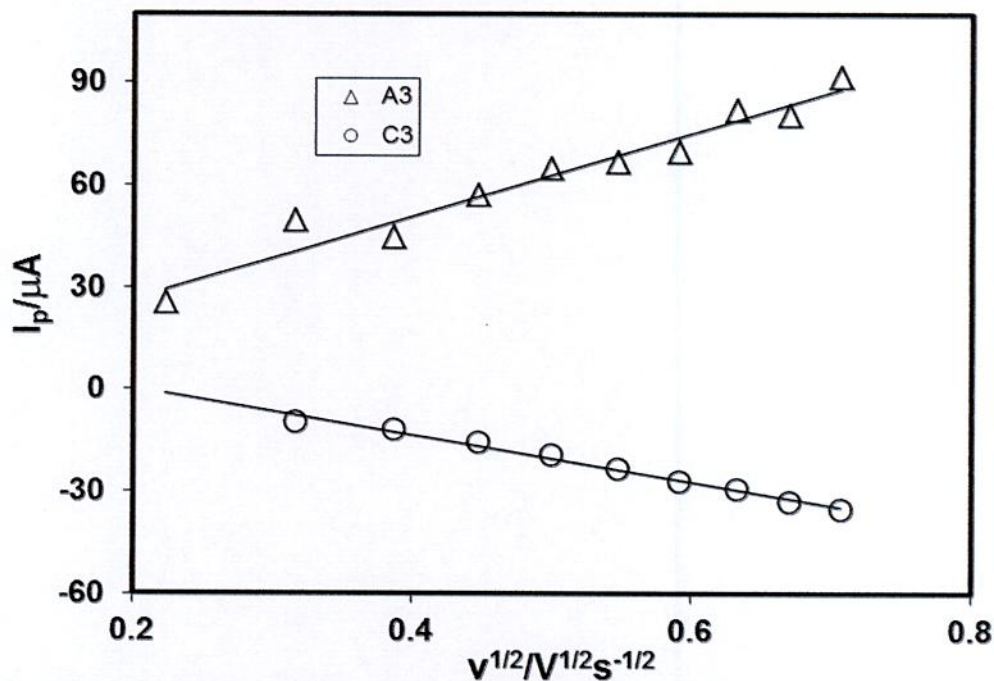

Fig. 4.74: Plots of peak current (I_p) versus square root of scan rate ($v^{1/2}$) of 2mM paracetamol + 150mM diisopropylamine of GC electrode in buffer solution (pH 7) (2nd cycle)
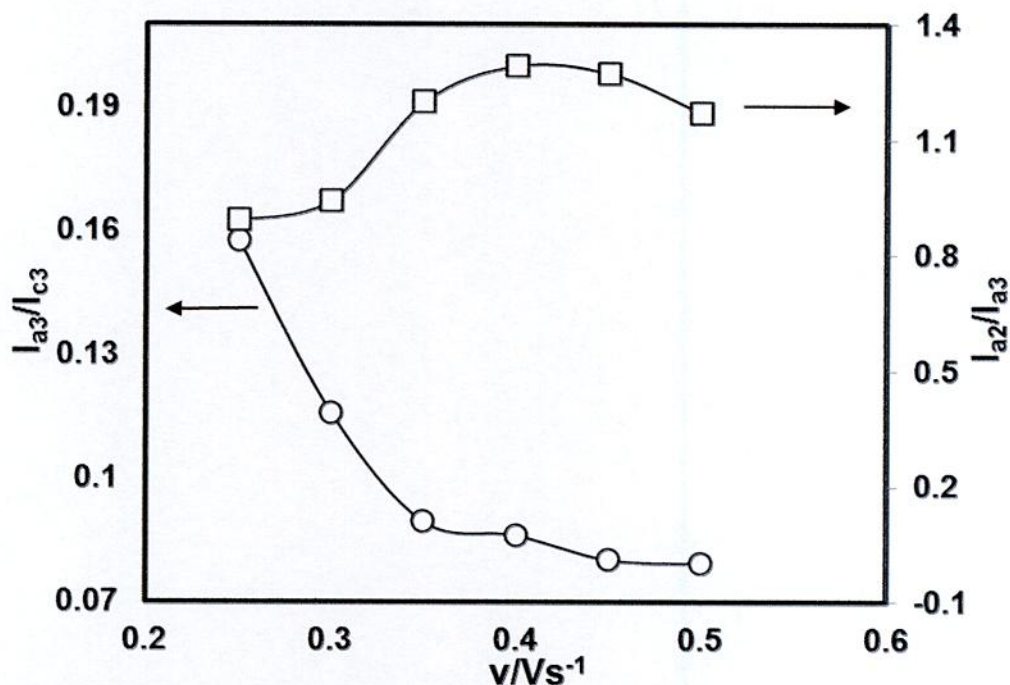
Fig. 4.75: Variation of peak current ratio of corresponding peak (I_{a3}/I_{c3}) and anodic peak (I_{a2}/I_{a3}) versus scan rate (v) of 150mM diisopropylamine + 2mM paracetamol of GC electrode in buffer solution (pH 7)
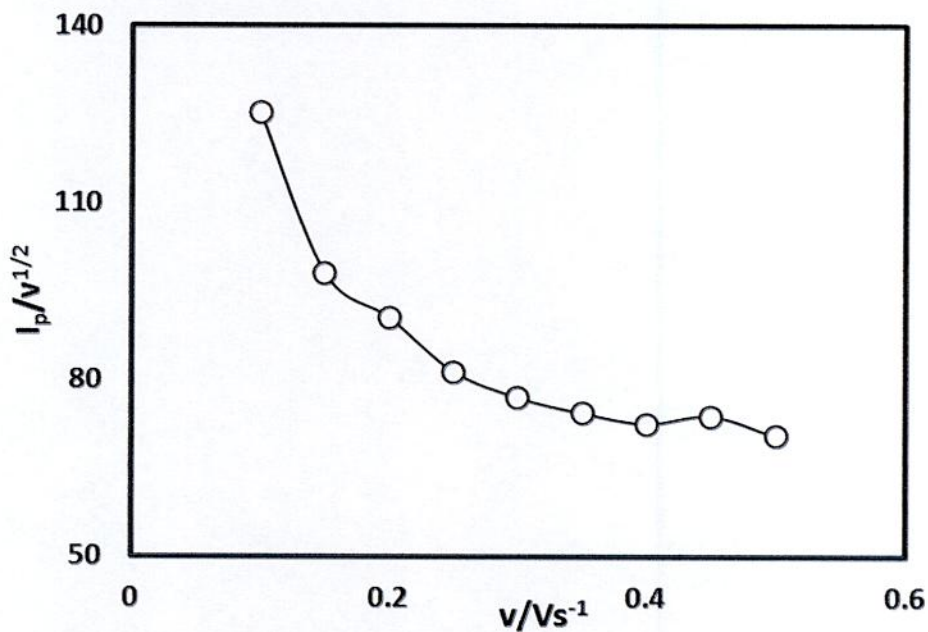
Fig. 4.76: Plots of current function ($I_p/v^{1/2}$) versus scan rate (v) of 150mM diisopropylamine + 2mM paracetamol of GC electrode in buffer solution (pH 7) at A_2 peak
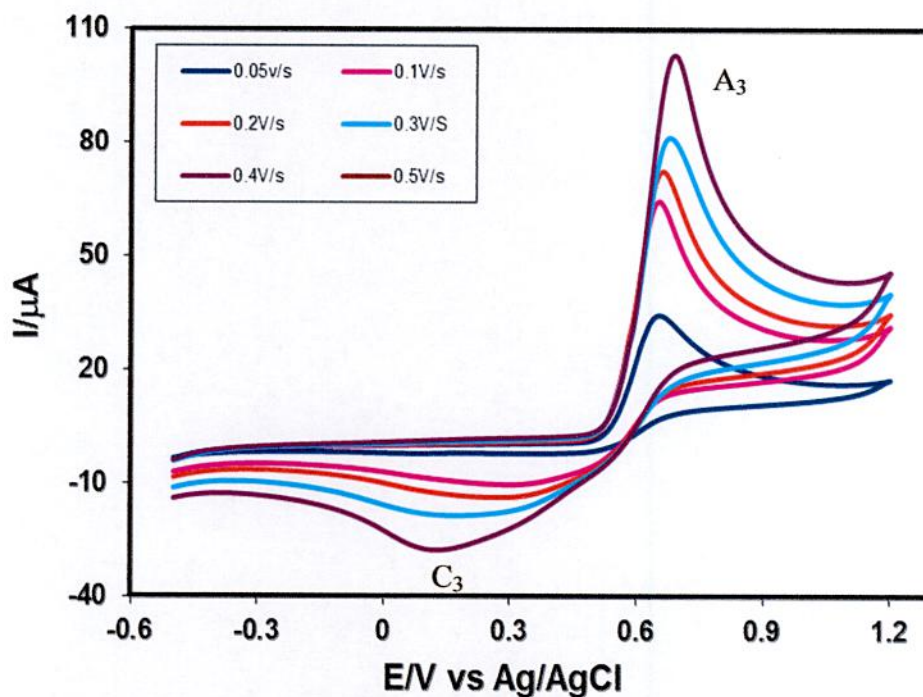
Fig. 4.77: Cyclic voltammogram of 2mM paracetamol + 150mM diisopropylamine of GC electrode in buffer solution (pH 3) at different scan rate (1st cycle)
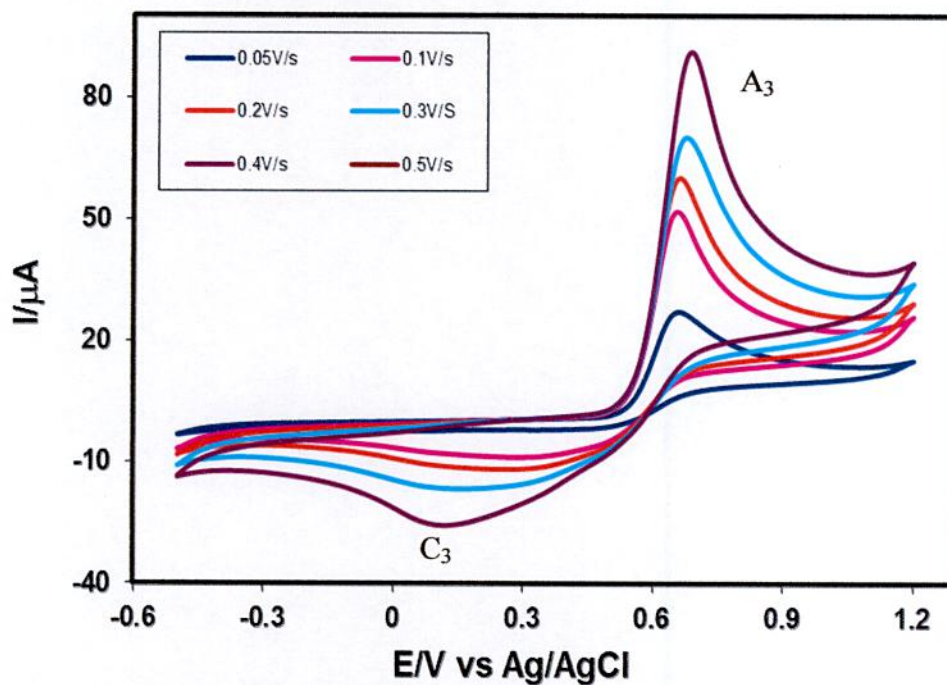
Fig. 4.78: Cyclic voltammogram of 2mM paracetamol + 150mM diisopropylamine of GC electrode in buffer solution (pH 3) at different scan rate (2nd cycle)
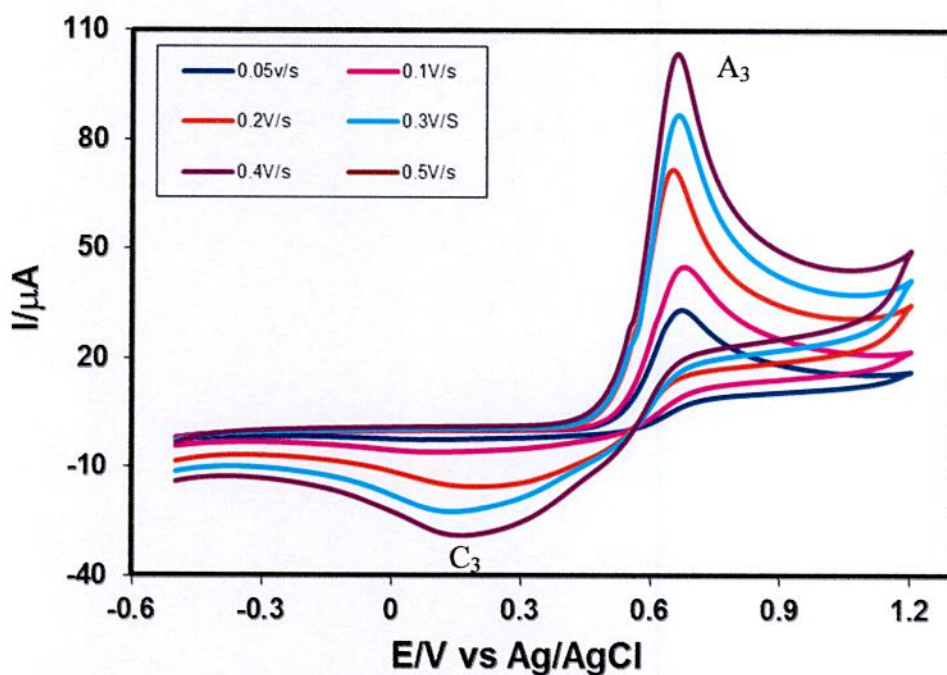
Fig. 4.79: Cyclic voltammogram of 2mM paracetamol + 150mM diisopropylamine of GC electrode in buffer solution (pH 5) at different scan rate (1st cycle)

Fig. 4.80: Cyclic voltammogram of 2mM paracetamol + 150mM diisopropylamine of GC electrode in buffer solution (pH 5) at different scan rate (2nd cycle)

Fig. 4.81: Cyclic voltammogram of 2mM paracetamol + 150mM diisopropylamine of GC electrode in buffer solution (pH 9) at different scan rate (1st cycle)

Fig. 4.82: Cyclic voltammogram of 2mM paracetamol + 150mM diisopropylamine of GC electrode in buffer solution (pH 9) at different scan rate (2nd cycle)
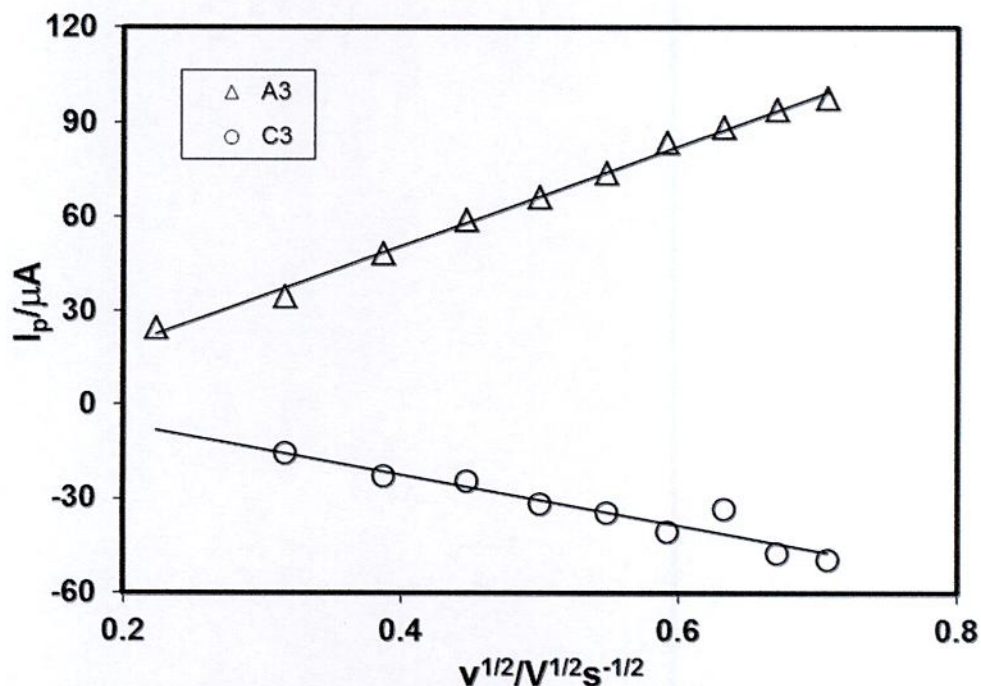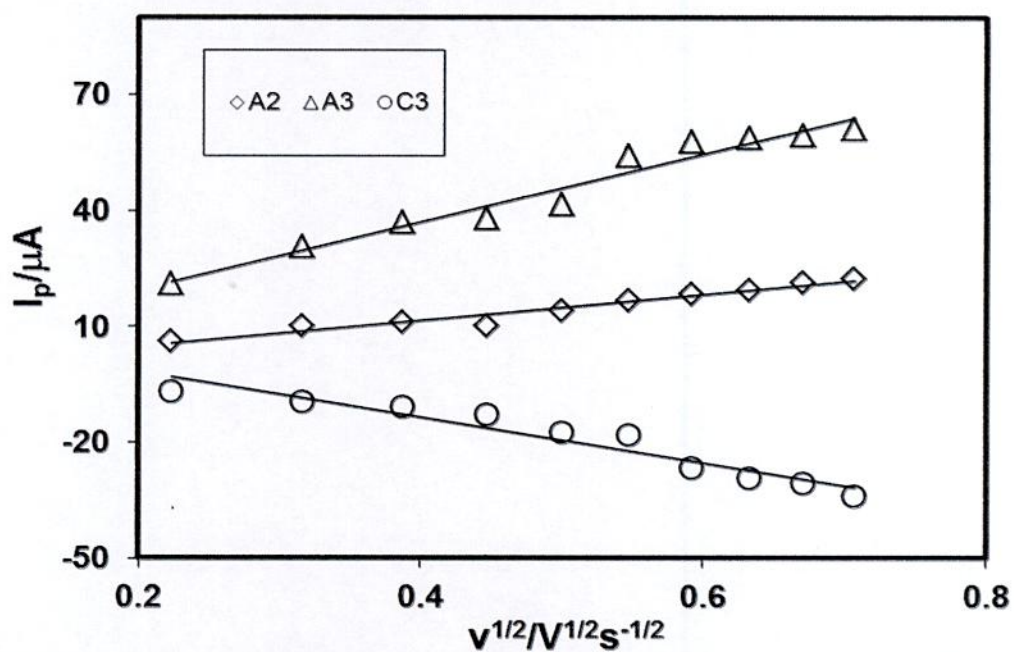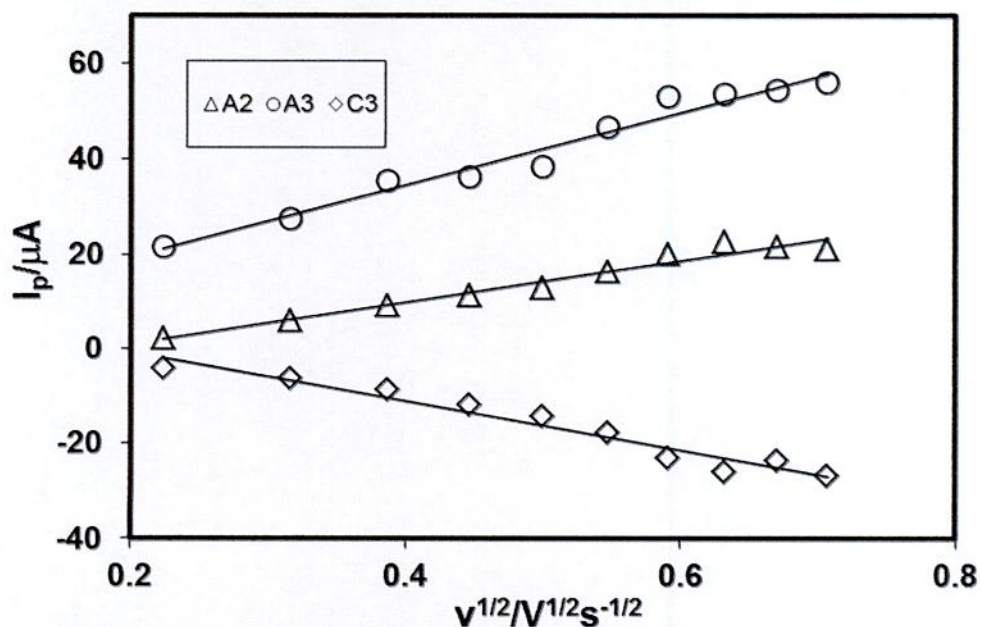
116

Fig. 4.83: Plots of peak current (I_p) versus square root of scan rate ($v^{1/2}$) of 2mM paracetamol + 150mM diisopropylamine of GC electrode in buffer solution (pH 3) (1st cycle)

Fig. 4.84: Plots of peak current (I_p) versus square root of scan rate ($v^{1/2}$) of 2mM paracetamol + 150mM diisopropylamine of GC electrode in buffer solution (pH 3) (2nd cycle)
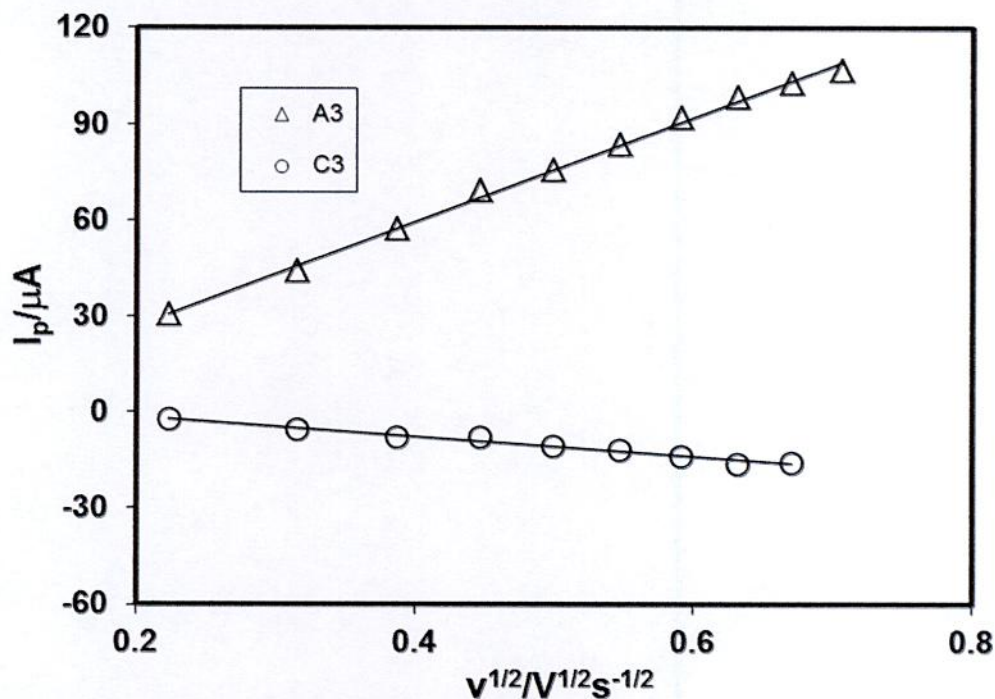
Fig. 4.85: Plots of peak current (I_p) versus square root of scan rate ($v^{1/2}$) of 2mM paracetamol and 150mM diisopropylamine of GC electrode in buffer solution (pH 5) (1st cycle)

Fig. 4.86: Plots of peak current (I_p) versus square root of scan rate ($v^{1/2}$) of 2mM paracetamol + 150mM diisopropylamine of GC electrode in buffer solution (pH 5) (2nd cycle)

Fig. 4.87: Plots of peak current (I_p) versus square root of scan rate ($v^{1/2}$) of 2mM paracetamol + 150mM diisopropylamine of GC electrode in buffer solution (pH 9) (1st cycle)

Fig. 4.88: Plots of peak current (I_p) versus square root of scan rate ($v^{1/2}$) of 2mM paracetamol + 150mM diisopropylamine of GC electrode in buffer solution (pH 9) (2nd cycle)
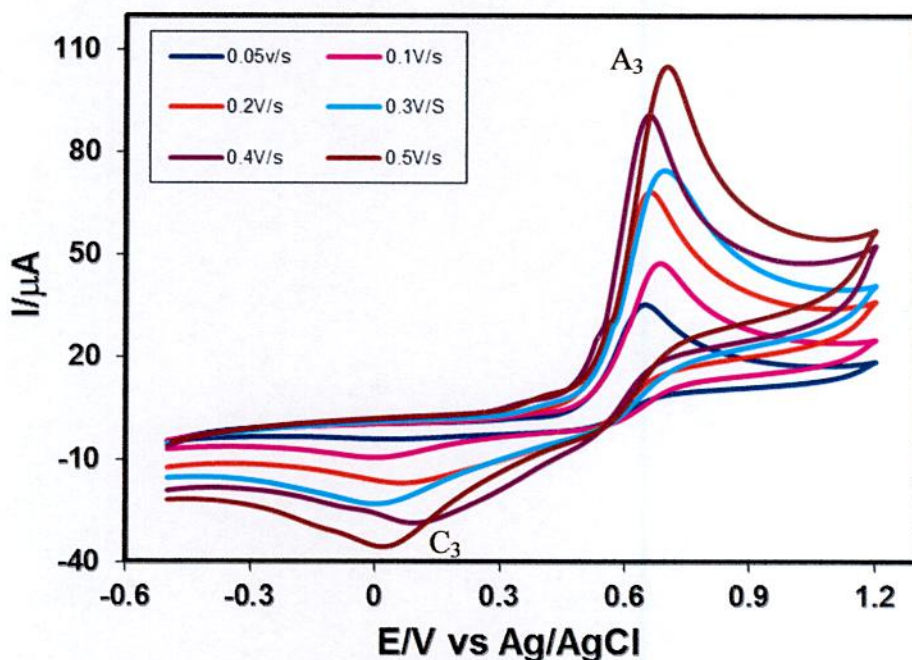
Fig. 4.89: Cyclic voltammogram of 2mM paracetamol + 100mM diisopropylamine of GC electrode in buffer solution (pH 7) at different scan rate (1st cycle)
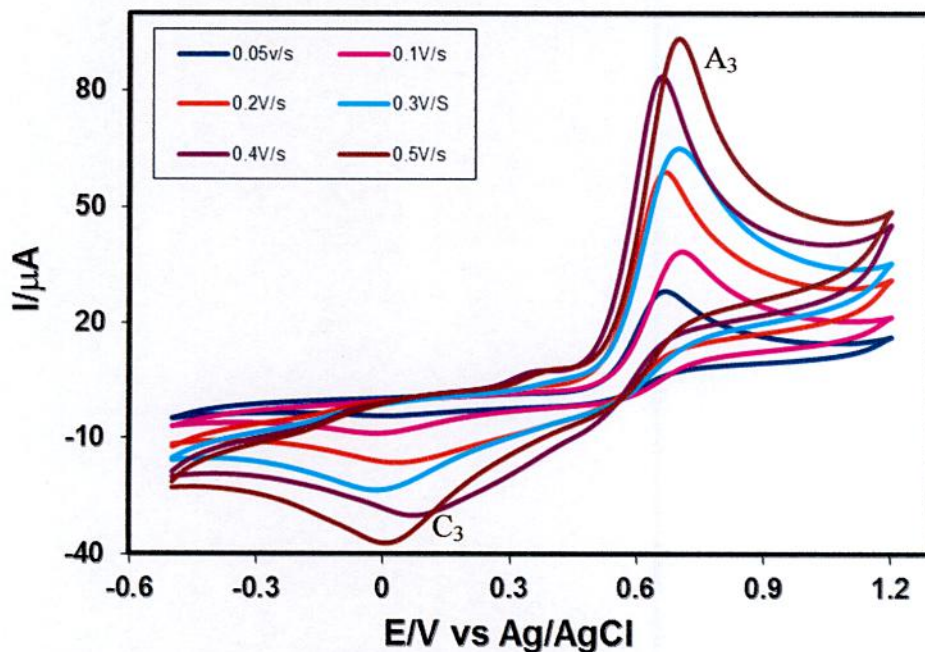
Fig. 4.90: Cyclic voltammogram of 2mM paracetamol + 100mM diisopropylamine in buffer solution (pH 7) of GC electrode at different scan rate (2nd cycle)
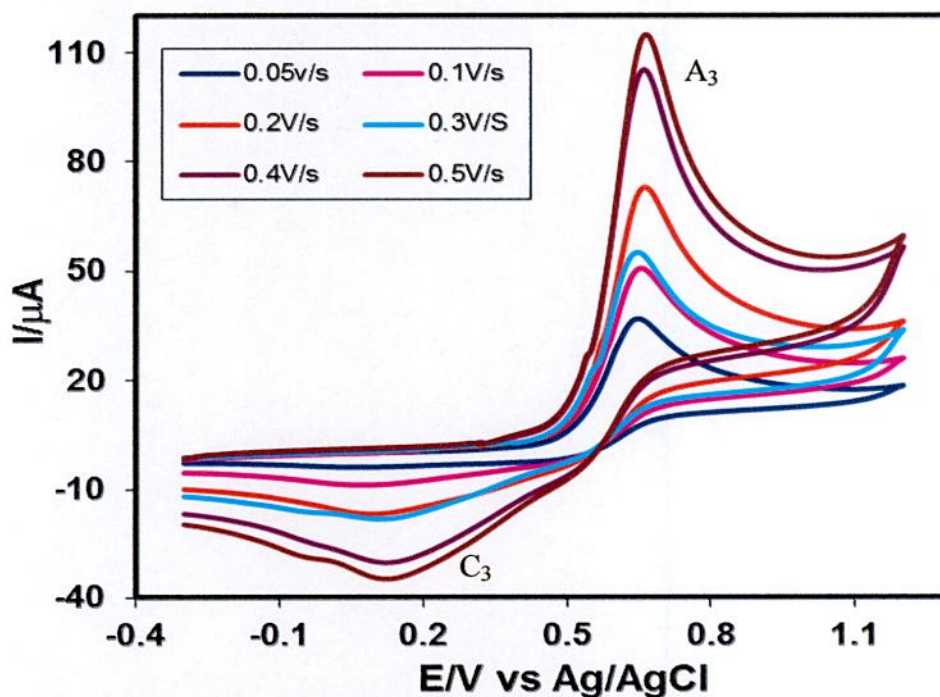
Fig. 4.91: Cyclic voltammogram of 2mM paracetamol + 200mM diisopropylamine in buffer solution (pH 7) of GC electrode at different scan rate (1st cycle)
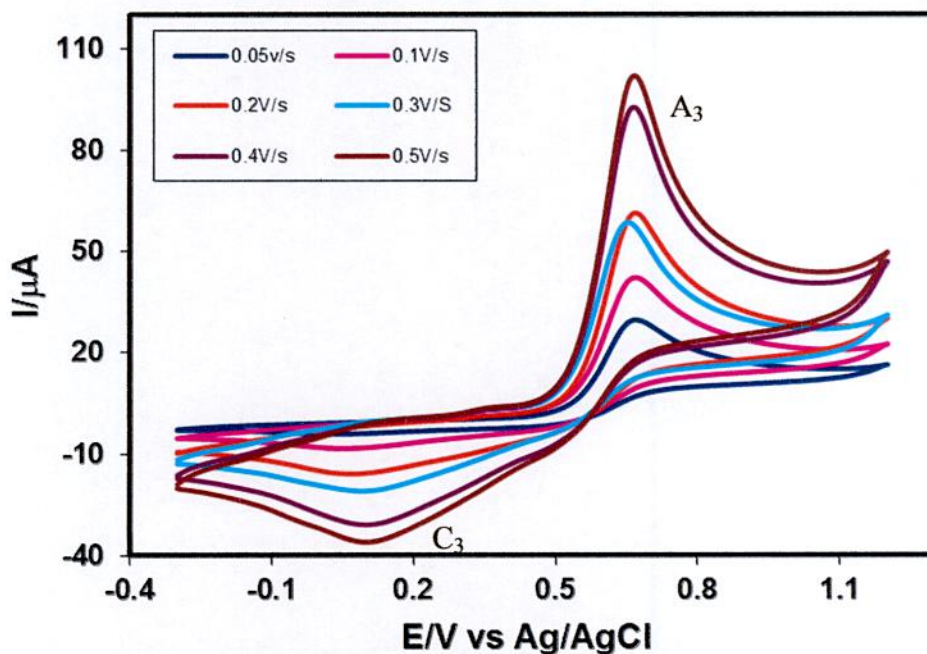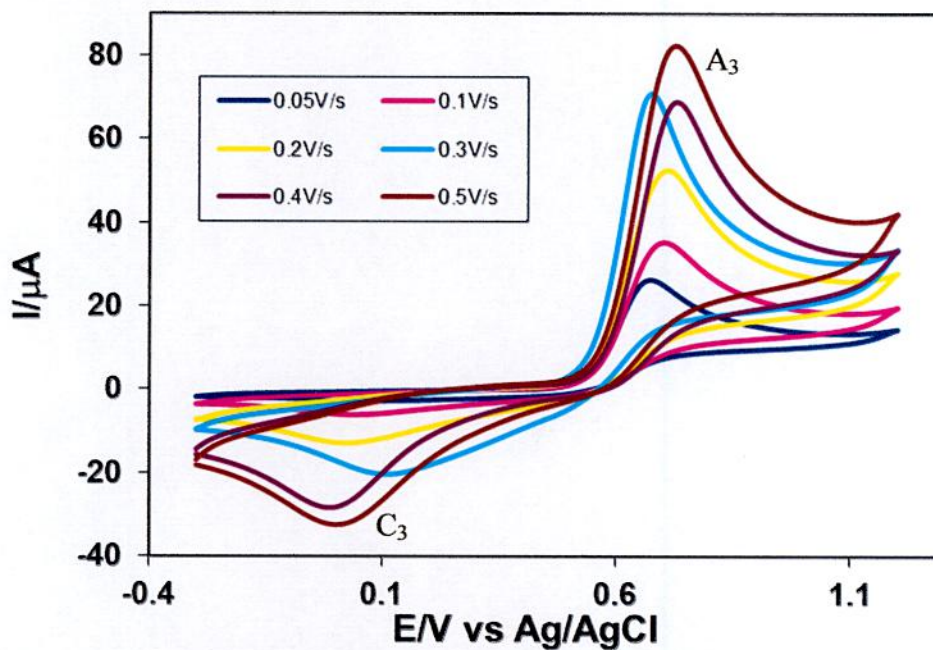

Fig. 4.92: Cyclic voltammogram of 2mM paracetamol + 200mM diisopropylamine in buffer solution (pH 7) of GC electrode at different scan rate (2nd cycle)

Fig. 4.93: Cyclic voltammogram of 2mM paracetamol + 250mM diisopropylamine in buffer solution (pH 7) of GC electrode at different scan rate (1st cycle)
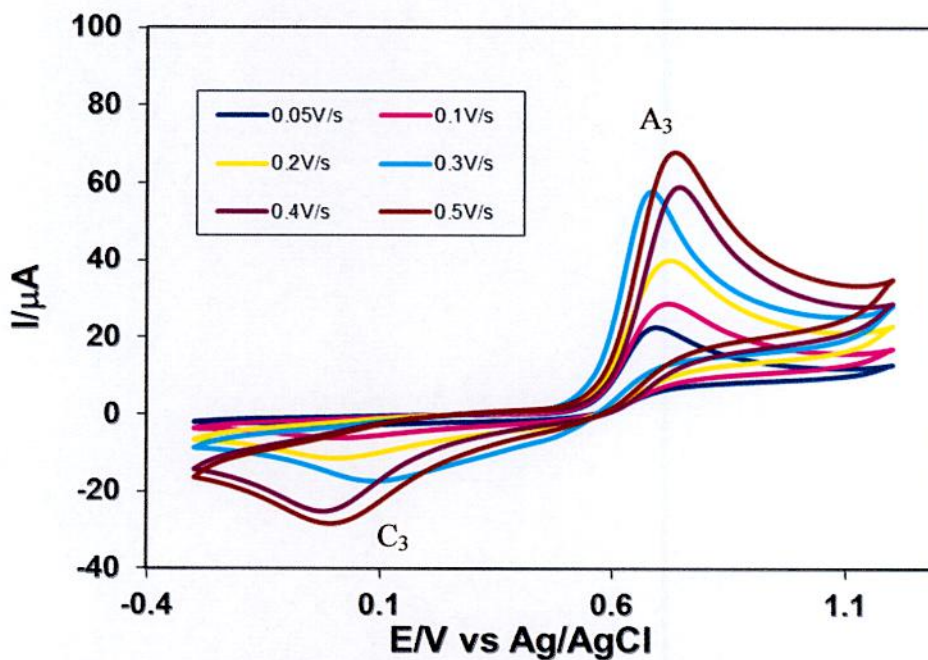

Fig. 4.94: Cyclic voltammogram of 2mM paracetamol + 250mM diisopropylamine of GC electrode in buffer solution (pH 7) at different scan rate (2nd cycle)
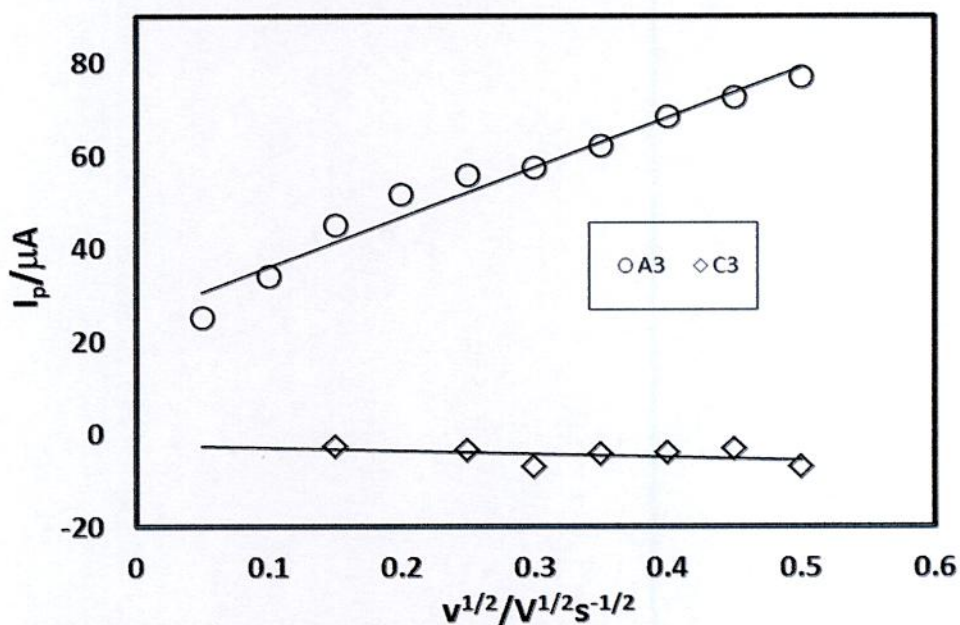
Fig. 4.95: Plots of peak current (I_p) versus square root of scan rate ($v^{1/2}$) of 2mM paracetamol + 100mM diisopropylamine of GC electrode in buffer solution (pH 7) (1st cycle)
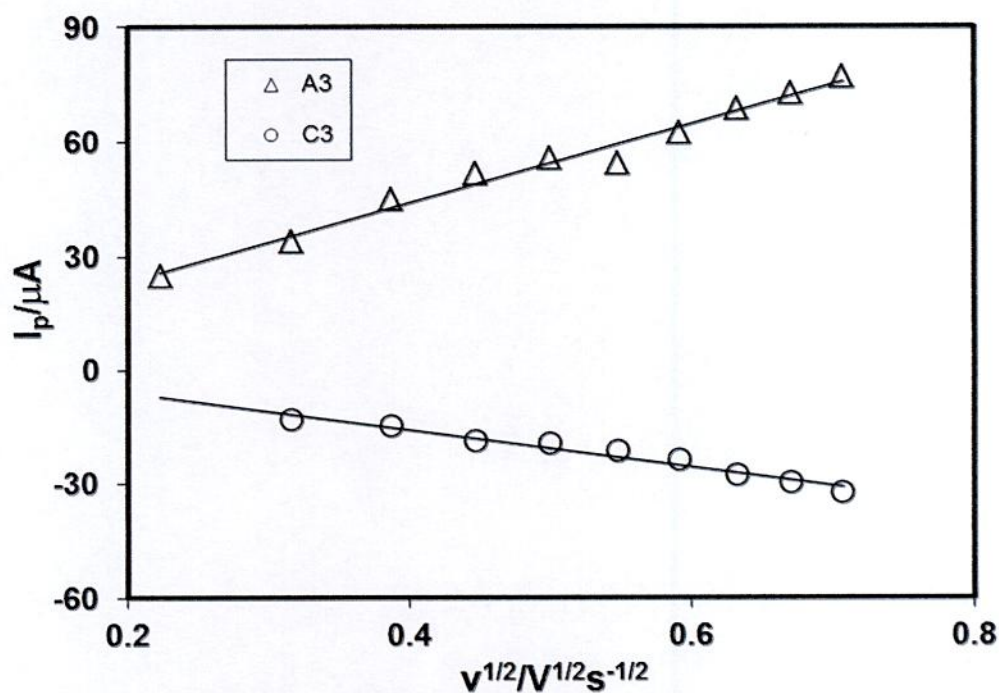

Fig. 4.96: Plots of peak current (I_p) versus square root of scan rate ($v^{1/2}$) of 2mM paracetamol + 100mM diisopropylamine of GC electrode in buffer solution (pH 7) (2nd cycle)
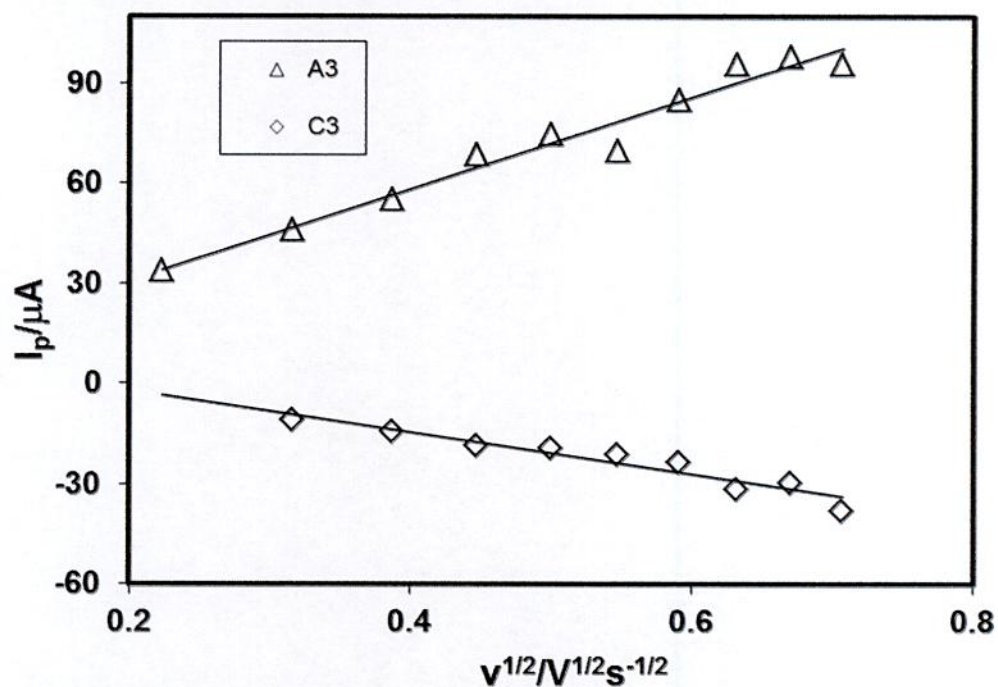
Fig. 4.97: Plots of peak current (I_p) versus square root of scan rate ($v^{1/2}$) of 2mM paracetamol + 200mM diisopropylamine of GC electrode in buffer solution (pH 7) (1st cycle)

Fig. 4.98: Plots of peak current (I_p) versus square root of scan rate ($v^{1/2}$) of 2mM paracetamol + 200mM diisopropylamine of GC electrode in buffer solution (pH 7) (2nd cycle)

124

Fig. 4.99: Plots of peak current (I_p) versus square root of scan rate ($v^{1/2}$) of 2mM paracetamol + 250mM diisopropylamine of GC electrode in buffer solution (pH 7) (1st cycle)
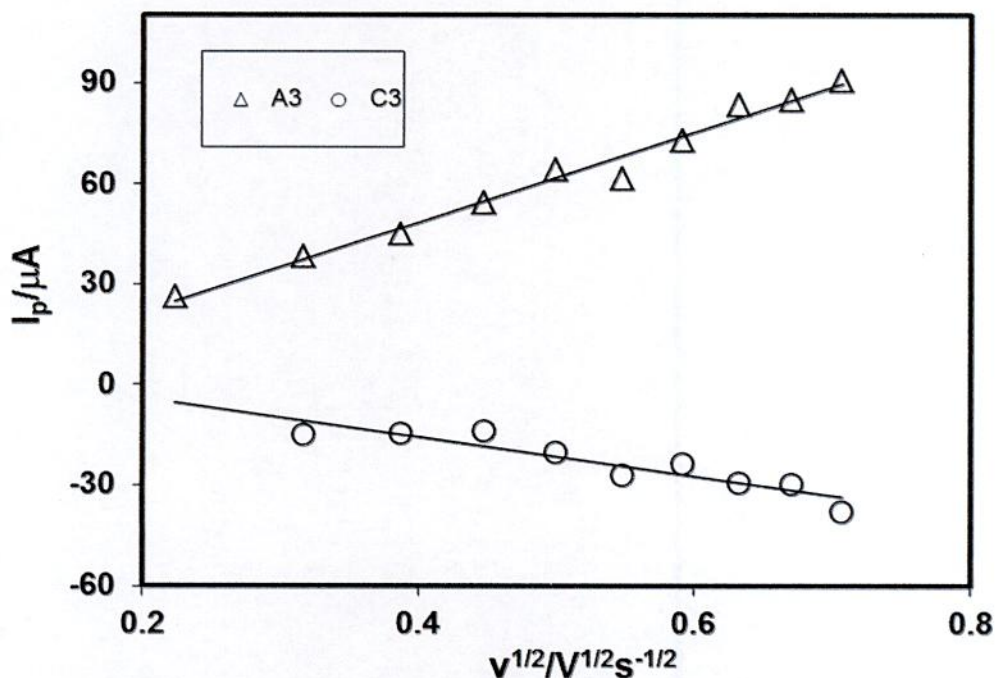

Fig. 4.100: Plots of peak current (I_p) versus square root of scan rate ($v^{1/2}$) of 2mM paracetamol + 250mM diisopropylamine of GC electrode in buffer solution (pH 7) (2nd cycle)
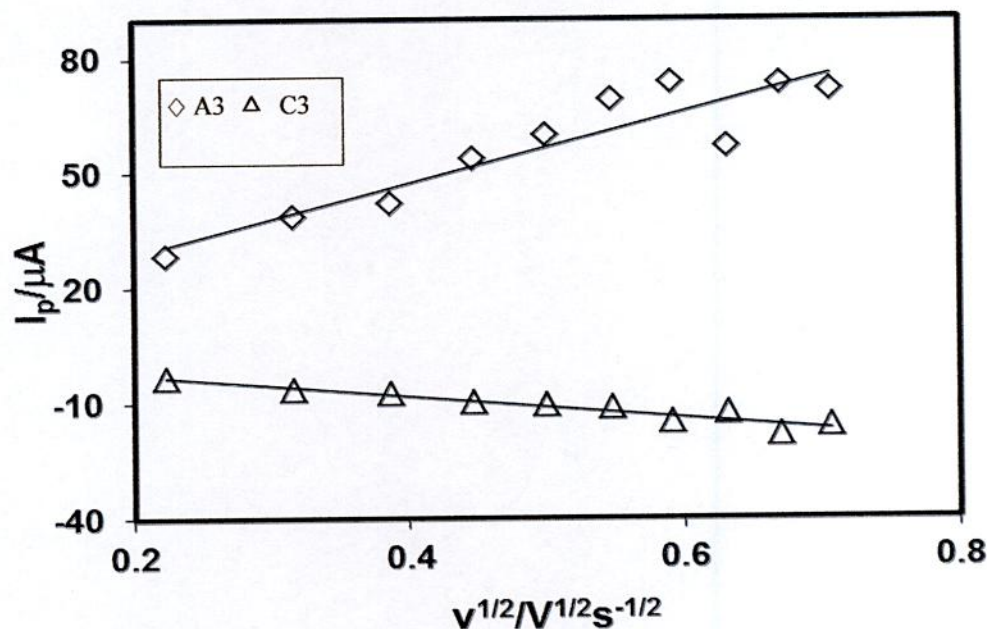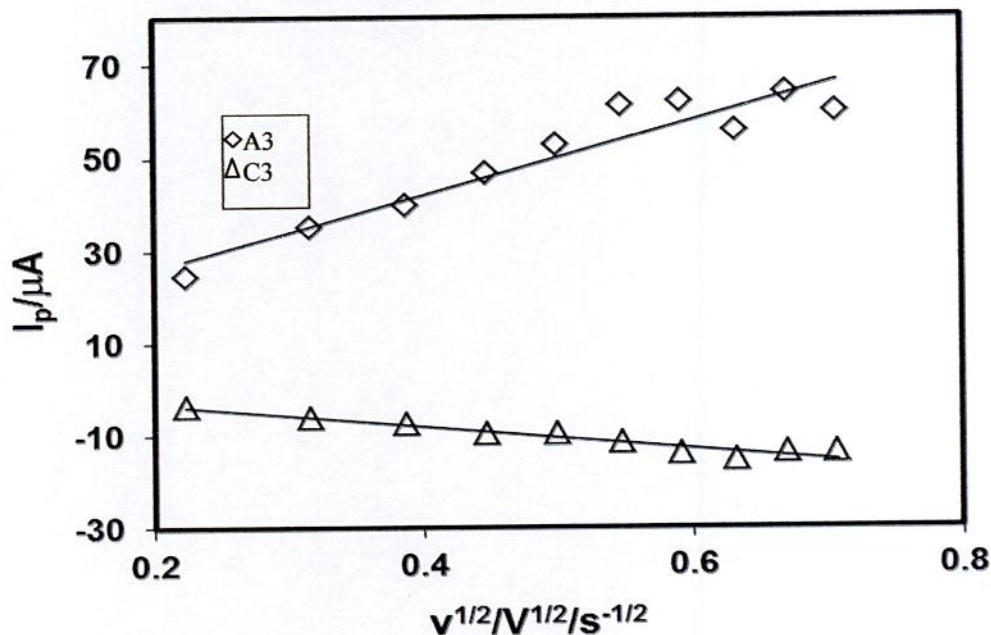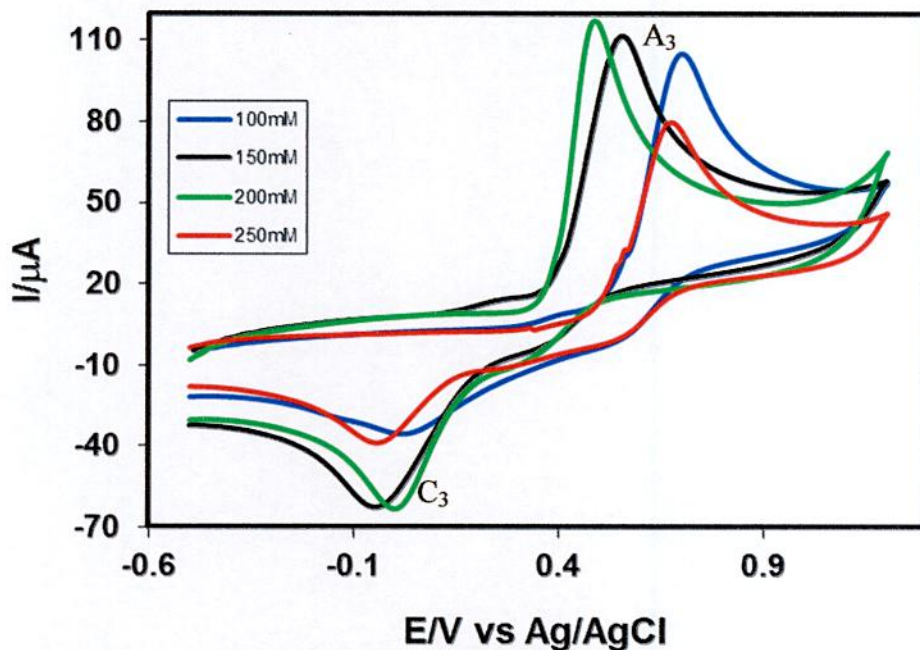
Fig. 4.101: Comparison of cyclic voltammogram of fixed 2mM paracetamol and different concentration (100, 150, 200 and 250mM) of diisopropylamine in buffer solution (pH 7) of GC electrode at scan rate 0.5V/s (1st cycle)
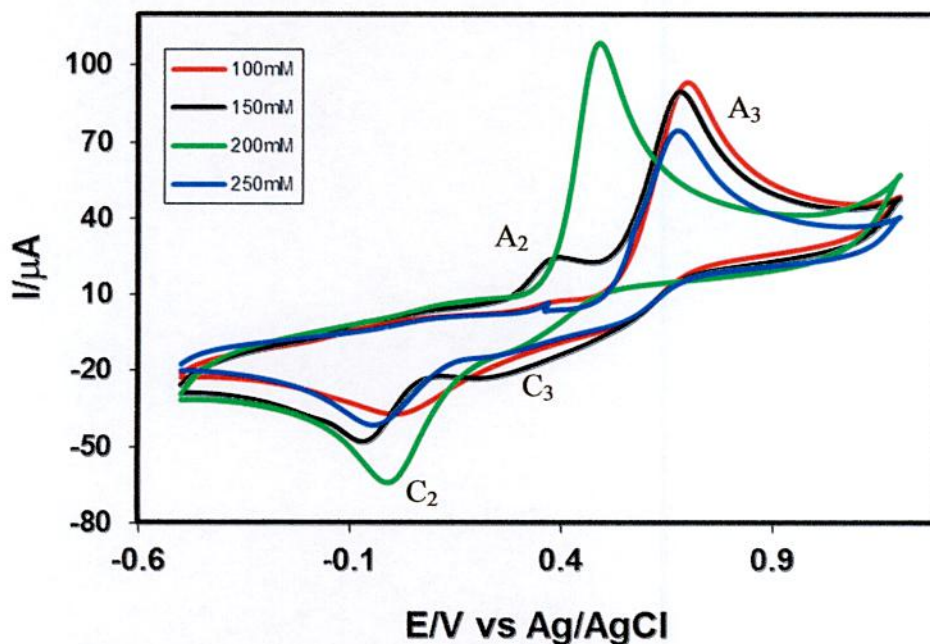

Fig. 4.102: Comparison of cyclic voltammogram of fixed 2mM paracetamol and different concentration (100, 150, 200, 250mM) of diisopropylamine in buffer solution (pH 7) of GC electrode at scan rate 0.5V/s (2nd cycle)

Fig. 4.103: Plots of peak current (I_p) versus concentration (C) of 2mM paracetamol (fixed) and different concentration (100, 150, 200 and 250mM) of diisopropylamine of GC electrode in buffer solution (pH 7) (2nd cycle)
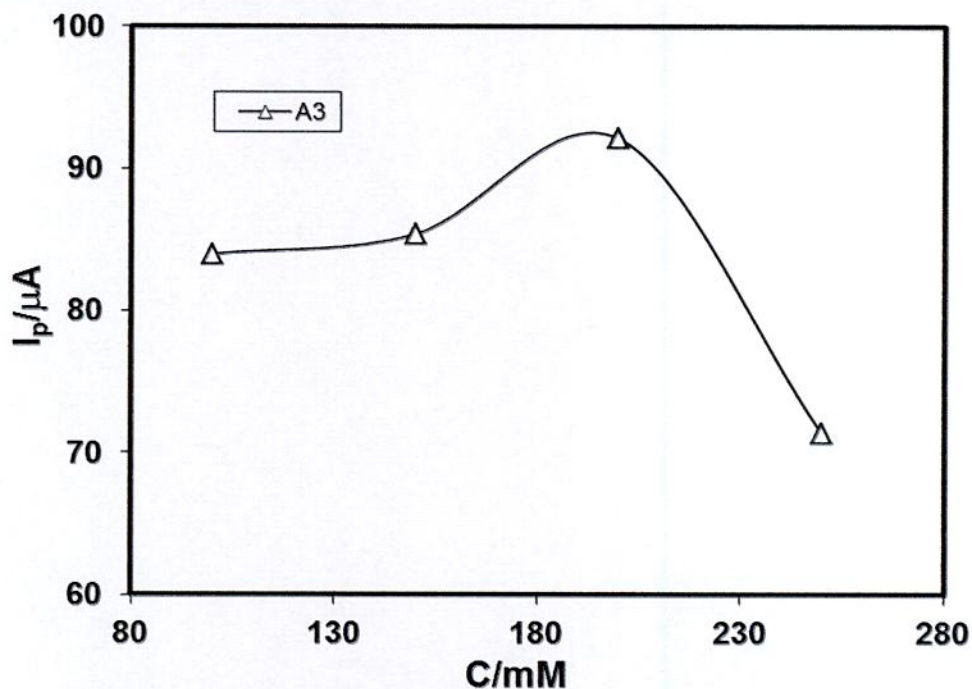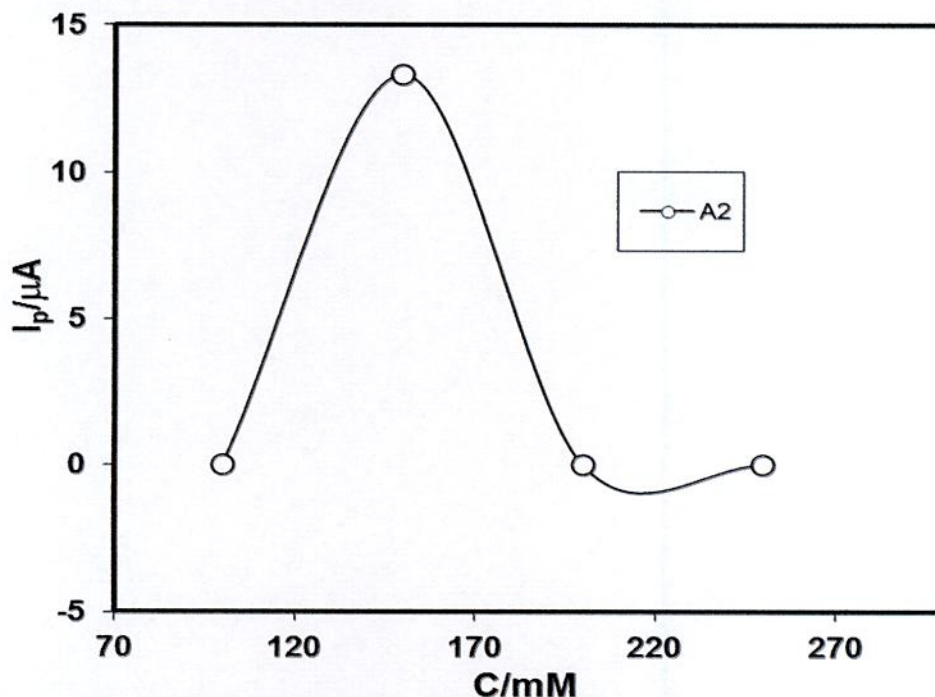

Fig. 4.104: Plots of peak current (I_p) versus concentration (C) of 2mM paracetamol (fixed) + different concentration (100, 150, 200 and 250mM) of diisopropylamine of GC electrode in buffer solution (pH 7) at scan rate 0.5V/s (2nd cycle)

Fig. 4.105: Comparison of cyclic voltammogram of fixed 150mM diisopropylamine and different concentration (2, 4, 6, 8mM) of paracetamol in buffer solution (pH 7) of GC electrode at scan rate 0.5 V/s (1st cycle)
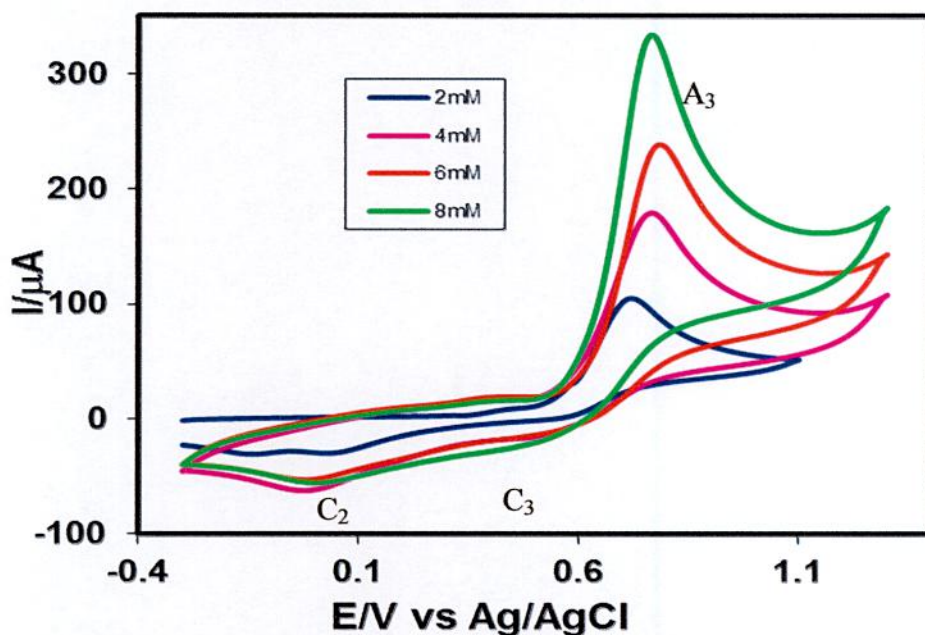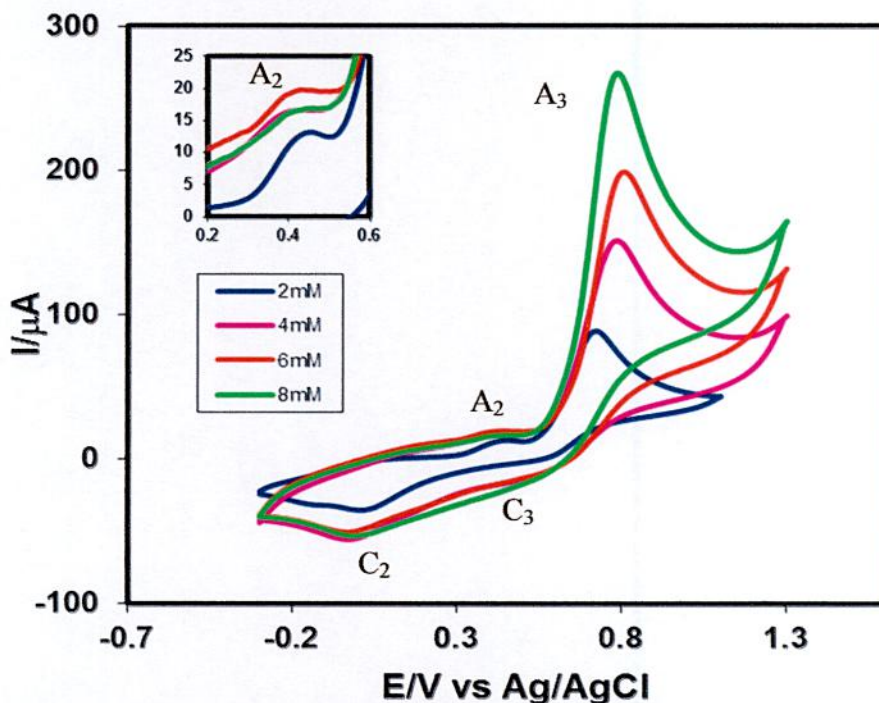

Fig. 4.106: Comparison of cyclic voltammogram of fixed 150mM diisopropylamine and different concentration (2, 4, 6 and 8mM) of paracetamol of GC electrode in buffer solution (pH 7) at scan rate 0.5V/s (2nd cycle), inset: appeared anodic peak (A$_2$)

128

Fig. 4.107: Plots of peak current (I_p) versus different concentration (C) (2, 4, 6 and 8mM) of paracetamol + fixed 150mM diisopropylamine of GC electrode in buffer solution (pH 7) at scan rate 0.5V/s (1st cycle) for anodic peak (A_3)

Fig. 4.108: Plots of peak current (I_p) versus different concentration (C) (2, 4, 6 and 8mM) of paracetamol + fixed 150mM diisopropylamine of GC electrode at scan rate 0.5V/s (2nd cycle) in buffer solution (pH 7) for appeared anodic peak (A_2)
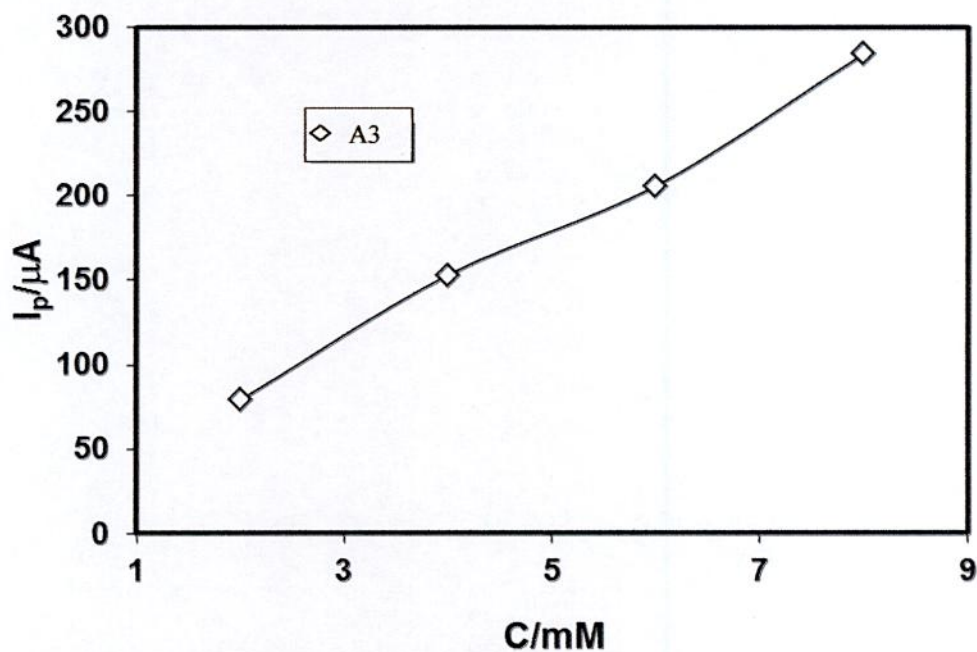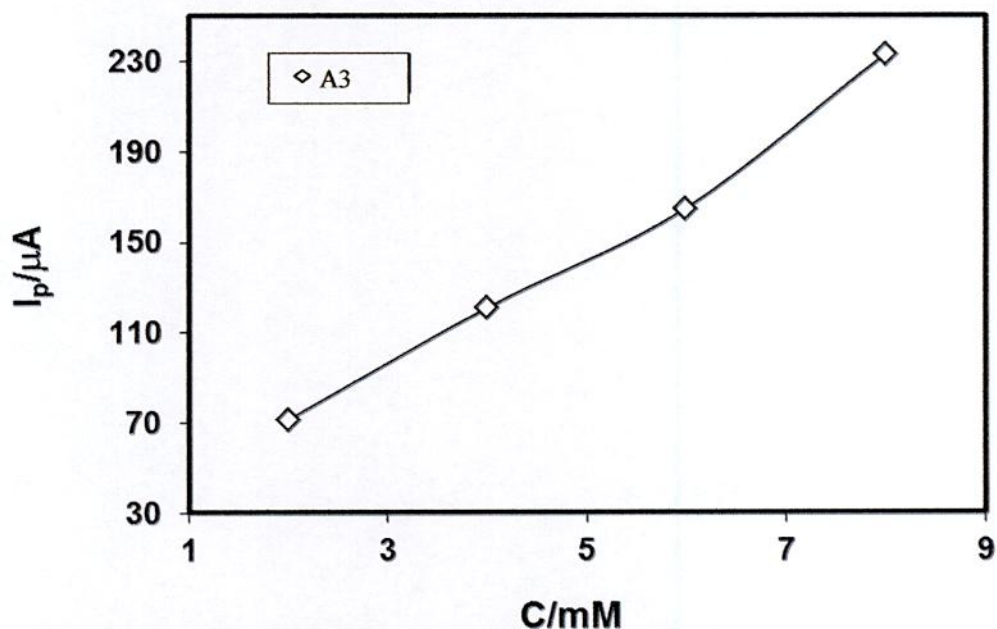
Fig. 4.109: Plots of peak current (I_p) versus different concentration (C) (2, 4, 6 and 8mM) of paracetamol + fixed 150mM diisopropylamine of GC electrode in buffer solution (pH 7) at scan rate 0.5V/s (2nd cycle) for anodic peak (A_3)
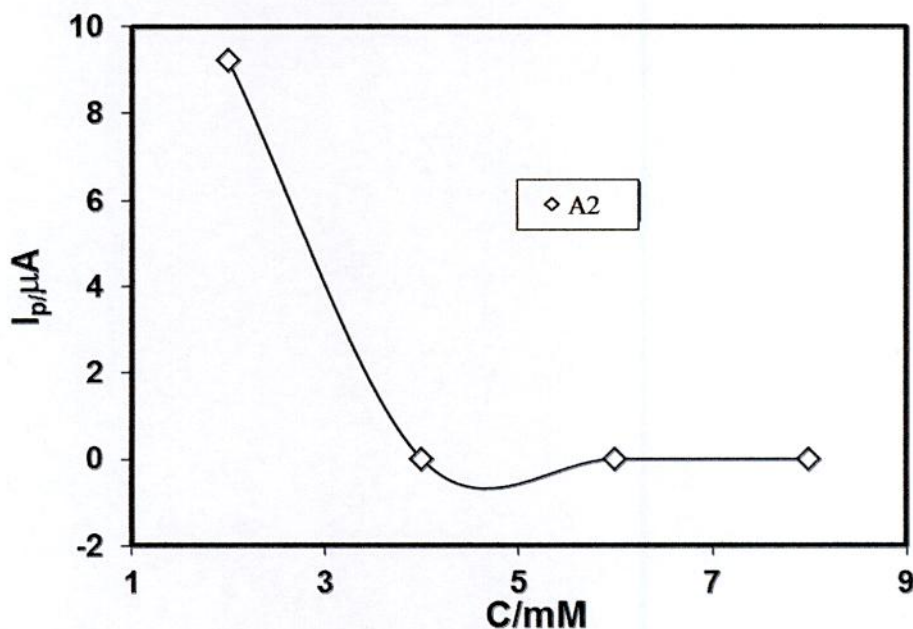

Fig. 4.110: Comparison of cyclic voltammogram of 2mM paracetamol + 150mM diisopropylamine of different electrodes (GC, Au, Pt) in buffer solution (pH 7) at scan rate 0.5V/s (1st cycle)

Fig. 4.111: Comparison of cyclic voltammogram of 2mM paracetamol + 150mM diisopropylamine of different electrodes (GC, Au, Pt) in buffer solution (pH 7) and at scan rate 0.5V/s (2nd cycle)

Fig. 4.112: Cyclic voltammogram of 2mM paracetamol + 150mM diisopropylamine during control potential coulometry of GC electrode in buffer solution (pH 7) at scan rate 0.1V/s

Fig. 4.113: Comparison of differential pulse voltammogram of 2mM paracetamol + 150mM diisopropylamine of GC electrode in different buffer solution of pH (3, 5, 7 and 9) at scan rate 0.5V/s (1st oxidation) where E_{pulse} 0.02V, t_{pulse} 20ms

Fig. 4.114: Comparison of differential pulse voltammogram of 2mM paracetamol + 150mM diisopropylamine of GC electrode in different buffer solution of pH (3, 5, 7 and 9) at scan rate 0.5V/s (2nd oxidation) where E_{pulse} 0.02V, t_{pulse} 20ms
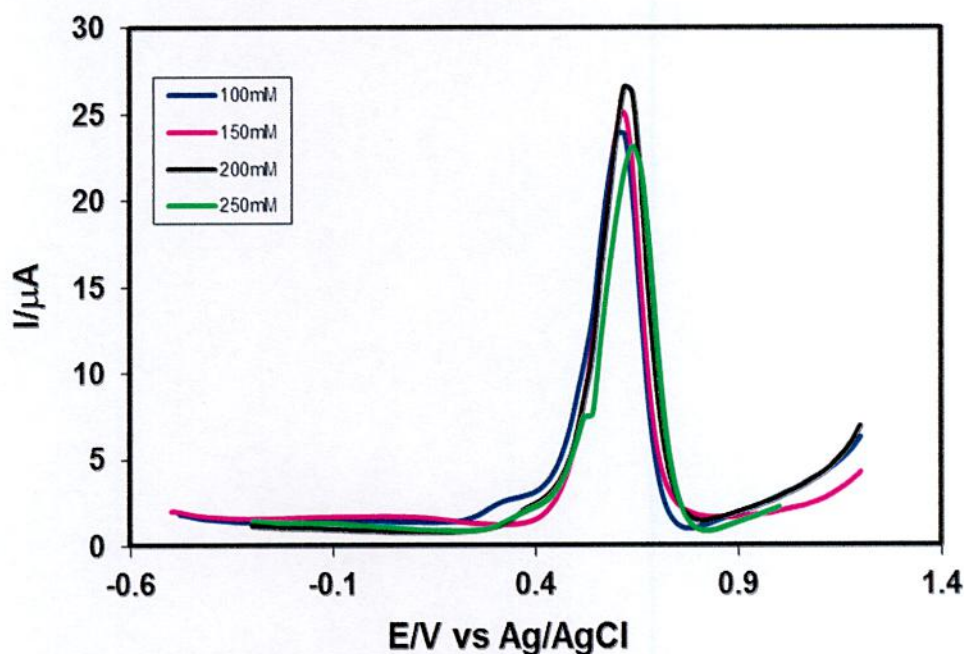
Fig. 4.115: Comparison of differential pulse voltammogram of fixed 2mM paracetamol + different concentration (100, 150, 200 and 250mM) of diisopropylamine of GC electrode in buffer solution (pH 7) at scan rate 0.5V/s (1st oxidation) where E_{pulse} 0.02V, t_{pulse} 20ms
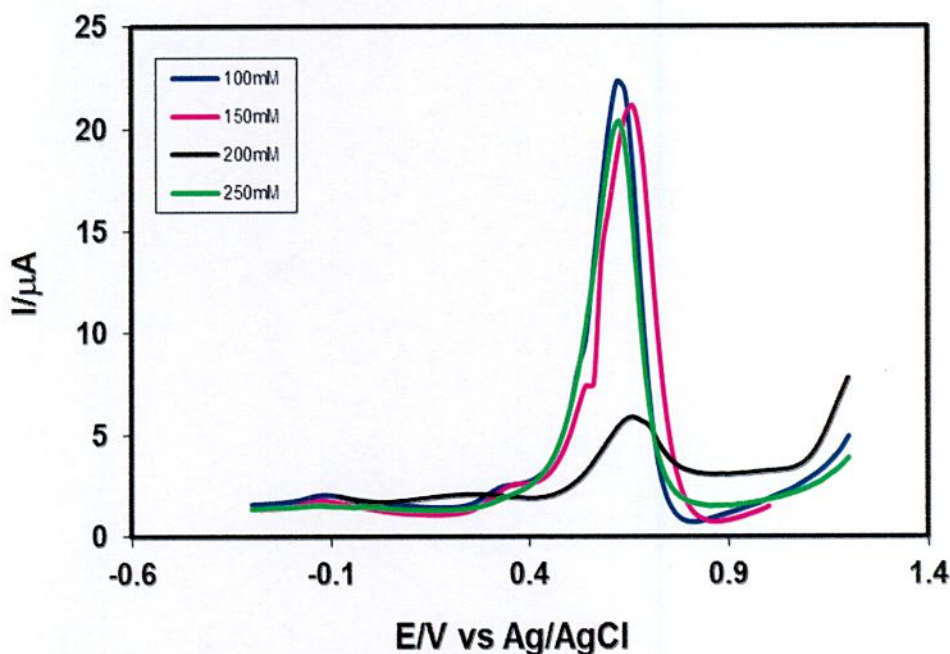
Fig.4.116: Comparison of Differential pulse voltammogram of fixed 2mM paracetamol + different concentration (100, 150, 200 and 250mM) of diisopropylamine of GC electrode in buffer solution (pH 7) scan rate 0.5V/s (2nd oxidation) where E_{pulse} 0.02V, t_{pulse} 20s
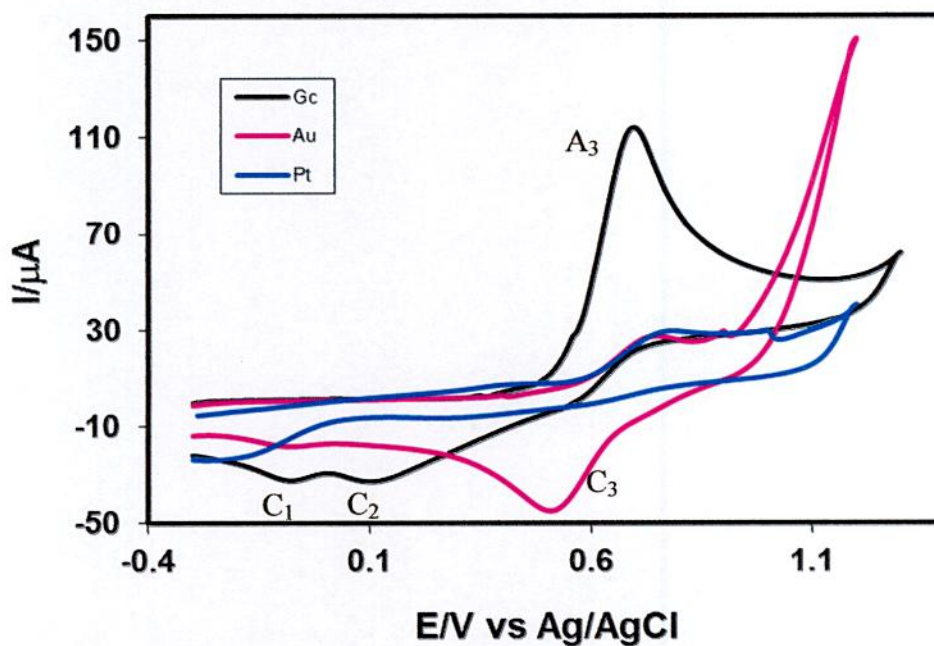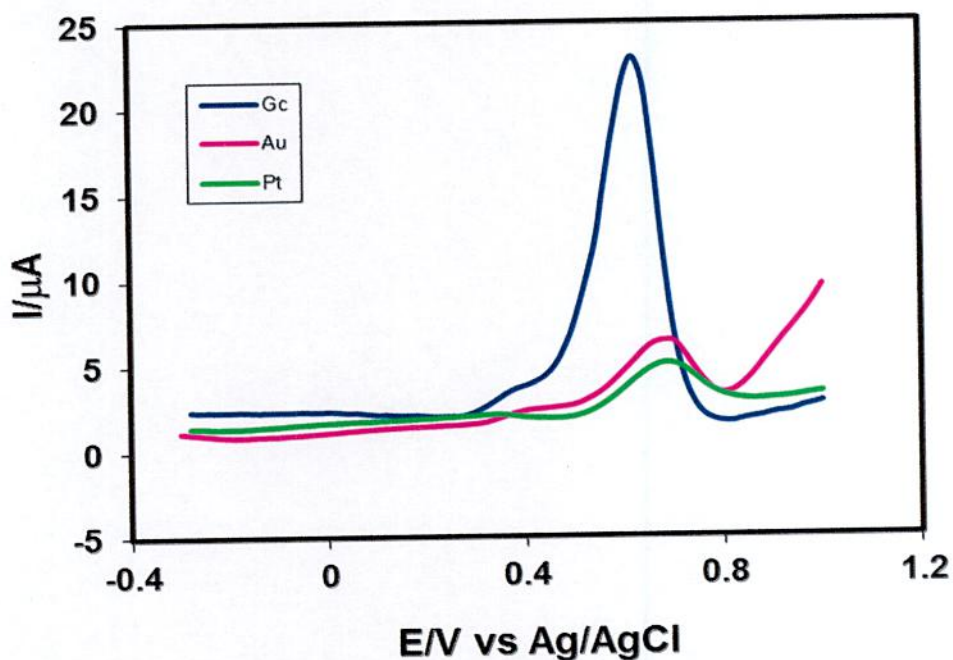
Fig. 4.117: Comparison of Differential pulse voltammogram of 2mM paracetamol + 150mM diisopropylamine of different electrode 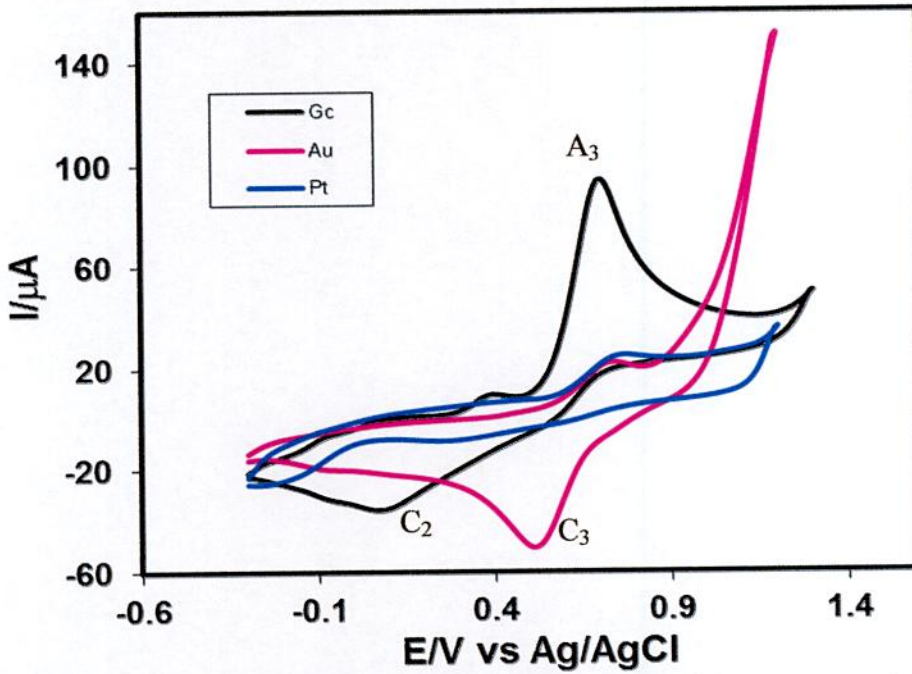(GC, Au, Pt) in buffer solution (pH 7) at scan rate 0.5V/s for 1st oxidation where E_{pulse} 0.02V, t_{pulse} 20ms
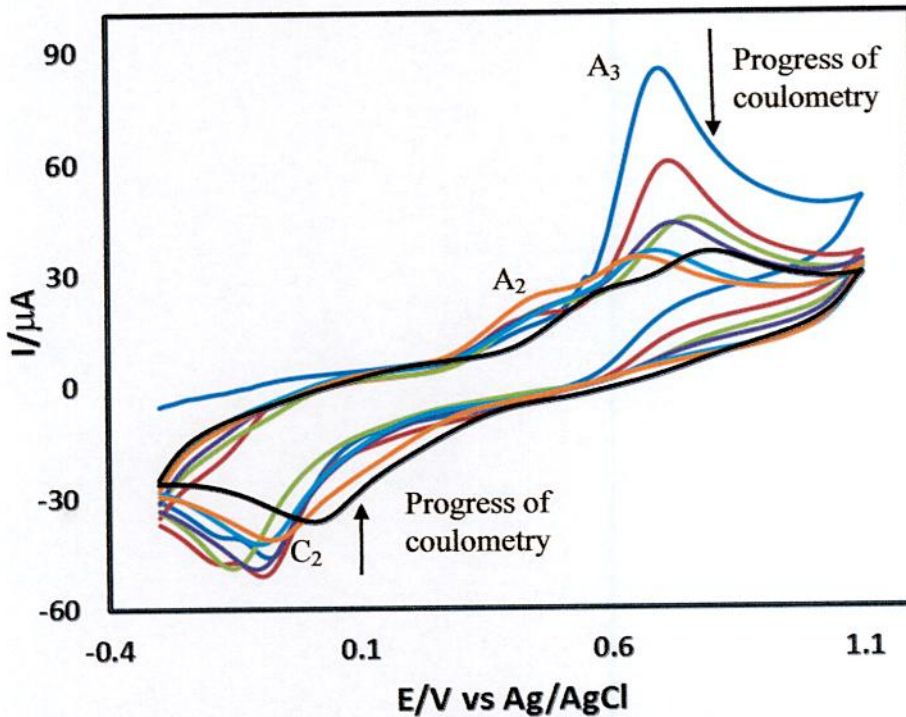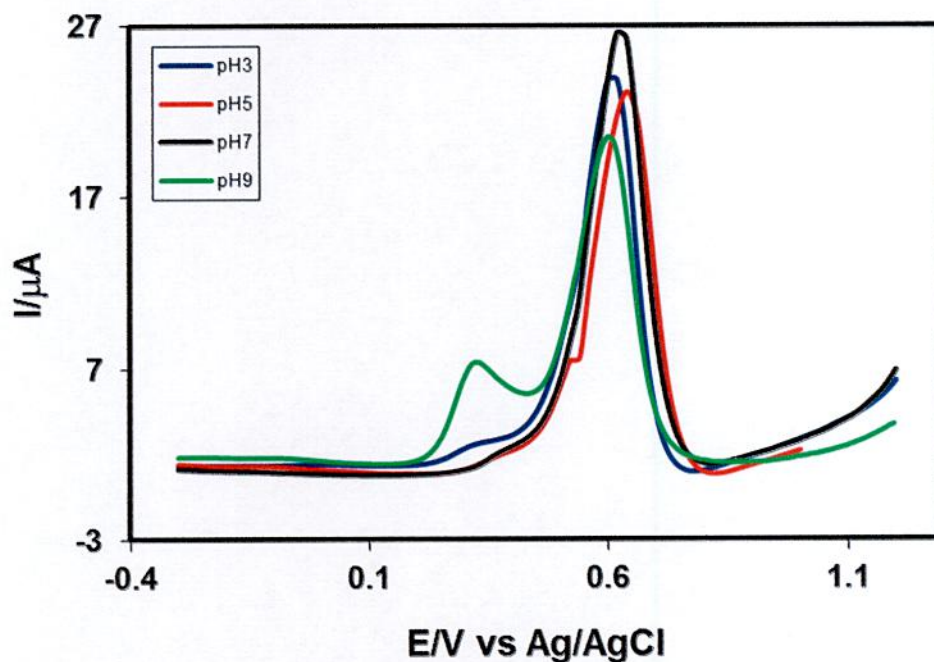

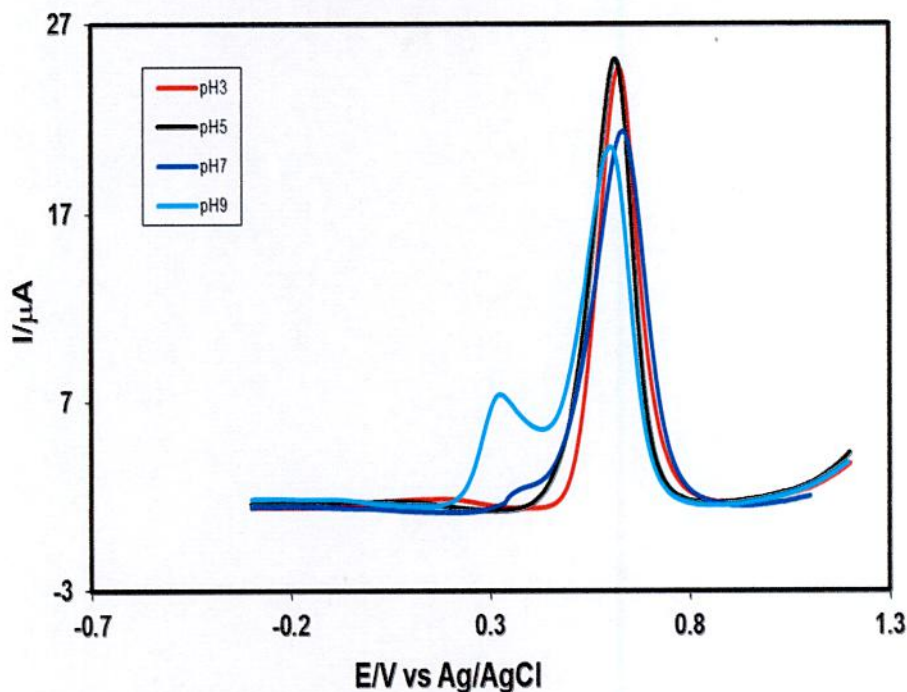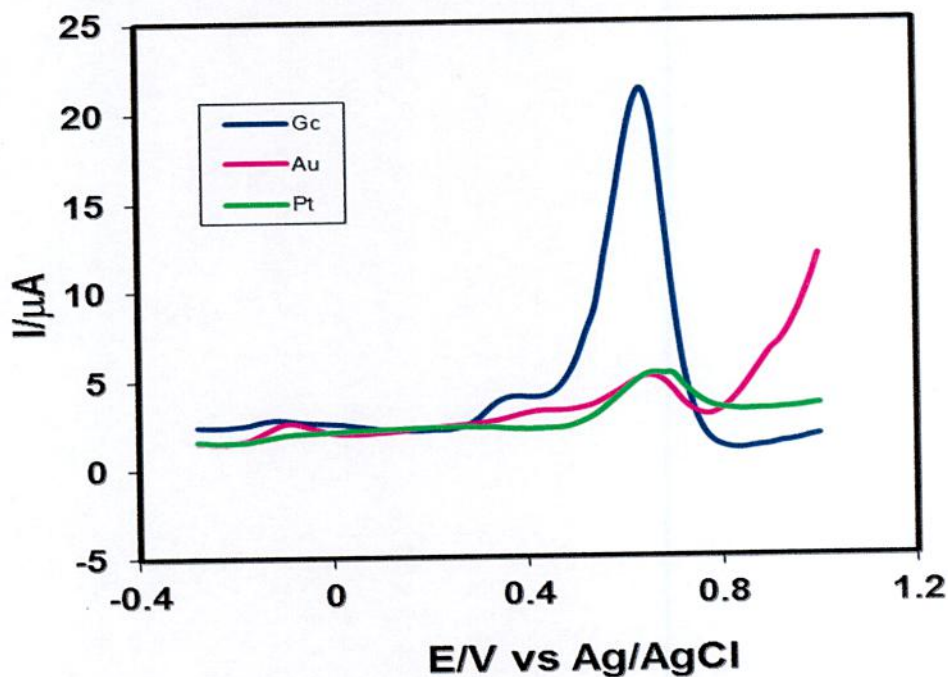Fig. 4.118: Comparison of Differential pulse voltammogram of 2mM paracetamol + 150mM diisopropylamine of different electrode (GC, Au, Pt) in buffer solution (pH 7) at scan rate 0.5V/s for 2nd oxidation where E_{pulse} 0.02V, t_{pulse} 20ms
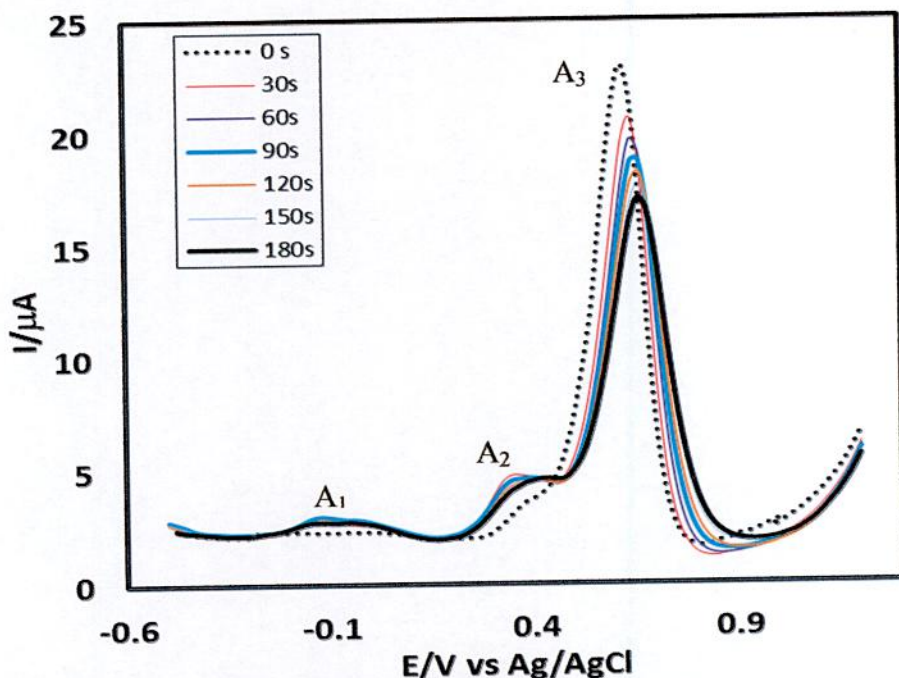
Fig. 4.119: Differential pulse voltammogram of deposition time change of 2mM paracetamol + 150mM diisopropylamine in buffer solution (pH 7) of GC electrode, where potential stepped 0.5V (E_{pulse} 0.02V, t_{pulse} 20ms)
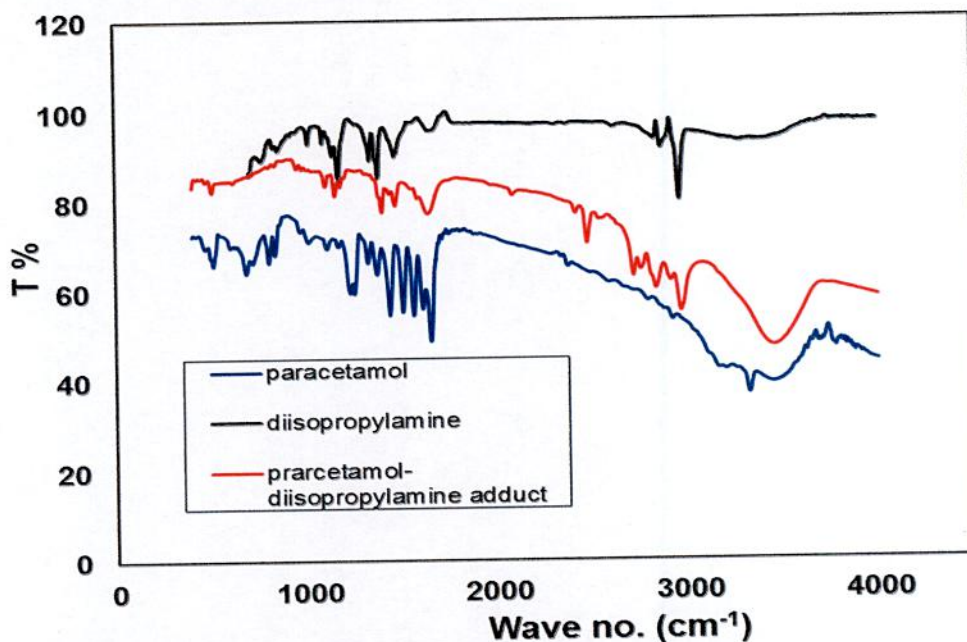
Fig. 4.120: Comparison of FTIR of only paracetamol, only diisopropylamine and paracetamol- diisopropylamine adduct
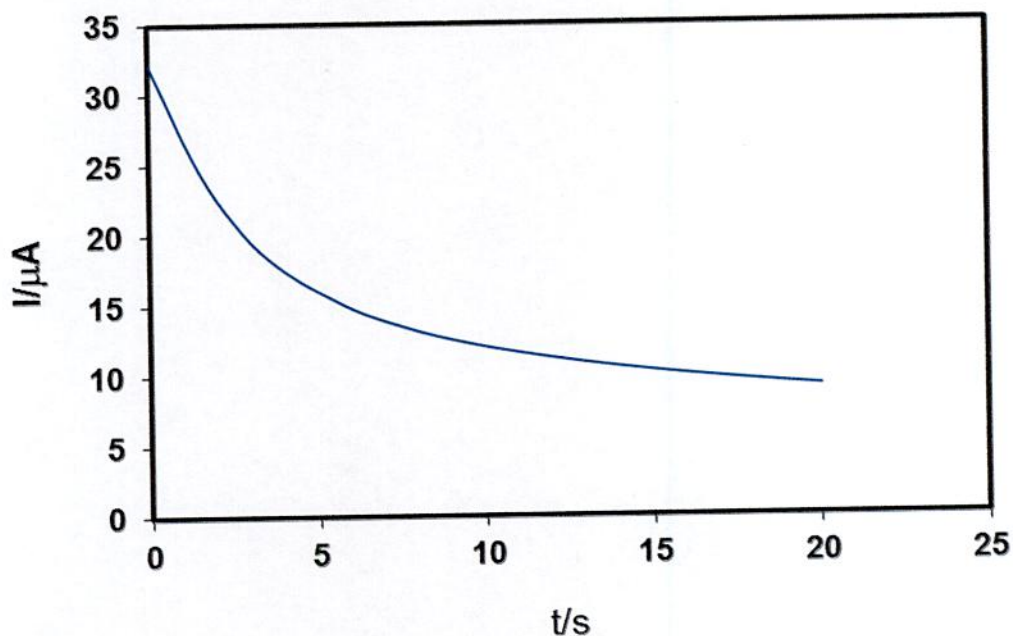
Fig. 4.121: Chronoamperogram of 2mM paracetamol + 150mM diisopropylamine of GC electrode in buffer solution (pH 7) at E_{pulse} 0.69V and time 20s
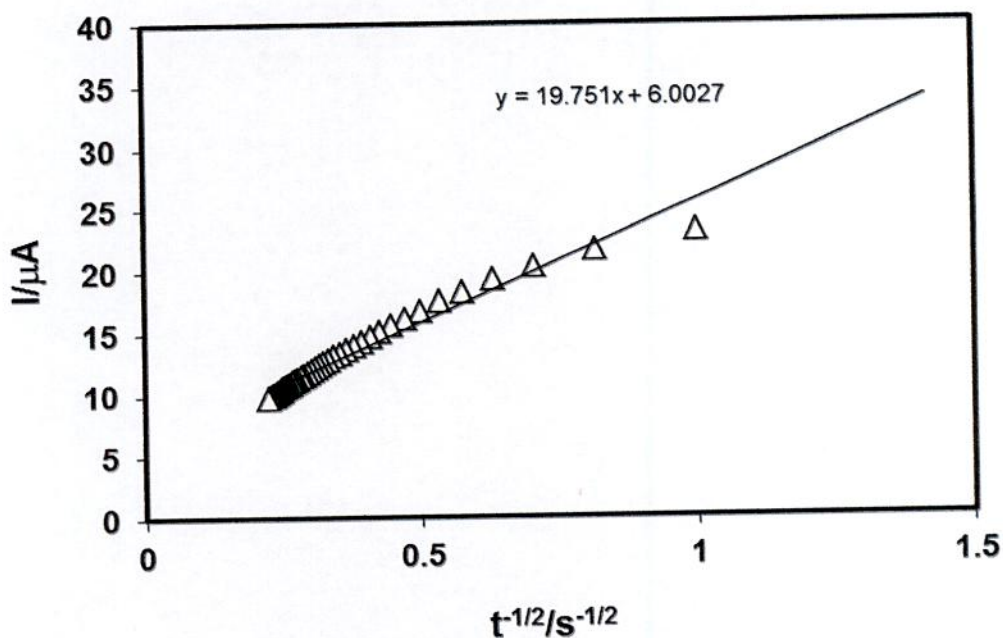
Fig. 4.122: Cottrell plots of the back-ground subtracted currents for 2mM paracetamol + 150mM diisopropylamine of GC electrode in buffer solution (pH 7) when the potential was stepped from 0.69V
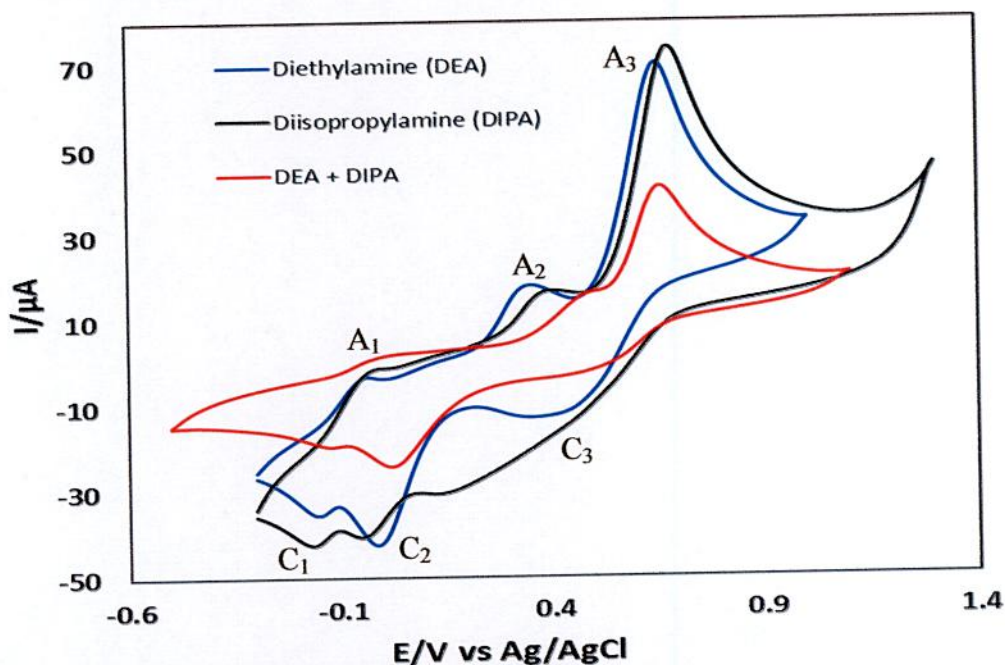
Fig. 4.123: Comparison of CV of 2mM paracetamol + 150mM diethylamine, 2mM paracetamol + 150mM diisopropylamine and 2mM paracetamol + 150mM diethylamine + 150mM diisopropylamine in pH 7 at scan rate 0.1V/s (2nd cycle)
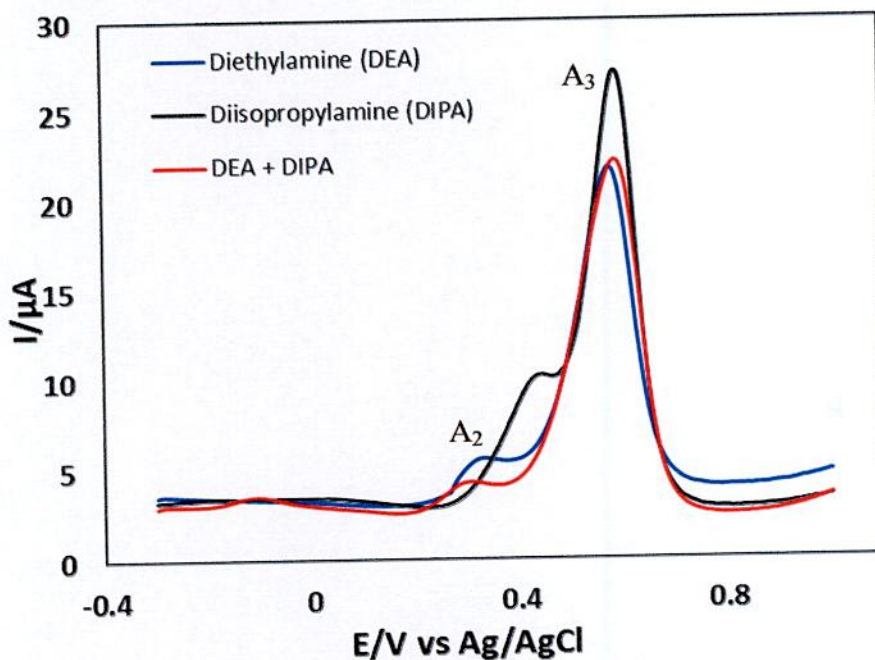
Fig. 4.124: Comparison of DPV of 2mM paracetamol + 150mM diethylamine, 2mM paracetamol + 150mM diisopropylamine and 2mM paracetamol + 150mM diethylamine + 150mM diisopropylamine in pH 7 at scan rate 0.1V/s (2nd cycle)

CHAPTER V

Conclusion

Two novel paracetamol adducts such as paracetamol-diethylamine and paracetamol-diisopropylamine were synthesized electrochemically. The formation of adducts were facilitated in neutral media. The electrochemical behaviors of the reaction are discussed in the thesis. The reaction of electrochemically generated p-quinoneimine from oxidation of paracetamol as Michael acceptors with diethylamine and diisopropylamine as nucleophiles has been studied in aqueous solution with various pH, different electrodes and different concentration of nucleophiles using Cyclic voltammetry (CV), Controlled potential coulometry (CPC), Differential pulse voltammetry (DPV) and Chronoamperometry (CA) techniques. The participation of reaction of p-quinoneimine with nucleophiles in the second scan of potential was observed.

The redox reactions of paracetamol are quasi-reversible. Diethylamine and diisopropylamine are electro-inactive. The products generated from the reaction that undergo electron transfer at more negative potentials than the paracetamol. The studied system shows that peak current of both the anodic and the corresponding cathodic peaks increases with the increasing of scan rate. The nearly proportionality of the anodic and corresponding cathodic peak suggest that the peak current of the reactant at each redox reaction is controlled by diffusion process. The current function decreased with the increasing of scan rate is ascribed that the nucleophilic addition of diethylamine and diisopropylamine occurs through an ECE mechanism.

The nucleophilic reactions are pH dependent. For diethylamine and diisopropylamine, the maximum peak current is obtained at pH 7. The oxidation reaction of paracetamol-diethylamine and paracetamol-diisopropylamine adduct preceded via the $2e^-/2H^+$ process. During the reaction not only electron but also proton are released from the paracetamol-amine adducts. The reactions are also concentration dependent. The reaction was mostly

favorable in 150mM of diethylamine and 150 mM diisopropylamine with fixed 2mM of paracetamol.

Electrode effects on CV and DPV of paracetamol in presence of diethylamine and diisopropylamine was investigated. The nature of voltammograms, peak position and current intensity for the studied systems are different for different electrodes. The voltammetric response of GC electrode is better than Au and Pt electrodes.

During the course of coulometry the appeared anodic and cathodic peak height was increase to the advancement of coulometry, parallel to the decrease in height of existing anodic and cathodic peaks. All anodic and cathodic peaks disappeared after consumption of 4-electrons. The electro-synthesized products originated from paracetamol with diethylamine and diisopropylamine were isolated. The formations of products were also confirmed by FTIR spectra.

REFERENCES

1. J. M. Saveant, 2006, "Elements of Molecular and Biomolecular Electrochemistry", Willey-VCH, New Jersey.

2. Nematollahi, D., Rafiee, M. and Fotouhi, L., 2009, "Mechanistic Study of Homogeneous Reactions Coupled with Electrochemical Oxidation", J. Iran. Chem. Soc., Vol. 6, No. 3, pp. 448-476.

3. Nematollahi, D. and Hedayatfar, V., 2011, "Diversity in electrochemical oxidation of dihydroxybenzenes in the presence of 1-methylindole", J. Chem. Sci. Vol. 123, No. 5, pp. 709–717.

4. H. Lund and O. Hammerich, 2001, "Organic Electrochemistry", Marcel Dekker, New York, 4th Ed.

5. Vermeulen, N. P., Bessems, J. G. and Van de Straat, R., 1992, "Drug Metab. Rev", Vol. 24, p. 367.

6. Prescott, L. F., 1996, "Paracetamol (Acetaminophen) a Critical Bibliographic Review", Taylor & Francis Ltd., London, pp. 285–351.

7. Bessems, J. G. M. and Vermeulen, N. P. E., 2001, "Crit. Rev. Toxicol", Vol. 31, p. 55.

8. Dahlin, D. C. and Nelson, S. D., 1982, "J. Med. Chem.", Vol. 25, p. 885

9. Potter, D.W. and Hinson, J. A., 1987, "J. Biol. Chem.", Vol. 262, p. 966.

10. Buckpitt, A. R., Rollins, D. E. and Mitchell, J. R., 1979, "Biochem. Pharmacol.", Vol. 28, p. 2941.

11. Fernando, C. R., Calder, I. C. and Ham, K. N., 1980, "J. Med. Chem.", Vol. 23, p. 1153.

12. Albano, E., Rundgren, M. and Harvison, P. J., 1985, "Mol. Pharmacol.", Vol. 28, p. 306.

13. Potter, D. W., Miller, D. W. and Hinson, J. A., 1986, "Mol. Pharmacol.", Vol. 29, p. 155.

14. Jollow, D. J., Thorgeirsson, S. S., Potter, W. Z., Hashimoto, M. and Mitchell, J. R., 1974, "Pharmacolog.", Vol. 12, p. 251.

15. Davis, M., Harrison, N. G., Ideo, G., Portmann, B., Labadarios, D. and William, R., 1976, "Xenobiotica.", Vol. 6, p. 249.

16. Bergman, K., Müller, L. and Teigen, S. W., 1996, "The genotoxicity and carcinogenicity of paracetamol: a regulatory review", Mutat Res., Vol. 349 (2), pp. 263–88

17. Testa, A. C. and Reinmuth, W. H., 1961, Anal. Chem., Vol. 33, p. 1320.

18. https://en.wikipedia.org/wiki/Diethylamine.

19. Shafiei, H., Haqgu, M., Nematollahi, D. and Gholami, M. R., 2008, "An Experimental and Computational Study on the Rate Constant of Electrochemically Generated N-Acetyl-*p*-Quinoneimine with Dimethylamine", Int. J. Electrochem. Sci., Vol. 3, pp. 1092–1107.

20. https://en.wikipedia.org/wiki/Paracetamol

21. S.C. Sweetman (Ed), 2002, "The Complete Drug Reference", Pharmaceutical Press, London, 33rd ed., p. 71.

22. https://en.wikipedia.org/wiki/Diethylamine.

23. https://en.wikipedia.org/wiki/Diisopropylamine

24. Alireza, A., Ameri, M., Ziarati, A. A., Radmannia, S., Amoozadeh, A., Barfi, B., and Boutorabi, L., 2015, "Electro-oxidation of paracetamol in the presence of malononitrile: Application for green, efficient, none-catalyst, simple and one-pot electro-synthesis of new paracetamols", Chinese Chemical Letters, Vol. 26, Issue 6, pp. 681–684.

25. Nematollahi, D., Shayani-Jam, H., Alimoradi, M. and Niroomand, S., 2009, "Electrochemical oxidation of acetaminophen in aqueous solutions: Kinetic evaluation of hydrolysis, hydroxylation and dimerization processes", Electrochimica Acta, Vol. 54, Issue 28, pp. 7407–7415.

26. Nematollahi, D., Feyzi Barnaji, B. and Amani, A., 2015, "Electrochemical Synthesis and Kinetic Evaluation of Electrooxidation of Acetaminophen in the Presence of Antidepressant Drugs", Iran J Pharm Res. Vol. 14(4), pp. 1115-22.

27. Moreira, A.B., Dias, I.L.T., Neto, G.O., Zagatto, E.A.G. and Kubota, L.T., 2006, Anal. Lett., Vol. 39, p. 349

28. Alves, J.C.L. and Poppi, R.J., 2009, Anal. Chim. Acta, Vol. 642, p. 212

29. Sena, M.M. and Poppi, R.J., 2004, J. Pharm. Biomed. Anal. Vol. 34, p. 27

30. Vidal, A.D., Reyes, J.F.G., Barrales, P.O. and Diaz, A. M., 2002, Anal. Lett., Vol. 35, p. 2433

31. Mot, A.C., Soponar, F., Medvedovici, A. and Saˆrbu, G., 2010, Anal. Lett., Vol. 43, p. 804

32. Han, Z.Z., Wu, S.G., Li, Q.Y., Wang, J., 2010, J Chinese Pharm., Vol. 45, p. 228

33. Sun, S., Liu, G. and Wang, Y., 2006, Chromatographia., Vol. 64, p. 719

34. Sullivan, C. and Sherma, J., 2003, J. Liquid Chrom. Related Tech., Vol. 26, p. 3453

35. Hadad, G.M. and Mahmoud, W.M.M., 2011, J. Liquid Chrom. Related Tech. Vol. 34, p. 2516

36. Goyal, R.N. and Singh, S.P., 2006, Electrochim. Acta, Vol. 51, p. 3008

37. Goyal, R.N., Gupta, V.K., Oyama, M. and Bachheti, N., 2005, Electrochem. Commun., Vol. 7, p. 803

38. Lau, O.W., Luk, S.F. and Cheung, Y.M., 1989, Analyst., Vol. 114, p. 1047

39. Zen, J.M. and Ting, Y.S., 1997, Anal. Chim. Acta, Vol. 342, p. 175

40. Lourenc‚a˜o, B.C., Medeiros, R.A., Rocha-Filho, R.C., Mazo, L.H., and Fatibello-Filho, O., 2009, Talanta, Vol. 78, p. 748

41. Sanghavi, B.J. and Srivastava, A.K., 2010, Electrochim. Acta, Vol. 55, p. 8638

42. Wangfuengkanagul, N. and Chailapakul, O., 2002, J. Pharm. Biomed. Anal. Vol. 28, p. 841

43. Habibi, B., Jahanbakhshi, M. and Pournaghiazar, M.H., 2011, Electrochim. Acta, Vol. 56, p. 2888

44. Habibi, B., Jahanbakhshi, M. and Pournaghiazar, M.H., 2011, Microchim. Acta, Vol. 172, p. 147

45. C.M.A. Brett and A.M.O. Brett, 1993, "Electrochemistry Principles, Methods and Applications", Oxford University Press.

46. M. E. Hossain, 2014, "Electrochemical sensor simultaneous detection and estimation of environmental toxic pollutants", M.Phil Thesis, KUET.

47. D.A. Skoog, F.J. Holler and T.A. Nieman, 2007, "Principles of Instrumental Analysis", Thomson Brooks/ Cole, 6th Ed., pp. 349-351.

48. P.T. Kissinger and W.R. Heineman, 1996, "Laboratory Techniques in Electroanalytical Chemistry", Marcel Dekker, Inc.

49. C.M.A. Brett and A.M.O. Brett, 1998, "Electroanalysis", Oxford University Press.

50. Chaires, J.B., Dattagupta, N. and Crothers, D.M., 1982, Biochemistry, Vol. 21, p. 3933.

51. Randles, J.E.B., 1948, Transactions of the Faraday Society, Vol. 44, p. 327.

52. Sevcik, A., 1948, Collection of Czechoslovak Chemical Communications, Vol. 13, p. 349.

53. Bott, A.W., 1994, Curr. Seps., Vol. 13, p. 49.

54. Klinger, R.J. and Kochi, J.K., 1981, Journal of Physical Chemistry, Vol. 85, p. 12.

55. Afzal Shah, 2010, "Redox Behavior and DNA Binding Studies of Some Electroactive Compounds", Ph.D Thesis, Department of Chemistry, Quaid-i-Azam University, Islamabad.

56. Nicholson, R.S., 1965, "Analytical Chemistry", Vol. 37, p. 135.

57. Matsuda, H. and Ayabe, Y.Z., 1955, Electrochimica Acta, Vol. 59, p. 494.

58. Andrews, L.J., 1954, Chem. Revs., Vol. 54, p. 713.

59. A.J. Bard and L.R. Faulkner, 1980, "Electrochemical Methods, Fundamentals and Applications", John Wiley, New York.

60. Eyring, H., Glasstone, S. and Laidler, K.J., 1939, The Journal of Chemical Physics, Vol. 7, p. 1053.

61. Reinmuth, W.H., 1962, "Analytical Chemistry", Vol. 34, p. 144.

62. Laviron, E., 1983, J. Electrochim. Interfac. Electrochim., Vol. 1, p. 148.

63. Polcyn, D.S. and Shain, I., 1966, Analytical Chemistry, Vol. 38, p. 370.

64. Aoki, K. and Osteryoung, J., 1981, Journal of Electroanalytical Chemistry, Vol. 122, p. 19.

65. Aoki, K. and Osteryoung, J., 1984, Journal of Electroanalytical Chemistry, Vol. 160, p. 335.

66. Flanagan, J.B. and Marcoux, L., 1973, Journal of Physical Chemistry, Vol. 77, p. 1051.

67. Heinze, J., 1981, Journal of Electroanalytical Chemistry, Vol. 124, p. 73.

68. Shoup, D. and Szabo, A., 1982, Journal of Electroanalytical Chemistry, Vol. 140, p. 237.

69. Gavaghan, D.J. and Rollett, J.S., 1990, Journal of Electroanalytical Chemistry, Vol. 295, p. 1.

70. Qian, W., Jin, B., Diao, G., Zhang, Z. and Shi, H., 1996, Journal of Electroanalytical Chemistry, Vol. 414, p. 1.

71. Ikeuchi, H. and Kanakubo, M., 2000, Journal of Electroanalytical Chemistry, Vol. 493, p. 93.

72. Jr. D.K. Gosser, , 1993, "Cyclic Voltammetry (Simulation and analysis of reaction mechanisms)", Wiley-VCH, Inc.

73. F.M. Hawkridgein, P.T. Kissinger and W.R.(Eds.) Heieman, 1996, "Laboratory Techniques in Electroanalytical chemistry", Marcel Dekker Inc., New York. 2nd Ed.

74. J. Wang, 1994, "Analytical Electrochemistry", VCH Publishers Inc., New York.

75. E.R. Brown, R.F. Larg, A. Weissberger and B.(Eds.) Rossiter, 1971, Physical Methods of chemistry, Vol.1-Part IIA, Wiley-Interscience, New York.

76. Armada, P.G, Losada, J. and Perez, S.V., 1996, "Cation analysis scheme by differential pulse polarography", Vol. 73, pp. 544-546.

77. Zhang, J., 1972, Journal of Electroanalytical Chemistry, Vol. 331, p. 945.

78. Nematollahi, D., Afkhami, A., Mosaed, F. and Rafiee, M., 2004, "Research on Chemical Intermediates", Vol. 30, p. 299.

79. Papouchado, L., Petrie, G. and Adams, R. N., 1972, J Electroanal Chem., Vol. 38, p. 389.

80. Papouchado, L., Petrie, G., Sharp, J.H. and Adams, R.N., 1968, J Am Chem Soc., Vol. 90, p. 5620.

81. Young, T.E., Griswold, J.R. and Hulbert, M.H., 1974, J Org Chem., Vol. 39, p. 1980.

82. Brun, A. and Rosset, R., 1974, J Electroanal Chem., Vol. 49, p. 287.

83. Stum, D.I. and Suslov, S.N., 1979, Bio. Zika, Vol. 21, p. 40.

84. Rayn, M.D., Yueh, A. and Yu, C.W., 1980, J Electrochem Soc., Vol. 127, p. 1489.

85. Md. Matiar Rahman, 2014, "Electrochemical characterization of biologically important electroactive metal ligand complexes with multi-electron transfer reaction", M.Phil Thesis, KUET.

86. Thibodeau, P.A. and Paquette, B., 1999, Free Radical Biology & Medicine, Vol. 27, p. 1367.

87. Mazzini, S, Monderelli, R, Ragg, E. and Scaglioni, L., 1995, J Chemi Soci, Perkin Transactions, Vol. 2, p. 285.

88.   Nematollahi, D. and Golabi, S.M., 2000, J Electroanal Chem., Vol. 481, p. 208.

89.   Kiani, A., Raoof, J.B., Nematollahi, D. and Ojani, R., 2005, Electroanalysis, Vol. 17, No. 19, pp. 1755–1760.

90.   Md. Alim Uddin, 2015, "Electrochemical study of catechol in presence of sulfanilic acid and diethylamine at different pH", M.Sc. Thesis, KUET.